UNIVERSITY OF CINCINNATI

Date: 10-May-2010

I, Mary McVey Buschmann **,**

hereby submit this original work as part of the requirements for the degree of:

Doctor of Philosophy

in Cell & Molecular Biology

It is entitled:

Laminin-332-Mediated Proliferation Control: Mechanisms Regulating Formation of the Epithelium

Student Signature: Mary McVey Buschmann

This work and its defense approved by:

Committee Chair: Susanne Wells, PhD
Susanne Wells, PhD

Karl Matlin, PhD
Karl Matlin, PhD

Susan Waltz, PhD
Susan Waltz, PhD

Anil Menon, PhD
Anil Menon, PhD

Jonathan Jones, PhD
Jonathan Jones, PhD

Laminin-332-Mediated Proliferation Control: Mechanisms Regulating Formation of the Epithelium

A dissertation submitted to the

Division of Research and Advanced Studies
of the University of Cincinnati

in partial fulfillment of the
requirements for the degree of

DOCTOR OF PHILOSOPHY

In the Department of
Cancer and Cell Biology
of the College of Medicine

2010

by

Mary McVey Buschmann

B.A. Concordia University, Ann Arbor, MI, 2003

Committee Members: Karl S. Matlin, PhD, Advisor
Susanne I. Wells, PhD, Chair
Jonathan C.R. Jones, PhD
Anil G. Menon, PhD
Susan E. Waltz, PhD

ABSTRACT

Normal epithelial cells rely on spatial cues from the extracellular matrix to proliferate, migrate, and survive. The extracellular matrix protein, laminin-332 (LM-332) seems to be particularly important in proliferation control during re-formation of a wounded epithelium. Inhibition of the LM-332-cell interaction prevents wound healing in keratinocytes and mammary epithelial cells. Treatment of normal renal epithelial cells with LM-332 rich medium increases the rate of proliferation, and inhibition of the LM-332-cellular interaction prevents proliferation in mammary epithelial and rat bladder carcinoma cells. Despite this information, the mechanism of LM-332-mediated proliferation control is largely unknown. The goal of the studies described here was to understand the requirement for LM-332 in proliferation control to form a polarized epithelium using the Madin Darby Canine Kidney (MDCK) cell model system. LM-332 expression was turned on at low cell density when cells were proliferative, and turned off and degraded upon re-formation of a quiescent epithelium. Furthermore, the suppression of LM-332 by expression of an shRNA targeted against the LMα3 subunit induced a G1 cell cycle arrest, likely through a mechanism mediated by p21waf1 inhibition of the cyclin E/cdk2 complex. The LMα3 shRNA-mediated proliferation arrest, however could not be validated, as the G1 block could not be rescued by plating cells on, or exposing cells to, endogenous LM-332, or by co-expression of human LMα3. Also, inhibition of the LM-332 receptors, integrins α3β1 and α6β4, did not cause proliferative arrest to a similar extent as cell expressing the shRNA, and last, expression of three additional siRNAs specific for the LMα3 chain did not alter proliferation. Instead, studies using the new siRNAs indicated that LM-332 is important for cell spreading and morphogenesis of the epithelium. All of the studies presented in this work

collectively suggest that deposition of LM-332 plays an important role in the regulation of cell spreading, morphogenesis, and possibly proliferation, to establish a polarized epithelium.

ACKNOWLEDGEMENTS

Many people have contributed to the excellent experience that I have had as a graduate student, and for them, I am truly grateful. I would like to offer thanks to the following people:

First, to my advisor, Karl Matlin. You seemed to know when it was best to let me figure things out on my own, and when I needed more guidance. You've had a knack for applying an appropriate mixture of correction and kindness. Thank you also for your unwavering support of my quest to achieve a work-life balance. You have set a standard by which all future colleagues will be compared.

To my thesis committee, Dr. Jonathan Jones, Dr. Anil, Menon, and Dr. Susan Waltz, and Dr. Susanne Wells, for not only offering invaluable advice, but also for your flexibility in helping me navigate my project despite finishing my studies at the University of Chicago. I'd specifically like to thank Dr. Susanne Wells for serving as my committee chair.

To the graduate program in Cancer and Cell Biology at the University of Cincinnati, specifically to Barbara Carter and Sharon Young, for helping on numerous occasions with administrative issues. Also, thank you to the Committee on Cancer Biology at the University of Chicago for welcoming me into your program.

To my "co-advisors", Kathleen Goss, Mirjam Zegers, Martin terBeest, and Carrie Rinker-Schafer. Thank you for the many, many times you edited my work, critiqued presentations, and offered advice. I've learned countless things from each of you, and for that I am sincerely appreciative.

To my fellow lab mates, past and present, Ignacio Calvo, Gina Kavanaugh, Patricia Gonzalez-Greciano, Grace Mak, Priya Mathur, Jose Moyano, Nisha Sipes, Jun Tang, and Holly Waechter. You've always made the lab an enjoyable place to be everyday. A special thanks to Jun Tang for all of your help with producing the adenoviruses used in these studies.

To my family, Daniel, Marjorie, and William McVey. Having a strong-willed child and sibling is no easy task. I was always determined to drive down my own road of life at 90 mph. Thank you for always ensuring that my car had gas and was equipped with seatbelts.

Last, to my wonderful husband, Joe. You've been by my side since the beginning. You quizzed me prior to exams my first year, helped me count nuclei for BrdU experiments, cooked and cleaned when I was working long hours, provided words of encouragement when things weren't going well, and lifted a glass with me when they were. In many ways, it feels like you should be the co-author of this work. As a little girl, I dreamed of what my life would be like. Thank you for helping make the reality so much better than the dream.

I dedicate this work to my beautiful daughter, Emilia. Your smiles bring new meaning to life and provide motivation for the future. I hope that whatever you choose to do with your life, that you are as richly blessed as I have been.

TABLE OF CONTENTS

LIST OF FIGURES

LIST OF TABLES

ABBREVIATIONS

β-gal	β-galactosidase
βGPP	β-glycerolphosphate
Ad-LacZ	Adenovirus-mediated delivery of the LacZ protein
Ad-shControl	Adenovirus-mediated delivery of an shRNA that does not target the canine genome
Ad-shLMα3	Adenovirus-mediated delivery of an shRNA against LMα3
AP-1	Activator Protein-1
APS	Ammonium Persulfate
ATP	Adenosine Tri-Phosphate
BCA	Bicinchoninic Acid
BLAST	Basic Local Alignment Search Tool
BM	Basement Membrane
BP buffer	Blocking and Permeabilization Buffer
BPB	Bromophenol Blue
BrdU	5-bromo-2-deoxyuridine
BSA	Bovine Serum Albumin
$CaCl_2$	Calcium Chloride
CAK	Cdk-activating Kinase
CDK	Cyclin Dependent Kinase
cDNA	Complementary DNA
CKI	Cyclin-dependent kinase inhibitor

CO_2	Carbon Dioxide
CPE	Cytoplasmic effect
CTN	Catenin
Cul-3	Cullin-3 E3 ubiquitin ligase
DAPI	4',6-diamidino-2-phenylindole
D5	Same as Ad-shLMα3 (Adenovirus-mediated delivery of an shRNA against LMα3)
DDM	Doublet Discrimination Mode
DMEM	Dulbecco's Modified Eagle Medium
DMSO	Dimethyl sulfoxide
DPI	Dots Per Inch
DTT	Dithiothreitol
ECM	Extracellular Matrix
EDTA	Ethylene diamine tetraacetic acid
EdU	5-ethynyl-2'deoxyuridine
EGFR	Epidermal Growth Factor Receptor
EGTA	Ethylene glycol tetraacetic acid
EHS	Engelbreth-Holm-Swarm sarcoma
ERK	Extracellular-Signal Regulated Kinase
FACS	Fluorescence Activated Cell Sorter
FAK	Focal Adhesion Kinase
FPLC	Fast Protein Liquid Chromatography
FSC	Forward Side Scatter

G0	Gap 0
G1	Gap 1
G2/M	Gap 2/Mitosis
GRGDSP	H-Gly-Arg-Gly-Asp-Ser-Pro-OH, blocking peptide
GSK-3β	Glycogen Synthase Kinase 3β
HBS	Hepes Buffered Saline
HCl	Hydrochloric Acid
HDAC	Histone Deacetylase
HEK	Human Embryonic Kidney-293 cells
HEPES	4-(2-Hydroxyethyl)-1-piperazineethane sulfonic acid
HRP	Horseradish Peroxidase
ILK	Integrin Linked Kinase
infU	Infectious units
IP	Immunoprecipitation
JNK	c-Jun N-terminal Kinase
LB broth	Luria Bertani broth
LE domain	Laminin domains III and V, which contain EGF-like repeats
LG domain	C-terminus of the Laminin α chain, contains five globular subdomains
LG4-5	The LG modules 4 and 5 within the LMα3 chain LG domain
LM	Laminin
LMα3ΔLG4-5	LMα3 construct encoding for the α3 chain lacking the LG4-5 domain
LM-332	Laminin-332
LN module	Domain VI of the laminin α, β and γ chains

MAPK	Mitogen Activated Protein Kinase
MDCK	Madin Darby Canine Kidney cells
MEM	Minimum Essential Medium medium
MeOH	Methanol
$MgCl_2$	Magnesium Chloride
$MnCl_2$	Manganese Chloride
MWCO	Molecular Weight Cut-off
NA	Numerical Aperature
NaCl	Sodium Chloride
NCBI	National Center for Biotechnology Information
NH_4OH	Ammonium Hydroxide
NMJ	Neuromuscular Junction
NLS	Nuclear Localization Sequence
No siRNA	A siRNA duplex control in which MDCK cells were electroporated with electroporation buffer alone
PAGE	Polyacrylamide Gel Electrophoresis
PBS-	Phosphate Buffered Saline, without ions
PBS+	Phosphate Buffered Saline, with Mg++ and Ca++ ions
PCNA	Proliferating Cell Nuclear Antigen
PCR	Polymerase Chain Reaction
PDGF	Platelet Derived Growth Factor
PFA	Paraformaldehyde solution
PI	Propidium Iodide
PI3K	Phosphoinositide 3-Kinase

PKC	Protein Kinase C
PMSF	Phenymethylsulphonyl fluoride
pRB	Retinoblastoma protein
Pre-LM-332	The LM-332 heterotrimer containing the full-length LMα3 chain
qPCR	Quantitative Real-Time PCR
RGES	Arg-Gly-Glu-Ser, RGD negative control peptide
RNAi	RNA interference
RPM	Rotations Per Minute
RPTK	Receptor Protein Tyrosine Kinase
RT	Room temperature, 20-25°C
RT-PCR	Reverse Transcriptase Polymerase Chain Reaction
S	Synthesis
SCF	Skp-Cul1-Fbox E3 ubiquitin ligase
SDS	sodium dodecyl sulfate
SFK	Src Family Kinase
shRNA	Short-hairpin RNA
siLMα3	siRNA duplexes specific for LMα3
siLuc	siRNA duplex targeting Luciferase
siRNA	Small-interfering RNA
SPARC	Secreted Protein Acidic and Rich in Cysteine
SSC	Side Scatter
TBST	Tris Buffered Saline with Tween
TE buffer	Tris EDTA buffer

TEMED	Tetramethylethylenediamine
TGFβ	Transforming Growth Factor β
Tris	2-Amino-2-hydroxymethyl-propane-1,3-diol
UTR	Untranslated Region

Chapter 1:
Introduction

1.1 Epithelia

1.1.1 Epithelia Structure and Function

Normal tissue function relies, at least in part, on the ability of epithelial cells to form and maintain continuous polarized epithelia. Indeed, loss of polarity is a hallmark of many epithelial derived diseases. The epithelium is a semi-permeable barrier that lines the outer surfaces of the body, providing protection from the outside environment and separating distinct chemical milieus. Epithelial cells can provide this barrier because they are apically and basolaterally, polarized. Polarization refers to the asymmetric organization of both the plasma membrane and cytoplasm along the apical-basal axis. The apical surface, depending on the tissue, opens to the exterior or to the luminal space, in such; that it always faces the outside world. The basolateral domain contains both the lateral and the basal cell surfaces. The lateral domain is involved in cell-cell adhesions, and the varieties of proteins localized to the lateral membrane are responsible for both physically linking epithelial cells together, and the selective permeability of the epithelium. The basal domain contains both the receptors for the underlying extracellular matrix (ECM) and the receptors and many transporters that maintain the physiological state of the cell (Fish and Molitoris, 1994; Fristrom, 1988; Schock and Perrimon, 2002).

1.1.2 Forming and Maintaining a Polarized Epithelium

The epithelium is formed early in embryogenesis by either compaction of cells at the blastula stage or from a mesenchymal-to-epithelial transition of mesenchymal cells (Schock and Perrimon, 2002; Thiery, 2002). Once the mature epithelium is formed, natural processes, such as cell-turnover, disrupt it. The epithelium can also be disrupted by injury and disease, which can result in large, denuded patches between cells. Rapid and precise cellular processes, such as spreading, migration and proliferation are required to replace lost cells to re-form the epithelium (Jacinto et al., 2001; Santoro and Gaudino, 2005). The process by which the epithelium is re-formed after injury is referred to as re-epithelialization. Re-epithelialization is triggered by several factors and occurs similarly in *in vivo* and *in vitro* epithelia. First, in the situation where the epithelium is disrupted by injury, damaged cells at the wound edge are transiently leaky to Ca^{2+}, which can transcriptionally activate expression of growth factors. Growth factor signaling promotes the expression and deposition of ECM proteins at the leading edge. The cells, in response to the newly deposited ECM, and in response to the original loss of cell-cell contacts, extend protrusions on the new substratum, and migrate into the wound (Friedl et al., 2004; Jacinto et al., 2001). For small wounds, migration alone is sufficient to re-form the epithelium (Fenteany et al., 2000). For larger wounds, however, cellular proliferation is also required (Jacinto et al., 2001). As proliferation is a much slower process than migration, migration proceeds first, then, if the epithelium has not re-formed within 24 hours, an upsurge of proliferation at the wound edge is observed (Matoltsy and Viziam, 1970). The processes of spreading, migration, and proliferation continue until cells again make contact with one another and re-establish continuity. The cessation of these events upon re-formation of the epithelium is referred to as density-dependent contact inhibition (Abercrombie, 1979), and failure of cells to undergo contact inhibition is a hallmark of many epithelial diseases, such as cancer

(Abercrombie, 1979). The long-term goal of our work is to understand how the newly deposited ECM promotes cellular events, such as adhesion, spreading, migration and proliferation to re-form the epithelium.

1.1.3 The MDCK In Vitro Model System

In vitro model systems have been useful for understanding the complex events required for re-formation of the epithelium. The Madin Darby Canine Kidney (MDCK) epithelial cell line was established in 1958 from the kidney of a normal female cocker spaniel (Madin et al., 1957; Sato, 1981) and has subsequently become one of the most important models for the study of epithelial biology. MDCK cells are ideal for the study of normal epithelial biology because they are not oncogenically transformed, unlike a number of other epithelial cell lines, and do not form tumors when injected into nude mice (Misfeldt et al., 1976; Sato, 1981; Simons and Fuller, 1985). MDCK cells share many physiological features of renal distal tubule and cortical collecting duct cells, and are responsive to hormones that regulate transepithelial transport (Herzlinger et al., 1982; Sato, 1981; Valentich, 1981). Importantly, MDCK cells re-form the epithelium in a manner similar to that of epithelia *in vivo*, that is, at low density in culture, cells secrete ECM proteins that they adhere to, and then spread, migrate, proliferate, and polarize to re-form cell-cell and cell-substratum connections, and then undergo density-dependent growth inhibition (Fenteany et al., 2000; Gaush et al., 1966; Misfeldt et al., 1976). MDCK cells secrete several ECM proteins, such as two forms of laminin, collagen IV, and proteoglycans, but it is unclear how these proteins may impact the formation of the epithelium in this cell type (Erickson and Couchman, 2001; Mak et al., 2006).

1.2 The Extracellular Matrix (ECM) Underlies Epithelia

Cellular adhesion to the ECM, in addition to providing structural support for the epithelium, also activates cellular signaling cascades that differentially control spreading, migration, proliferation, and survival. Injury to the epithelium disrupts cell-substratum adhesions; therefore, deposition and assembly of new ECM proteins are prerequisite for re-formation of the epithelium.

In mature epithelia, the ECM is divided into two structures: the basement membrane (BM) and the interstitial connective tissue. The BM is a thin 40-120nm sheet of matrix molecules that underlies all epithelia (Alberts, 2008). By electron microscopy, the BM is visible as three structures: the *lamina lucida externa, the lamina densa*, and the *lamina lucida interna*. The core of the BM is the *lamina densa,* and is composed mainly of laminin isoforms, collagen IV, nidogen, and perlecan (Hay, 1991). From tissue-to-tissue, the composition of BM proteins is heterogeneous, and likely contributes to the distinct functionality of that tissue.

The second component of the ECM is the interstitial connective tissue, which underlies the BM *in vivo*. Fibroblastic secretions of matrix molecules, such as collagen and fibronectin generate the connective tissue (Alberts, 2008). Assembly of these matrix proteins is important for increasing the tensile strength of a tissue, and may also be important for assembly of the basement membrane (Furuyama and Mochitate, 2000; Sanderson et al., 1986). The matrix proteins within the connective tissue and the BM are mostly unique, but some examples exist of proteins that are found in both the ECM and BM. As the connective tissue is not present *in vitro,* and it is the BM that contacts epithelia and regulates epithelial function both *in vivo* and *in vitro,* the BM will be the focus of this discussion.

1.3 The Laminin Family of Basement Membrane Proteins

1.3.1 Introduction

The laminin family of BM proteins has been widely implicated in the formation of the epithelium. Their importance in promoting and maintaining the integrity of the epithelium is evidenced by the plethora of diseases that are caused by loss or mutation of the proteins (Table 1.1). Laminins were originally discovered as a major component of the mouse Engelbreth-Holm-Swarm (EHS) sarcoma. Antibodies raised against the EHS sarcoma matrix were used to purify laminin from the tumor and to immunolocalize the protein to the BM of tissues throughout the body (Timpl et al., 1979). Members of the laminin family are characterized by the presence of unique α, β, and γ chains that interact to form a heterotrimeric glycoprotein (Figure 1.2) (Beck et al., 1990; Engel et al., 1981). The individual chains are joined through a long coiled-coil, producing a molecule with one long arm, and as many as three short arms (Beck et al., 1993). Combinations of five α, four β, and three γ chains have been identified. These join to form 16-18 different laminin isoforms that are differentially found within the BM of epithelia, muscle and nerve cells in mammals (Durbeej, 2010; Miner and Yurchenco, 2004). Laminins are named based on their chain composition. For example, laminin-332 (LM-332) is a heterotrimer consisting of the α3, β3, γ2 subunits and laminin-511 (LM-511) consists of α5, β1, and γ1 subunits (Aumailley et al., 2005). Table 1.2 lists the chain compositions and tissue localizations of each laminin.

Table 1.1 Diseases Associated with the Loss or Mutation of Laminin Chains

Laminin chain	Null/mutated Phenotype	Human disease	Reference
α1	Embryonic lethal (Ds)		(Yurchenco and O'Rear, 1994)
α2	Adult lethal, muscular dystrophy and peripheral nerve dysmyelination (Ms)	Congenital muscular dystrophy	(Miyagoe et al., 1997) (Patton et al., 1999) (Patton et al., 1997) (McGowan and Marinkovich, 2000)
α3	Neonatal lethality and severe skin blistering (Ms)	Epidermolysis bullosa	(Ryan et al., 1999)
α4	Endothelial defect, hemorrhages, misalignment of neuromuscular junction active zones and infoldings, cardiac hypertrophy, heart failure (Ms)	Cardiomyopathy	(Knoll et al., 2007; Patton et al., 2001; Thyboll et al., 2002)
α5	Embryonic lethal with defects in the kidney, neural tube, limb, and placental vessels		(Miner and Li, 2000)
β2	Adult lethal, glomerular defects with proteinuria, abnormal neuromuscular junction (Ms)	Nephritic syndrome	(Noakes et al., 1995a; Noakes et al., 1995b)
β3	Neonatal lethality and severe skin blistering (Ms)	Epidermolysis bullosa	(Ryan et al., 1999)
γ1	Embryonic lethal, failure of blastocyst		(Smyth et al., 1999)
γ2	Neonatal lethality and Severe skin blistering (Ms)	Epidermolysis bullosa	(Meng et al., 2003; Pulkkinen et al., 1994)

(Ds) Drosophila, (Ms) Mouse

Table 1.2 Chain Compositions of the 16-known Laminins

Laminin	Chain Composition	Old name	Tissue Localization[1]
Laminin-111	α1β1γ1	Laminin-1, EHS laminin, classical laminin	Kidney, live, testis, ovary, and embryonic epithelium, brain blood vessels
Laminin-211	α2β1γ1	Laminin-2, merosin	Placenta
Laminin-121	α1β2γ1	Laminin-3, s-laminin	Muscle, heart, peripheral nerve, testis
Laminin-221	α2β2γ1	Laminin-4, s-merosin	Muscle, heart, peripheral nerve, NMJ
Laminin-3A32	α3Aβ3γ2	Laminin-5, kalinin, nicein	Epidermis, placenta, mammary gland
Laminin-3B32	α3Bβ3γ2	Laminin-5B	Epidermis, uterus, lung
Laminin-311	α3β1γ1	Laminin-6, K-laminin	Epidermis, amnion
Laminin-321	α3β2γ1	Laminin-7, KS-laminin	Epidermis, amnion
Laminin-411	α4β1γ1	Laminin-8	Endothelium, smooth muscle, fat, peripheral nerve
Laminin-421	α4β2γ1	Laminin-9	Endothelium, smooth muscle, NMJ
Laminin-511	α5β1γ1	Laminin-10	Epithelium (mature and developing), endothelium, smooth muscle
Laminin-521	α5β2γ1	Laminin-11	Epithelium, endothelium, smooth muscle, NMJ
Laminin-213	α2β1γ3	Laminin-12	Placenta, testis
Laminin-423	α4β2γ3	Laminin-14	Retina/CNS
Laminin-523	α5β2γ3	Laminin-15	Retina/CNS
Laminin-522	α4β2γ2	None	Bone marrow

[1] From Durbeej, 2010

1.3.2 Structure of the Laminin Heterotrimer

The unique structure of laminin isoforms has a direct effect on its ability to assemble into a BM and to mediate cell function. Rotary shadowing electron microscopy has shown that the three subunits combine to form a cruciform structure (Figure 1.2) (Engel et al., 1981; Yurchenco et al., 1985). Many of the original laminin structural studies were performed by analysis of laminin-111, but several of the features within this laminin are also observed in other members of the laminin family (Miner and Yurchenco, 2004). Laminin-111 and laminins-211, -121, -211, -511, and -521 are called the 'prototypical' laminins because they are all structurally similar to the originally identified laminin-111. Within the prototypical laminins, the individual α, β, and γ chains are homologous in domain structure. Each chain contains six domains, named I-VI. The long arm of the cross-like laminin protein is comprised of domains I and II. This rod-like domain forms α-helices that are stabilized by disulfide linkages between the chains at the N-terminus and at the junction between domains II and III (Beck et al., 1990). Each α helix contains roughly 600 amino acids arranged in a series of heptad repeats. Of these repeats, the first and fourth amino acids generally are the hydrophobic leucine, isoleucine, or valine residues, the fifth and seventh are charged, and the second, third, and sixth are hydrophilic (Paulsson et al., 1985; Tunggal et al., 2000). Because of the electrical charges of the fifth and seventh amino acids, identical or homologous chains cannot form stable coiled-coils, which may explain why laminins form heterotrimers, and the particular combinations of trimers that are observed (Beck et al., 1993).

The biggest deviation between the structure of the prototypical laminins and that of other laminins, specifically laminins -332, -321, -411, -311, and -421, is the presence of domains III-VI within the α chain. With the exception of laminin-332, all laminins have domains III-VI in the β and γ chains (Miner and Yurchenco, 2004). Domains III-VI form the short arms of the

laminin molecule. Domains III and V are rod-like in structure, and are separated by domains IV and VI, which are globular. Domains III and V contain three to eight EGF-like repeats that are stabilized by disulfide bonding (Engel, 1989). These are referred to as the 'LE' domains (Aumailley et al., 2005). The EGF-like repeats within this domain have the same basic structure as EGF, but differ from the classical EGF by two extra cysteine residues at the C-terminal end. It is currently unclear if the EGF-like sequences within laminin act merely as spacers or whether they act mitogenically (Engel, 1989). Domain IV is a cysteine-rich, globular domain. The α chains contain two IV domains, which are termed IVa and IVb. Domains IVa of the α chains and IVb of the α1 and α2 chains are homologous to domains IV of the γ chains (Beck et al., 1990; Tunggal et al., 2000). Domain VI is an N-terminal globular domain that is the most highly conserved region of the molecule. This domain is also referred to as the LN module (Aumailley et al., 2005). The interactions between domain VI of like chains (i.e. α-with-α, β-with-β, γ-with-γ) is critical for assembly of laminins into sheets within the basement membrane (described in *1.3.4*) (Yurchenco and O'Rear, 1994; Yurchenco et al., 1985).

At the C-terminus of the α chain are five large globular subdomains, which are called LG modules. Each LG module is highly homologous and contains around 200 amino acids (Timpl et al., 2000). The LG modules together comprise the LG-domain (Aumailley et al., 2005). The entire domain comprises one-third of the α chain amino acid sequence. The cell-laminin interaction occurs by receptor recognition of sequences within the LG-domain.

1.3.3 Laminin Glycosylation, Assembly, and Secretion

As laminins are heterotrimeric glycoproteins, proper glycosylation and heterotrimer assembly are required for secretion from the cell. Laminin-111 is predicted to be glycosylated on 14 glycosylation sites within the α chain, 13 sites within the γ chain, and 11 sites within the β

chain (Howe and Dietzschold, 1983). Similarly, the laminin α2 chain also contains 30 potential glycosylations sites (Bernier et al., 1995). Although the other laminin chains are also known to be glycosylated, glycosylation sites have not been mapped in these molecules. In laminin-111, the α, β, and γ chains are glycosylated with asparagine-linked high mannose oligosaccharides in the endoplasmic reticulum. Chains containing these oligosaccharides are referred to as the laminin precursors. Also in the endoplasmic reticulum, dimeric βγ complexes form containing the precursor β and γ subunits. Glycosylation is not required for the βγ interaction, however (Matsui et al., 1995; Peters et al., 1985; Yurchenco et al., 1997). This complex forms in the absence of the α subunit. Once the α chain is expressed, it associates with the βγ dimer (Matsui et al., 1995; Yurchenco et al., 1997). After the αβγ trimer forms, the proteins are translocated from the endoplasmic reticulum to the golgi apparatus. Here, high mannose oligosaccharides are processed to complex oligosaccharides, which are observed in the mature laminin. After processing, laminin is quickly externalized from the cell via recognition of a signal sequence at the N-terminus, and is not stored intracellularly (Peters et al., 1985). At least in regards to LM-332, processing of the oligosaccharides is required for cell migration and adhesion (Kariya et al., 2008; Kariya et al., 2010), suggesting that the regulation of laminin glycosylation is an important event that can alter cell function.

1.3.4 Laminin Assembly into the BM

Polymerization of the prototypical laminins into a sheet-like structure is a feature that sets the prototypical laminins apart from the rest of the laminin family. These laminin molecules are secreted as individual proteins, but quickly polymerize into a sheet-like structure, which provides a substrate for cell adhesion, and in some cases, migration. Laminin assembly into the BM has been studied in laminin-111 and laminin-211, but is thought to hold true for the other

prototypical laminins as well. Once individual laminin heterotrimers are secreted from the cell, LG modules 4-5 (LG4-5) within the C-terminus of the α chain are anchored to the plasma membrane by interaction with sulfated glycolipids, called sulfitides, and dystroglycan (Li et al., 2005b; McKee et al., 2009; Weir et al., 2006). The globular domain VI within the α, β, and γ chains then self associate with the α, β, and γ globular domain VI of neighboring laminin molecules in a Ca^{2+} dependent reaction (Yurchenco et al., 1985). Continued α-α, β-β, and γ-γ interactions between the domain VI of multiple laminin molecules generates a laminin polymer (Yurchenco and O'Rear, 1994). Laminin polymerization draws sulfitides and dystroglycan receptors together and triggers signaling events that promote a myriad of cellular events (Li et al., 2005b). Once laminin has polymerized, the sheet is stabilized by indirect interaction with collagen IV, which, prior to interacting with laminin, also polymerizes to form a collagen IV network (LeBleu et al., 2007). The laminin and collagen IV sheets are linked together by small proteins, mainly nidogen/entactin that are singularly secreted. These proteins bind to both laminin and collagen IV through sites that are unique to both proteins. Specifically, nidogen/entactin interacts with the laminin γ chain, and with the collagenous domain of collagen IV (Yurchenco and O'Rear, 1994). Many other proteins may also be present that aid in BM stabilization. Perlecan, for example, is a proteoglycan that has binding sites for collagen IV and nidogen/entactin, and for the integrin receptors on the basal cell surface. Other minor protein components are present in the BM, but the function attributed to each is poorly understood. Secreted Protein Acidic and Rich in Cysteine (SPARC), agrin, collagen XV, and collagen XVIII are examples of such proteins (LeBleu et al., 2007).

1.3.5 The Laminin Receptors

All laminins interact with the cell through binding of cellular receptors. The three largest families of laminin receptors are the integrins, dystroglycan, and syndecans (Table 1.3). Each of these protein families have a cytoplasmic C-terminal region that, upon activation, promote signaling cascades that differentially regulate cellular functions ranging from adhesion to apoptosis. The integrins are heterodimeric membrane proteins consisting of an α and β subunit, which combine to form 24 different integrins that differentially bind to ECM proteins. The α and β subunits contain extracellular, membrane, and cytoplasmic regions. Upon laminin binding to the extracellular region of the integrin, integrin conformational changes allow for the recruitment of cell signaling intermediates. Dystroglycan is a glycoprotein that is originally expressed as a single molecule, but is then cleaved into an α and β subunit (Higginson and Winder, 2005). The α subunit binds to laminin at the C-terminus within LG4-5 (Talts et al., 1999). Syndecans are a family of four proteins that are type I transmembrane cell surface proteoglycans. Syndecan-1 is primarily found in epithelia and is known to bind to several members of the laminin family, additionally, syndecans-2 and -4 have also been shown to interact with laminins α1 and α3 within the globular domains at the C-terminus (Xian et al., 2010). MDCK cells express the laminin receptors α3β1, α2β1, and α6β4 (Schoenenberger et al., 1994), dystroglycan (Masuda-Hirata et al., 2009), and at least syndecan-1, of the syndecans (Erickson and Couchman, 2001).

Table 1.3 The Laminin Receptors

Receptor	Laminin Ligand
α1β1	α1, α2 (LN domain)
α2β1	α1, α2 (LN domain)
α3β1	α2, α5, α3, α4 (LG domain)
α6β1	α1, α2, α5, α3, α4 (LG domain)
α7β1	α1, α2 (LG domain)
α6β4	α1, α2, α5, α3 (LG domain)
Dystroglycan	α1, α2, α3, α4, α5 (LG domain)
HNK-1	α1 (LG domain)
Lutheran	α5 (LG domain)
Sulfatides	α1, α2 (LN domain); α1, α2, α3, α4, α5 (LG domain)
Syndecan-1	α1, α2, α3 (LG domain)
Syndecan-2	α1, α3, α5 (LG domain)
Syndecan-4	α1, α3 (LG domain)

1.4 Laminin-332

1.4.1 Laminin-332 Structure and Function

The predominant laminins found in mature epithelial tissues are laminins-332 and -511. Laminin-332 (LM-332) in particular, is required for re-formation of the epithelium (Goldfinger et al., 1999). Within hours of wounding a quiescent epidermis, LM-332 is transcribed and deposited by cells at the wound edge and the deposition has been connected with cellular adhesion, migration, spreading, and proliferation (Marinkovich, 2007; Nguyen et al., 2000).

LM-332 is unique to the laminin family in several ways (Figure 1.3). First, the α3 chain is the only laminin chain which has variants, termed α3A and α3B. LMα3B is roughly 335 kD, and is structurally similar to the prototypical laminins in that it contains domains III-VI at the N-terminus (Galliano et al., 1995; Kariya et al., 2004). LMα3A however, is truncated between domains III and IV and is not capable of self-assembly into a network like the prototypical laminins (Cheng et al., 1997). LMα3A and B chains are products of the same gene, but their expression is regulated by distinct promoters and alternative splicing of the same transcript

(Ferrigno et al., 1997; Galliano et al., 1995; Ryan et al., 1994). The isoform expression varies by tissue, and its affect on cellular function may also differ by tissue type (Kariya et al., 2004). LMα3B can also be cleaved between domains III and IV, likely by the protease BMP-1, yielding a 190kD product that is nearly identical to LMα3A (Kariya et al., 2004). It is therefore difficult to decipher LMα3A versus cleaved-LMα3B expression. Importantly, both the full length and cleaved LMα3B and LMα3A are capable of promoting adhesion, migration and proliferation, both heterotrimerize with the β3 and γ2 chains, and both are identical at the C-terminus (Ferrigno et al., 1997; Kariya et al., 2004). Most studies to do not indicate whether LMα3A or LMα3B were examined, therefore attributing unique functionality to either variant is also difficult. For this reason, LMα3 will be referred to generically in this discussion.

LM-332 is also structurally unique in that the β3 and γ2 chains are shorter than the β or γ chains of the prototypical laminins (Rousselle et al., 1991). The β3 chain contains a globular LN domain at the N-terminus, and may be able to self associate with the β3 chain of other β3 containing laminins (Odenthal et al., 2004). Because of the truncations within the other two chains, however, LM-332 is unable to form a self-assembled network (Cheng et al., 1997).

Perhaps the feature of LM-332 that has the biggest impact on cellular function is that LM-332 is vulnerable to cleavage at many places within the molecule, most famously, within the LG domains of the α chain. The LG domain contains several sites that interact with cell surface receptors. Processing events impact LM-332 receptor binding. The full length LMα3A is secreted as a pre-cursor that is 190-200kD (pre-LM-332). This precursor should not be confused with the intracellular LMα3 precursor that contains high mannose oligosaccharides. Pre-LM-332 contains all five LG modules at the C-terminus, which are required for LM-332 secretion (Sigle et al., 2004; Tsubota et al., 2005). Shortly after pre-LM-332 is secreted, the LG domain of the α3 chain is cleaved by the protease plasmin between LG3 and LG4 domains, releasing a 35kD

fragment (Goldfinger et al., 1998) Processed LM-332 is often observed in the BM of mature epithelia, but pre-LM-332 is rarely observed other than in situations when the epithelium is re-forming, such as after injury (Sigle et al., 2004). Indeed, the LG4 and LG5 are important for cell proliferation, and the removal of these domains promotes adhesion and migration in keratinocytes (Shang et al., 2001; Tran et al., 2008).

1.4.2 LM-332 and Proliferation Regulation

It has long been appreciated that cell-substratum interactions are required for growth, as cells in suspension fail to divide. This dependency is referred to as 'anchorage-dependent growth' (Assoian, 1997; Stoker et al., 1968). Proliferation is also a key cellular event for re-formation of an epithelium, and is equally impacted by interaction with the substratum. Indeed, failure to re-form the epithelium is often caused by failure to proliferate.

LM-332 has been implicated in proliferation control of both normal and diseased cells. During re-formation of the epithelium, the full-length, pre-LM-332 is expressed at the leading edge in multiple cell types including keratinocytes and MDCK cells, at roughly the same geographical location where cellular proliferation is occurring (Matoltsy and Viziam, 1970; Nguyen et al., 2000; Moyano, unpublished). Overexpression of LM-332 has also been shown to accelerate the proliferation rate of fibrosarcomas (Mizushima et al., 2002), as has exogenous exposure of LM-332 to kidney epithelial cells and mesenchymal stem cells (Hashimoto et al., 2006; Joly et al., 2006). The presence of the LG4 and LG5 domains within the pre-LMα3 chain seems to required for LM-332 mediation proliferation control, as expression of a construct coding for LMα3 lacking the G4-5 domains, LMα3ΔG45, in primary keratinocytes prevented cell proliferation and tumorigenicity in nude mice, whereas cells expressing the full length pre-LMα3 were hyper-proliferative and tumorigenic (Tran et al., 2008). Gonzales and colleagues

provided perhaps the best evidence that LM-332 is required for epithelial proliferation. They inhibited the cellular-LM-332 association through treatment with function blocking antibodies specific for the LMα3 globular domain in both MCF-10A mammary epithelial cells and 804G rat bladder carcinoma cells. Treatment with these antibodies resulted in decreased proliferation and downregulation of the ERK signaling pathway in both cells types (Gonzales et al., 1999). Despite an obvious role of LM-332 in proliferation regulation, the mechanism for this control is still largely unknown.

1.4.3 The LM-332 Integrin Receptors and Proliferation Regulation

The best-characterized LM-332 cellular receptors implicated in proliferation control are the integrins, α3β1 and α6β4. Integrin signaling is a complex topic, and the thorough discussion of which, is beyond the scope of this introduction (for a full review, see Giancotti and Tarone, Annu Rev Cell Dev Biol, 2003). On the most rudimentary level, integrins, upon binding to ligand, associate with elements of the cytoskeleton, and provide stable adhesions between the cell and the BM. A common phenotype associated with the inhibition of α3β1 and α6β4 binding to LM-332 is a loss of, or weakened cell adhesion. More specifically however, LM-332 binding to the α3β1 integrins induces conformational changes that transform the integrins into potent signaling molecules that regulate cellular adhesion, spreading, migration, proliferation, and apoptosis. The integrin α3β1 signals by recruiting adaptor proteins and kinases into physical structures called focal adhesions. Signaling from the kinases, such as Focal Adhesion Kinase (FAK) and Integrin Linked Kinase (Sonnenberg et al.) can then activate members of the Src Family Kinase (SFK) and Receptor Protein Tyrosine Kinase (RPTK) signaling pathways, ultimately regulating gene expression and cellular events (Giancotti and Tarone, 2003). The LM-332 receptor, integrin α6β4 is a unique integrin in that the β4 subunit has a long cytoplasmic

domain that contains many tyrosine phosphorylation sites that are phosphorylated upon ligand binding (Mainiero et al., 1997). The phosphorylated β4 subunit can then activate SFKs and the PI3K pathway (Dans et al., 2001; Shaw, 2001). In the case of α6β4 and probably α3β1, growth factor receptors are also activated following ligand binding through either direct interaction, or through SFK-mediated cross-talk (Alam et al., 2007; Giancotti and Tarone, 2003).

Both α3β1 and α6β4 integrins have been widely examined in formation of the epithelium and proliferation. Inhibition of either α3β1 and/or α6β4 integrins through function blocking antibodies prevents the closure of scrape wounds in mammary epithelial cells (Gonzales et al., 1999). The inhibition of α6β4 by truncation of the cytoplasmic domain of the β4 subunit in mouse primary keratinocytes prevents proliferation (Murgia et al., 1998; Nikolopoulos et al., 2005), inhibition or loss of α3β1 integrin prevents proliferation in mouse mammary epithelial cells, rat bladder epithelial cells, and keratinocytes (Gonzales et al., 1999; Li et al., 2005a), and inhibition or loss of β1 integrin promotes expression of the cell cycle inhibitor, p21 in mammary epithelial cells, and prevent proliferation in the mouse epidermis (Clarke et al., 1995; Li et al., 2005a). Despite the large number of studies that suggest a requirement for either α3β1 or α6β4 in epithelial proliferation, it is unclear to what extent these integrins are required for proliferation in tissues other than the epidermis, breast, or intestine. Additionally, in some studies, inhibition of β1 integrin resulted in proliferative arrest, and in others, β4 integrin had this effect. Reconciling the necessity for both integrins in proliferation control of other tissues, and understanding why these differences occur are therefore important issues.

1.4.4 The LM-332 Non-Integrin Receptors and Proliferation Regulation

LM-332 has other receptors within epithelial cells that may be important for proliferation. These are the syndecans and dystroglycan. Of the four syndecan family members, syndecan-1, -

2, and -4 are often found in epithelial cells. Syndecans, upon ligand binding, are thought to signal through their cytoplasmic domain by both coordination with growth factor receptors and activation of PKCα and PKCδ (Fears and Woods, 2006). Syndecan-1 interacts with the α3 chain within the LG4-5 domain, and syndecan-2 and -4 have been shown to interact with the LG4 domain (Okamoto et al., 2003; Utani et al., 2001). Expression of syndecan-1 is transiently increased in the epidermis following injury, and its inhibition delays wound repair *in vivo* likely because of a decrease in cellular proliferation (Elenius et al., 1991; Elenius et al., 2004; Ojeh et al., 2008). Furthermore, in the absence of syndecan-1, *in vivo* corneal wounds do not undergo a proliferative "burst" 24 hours after wounding (Stepp et al., 2002). Syndecan-4 protein expression is also increased during epidermal repair and is required for cellular migration in this process (Echtermeyer et al., 2001; Gallo et al., 1996; Lin et al., 2005; Midwood et al., 2004). The dystroglycan complex is best known for binding laminins-111, -211, and -511, but it is unclear if LM-332 also interacts with dystroglycan. The LMα3 chain contains a potential dystroglycan binding site within LG4-5, and the LMα3-containing LM-311 can interact with dystroglycan in lung epithelia (Jones et al., 2005; Suzuki et al., 2010), which suggests that the α3 chain in LM-332 may also bind to dystroglycan. It is also unclear to what extent a LM-332-dystroglycan interaction might regulate proliferation in epithelial cells. In *Xenopus* embryos, loss of dystroglycan resulted in a reduction of proliferation in pronephric cell progenitors (Bello et al., 2008), but suppression of α-dystroglycan had no affect on myoblast proliferation (Montanaro et al., 1999). There are indications that dystroglycan associates with signaling proteins that are involved in proliferation control. For example, in muscle cells, β-dystroglycan interacts with Grb-2 (Yang et al., 1995).

1.5 Anchorage Dependent Proliferation Control and Cell Cycle Regulation

1.5.1 Introduction

As previously stated, it has long been appreciated that cell-substratum interactions are required for growth, as cells in suspension fail to divide. This dependency is referred to as 'anchorage-dependent growth' (Assoian, 1997; Stoker et al., 1968). Fibroblasts have been the cell line of choice to study "anchorage dependent growth" because epithelial cells in suspension typically undergo apoptosis (Frisch and Francis, 1994). It is unclear to what extent epithelial cells use similar mechanisms to regulate proliferation. Fibroblasts and epithelial cells have some overlap in integrin receptors, specifically αvβ3 and α2β1. The epithelial integrins, α6β4 and α3β1 are not typically found in normal fibroblasts. Also, the matrix environment of fibroblasts is vastly different than epithelial cells. *In vivo,* fibroblasts secrete, attach to, and reside in the collagen I-rich connective tissue of the ECM, and not the laminin and collagen IV-rich BM, which underlies epithelia (Alberts, 2008). None-the-less, anchorage-dependent growth studies suggest that integrin signaling is required for proliferation, which has also been shown for epithelial cells, and therefore may provide useful clues pertaining to the potential mechanism used by LM-332 to regulate proliferation in epithelia.

1.5.2 The Cell Cycle

To understand how the LM-332-cellular interaction may regulate the cell cycle, it is first necessary to have an appreciation for the mechanisms of normal cell cycle progression. The cell cycle is the process by which the cell first grows, replicates DNA, and then divides into two cells. These stages are referred to as Gap 1 (G1), Synthesis (S), and Gap 2/Mitosis (G2/M) phases, respectively. The order of these phases is crucial, and the cell has devised ingenious mechanisms to ensure that one phase does not begin before the other is complete. Cell cycle

progression is regulated by three main mechanisms: expression of cyclins, heterodimerization of cyclins with kinases, known as cyclin-dependent kinases (cdks), and nuclear localization and activation of the cyclin/cdk complexes. The coordination of these events then culminates in the expression of proteins both required for the next stage of the cell cycle and for the nuclear export and/or degradation of proteins that were used in the previous stage. Both studies in which LM-332 or the integrin receptors were inhibited in epithelial cells, and studies in suspended cells, suggest that cell-substratum interaction is required for G1 progression to S phase (D'Amico et al., 2000; Gonzales et al., 1999; Guadagno et al., 1993; Li et al., 2005a; Murgia et al., 1998; Nikolopoulos et al., 2005; Raghavan et al., 2000; Zhao et al., 2001; Zhu et al., 1996), therefore, a presentation of the regulation of G1 phase will be presented in the following section.

1.5.3 Cell Cycle Progression to S Phase

Quiescent epithelial cells, such as those in a confluent epithelium, are growth arrested in a cell cycle phase referred to as G0. Within G0, cyclin proteins are not expressed. Cells exit G0 upon an influx of cell signaling events, which result in expression of the G1 cyclin, cyclin D1 (Figure 1.5). Specifically, cyclin D1 mRNA and protein expression can be activated by GF signaling, such as through EGFR or PDGF (Pennock and Wang, 2003; Weber et al., 1997a; Weber et al., 1997b). Signaling through these proteins can activate mediators such as the Rho-GTPases and members of the MAPK pathway, particularly ERK and JNK (Meloche and Pouyssegur, 2007; Weber et al., 1997a; Weber et al., 1997b). These pathways culminate in the activation of transcription factors, which bind to the cyclin D1 promoter, and activate its transcription (Karin, 1995; Shaulian and Karin, 2001; Shaulian and Karin, 2002). Cyclin D1 protein then interacts with its cdk partners, cdk4 or cdk6 in the cytoplasm, inducing a partial conformational change within the cdk4/6, which is prerequisite for phosphorylation and

activation of the complex. Specifically, based on structural studies of the similar cdk2 protein, cdk4/6 interaction with cyclin D1 is thought to reveal the substrate-binding site, a threonine residue, and reorients several side chains that lead to the correct positioning of the ATP phosphates that are required for a phosphotransfer reaction (Jeffrey et al., 1995; Morgan, 1997). The cyclin D1/cdk4/6 complex is then transported into the nucleus. Neither cyclin D1 nor cdk4/6 contain a nuclear localization sequence (NLS) (Yang and Kornbluth, 1999), evidence suggests, however, that the complex "piggybacks" into the nucleus by binding to proteins that do contain a NLS (Alt et al., 2002; Diehl and Sherr, 1997).

Once in the nucleus, cdk4/6 is phosphorylated at the exposed threonine residue by cdk-activating kinase (CAK), activating the cdk. The cdk4/6 kinase then phosphorylates and inactivates the retinoblastoma protein (RB). Phosphorylation of RB is a major point of regulation within G1 phase of the cell cycle. In quiescent cells, RB is hypophosphorylated and bound to the E2F family of transcription factors. Hypo-phosphorylated RB is found in two distinct E2F repressional complexes. The first contains histone deacetylase (HDAC) and SWI/SNF, and the second contains only SWI/SNF (Brehm et al., 1998; Zhang et al., 2000). RB contains sixteen Ser/Thr-Pro phosphorylation sites, which are phosphorylated by different cyclin/cdk complexes. When cyclin D1/cdk4/6 phosphorylates RB, RB is dissociated from HDAC, and the E2F transcription factor is activated sufficiently to promote transcription of the second G1 cyclin, cyclin E (Brehm et al., 1998; Zhang et al., 2000). Cyclin E differs somewhat from cyclin D1 in that it contains a NLS, and that, upon binding to its cdk partner, cdk2, the complex is transported directly into the nucleus (Moore et al., 1999), where cdk2 is activated similarly to cdk4/6. The cyclin E/cdk2 complex then further phosphorylates RB, disrupting the remaining RB/SWI/SNF/E2F complex, and freeing E2F to activate the expression of genes required for S

phase entry, particularly the S phase cyclin, cyclin A (Zhang et al., 2000), whose expression is prerequisite for DNA replication.

At the end of G1 phase, it is important that cyclin D1 and cyclin E are rapidly removed from the nucleus and degraded. The consequence of continuous expression of these cyclins is unregulated cellular proliferation. For this reason, it is not surprising that high levels of cyclin D1 and cyclin E are often observed in malignancies (Diehl, 2002; Gong et al., 1994; Hwang and Clurman, 2005). The degradation of both cyclin D1 and cyclin E are triggered by phosphorylation events. Proteolysis of cyclin D1 is initiated when the protein is phosphorylated at Thr-286 by glycogen synthase kinase 3 beta (GSK3β) (Diehl et al., 1998). This phosphorylation recruits the nuclear exportin, CRM1, which shuttles cyclin D1 out of the nucleus (cyclin D1 does not have a nuclear export sequence). In the cytoplasm, phospho-cyclin D1 is ubiquitinated by the Skp-Cul1-F box (SCF) E3 ubiquitin ligase and is targeted for destruction (Gladden and Diehl, 2005; Lin et al., 2006). The mechanism of cyclin E degradation depends on whether the protein is monomeric, or in an active complex with cdk2. If cyclin E is monomeric, it is ubiquitinated and targeted for destruction by the E3 ubiquitin ligase, cullin-3 (Cul-3) (Singer et al., 1999). Degradation of cyclin E that is in an active complex with cdk2 however, is regulated by auto-phosphorylation from cdk2 at Thr-62, Thr-380, and Ser-384. Upon phosphorylation, the ubiquitin ligase, Fbw7 binds to cyclin E and promotes its degradation (Hwang and Clurman, 2005).

1.5.4 Cell Cycle Inhibition by Cyclin-Dependent Kinase Inhibitors (CKIs)

CKIs are potent inhibitors of cyclin/cdks and cell cycle progression, and loss of their expression is also commonly observed in human cancers. CKIs are comprised of two main families: INK4 and Cip/Kip. The INK4 family consists of four members, p15, p16, p18, and p19,

which are named based on their molecular weight. INK4 proteins bind directly to cdk4 or cdk6, which inhibit the kinase activity by causing a dissociation of the cyclin D1/cdk4/6 complex (Ragione et al., 1996). The regulation of INK4 protein expression varies by individual family member. INK4 protein, p16, for example can be regulated by the JunB component of the AP-1 transcription factor, which is normally activated under situations of cell stress, whereas the promoter of p18 is activated in response to E2F-1 binding and may represent a normal feedback mechanism to inhibit cyclin D1/cdk4/6 activity at the end of G1 phase (Pei and Xiong, 2005).

The Cip/Kip family, consisting of p21cip1/waf1, p27kip1, and p57kip2, has been connected with diverse functions that do not always result in cell cycle arrest (Besson et al., 2008; Pei and Xiong, 2005). For the purposes of this introduction, only the inhibitory functions of these proteins will be addressed. Different genes encode the three family members, and their sequences are divergent in all but their cyclin and cdk binding N-terminal domains. The signaling pathways regulating the expression of the Cip/Kip family are numerous and vary by protein and by cell type. In broad terms, the expression of p21waf1 is typically elevated following DNA damage, although it has also been observed in non-adherent cells (Bao et al., 2002; Zhu et al., 1996). Inhibitory protein p27kip1 levels are elevated in response to mitogen starvation and within the cellular quiescent state, and p57kip2 is an important regulator of the cell cycle during embryonic development. As cdk inhibitors, these proteins primarily inhibit cdk2 and cdk1 containing kinases. Cip/Kip proteins can bind to the cyclin or cdk alone, or to the cyclin/cdk complex, with the latter being thermodynamically favored. Structural analysis of the N-terminus of cyclin A in a complex with cdk2 and p27kip1 (amino acids 22-106) showed that p27kip1, and likely the other Cip/Kip family members, can inhibit the kinase activity of the complex by occluding the substrate interaction domain on the cyclin, and insert itself into the catalytic cleft of cdk2 (Russo et al., 1996).

1.5.5 Anchorage-dependent Cell Cycle Regulation

Studies in suspended cells, or cells in which some aspect of integrin-mediated signaling was inhibited, suggest two primary mechanisms for G1 proliferation control. First, fibroblasts in suspension do not express cyclin D1. The failure to induce cyclin D1 expression may be due to integrin signaling, as expression of a dominant negative Focal Adhesion Kinase (FAK) also prevented cyclin D1 expression (Zhao et al., 2001). Studies using the mammary epithelial cell line, MCF-7, also suggest that signaling through Integrin-Linked Kinase (ILK) is required for cyclin D1 expression (D'Amico et al., 2000). In both studies, although FAK and ILK are kinases associated with focal adhesions that are typically activated following adhesion, the actual requirement for integrin activation to mediate cyclin D1 expression was not examined. A second mechanism of G1 cell cycle arrest in suspended fibroblasts has also been identified. In these studies, in addition to reduced cyclin D1 mRNA and protein levels, the cyclin E/cdk2 complex was also inactivated by increased association with p21waf1 and p27kip1, and failed to phosphorylate RB, leading to a decrease in cyclin A expression and a failure to enter S phase (Guadagno et al., 1993; Zhu et al., 1996). Last, as discussed previously, inhibiting the $\alpha 3\beta 1$ interaction with LM-332 prevented proliferation and ERK phosphorylation in mammary and intestinal epithelial cells, but the impact on the cell cycle machinery was not examined.

Despite this information, much remains unknown as to the involvement of LM-332 for proliferation regulation. First, it is unknown if LM-332 is also required for G1 proliferation control of kidney epithelial cells. Second, in both the kidney epithelium, and within other epithelial cell types, it is unknown if the LM-332-interaction is required for cyclin D1 expression and/or cyclin E/cdk2 kinase activity. Last, since LM-332 binds to different integrin receptors, and the requirement for either $\alpha 3\beta 1$ or $\alpha 6\beta 4$ in proliferation control has often been

contradictory, it remains unclear which integrin receptor might bind to LM-332 to promote proliferation.

1.6 A Model for LM-332-mediated Proliferation Control to Re-form the Epithelium

Based on the studies presented in this chapter suggesting a requirement for LM-332 in proliferation control to re-form the epithelium, in conjunction with what is known about the requirement for the integrin receptors in proliferation control, the following model is proposed (Figure 1.5): MDCK cells, at subconfluence or following wounding, deposit the full-length LM-332. LM-332 binds to its integrin receptors, $\alpha3\beta1$ and $\alpha6\beta4$, initiating signaling cascades that promote the expression of cyclin D1, and the cell proliferates. If this interaction is inhibited, cyclin D1 will not be expressed, expression of the cell cycle inhibitory proteins p21waf1 and p27kip1 will increase and inhibit the activity of cyclin E/cdk2, preventing pRB phosphorylation and progression to S phase. Upon confluence, LM-332 will either be cleaved within the LM$\alpha3$ chain to the processed form, or LM-332 will no longer be expressed.

1.7 Summary and Hypothesis

Maintenance of normal tissue structure and function is dependent upon the complex functions of epithelial cells. It is, therefore essential that epithelia have tightly regulated mechanisms to repair epithelial injury. Upon epithelial injury, cells adjacent to the wound site secrete new extracellular matrix, migrate along the newly deposited matrix, and begin to proliferate to replace lost cells. Proliferation ceases upon re-formation of the epithelium.

LM-332 is BM protein of the laminin family that is required for formation of the epithelium and proliferation in many epithelial cell types. This protein interacts with the cell mainly through integrin receptors, $\alpha6\beta4$ and $\alpha3\beta1$, and much of its function is mediated through

integrin signaling. Indeed, α6β4 and α3β1 integrins are also required for formation of the epithelium and proliferation. The mechanism of LM-332-mediated proliferation control, however, is largely unknown; particularly which integrin receptors are utilized, and downstream, how the LM-332/integrin interaction may regulate the cell cycle machinery.

This work tested the hypothesis that **LM-332 regulates proliferation of MDCK epithelial cells through interaction with α6β4 and α3β1 integrins and subsequent signaling to G1 cell cycle regulatory proteins.** To test this hypothesis: first, the proliferation mechanisms of normal MDCK cells were characterized during formation of the epithelium. Second, an shRNA specific for LMα3 was designed and characterized, and then used to determine the requirement and mechanism of LM-332 in MDCK proliferation control. Last, the specificity of this knockdown was analyzed, and the requirement for the integrin receptors was assessed.

Chapter 1 Figures

Figure 1.1 Re-formation of the Epithelium

The formation and maintenance of a continuous, polarized epithelium is critical for normal tissue functionality. The epithelium can be disrupted by cell-turnover, injury, and disease (1). Following disruption of the epithelium, new ECM is deposited at the wound edge, and cells at the leading edge extend protrusions and migrate onto the new matrix (2). After roughly 24 hours, cells at the wound edge begin to proliferate (3). The processes of matrix deposition, spreading, migration, and proliferation continue until cells re-establish cell-cell contacts and re-form a continuous monolayer (4).

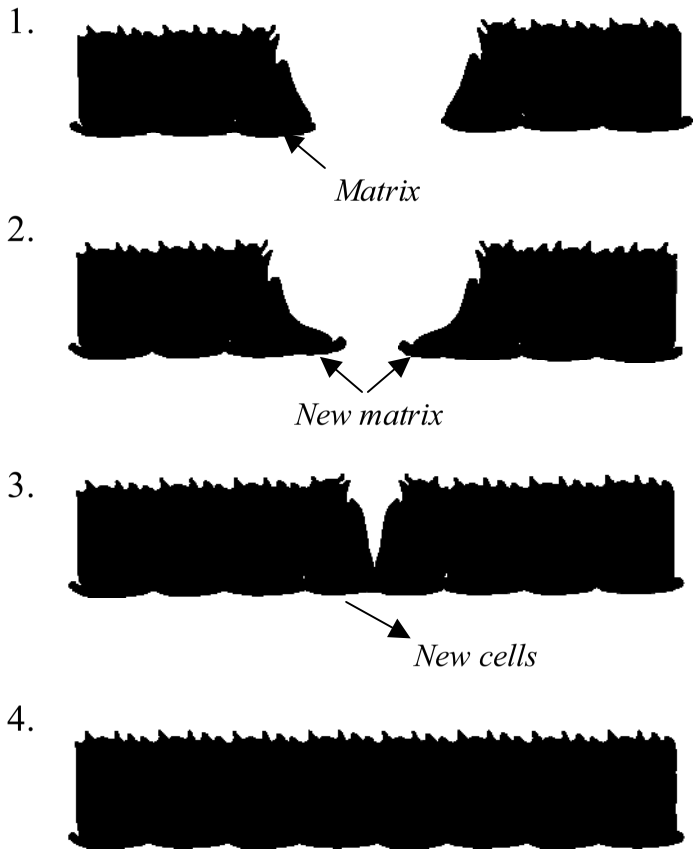

Epithelium is wounded

↓

Secretion of new matrix
and cellular migration

↓

Cellular proliferation

↓

Re-formed,
quiescent epithelium.

Figure 1.2 The Prototypical laminin

The prototypical laminins, -111, -211, -121, -221, -511, and -521, have a cruciform structure formed by coiled-coil interactions between domains I and II of the α, β, and γ chains. Domains III-VI of each chain make up the free arms of the heterotrimeric molecule. Laminin molecules polymerize with like laminins through α-α, β-β, and γ-γ interactions between domain VI, referred to as the LN module, of other laminin molecules. At the C-terminus of the α chain are the LG modules, which contains multiple cellular binding sites.

The α chain is depicted in black, the β chain in blue, and the γ chain in green.

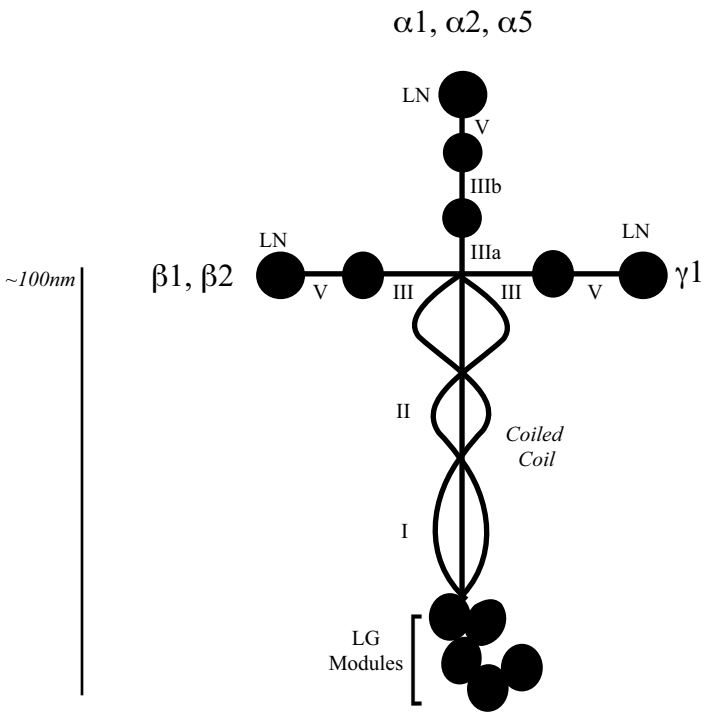
α1, α2, α5
LN
V
IIIb
LN
IIIa
LN
β1, β2
V
III
III
V
γ1
~100nm
II
Coiled
Coil
I
LG
Modules

Figure 1.3 Structure and Processing of Laminin-332

The structure of laminin-332 differs significantly from the prototypical laminins (compare to Figure 1.2). First, the laminin α3 chain is the only laminin chain to have variants, α3A and α3B, which arise from alternative splicing. Laminin α3A is truncated at domain III, whereas laminin α3B contains domains III-VI. Next, the β3, and γ2 chains, which are identical in laminin-3A32 and laminin-3B32, are truncated, which prevents polymerization of this laminin. The molecule can also be proteolytically processed within all chains. Select cleavage locations are depicted in the figure (see inset for γ2 cleavage sites). Cleavage of LNγ2 by MMP-3, MMP-12, MMP-13, and MMP-20 has also been described, but is not depicted (@ Remy, Cancer Res, 2006). Figure adapted from Miner and Yurchenco, 2004 and Marinkovich, 2007 (Marinkovich, 2007; Miner and Yurchenco, 2004).

Laminin-3A32

Laminin-3B32

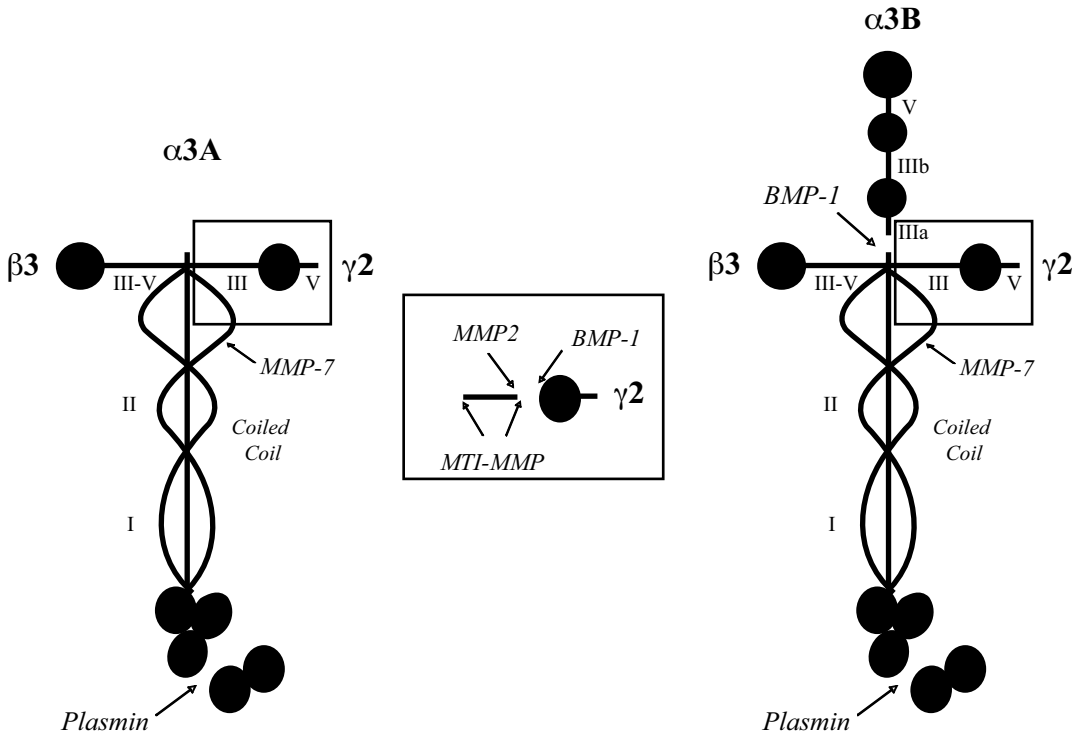

Figure 1.4 The G1 Cell Cycle Signaling Cascade

In proliferative cells, normal G1 cell cycle progression is initiated by membrane receptor activation (i.e. integrins or growth factor receptors), and subsequent activation of MAPK pathway signaling. The MAPKs, ERK1/2, p38, or JNK can activate transcription factors that lead to expression of the G1 cyclin, cyclin D1. Expression and activation of the G1 cyclin/cdk complexes, cyclin D1/cdk4 and cyclin E/cdk2 sequentially inactivate pRB, promoting expression of proteins required for S phase entry and progression.

First wave:

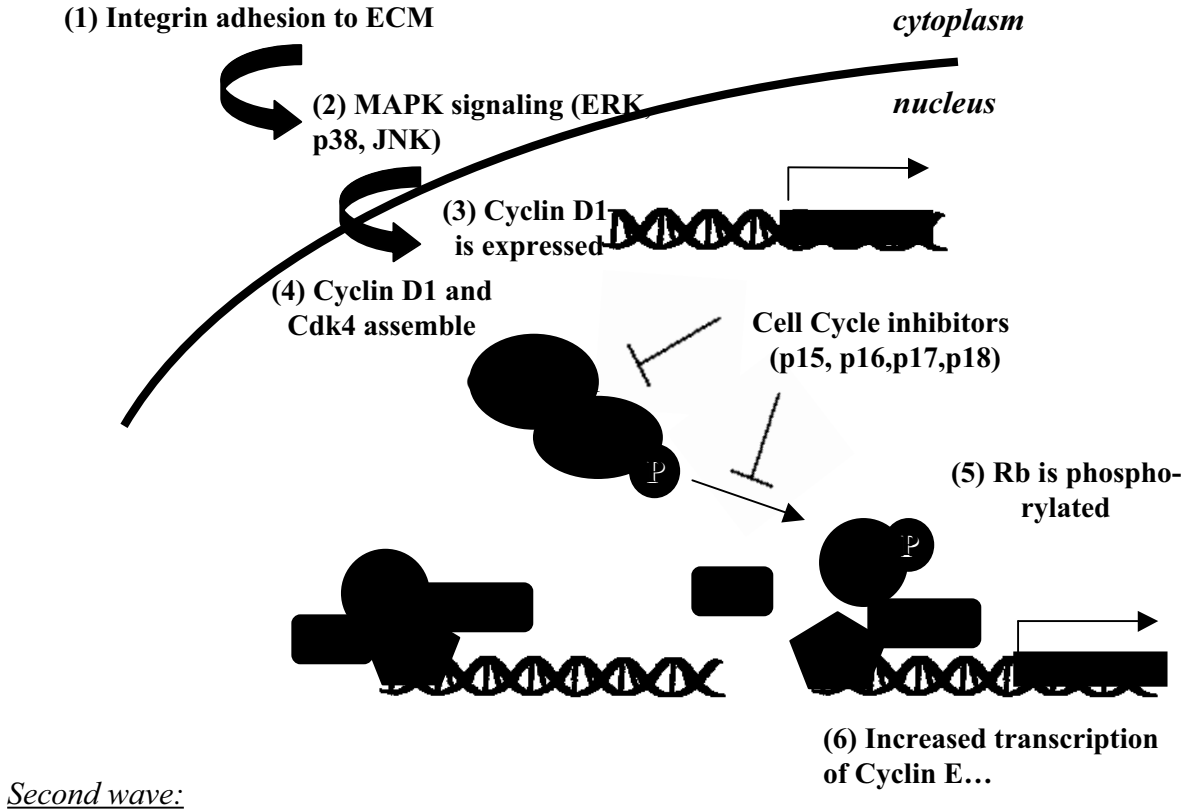

Second wave:

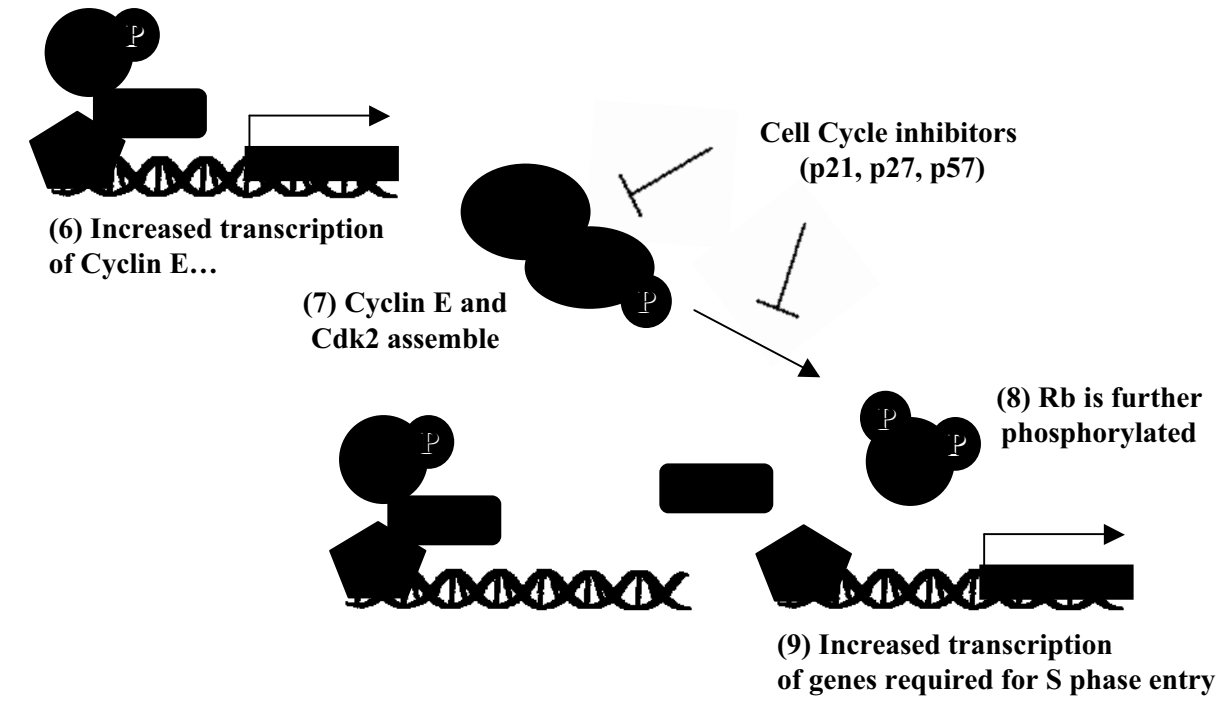

Figure 1.5: A Model for LM-332-mediated Proliferation Control to Re-form the Epithelium

(1) MDCK cells, at subconfluence or following wounding, deposit LM-332 containing the full-length LMα3 chain. LM-332 binds to its integrin receptors, α3β1 and α6β4, initiating signaling cascades that promote the expression of cyclin D1, and cell proliferates. (2) If the LM-332 interaction is inhibited or LM-332 is not expessed, cyclin D1 will not be expressed; expression of the cell cycle inhibitory proteins p21waf1 and p27kip1 will increase, and will inhibit the activity of cyclin E/cdk2, preventing pRB phosphorylation and progression to S phase. (3) Upon confluence, LM-332 will either be cleaved within the LMα3 chain to the processed form, or LM-332 will no longer be expressed.

1.

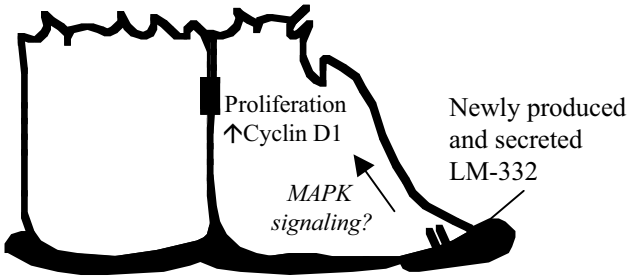

<u>Subconfluence and wounding</u>: Cell produces and secretes LM-322. Cells proliferate to re-form the epithelium.

2.

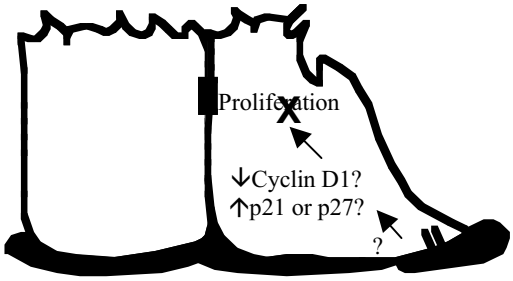

<u>Inhibition of LM-332</u>:In the absence of the LM-332-integrin interaction in a subconfluent epithelium, cyclin D1 will not be expressed and/or p21waf1 and/or p27kip1 will be expressed and inhibit cyclin E/cdk2. Proliferation will arrest.

3.

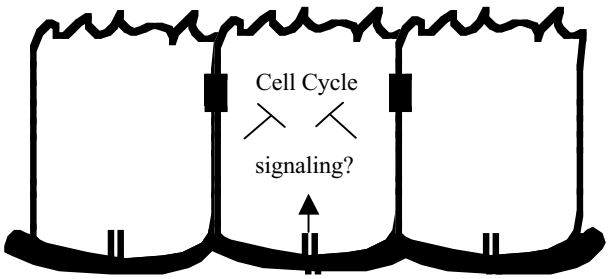

<u>Confluence</u>: LM-332 is no longer produced or secreted or LMα3 is processed. The epithelium is quiescent.

|| *Integrin α3β1 and/or α6β4*

▮ *Cell-Cell Contact*

Chapter 2:

Materials and Methods

GENERAL

2.1. Cell Culture

2.1.1 Cell Lines

Unless otherwise noted, cultures of MDCK cells (strain II, Heidelberg isolate, passages 7-35 (Matlin et al., 1981), were used in all studies. Cells were grown in high glucose DMEM (Gibco or Mediatech), supplemented with 5% fetal bovine serum (Mediatech), 10mM HEPES, pH7.3 (Fisher Scientific), and 2mM l-glutamine (Sigma) (Referred to as 'MDCK growth medium'), and incubated at 37°C in the presence of 5% CO_2. Stock cells were maintained in MDCK growth medium and were passaged 1:5 every three days.

Caco-2 cells (clone C2BBe, originally cloned by, and obtained from M. Mooseker, Yale University, passages 30-50 (Peterson et al., 1993; Peterson and Mooseker, 1992), which were derived from human colonic adenocarcinoma, but resemble intestinal epithelium, were used for select studies. Cells were grown in high glucose DMEM, supplemented with 10% fetal bovine serum, 10mM HEPES, pH7.3 (Fisher Scientific), and 2mM l-glutamine, and incubated at 37°C in the presence of 5% CO_2.

Human Embryonic Kidney (HEK) -293 adenoviral packaging cells were obtained from ATCC (CRL-1573) and were grown in high glucose DMEM, supplemented with 10% fetal

bovine serum, 10mM HEPES, pH7.3 and 2mM l-glutamine (Referred to as 'HEK growth medium'), and incubated at 37°C in the presence of 5% CO_2. Cells were kept at low passage (p6-13) and not allowed to reach a density greater than 90%.

All stock cells were maintained in polycarbonate tissue culture treated dishes (BD Falcon). For most experiments, cells were released from dishes by treatment with .05% trypsin-EDTA (Gibco or Mediatech), and seeded onto polycarbonate tissue culture treated dishes or glass coverslips (Bellco) at varying densities.

2.1.2 Plating Conditions for Time-course Experiments

MDCK stock cells, three days post-passage, were trypsinized, resuspended in MDCK growth medium and counted. For experiments using 35mm tissue culture dishes, .75x10^6 cells were plated. For 100mm tissue culture dishes, 8x10^6 cells were plated. Cells were allowed to grow for seven days, with time-points being harvested on days indicated by individual experiments. Cells were fed with fresh MDCK growth medium every two–to-three days.

2.1.3 Plating on Pre-coated Matrices

To generate endogenous matrix for Ad-shLMα3 rescue experiments, antibody perturbation experiments, and adhesion assays, 10^6 MDCK cells were plated into 35mm dishes or 25,000 cells were plate into 96 well plates and allowed to grow for two days. At this time, cells were 90-95% confluent. To remove the cells with minimal disturbance to the underlying matrix, cells were washed one time briefly with sterile de-ionized water, and then incubated in de-ionized water for 2 minutes. Water was then removed, and sterile 20mM NH_4OH was added for 5 minutes to lyse cells. The matrix was then washed three times with cold phosphate buffered saline (PBS-, '-' refers to PBS without added Mg^{++} or Ca^{++} ions). The matrix was then blocked

2hrs-overnight at 4°C in 1%BSA/PBS- to block non-specific binding sites. Prior to plating cells, plates were washed two more times with cold PBS-.

For rescue experiments and adhesion assays requiring collagen I coating, the day prior to the experiment, Type I Collagen prepared from rat-tail (Sigma-Aldrich) was diluted to a working stock concentration of 1 mg/ml in PBS-. Plates were then coated with 10μg/cm^2 of collagen. For 96 well plates, 3μg of collagen in 100μl was used, for 35mm dishes, ~100μg in 1.2ml was used. After adding collagen, plates were incubated at 37°C for two hours in the tissue culture incubator. Collagen solution was then aspirated, and plates were placed back at 37°C for 30 minutes. 1% BSA/PBS- was then added and plates were incubated from 2hrs-to-overnight at 4°C to block non-specific binding sites. Prior to plating cells, wells were washed two times with cold PBS-.

Bovine Serum Albumin (BSA) (Sigma-Aldrich) was dissolved in PBS- to generate a 5% stock solution. Solution was then spun for 20 minutes at 3500rpm, sterile filtered through a .22μm filter device, and stored in aliquots at -20°C. For BSA controls used in adhesion assays, a 1% BSA/PBS- solution was added to the appropriate wells of a 96 well plate at the same time as collagen I. The same incubation and blocking procedure was followed.

2.1.4 Treatment with JNK Inhibitor, SP600125

The inhibitor SP600125 was obtained in solution (50mM in DMSO) from Calbiochem (#420128). Stock solution was aliquoted and stored at -20°C. For experiments, SP600125 was further diluted into MDCK growth medium containing .3% DMSO (the manufacturer recommended adding .1% DMSO per 10μM of drug to enhance solubility), for a final concentration of SP600125 of 30μM. For DMSO control, and equal volume of DMSO was

added to a second set of samples. Cells were incubated with the drug for 16hrs, and then harvested for immunoblot.

2.2. Antibodies

2.2.1 Primary and Secondary Antibodies

Listed below are the antibodies used in the present studies. For primary antibodies, refer to individual experiments for concentration and application. For secondary antibodies, in immunoblot experiments, a concentration of 1:2500 was used, and for immunofluorescence, 1:500 was used.

Table 2.1: Primary Antibodies used in Present Studies

Specificity[1]	***Type***[2]	***Source***
Actin (Ck)	*Ms m*	*James Lessard*
Akt (ms)	*Rb p*	*Cell Signaling (9272)*
Akt (Ser473) (ms)	*Rb p*	*Cell Signaling (9271)*
BrdU	*Rt m*	*Abcam (ab6326)*
BrdU	*Ms m*	*Calbiochem (D36952)*
Cdk1/Cdc2 (hu)	*Rb p*	*BD Pharmingen (559800)*
Cdk1/Cdc2 (hu)	*Ms m*	*BD Transduction (610037)*
Cdk2 (hu)	*Ms m*	*BD Transduction (610145)*
Cdk4 (DCS156) (hu)	*Ms m*	*Cell Signaling (2906)*
Cdk4 (H22) (hu)	*Rb p*	*SCBT (sc601)*
Cyclin B1 (hu)	*Ms m*	*Stressgen (CC195)*
Cyclin B1 (hu)	*Rb p*	*SCBT (sc594)*
Cyclin D1 (DCS6) (hu)	*Ms m*	*Cell Signaling (2926)*
Cyclin D1 (hu)	*Rb p*	*Cell Signaling (2922)*
Cyclin E (M20)(rt)	*Rb p*	*SCBT (sc481)*
ERK1	*Rb p*	*SCBT (sc93)*
ERK2	*Rb p*	*SCBT (sc154)*
gp-135 (#3F21D8)	*Ms m*	*G. Ojakian, SUNY*
Integrin β1 (AIIB2) (ms)	*Rt m*	*Dev Studies Hybridoma Bank*
Integrin β1 (hu)[4]	*Rb p*	*Research Genetics*
Integrin β4 (hu)	*Gt p*	*SCBT (6628)*
Integrin α6 (GOH3)	*Rt m*	*BD Pharmingen (555734)*
JNK (hu)	*Rb p*	*SCBT (sc474)*
Laminin-332 (hu) (8LN5)	*Rb p*	*Manuel Koch*
Laminin-332 (hu) (9LN5)	*Rb p*	*Manuel Koch*
LMα3 (hu) (RG13)	*Ms m*	*Jonathan Jones*
LM-β3 (Kalinin B1) (hu)	*Ms m*	*BD Pharmingen (610423)*
LM-111 (hu)	*Rb p*	*Sigma*
p21waf1 (hu)	*Rb p*	*SCBT (sc397)*
p27kip1 (ms)	*Ms m*	*BD Transduction (25020)*
p38 MAPK	*Rb p*	*Cell Signaling (9212)*
Phospho- p42/44 MAPK	*Rb p*	*Cell Signaling (9101)*
Phospho-p38 MAPK	*Rb p*	*Cell Signaling (9211)*
PKCα (hu)	*Rb p*	*Cell Signaling (2056)*
SAPK/JNK (Thr183/Tyr185) (hu)	*Rb p*	*Cell Signaling (9251)*

1. Antibodies raised against proteins or peptides based on peptide sequences of human (hu), mouse (ms), rat (rt), or chicken (ck) origin.
2. Host species: rabbit (rb), mouse (ms), rat (rt), or goat (gt).
3. Antibody type: monoclonal (m) or polyclonal (p)
4. Integrin β1 antibody was prepared against a peptide from the carboxy-terminal 37 amino acids of the human integrin β1

Table 2.2 Secondary Antibodies used in Present Studies

Antibody	***Source***	***Application***
Donkey anti-MouseHRP	*Jackson Immunoresearch (715-035-151)*	*Immunoblot*
Donkey anti-RabbitHRP	*Jackson Immunoresearch (711-035-152)*	*Immunoblot*
Donkey anti-GoatHRP	*Jackson Immunoresearch (705-035-147)*	*Immunoblot*
Goat anti-Mouse AlexaFluor488	*Molecular Probes, Invitrogen (A11034)*	*IF*
Goat anti-Mouse AlexaFluor555	*Molecular Probes, Invitrogen (A21429)*	*IF*
Goat anti-Rabbit AlexaFluor488	*Molecular Probes, Invitrogen (A11034)*	*IF*
Goat anti-Rabbit AlexaFluor555	*Molecular Probes, Invitrogen (A21424)*	*IF*
Goat anti-Rat AlexaFluor488	*Molecular Probes, Invitrogen (A11006)*	*IF*
Goat anti-Rat AlexaFluor555	*Molecular Probes, Invitrogen (A21432)*	*IF*

2.2.2 Reviving AIIB2 Hybridomas and Subsequent Antibody Purification from Supernatant

The AIIB2 hybridoma cell line that secretes antibodies specific for β1 integrins, was obtained from the Developmental Studies Hybridoma Bank. To revive, cells were thawed quickly in a 37°C water bath and reconstituted in high glucose MEM, containing pyruvate, 10-20% FBS, Antibiotic/Antimycotic (Gibco), 1X OPI Supplement (Sigma), and 1X OptiMab (Gibco) (Referred to as "Hybridoma media"). Cells were maintained in Hybridoma media, and passaged every few days so that cells never reached high density. To collect supernatant, hybridoma suspensions were collected in tubes, and spun to separate the cellular contents from the medium, which contained the antibody. The medium was then removed from the pellet and stored at -20°C.

AIIB2 was purified from hybridoma supernatants via Fast Protein Liquid Chromatography (FPLC) (GE Healthcare $AKTA_{FPLC}$) using a HiTrap Protein G HP column (GE Healthcare), and Unicorn 5.1 (GE Healthcare) analysis software. Prior to subjecting samples to

FPLC, samples were first dialyzed overnight in 10,000 molecular weight cut-off (MWCO) dialysis tubing (Pierce) against column binding buffer (20mM sodium phosphate buffer, pH 7.0) to remove salts and adjust samples to the composition of the binding buffer. Samples were then passed through a .22μm filter to remove any remaining particulate material. The pump was filled with, and the column washed with binding buffer. The samples were then applied to the column. After all of the sample had passed through the column, the column was washed with binding buffer, and eluted with .1M glycine-HCl, pH 2.7 into collection tubes containing 1M Tris-HCl, pH 9.0. Purified antibodies were then removed from the appropriate collection tube, and dialyzed overnight in a 3,500 MWCO dialysis cassette (Pierce) against binding buffer to ensure a neutral pH of the final product. Concentrations of the antibodies were measured on the Nanodrop spectrophotometer (ThermoFisher). The final products were diluted 1:1 in sterile glycerol, and stored at -20°C.

2.2.3 Antibody-mediated Integrin Perturbation Experiments

For antibody perturbation experiments, two days prior to the experiment, MDCK stock cells were split 1:10 so as to be subconfluent on the day of the experiment. Cells were washed once with PBS-, and then removed from the plate with treatment of 4mM EDTA/1mM EGTA/PBS- for ~45 minutes. While cells were detaching, antibodies were diluted into 1ml MDCK growth medium containing 5% heat treated FBS at the following concentrations: AIIB2, 10μg/ml and GOH3, 5μg/ml. Additionally, 150μg/ml of H-Gly-Arg-Gly-Asp-Ser-Pro (GRGDSP) (Calbiochem, #03-34-0035) and Arg-Gly-Glu-Ser (RGES) (Sigma, #A5686) peptides were included. (Peptides were obtained as a powder and diluted in water to a stock concentration of .95mg/ml, ~pH7.0. After cells had detached, they were collected by centrifugation, and the pellet was resuspended in MDCK growth medium containing 5% heat-

treated FBS. Cells were counted and diluted to .25x10^6 cells/ml. 1ml of this suspension was added to tubes containing the antibodies, peptides, or medium alone (untreated control). Cells were incubated with antibodies and peptides for 30 minutes on ice, mixing by gentle agitation every 5-10 minutes. At the end of the incubation, cells were plated onto coverslips in 35mm dishes that were coated with MDCK endogenous matrix (see section 2.1.3). Cells were then allowed to grow for 17-19hrs, at which time they were harvested for experimentation.

2.3 Immunofluorescence

2.3.1 Indirect Immunofluorescence on Glass Coverslips

MDCK cells were plated onto glass coverslips at densities and conditions dictated by individual experiments. Upon harvest, coverslips were washed with PBS-, and cells were fixed in either 3% Paraformaldehyde (PFA) solution containing 10μM $CaCl_2$ and 10μM $MgCl_2$, and 1X PBS- for 20-30 minutes, 10 minutes in ice cold methanol (MeOH) at -20°C, or 5 minutes in ice cold acetone on ice, depending on the fixation requirements for particular antibodies. PFA fixed samples were then quenched for 10 minutes in 50mM NH_4Cl/PBS-, and then permeabilized in .1%Triton-X100/PBS- for 4 minutes. Regardless of fixation conditions, cells were then washed twice for 5 minutes with blocking buffer (.2% fish skin gelatin in PBS-), and twice for 5 minutes in PBS-. Primary antibody incubation was carried out in a moist chamber containing parafilm. Coverslips were inverted onto a 30-50μl drop of primary antibody diluted in blocking buffer and incubated in the moist chamber for 20-30 minutes at RT. Coverslips were then removed from the moist chamber and placed back in dishes. Blocking and wash steps were repeated as before. Secondary antibodies conjugated to fluorophores (Molecular Probes, Invitrogen) were also incubated in a moist chamber, as described above. When filamentous actin was stained, fluorescent phalloidin (Molecular Probes, AlexaFluor Phalloidin488, used at 1:100) was included

with the diluted secondary antibody. Blocking and wash steps were again repeated. Coverslips were then mounted onto a microscope slide containing one drop of Vectashield HardSet mounting medium with DAPI (Vector Laboratories). Mounting medium was given 15 minutes to initially set-up, coverslips were sealed with nail polish, and slides were placed at 4°C overnight to allow complete solidification of mounting medium. Slides were then viewed on a Zeiss Axioskop fluorescence microscope with a 63X, 1.4 numerical aperture (NA), PlanApo, or 40X 1.3 NA PlanNeofluor oil immersion objective and Nomarski optics, and imaged with an Axiocam MRm digital camera using AxioVision (Carl Zeiss) software. Images were optimized with Adobe Photoshop software (Adobe systems) using linear adjustment of levels, contrast, and brightness.

2.3.2 Indirect Immunofluorescence of MDCK cells Grown in Transwell chambers.

MDCK cells grown in Transwell chambers (2.4 cm diameter) were fixed for 30 minutes at room temperature with 3% PFA solution at room temperature, washed in PBS-, and quenched for 15 minutes with 0.1% $NaBH_4$/PBS- at room temperature with gentle shaking. Cells were then washed twice with PBS-, permeabilized with 0.1% Triton X100/PBS- for 4 minutes, and then washed again with PBS-. At this point, the filters were cut from their plastic support with a scalpel blade, transferred cell-side-up to individual 35 mm plastic Petri dishes, and blocked for 30 minutes at room temperature with 10% goat serum in PBS-. After aspiration of the blocking solution, the filters were cut into quarters for staining.

Antibody staining was conducted in a moist chamber at room temperature by placing filter quarters cell-side-up over 100µl droplets of diluted antibody on sheets of parafilm, and then gently covering the cell side with an additional 100µl of diluted antibody. The filters were then incubated with the antibody for 30 minutes at room temperature. Following primary antibody

incubation, filters were washed 4 times with PBS- for 5 minutes each in individual 35 mm dishes. Staining with secondary antibodies was conducted identically. When filamentous actin was stained, fluorescent phalloidin was included with the diluted secondary antibody.

After antibody staining, filter quarters were washed twice with PBS- for 5 minutes and twice with 0.1% Triton X100/PBS- for five minutes. They were then post-fixed with 3% PFA for 5 minutes and, finally, washed twice with PBS-. Filter pieces were mounted on glass slides in Vectashield HardSet mounting medium under a 22mm square coverslip supported by 4 hardened nail polish "feet", and edges sealed with additional nail polish. Stained filter quarters were imaged with a Zeiss LSM-510 confocal laser-scanning microscope in either the XY plane or as a Z-line orthogonal image using a 63X, 1.4 NA PlanApo oil immersion objective. For XY images, the optical slice was about 1.0μm with a frame size of 1024x1024 pixels. For Z-lines, the frame size was 2048x2048 pixels with a step size of 0.48μm. Images were again optimized with Adobe Photoshop software (Adobe systems) using linear adjustment of levels, contrast, and brightness.

2.4 Statistical Analysis

All statistical analysis (averages, standard deviation, and significance) were performed with Excel software (Microsoft Excel for Mac 2004, version 11.3.3). Statistical significance was determined by paired two-sample for means student's t-test, which generated a p-value based on two-tailed analysis.

2.5 Adhesion Assays

Prior to performing adhesion assays, plates coated with endogenous extracellular matrix proteins, collagen I or BSA were prepared as described in section 2.1.3. On the day of the experiment, prior to plating cells, plates were removed from 4°C, and washed 2X with PBS+ (PBS containing 1mM $CaCl_2$ and .5mM $MgCl_2$).

To prepare cells, MDCK cells were passaged 1:10 into 5- 10cm tissue culture dishes two days prior to experiments to yield subconfluent cultures on the day of the experiment. After two days, cells were washed 1X with PBS-, 1X with 4mM EDTA/1mM EGTA/PBS- solution, and then incubated for 40-50 minutes with 5ml of EDTA/EGTA solution to dissociate cells. Cells were recovered into a 50ml conical tube, spun down to pellet, resuspended in 4-6ml serum free SMEM, and counted. Cells were diluted to 4x10^6 cells/ml or 1x10^5 cells/25µl. All treatment parameters contained 4 wells. After plating, cells were given 60 minutes to attach by incubating at 37°C, 5% CO2. At the end of the incubation, the plate was carefully washed 2X with 100µl of .5% BSA/PBS+, then again with 100µl of PBS+. Cells were then fixed with 100% Methanol for 10 minutes at room temperature. Methanol was then flicked off, and plate was allowed to completely dry. While plate was drying, a .1% Crystal Violet solution was filtered through a .22µm filter. Once plate was dry, 100µl of freshly filtered Crystal Violet solution was added to each well and incubated for 5 minutes. Wells were then washed 4X with 200µl of sterile deionized water. Plate was again allowed to dry completely. 100µl of 1% sodium deoxycholate was then added, and incubated until the Crystal Violet dye was completely dissolved. Absorbance was then read at 590nm on a M5 plate reader (Molecular Devices). Raw data was imported into Excel, and background (from wells containing no cells) was subtracted. Absorbance readings from wells with like treatments was averaged, and graphed. Absorbance data from wells containing known plating or experimental errors were removed prior to analysis. Error bars represent the standard deviation between wells of like treatment.

2.6 Analysis of Cell Area

MDCK cells expressing siRNAs specific for LMα3 or controls (described in 2.19), were trypsinized and replated at low density on glass coverslips and incubated at 37°C, 5% CO_2

overnight. After incubation, cells were fixed with 3% PFA solution for 20 minutes, permeabilized with .1% triton X-100 in PBS- for 4 minutes, then blocked 2X with .2% fish skin gelatin/PBS- for 5 minutes, and washed 2X with PBS- for 5 minutes. The actin cytoskeleton was stained with Phalloidin AlexaFluor488 (Molecular Probes, Invitrogen) for 10 minutes in a moist chamber. Blocking and wash steps were repeated, and coverslips were mounted with Vectashield HardSet mounting medium containing DAPI. Cells were visualized on the Axioskop fluorescence microscope, described above, using the 63X objective. Total spread area was measured from digital micrographs using phalloidin staining, and the threshold setting in ImageJ analysis software. The software quantified cell area by measuring the number of pixels within the threshold. Cell number was determined by manually counting DAPI stained nuclei. Area per cell was determined by comparing the total cell area to total cell number.

2.7 Proliferation Assays

2.7.1 Bromodeoxyuridine (BrdU) Incorporation Assays

BrdU was obtained from Calbiochem, diluted to 5mM stocks in sterile ddH20, and stored in small aliquots at -20°C.

MDCK cells treated as described in individual experiments were plated at low density (2.5x10^5 cells per 35mm dish) on glass coverslips and incubated at 37°C, 5% CO_2 overnight. The next day, roughly 17-19hrs after plating, a new 5mM BrdU stock vial was thawed, and added directly to tissue culture medium, for a final concentration of 50μM. Cells were incubated with BrdU for 6hrs. At the end of the labeling period, cells were washed 3X with PBS- at room temperature, and fixed for 30 minutes with 3% PFA at room temperature. Cells were then washed 2X with PBS- and quenched for 10 minutes with 50mM NH_4Cl/PBS-, quench solution. In experiments where antigens other than BrdU wished to be maintained, the blocking step

immediately followed quenching. In experiments where only BrdU incorporation wished to be observed, cells were treated with 2M HCl for 10 minutes at 37°C to denature DNA. At the end of incubation, samples were neutralized with borate buffer, pH 9.0 (.2M Sodium Tetraborate, .2M Boric Acid). Coverslips, regardless of procedure, were then washed 2X with PBS- and blocked and permeabilized with Blocking and Permeabilization (BP) buffer (5% goat serum, .1% Triton X-100, PBS-) for 30 minutes at room temperature. Coverslips were then washed 2X with PBS-. For experiments where cells were not previously treated with HCl to denature DNA, cells were stained in primary antibody solution containing DNase (10mM NaCl, 1mM $CaCl_2$, 6mM $MgCl_2$, .05U/μl DNase I (Roche), anti-BrdU primary antibody, an antibody against a second antigen, and BP buffer) for 1hr at 37°C in a moist chamber. For samples previously denatured, cells were stained with a primary antibody solution containing only anti-BrdU primary antibody diluted in BP buffer. These samples were also incubated with antibody solution for 1hr at 37°C. After primary antibody incubation, samples were treated the same regardless of how DNA was denatured. After staining, coverslips were transferred from the moist chamber to dishes and washed 4X, 5 minutes each with PBS-/0.1% TritonX-100. Secondary antibodies specific for the species of origin of the primary antibody(ies), which were coupled to fluorophores, were diluted in BP buffer. Coverslips were transferred back to a moist chamber, and inverted onto 50μl droplets of secondary antibodies. Samples were incubated with secondary antibody solution for 30 minutes at room temperature, protected from light. Following staining, wash steps were repeated. Coverslips were then mounted onto coverslips with HardSet mounting medium containing DAPI. Cells were observed on the AxioSkop fluorescent microscope using the 40X 1.3 NA PlanNeofluor oil immersion objective. Enough images were taken so as to obtain a minimum of 1000 cells per treatment group. To quantify total nuclei, DAPI stained nuclei were counted manually by opening images in Photoshop and placing dots on each nuclei to indicate

that it had been counted. BrdU staining was quantified similarly. Counts were then analyzed for percent of BrdU incorporation by dividing the number of BrdU positive cells by the total number of nuclei. Results were graphed in Excel, either as a percentage of BrdU incorporated, or as a fold change compared to untreated controls.

2.7.2 FACS Analysis

MDCK cells, treated as described in individual experiments, were washed 1X with PBS-, then incubated for 5 minutes in 4mM EDTA/1mM EGTA/PBS- for 5 minutes, then trypsinized with .05% Trypsin/EDTA for 30 minutes to create a single cell suspension. Trypsinization was stopped by the addition of MDCK growth medium. Cell suspension was then pelleted by centrifugation, resuspended in 5ml MDCK growth medium, and counted. 1-2x10^6 cells, depending on the experiment, were then removed and placed in a new 15ml conical tube. Cells were again pelleted by centrifugation, and washed 1X with PBS-. Following the wash, cells were resuspended in 500µl of PBS-. Meanwhile, 15ml conical tubes were prepared with ice cold ethanol. With a vortex set on '2', cell suspension was added slowly, dropwise, into the ethanol, for a final ethanol concentration of 70%. Cell/ethanol suspension was then placed at -20°C for a minimum of 24hrs for fixation. After fixation, cells were pelleted by centrifugation, ethanol was removed, and cells were washed with 1ml PBS-. Cell suspension was then transferred to a 1.5ml eppendorf tube, and spun at 5-14krpm to recover cells. Cells were then resuspended in 1ml of 1X propidium iodide (PI) stain (.1% Triton/PBS-, .2mg/ml RNaseA (Qiagen), .02mg/ml Propidium Iodide), and incubated at room temperature. In some cases, cells could not be recovered from PBS- after fixation. In this scenario, Triton X-100, RNaseA, and Propidium Iodide were added directly to the PBS- to yield the appropriate final concentration. This practice had no affect on sample quality or data. Following PI staining, flow cytometric analysis was performed on the BD

LSR II, in early experiments, and the BD FACScan in later experiments. All samples were read with a low flow rate, a threshold of 52, Linear amp gain for forward side scatter (FSC) and side scatter (SSC), and the DDM set for FL2, which reads total area fluorescence. In each experiment, voltages were set so that the G0/G1 peak was at a value of 200 on the FL2-H parameter. Acquisition and Storage were set so that 10,000 events were counted in the single cell gate. Data were analyzed using FlowJo software (Tree Star, Inc), specifically using the algorithm described by Watson, *et al* (Watson et al., 1987).

2.7.3 Counting

MDCK cells were plated as described in section 2.1.2. Each day, cells were washed one time with PBS-, then trypsinized with .05% Trypsin/EDTA for 15-40 minutes (cells took longer to trypsinize after the epithelium had formed). Trypsinization was stopped by the addition of 7ml MDCK growth medium. Cells were then collected and resuspended in 10-15ml of MDCK growth medium. Cells were then counted from eight different quadrants on a hemacytometer. Quadrants were then averaged and plotted on a line-graph in Excel.

2.7.4 Click-iT 5-ethynyl-2'-deoxyuridine (EdU) Incorporation Assay

The Click-iT EdU incorporation assay components were obtained as a kit from the Invitrogen corporation (Product #C10214). This protocol was optimized for our system based on the manufacture's protocol. To measure proliferation of MDCK cells co-expressing human LMα3 (see section 2.17) and the shRNA specific for LMα3 (see section 2.18), 8,300 cells, at the replating step, were plated into a 96 well black, clear bottom tissue culture plate (Greiner, Product #655090). Extra wells of non-infected controls were included as a "no EdU control". The next day, 30μM of the nucleoside analog EdU was diluted into MDCK growth medium

containing Hygromycin. A final volume of 100µl was added to each well. Cells were incubated with EdU for 6hrs. Cells were then washed with 200µl PBS-. 50µl of fixative solution was then added and incubated for 5 minutes. After incubation, 50µl of Click-it Reaction Cocktail was added directly to the fixative. The mixture was then incubated with gentle agitation for 25 minutes, protected from light. Cells were then washed two times with 200µl of Blocking Buffer. 50µl of Anti-Oregon GreenHRP antibody (1:400) was then added to cells and incubated for 30 minutes protected from light. Cells were then washed twice with 200µl Amplex UltraRed Buffer. Cells were then incubated with 100µl of Amplex UltraRed reaction mixture for 15 minutes on rotator protected from light. The reaction was stopped with the addition of Amplex UltraRed stop solution. The plate was read on a M5 plate reader (Molecuar Devices) for excitation/emission 568nm and 585nm. Readings from the "No EdU" control were also included to control for background fluorescence. Readings from all wells of each parameter were averaged and plotted in Excel.

BIOCHEMICAL METHODS

2.8 Extraction Methods

Table 2.3 depicts the extraction methods used in the present studies.

Table 2.3: Extraction Methods used in Present Studies:

Buffer	Assay	Components	Additives
SDS Buffer	Immunoblot	50mM Tris-HCl, pH 8.8 2% (w/v) SDS 5mM EDTA	a) 1X Complete Phosphatase inhibitor cocktail (Sigma) b) 1X Complete Protease inhibitor cocktail (Roche)

Buffer	Assay	Components	Additives
Radio-immunoprecipitation Assay (RIPA) Buffer	IP Immunoblot	10mM Tris-Cl, pH 7.5 0.5% (w/v) SDS 1.0% (w/v) IGEPAL .15M NaCl	a) 1X Complete Phosphatase inhibitor cocktail (Sigma) b) 1X Complete Protease inhibitor cocktail (Roche) c) 1.0% (w/v) Sodium Deoxycholate
Cdk4 Kinase Assay Buffer	Cdk4 kinase assay	50mM Hepes, pH 7.5 150mM NaCl 2.5mM EGTA 1mM EDTA 0.1% (w/v) Tween 20 10% (w/v) Glycerol	a) 1X Complete protease inhibitor cocktail, EDTA free (Roche) b) .1mM phenylmethylsulphonyl fluoride (PMSF) c) 1mM Dithiothreitol (DTT) d) 10mM β-glycerophosphate (βGPP) e) 1mM Sodium Fluoride f) .1mM Sodium Orthovanadate
Cdk4 Kinase Assay Buffer	Cdk2 kinase assay	10mM Tris-HCl, pH 7.5 5mM EDTA 130mM NaCl 1.0% Triton X-100	a) 1X Complete protease inhibitor cocktail, EDTA free (Roche) b) 1X Complete Protease inhibitor cocktail (Roche) c) 1mM DTT
Rho-binding Lysis Buffer	MAPK signaling immunoblots	50mM Tris, pH 7.2 500mM NaCl 10mM $MgCl_2$ 1.0% (v/v) TritonX-100 0.1% (w/v) SDS	a) 1X Complete protease inhibitor cocktail, EDTA free (Roche) b) 40mM βGPP c) 50mM NaF d) 1mM PNPP e) 0.5%Sodium Deoxycholate

2.8.1 SDS-Gel Electrophoresis and Immunoblotting:

Polyacrylamide gels were prepared in the Mini-Protean II apparatus (Bio-Rad). "Running" gels contained 5-15% polyacrylamide, 0.16-0.4% bis-acrylamide, 37.5mM Tris-Cl, pH 8.8, 1% ammonium persulfate (APS), and .05% Temed, and "stacking" gels contained 5% polyacrylamide, .13% bis-acrylamide, 125mM Tris-Cl, pH 6.8, 1% APS, and .05% Temed.

Cell cultures were extracted directly with either SDS extraction or RIPA buffer. For SDS extraction, cells were washed 2X with cold PBS-. One sample at a time, SDS extraction buffer was added to wells, and dish was immediately scraped with a rubber policeman. The lysate was collected with a 22- or 25-gauge needle, placed into a sterile 1.5ml microcentrifuge tube, and sheered with the needle. Sample was then immediately boiled for 3 minutes. Once all samples had been sheered and boiled, the BCA Protein assay (Pierce) was performed to assess protein concentration. In most experiments, lysates were then normalized. Lysates were then mixed with sample buffer to achieve a final concentration of 40% sucrose/5mM DTT/.08% Bromophenol Blue (BPB), and again boiled for 3 minutes. Samples were then permitted 5 minutes to cool. 4mM iodoacetamide (IAA) was then added and samples were alkylated at 37°C for 15 minutes. Samples were then spun to recover contents and 10-20μg of total protein was loaded onto a polyacrylamide gel. For RIPA buffer extraction, cells were washed 2X with cold PBS-, then incubated with .75-1ml of cold RIPA, on ice, for 15minutes, with agitation. After incubation, wells were scraped with a rubber policeman, collected with a 22- or 25-gauge needle, placed into a sterile 1.5ml microcentrifuge tube, and sheered with the needle. The BCA protein assay was performed to determine protein concentration. In most experiments, lysates were normalized. A sample buffer was then mixed with lysates (final concentration, 40% sucrose, 5mM DTT, 2% SDS, and .08% BPB), and samples were boiled 3-5 minutes. Samples were then alklyated and loaded onto a polyacrylamide gel as describe above. An electrode buffer (50mM Tris base,

400mM glycine, and .1% SDS) was added to gel apparatus, and 200V were applied. Gels ran for varying lengths of time, depending on the experiment. Gels were then transferred onto polyvinylidene difluoride (PVDF) membranes using a Semi-dry transfer apparatus (Bio-Rad). Following transfer, membranes were blocked 1hr to overnight in 5% Milk/Tris Buffered Saline with Tween (TBST) or 5% BSA/TBST. Membranes were then incubated with a primary antibody solution for 1hr-overnight, depending on the antibody. Membranes were then washed 4X with TBST, then incubated for 1hr at RT with either a secondary antibody coupled to horseradish peroxidase (HRP). Wash steps were repeated. Membranes were then incubated with ImmunoStar Chemiluminescent reagent (Bio-Rad) for 2-5 minutes. Membranes were then exposed to x-ray film and developed. Films were then scanned at a minimum of 600 dpi resolution. Image optimization was performed using Photoshop software. When detection of a second antigen, such as actin, was desired, after membrane was treated with chemiluminescent reagent and developed, the membrane was "stripped" to detach primary antibodies from the membrane. Briefly, Stripping Buffer (2% SDS, 62.5mM Tris-Cl, pH 6.7, 100mM β-mercaptoethanol) was added to membranes in plastic bags. Bags were incubated in 50°C water bath for 30 minutes. Membrane was then removed, and washed 3X quick, and 3X 10 minutes in TBST. After washes, the immunoblotting procedure was repeated starting at the blocking step. Primary antibody detection was then repeated using the desired antibody.

2.8.2.Extracting MDCK Endogenous Matrix for Immunoblot Analysis

10^6 MDCK cells were plated into 35mm tissue culture dishes and allowed to grow for two days. To remove the cells with minimal disturbance to the underlying matrix, cells were washed one time briefly with deionized water, and then incubated in deionized water for 2 minutes. Water was removed, and 20mM NH_4OH was added for 5 minutes to lyse cells.

Remaining matrix was then washed 2 times with cold PBS-. Extraction using SDS extraction buffer then proceeded as above, followed by immunoblot analysis.

2.8.3 Densitometry

Densitometric analysis was performed using Quantity One software (Bio-Rad). Images of scanned films, previously saved as .tiff files were opened in the software. Bands and background area were selected using the 'Volume Rectangle Tool', a volume analysis report was then generated, which measured the density (intensity/mm^2) of each selected area. Data were then exported to Excel. Background density was subtracted from each band reading. This value was then normalized to the density of the corresponding actin band. Data from each experiment were then combined and averaged. Error bars represent the standard deviation. Statistical significance was determined by two-tailed Student's t-test

2.8.4 Blocking Peptides

In immunoblotting and immunofluorescence experiments where specificity of the primary antibody was in question, particularly, p21waf1 and Cyclin E experiments, a primary antibody solution was made exactly as described above in two separate tubes. To the second tube, the blocking peptide was added at a concentration double that of the primary antibody. The primary antibody/blocking peptide solution was then incubated for 1hr with rotation. After the incubation, the membrane or coverslip was incubated with both solutions in the exact manner as is typical for primary antibody incubation. Immunoblotting and immunofluorescence experiments then proceeded as described above.

2.9 Immunoprecipitation

Cells were plated at a density of 3.5-8.0x10^5 cells/cm^2 24hrs prior to harvest. To harvest, cells were washed 2X with ice cold PBS-. Cells were extracted by adding 0.5-1.0ml cold RIPA buffer and incubated for 15 minutes, on ice, with agitation. Dishes were then scraped with a rubber policeman and lysate was transferred to a 1.5ml microcentrifuge tube. Samples were briefly vortexed, then spun for 10 minutes at 14 krpm at 4°C. Supernatant was then transferred to a centrifugal filter unit, and spun again to filter at 2 krpm, for 5 minutes. Protein concentrations of the lysates were then determined by the BCA Protein Assay. Samples were normalized, and 1-5μg of primary antibody was added to the lysate. Samples were incubated from 2hrs-24hrs, depending on the primary antibody, with rotation at 4°C. 30μl of Protein A or Protein G beads (Pierce) that were pre-washed 3X in RIPA buffer, and the beads reconstituted at a 1:1 ratio with RIPA buffer, were added to the lysate/primary antibody mixture. Beads were incubated for 1-2hrs at 4°C with rotation. The slurry was then pelleted by centrifugation. The supernatant was removed and either re-probed with a different primary antibody, or discarded. The beads were washed 3X with cold RIPA buffer, and one time with 10mM Tris-Cl, pH 8.6. Immunoprecipitated proteins were then solubilized from the beads and reduced by adding SDS-gel sample buffer (0.16M Tris-Cl, pH 8.8, 4mM EDTA, 16% sucrose, 0.16% BPB, 20mM DTT, and 2% SDS), and boiling for 3-5 minutes. Samples were then alklyated with 4mM IAA, and SDS-PAGE, and immunoblotting were performed. When complex detection was desired, after membrane was treated with chemiluminescent reagent and developed, the membrane was "stripped" and primary antibody detection was then repeated using a primary antibody directed against the second complex protein.

2.10 Metabolic Labeling

MDCK cells or Caco-2 cells prepared as described in individual experiments were radiolabeled with ^{35}S Methionine/Cysteine as either a pulse label (less than 30 minutes), short-term label (4h), or long-term label (18-24hrs). For both pulse and short-term labeling, cells grown in either 35mm or 60mm dishes at a density of 6.0-8.0x10^5 cells/cm^2. Prior to label, cells were incubated for 15 minutes in serum-free MDCK growth medium lacking methionine and cysteine (referred to as "Labeling medium") at 37°C, 5% CO_2 to deplete amino acid pools. At the end of the incubation, Labeling medium containing 50μCi/ml ^{35}S Methionine/Cysteine (Perkin-Elmer) was added to cells. Cells were then placed back at 37°C, 5% CO_2, for required labeling period. For long-term labeling experiments, cells were incubated directly, with no amino acid depletion step, in MDCK growth medium containing .1X methionine/cysteine and 50μCi/ml ^{35}S Methionine/Cysteine. Cells were then placed at 37°C, 5% CO_2 for 18-24hrs. At the end of the labeling period, regardless of labeling duration, medium was removed from cells. Cells were extracted by adding 0.5-1.0ml ice cold RIPA buffer, then incubated for 15 minutes, on ice, with agitation. Dishes were then scraped with a rubber policeman and lysate transferred to a 1.5ml microcentrifuge tube. Samples were briefly vortexed, then spun for 10 minutes at 14 krpm at 4°C. Supernatant was then transferred to a centrifugal filter unit, and spun again to filter at 2 krpm, for 5 minutes. When necessary, protein concentration of the lysate was determined by the BCA Protein Assay. Samples were normalized, and 1-5μg of primary antibody was added to the lysate. Immunoprecipitation and sample prep then proceeded as described in sections 2.9 and 2.8, respectively. SDS-PAGE was then performed as described previously. Gels were then fixed in Destain solution (50% methanol, 10% acetic acid) for 10 minutes. To visualize precipitated proteins, gels were incubated with Enhance (Perkin-Elmer), dried, and exposed to x-ray film for

1-7days in a cassette, stored at -80°C. Films were then developed and scanned with a minimum resolution of 600 dpi.

2.11 Kinase Assays:

2.11.1 Cdk4 Kinase Assay

1.25x10^6 MDCK cells infected with adenovirus containing short-hairpin RNA sequences specific for canine LMα3, or short-hairpin RNA sequences specific for controls were plated in 60mm dishes and incubated at 37°C, 5% CO_2 for 18-24hrs. Cells were then washed 2X with 2ml PBS- on ice. 750µl Cdk4 lysis buffer was added to each plate and incubated on ice with rocking for 20 minutes. Plates were then scraped, lysates were collected into 1.5ml microcentrifuge tube, and tubes were placed on tube rotator for another 30 minutes at 4°C. Lysates were then spun at 14krpm for 7 minutes at 4°C, then filtered through centrifugal filter unit by spinning again at 2000rpm for 6 minutes at 4°C. To pre-saturate Protein A beads with primary antibody, 15µl of beads, pre-washed with Cdk4 lysis buffer, were placed in1.5ml microcentrifuge tubes, and 7.5µg of Rabbit anti-Cdk4 or IgG control, was added to bead bed. The bead and antibody slurry was then incubated 1-2hr on rotator at 4°C. While beads were incubating, lysates were pre-cleared by adding 15µl of pre-washed protein A beads to lysates with 2µl of 5% BSA and incubated for 30 minutes on rotator at 4°C. Lysates were then briefly spun to pellet beads. Lysates were removed from the tube and placed in the tubes containing the bead/primary antibody slurry. Samples were then incubated on tube rotator for 3-4 hrs, at 4°C. Beads were then washed 3X with 1ml complete Cdk4 lysis buffer, 1X with 1ml 50mM Hepes/1mM DTT, and 1X with 1ml of Rb kinase buffer (50mM Hepes, 10mM MgCl2, 5mM MnCl2, 1mM DTT). Beads were spun down one final time to remove all residual buffer. 50µl of Rb kinase buffer containing ^{32}PγATP (50mM Hepes, pH7.5, 10mM $MgCl_2$, 5mM $MnCl_2$, 1mM DTT, 0.1mM Sodium Orthovanadate, 1mM NaF, 10mM βGPP, 2.5mM EGTA, 0.2mg/ml BSA,

2μg purified C-terminal Rb protein (Cell Signaling Technology), 50μM ATP (Ambion), and 5μCi ^{32}PγATP-6000Ci/mmol (Perkin Elmer)) was added to each sample. Samples were then placed into a 30°C water bath and incubated 30 minutes with frequent agitation. 4X Sample buffer (100mM Tris-Cl, pH 6.8, 4% SDS, 20% glycerol, 200mM DTT, BPB) was then added to beads, and samples were boiled for 15 minutes to solubilize and reduce samples. Samples were allowed 5 minutes to cool, and then were loaded onto a 12% gel and subjected to SDS-PAGE as described previously. Gels were ran at 200V and stopped just prior to dye front running off. Gels were then transferred to PVDF membrane as described previously. Membrane was then wrapped in plastic and exposed to x-ray film for 4 days in a cassette, stored at -80°C. Films were then developed. As a control, membranes were then immunoblotted for total Cdk4 protein.

2.11.2 Cdk2 Kinase Assay

2.0x10^6 MDCK cells infected with adenovirus containing short-hairpin RNA sequences specific for canine LMα3, or short-hairpin RNA sequences specific for controls were plated in 10cm dishes and incubated at 37°C, 5% CO_2 for 18-24hrs. To harvest, cells were washed 2X with 2ml PBS- on ice. 1ml of Cdk2 lysis buffer was added, and plates were incubated on ice for 15 minutes with agitation. Plates were then scraped, and lysates placed into 1.5ml microcentrifuge tubes. Lysates were spun down at 14krpm for 6 minutes at 4°C. The resulting supernatant was placed in centrifugal filter unit, and spun to filter at 2000rpm for 5 minutes. Lysates and 15μl of protein A beads that had been pre-washed with Cdk2 lysis buffer, and 2μl of 5% BSA were added to new microcentrifuge tubes and samples were pre-cleared by rotating 30 minutes at 4°C. Meanwhile, to pre-saturate Protein A beads with primary antibody, 15μl of beads, pre-washed in Cdk2 wash buffer, were placed into microcentrifuge tubes. To beads in appropriately labeled tubes, 5μg of Rabbit anti-Cdk2 or Rabbit IgG was added and tubes were

placed on rotator at 4°C for 1-2hrs. In tubes containing the lysate/bead slurry, beads were spun down from lysates, at 14kpm, 4°C. Lysate was then added to tubes with beads and antibody and incubated for 2-3hrs with rotation at 4°C. Beads were then spun down briefly at RT and washes performed as follows: washes 1-2: Cdk2 buffer containing 500mM NaCl, washes 3-4: Cdk2 buffer containing 200mM NaCl, washes 5-6: Cdk2 buffer, and washes 7-8: Cdk2 Kinase buffer (25mM Tris-Cl, pH7.5, 10mM $MgCl_2$, 1mM DTT). After the last wash, beads were resuspended in 35µl "complete" Cdk2 kinase buffer (25mM Tris-Cl, pH7.5, 10mM $MgCl_2$, 1mM DTT, 1.5µg Histone H1 (Sigma-Aldrich), 150µM ATP (Ambion), and 25µCi ^{32}PγATP-6000Ci/mmol (Perkin Elmer)). Samples were then placed into a 30°C water bath and incubated 30 minutes with frequent agitation. 4X Sample buffer (100mM Tris-Cl, pH 6.8, 4% SDS, 20% glycerol, 200mM DTT, BPB) was then added to beads, and samples were boiled for 5 minutes to solubilize and reduce samples. Samples were allowed 5 minutes to cool, and then were loaded onto a 12% gel and subjected to SDS-PAGE as described previously. Gels were ran at 200V and stopped just prior to dye front running off. Gels were transferred to a PVDF membrane. Membrane was then wrapped in plastic and exposed to x-ray film for 2 days in a cassette, stored at -80°C. Films were then developed. As a control, membranes were immunoblotted for total Cdk2 protein.

DNA AND RNA METHODS

2.12 Polymerase Chain Reaction (PCR)

2.12.1 RNA Extraction and Reverse Transcriptase (RT) PCR

Total RNA was isolated from MDCK cells using the RNeasy kit. RNA was treated with DNase I (Invitrogen) to remove any remaining DNA. RT-PCR was performed using the Superscript III Reverse Transcriptase kit (Invitrogen) using the manufacturer's protocol. This kit uses primers against random hexomers, and 1.0µg of RNA per 20µl reaction. The reverse

transcriptase reaction was performed on a DNA Engine Dyad, Peltier ThermoCycler, using a 10 minute annealing step at 25°C, and a 50 minute reverse transcriptase reaction at 50°C. The resulting cDNA was then treated with RNaseH to remove any remaining RNA.

2.12.2 Conventional PCR Conditions and Primers

For amplification of both MDCK cDNA and plasmids, 1μg of DNA was amplified in 25-50μl reactions containing 1X AmpliTaq buffer, 1.5mM MgCl2, .5μM of each primer, and .2mM dNTPs, and .1U/μl AmpliTaq DNA Taq polymerase (Applied Biosystems). PCR reactions were performed in a DNA Engine Dyad, Peltier ThermoCycler (Bio-Rad) with conditions described in Table 2.4. The products were visualized by agarose gel electrophoresis with Sybr Safe (Invitrogen) or ethidium bromide, imaged on a Bio-Rad Gel-Doc, and analyzed with Quantity One software.

Table 2.4: PCR Primers and Conditions

Gene or Plasmid	**Sequence 5'→3'**	**PCR Conditions**
LMα3[1]	F- ACAGATGGAGAGGGAAACAAC R- ATTGCCTGCTTGGCTTGG	25°C x 10 min 42°C x 12 min 95°C x 10 min Cycle: 94°C x 20 sec 50°C x 45 sec 72°C x 30 sec For 30 Cycles 72°C x 7 min
LMα5[1]	F- GCGACAACTGCCTCCTCTAC R- CCAGGTGGTCCTGGGTATC	95°C x 2 min Cycle: 95°C x 1 min 50°C x 45 sec 72°C x 60 sec For 35 Cycles 72°C x 10 min
β-actin[2]	F- CAAAGCAACCGTGAGAAG R- CAGAGTCCATGACAATACCAG	25°C x 10 min 42°C x 12 min 95°C x 10 min Cycle: 94°C x 20 sec 50°C x 45 sec 72°C x 30 sec For 30 Cycles 72°C x 7 min
Adeno-X	F- TAGTGTGGCGGAAGTGTGATGTTGC R- CGCCCAGATCTTCGAGT	95°C x 6 min Cycle: 94°C x 2 min 94°C x 15 sec 68°C x 2 min For 25 Cycles 68°C x 3 min
pcDNA3.1*Hygro*	F- TAATACGACTCACTATAGGG R- TAGAAGGCACAGTCGAGG	95°C x 5 min Cycle: 94°C x 1 min 49°C x 45 sec 72°C x 60 sec For 35 Cycles 72°C x 10 min

[1] Primers based on the sequences of human transcripts
[2] Primers based on the sequences of canine transcripts

2.12.3 Quantitative Real-time Polymerase Chain Reaction (qPCR)

.2μg of cDNA prepared as described above, was mixed with SYBR Green 1X master mix (Qiagen), and 1X of primers specific for LAMA3 or LAMA5 (Quantitect primers from Qiagen, product #s QT01465975 and Q501450638, respectively) in a 50μl reaction. All samples were analyzed in triplicate. Serial dilutions of plasmids containing the LAMA3 or LAMA5 PCR products were also run to generate a standard curve by which to determine nanogram values of LMα3 or LMα5 mRNA. (Plasmids were generated by cloning the PCR products from LAMA3 and LAMA5 primers into the pCR2.1-TOPO vector within the TOPO-TA cloning system (Invitrogen, Kit #K4500-01)). qRT-PCR was performed on the DNA Engine Opticon II thermocycler (Bio-Rad), using the following program with the Opticon Monitor 2 software:

15 minutes x 95°C
Cycle: 15 seconds x 94°C
30 seconds x 55°C
40 seconds x 72°C
Read plate
For 34 Cycles
Melting curve, read each 1°C, hold 5 seconds

To analyze fluorescent output, the threshold (C(t)) was manually set at .1, which was within the linear range of the sigmoidal-shaped amplification curve for all samples and standards. A standard curve was generated within the software by comparing base-10 logarithm of the initial nanogram concentrations of the LAMA3 or LAMA5 plasmids to the C(t) values generated from these plasmids. The software automatically fit a linear line to these values and generated an equation in the form of y=mx+b, where m was the slope and b was the y-intercept. Nanogram quantities of each sample were then determined by fitting the C(t) values to the standard curve generated by the plasmids. The nanogram quantities for each sample were then averaged in Excel and plotted as a bar graph.

2.13 Human LMα3(hLMα3)-pcDNA3.1 Hygro and pcDNA3.1 Hygro

The hLMα3-pcDNA3.1 plasmid was obtained, on Whatman filter paper, from Jonathan Jones, Northwestern University. To recover the plasmid, a circle was cut around the plasmid, and the paper was placed in a microcentrifuge tube. 50µl of 10mM Tris, pH7.6 was added, and the tube was vortexed. After a 5 minute incubation, the tube was briefly centrifuged to recover contents. Concentration of the recovered plasmid were determined on a Nanodrop spectrophotometer. The pcDNA3.1Hygro empty vector was obtained from the Invitrogen Corporation.

2.14 Transformations and Plasmid Amplification

Plasmids were diluted to 10ng/µl in sterile ddH20. To transform DH5α competent *E. coli* (Invitrogen), bacteria were thawed gently on ice, and then 50µl was aliquoted into sterile 5 ml tubes. 10ng of plasmid was then swirled gently into bacteria and incubated on ice for 30 minutes. Samples were then heat shocked for 20 seconds in a 37°C water bath and placed immediately on ice. Pre-warmed sterile Luria Bertani (LB) broth was then added to each tube and incubated at 37°C for 1hr with gentle agitation. 20-200µl of transformed bacteria were then plated on LB Agar plates containing 100µg/ml ampicillin or 50µg/ml kanamycin. Bacteria grew overnight at 37°C. Resulting colonies were selected and grown up in 5ml LB broth mini-culture containing 100µg/ml ampicillin or 50µg/ml kanamycin, for 6-8hrs. 500µl of culture was saved as a glycerol stock, from the remainder, plasmid DNA was purified from the culture using the QIAPrep Spin Mini-prep kit (Qiagen). Plasmids were screened via PCR or restriction digest. A positive clone was selected, and a large bacterial culture was generated by adding 30µl of glycerol stock to 250ml of LB Broth containing 100µg/ml ampicillin or 50µg/ml kanamycin, and growing overnight with agitation. Plasmids were then purified from bacteria using the HiSpeed

Maxi kit (Qiagen). Concentrations were measured on a Nanodrop spectrophotometer (Thermo-Fisher), and plasmids were again confirmed to be correct by PCR and/or restriction digest.

2.15 Restriction Digests

For restriction digest of plasmid DNA from mini-cultures, 5μl of mini-prep product was digested, and for digestion of plasmid from overnight cultures, 1μg of plasmid was used. Reactions were carried out by incubation of DNA with 1X restriction enzyme buffer, 1X BSA, and 10U of restriction enzyme, for 2hrs at 37°C. The products were visualized by agarose gel electrophoresis with Sybr Safe, imaged on a Bio-Rad Gel-Doc, and analyzed with Quantity One software.

2.16 Transient Expression

2.16.1 Electroporation

A day before electroporation, MDCK cells were split 1:4 so that cells would be around 70% confluent and in the logarithmic phase of growth the following day. 1.0x10^6 cells were electroporated with 2μg of duplex siRNA or 4μg of plasmid, in suspension using the Lonza (formerly Amaxa) Nucleofection kit – L and the Nucleofector II electroporation system (Lonza). After electroporation, cells were plated in 35mm dishes, and incubated 24-48hrs prior to assaying. In experiments where subconfluent cellular conditions were required, cells were split 1:1 24 hours after electroporation, allowed to grow for another 24 hours, and then harvested for experimentation.

2.16.2 Lipofectamine 2000

The day prior to transfection, MDCK cells were plated in antibiotic free MDCK growth medium at high density into 35mm dishes, so that cells would be 90-95% confluent upon transfection. On the day of transfection, 4μg of plasmid DNA was diluted into OptiMEM I Reduced Serum Medium. This suspension was then added to Lipfectamine 2000 transfection reagent (Invitrogen), which was pre-diluted in OptiMEM. Lipofectamine 2000 reagent and DNA were then incubated for 20-30 minutes at RT to allow complexes of transfection reagent and DNA to form. The suspension was then slowly swirled into the growth medium of dishes containing MDCK cells. After 24hrs, medium was replaced new antibiotic free MDCK growth medium. After another 24hrs, cells were harvested for experimentation.

2.17 Stable Expression of hLMα3-pcDNA3.1Hygro and pcDNA3.1Hygro Vector

2.17.1 Calcium Phosphate Transfection

A day before transfection, MDCK cells were split 1:4 so that cells would be subconfluent and in the logarithmic phase of growth the following day. On the day of transfection, 20μg of hLMα3-pcDNA3.1Hygro and empty vector were incubated with sterile Hepes Buffered Saline (HBS) and 2M $CaCl_2$ for 30 minutes at RT, to generate a DNA/Ca^{2+} co-precipitate. Meanwhile, MDCK cells were trypsinized, counted, and resuspended to final concentration of .5-1.0x10^6 cells/ml. DNA co-precipitate was then added to 1ml of cell suspension in a 10cm plate, and incubated for 15-20 minutes. Antibiotic free MDCK growth medium supplemented with 200μM chloroquin and cell suspension was then added to the plate with the DNA/cell suspension, and incubated for 6hrs at 37°C, 5% CO_2. Cells were then "shocked" by adding 15% glycerol in HBS for exactly 1 minute. Cells were then promptly washed gently 2X with MDCK growth medium.

10ml of growth medium was then added, and cells were incubated at 37°C, 5% CO_2 for 2-3 days to allow culture to divide several times.

2.17.2 Selection of Resistant Clones and Generation of Stable Cell Lines

After performing the calcium phosphate transfection, transfected cells were trypsinized, spun, and diluted at very low density in MDCK growth medium containing 300μg/ml hygromycin (appropriate concentration of hygromycin was previously determined by performing a killing curve). Cells were then plated at very low density in 10cm dishes and allowed to grow until colony formation was apparent, typically 7-10 days. One plate was also prepared at higher density as a "pool". Once colonies were large enough, yet still well distinguished from other colonies, plates were washed carefully, 2X with PBS-. Sterile cloning cylinders were then placed around colonies, and 150μl of .05% trypsin/EDTA was added to the cylinder to lift the individual colony from the plate. 20-24 colonies were selected of hLMα3 and empty vector lines. Colonies were placed into 24 well plates containing MDCK growth medium with hygromycin. Once wells became confluent, generally another 5-7 days, individual wells were trypsinized and split 1:1, with half plated onto coverslips in 12 well plates for screening, and the other plated into 12 well plates to continue growing. Positive LMα3 clones were screened by immunofluorescence using the RG13 antibody, which detects human, but not canine LMα3. Empty vector clones were screened by harvesting RNA, generating cDNA, and performing PCR. Stable pools, and two clones each of hLMα3 expressing cells and empty vector were chosen based on expression levels.

RNAi AND ADENOVIRUS PRODUCTION

2.18 Adenovirus-mediated shRNA Suppression

2.18.1 Identification of shLMα3-D5 RNAi target sequences

RNAi target sequences used in the present studies are described in Table 2.5. To identify the shLMα3-D5 target sequence, the LAMA3 gene was first partially sequenced (University of Cincinnati College of Medicine Core Sequencing Facility) by using the LMα3 primers described in Table 2.4. Potential siRNA targets were identified in the sequence using the computerized algortithm provided at www.ambion.com (Ambion).

Table 2.5 siRNA and shRNA Target Sequences

Name	Sequence 5'→ 3'	Species of origin	Location in coding sequence[1]	Type
shLMα3-D5[2,3]	ATGACTACGAAGCCAAACT	Canine	1259-1278	Adenovirus-short hairpin (sh)
siLMα3-1	TCGTTCTGCCATTTCAAATCATG	Canine	804-826	RNA duplex-Small interfering (si)
siLMα3-2	ACGGAACCGCAACTTTGGAAAGC	Canine	1113-1135	RNA duplex (si)
siLMα3-3	CTCGAGAGACAAGTTAAAGAAAT	Canine	1369-1391	RNA duplex (si)
siLMα3-4	AGGGTTGATCGACACCAATATCA	Canine	1950-1972	RNA duplex (si)
siLMα3-5	AACCACCTTTCCTAATGTTGCTT	Canine	3962-3984	RNA duplex (si)
siLuc	GTGCGTTGCTAGTACCAAC	Firefly	276-294	RNA duplex (si)
shLacZ[4,5]	GCTACACAAATCAGCGATTT	E. coli	Unknown	Adenovirus-(sh)
shPKCα[4]	GCCTCCATTTGATGGTGAAGA	Human	1649-1669	Adenovirus-(sh)

[1]Location in coding sequence: Canine LMα3 targets were generated from Reference sequence AF236865.1, Firefly, from EU684088.1, and Human, from NM_002737.2.
[2]Referred to as Ad-D5 in early studies, and shLMα3 in later studies.
[3] shLMα3-D5 was originally designed as a RNA duplex, and later, the target sequence was used to generate a short hairpin RNA.
[4]Created and generously provided by Dr. Jun Tang, the University of Chicago
[5]LacZ control sequences were provided from the Block-It RNAi suppression kit (Invitrogen), and cloned into adenoviral plasmids by Dr. Tang.

2.18.2 Screening siLMα3 siRNA Duplexes for LMα3 Suppression

The target sequence identified in 2.18.1 was obtained as synthetic RNA molecules from the Ambion corporation and were annealed according to recommendations by the manufacturer. The duplex was referred to as siLMα3. The efficacy of the siLMα3 siRNA target sequence was

confirmed by transient transfection of RNA duplexes, into MDCK cells. After 48 hours, RNA was prepared and suppression of LMα3 transcripts was determined by RT-PCR.

2.18.3 Generation of shLMα3 Adenoviral Vectors

To generate an adenoviral vector capable of driving expression of the siLMα3 target sequence as a short hairpin RNA (shRNA), oligonucleotides were designed and obtained (Integrated DNA Technologies) that contained the sense and antisense target sequences of siLMα3, separated by the hairpin sequence TTCAAGAGA, and flanked with the terminator sequence, TTTTTT, a unique *KpnI* restriction site, a 5' *BamHI* site, and a 3' *EcoRI* site. To generate adenovirus, the BD Knockout Adenoviral System 1 (BD Biosciences, Clontech) was used. Upon receipt, lyophilized oligonucleotides were resuspended in sterile deionized water to a concentration of 100μM. 10μg each of sense and anti-sense oligonucleotides were annealed by mixing strands 1:1 in a microcentrifuge tube. Tubes were then boiled in a large beaker of water for 5 minutes. The beaker of water was then removed from the heat source and allowed to cool below 50°C. Annealed product was then ligated into pre-linearized pSIREN-Shuttle vector by mixing 2μl of pSIREN-Shuttle, .5μM annealed oligonucleotide, 1.5μl 10X T4 DNA Ligase Buffer, .5μl 100X BSA, 9.5μl deionized water, and .5μl T4 DNA Ligase. The mixture was then incubated for 3hr at RT. DH5α competent cells were then transformed using 2μl of ligation mixture, and plated onto LB plates containing 50μg/ml kanamycin. Positive colonies were identified by restriction digest using the *KpnI* restriction enzyme. A positive clones selected and grown up in large-scale bacterial cultures and plasmids were purified using a Maxi-Prep kit (Qiagen). The "shuttle" site of the plasmid, which contained the hairpin sequence and RNA polymerase promoter, was digested out of the vector with *I-CeuI* and *PI-SceI*. The digested "insert" was then ligated into pre-linearized Adeno-X Viral DNA vector by mixing 2μl of the

insert, 2µl of sterile deionized H20, 3µl of the vector (250ng/µl), and 2µl of T4 DNA Ligase (.4U/µl), and incubating overnight at 16°C. Ligation product was then digested with *SwaI*, which linearized the non-recombinant/self-ligated pAdeno-X DNA, and is thought to reduce the frequency of non-recombinant clones during transformation. After digestion, digestion product was purified away from restriction enzymes by ethanol precipitation and resuspended in sterile TE buffer (10mM Tris, 1mM EDTA, pH 7.5). 2µl of this product was then used to transform DH5α competent cells. Transformed cells were plated and grown up on LB Agar plates containing 100µg/ml ampicillin. Proper insertion of the hairpin into the Adeno-X viral DNA vector was confirmed by PCR, restriction digest using *I-CeuI* and *PI-SceI* restriction enzymes, and sequencing of the plasmid using the same primers as were used for PCR. The positive clone, D5, was chosen and grown up in a large-scale culture, which was again purified by Maxi-Prep. The plasmid was referred to as Ad-shLMα3-D5.

2.18.4 Virus Generation of Ad-shLMα3-D5

Adenovirus containing the shLMα3-D5 was produced in HEK-293 packaging cells (ATCC). The day prior to transfection, HEK-293 cells were passaged 1:6 into 10cm dishes so that cells would be 50-70% confluent for transfection in HEK growth medium without antibiotics. Also prior to transfection, the AdX-shLMα3 plasmid was digested with the restriction enzyme *PacI*, which supports the formation of the adenovirus replication complex by exposing inverted terminal repeats that contain the origins of adenovirus DNA replication. After digestion, *PacI* digested DNA was ethanol extracted and confirmed on an agarose gel. The next day, the AdX-shLMα3-D5 plasmid was transfected into several plates of HEK-293 cells using the Lipofectamine2000 reagent and transfection procedure. 24hrs later, antibiotic/antimycotic solution was diluted into the medium (final concentration 1X). Adenovirus was harvested from

cells once cytoplasmic effect (CPE) was evident, and more than 50% of cells had detached. Cells were harvested by first mechanically dislodging them from the plate by either agitation or pipeting medium against the cell later. The cell suspensions were then collected into a 50ml conical tube and spun at 3000rpm to pellet cells. The supernatant was then discarded and the pellet was resuspended in 500μl of PBS- for each original plate of cells (for example, three plates of cells require 1.5ml of PBS-). To collect adenovirus from the packaging cells, the cell suspension was lysed by three consecutive freeze-thaw cycles. Cell debris was pelleted by centrifugation, and supernatant containing adenovirus was removed and stored. This batch was considered the "primary amplification". To yield high titer virus, a second round of infection was performed, termed the "secondary amplification". 250μl of the primary amplification stock was added directly to HEK cells (in HEK growth medium) that were 50-70% confluent. Once CPE was again evident, adenovirus was collected from the cells through freeze-thaw cycles, as described above. The infection procedure was performed one additional time using the secondary amplification, to generate the "high titer stock", this time infecting several plates to generate a larger volume of virus. The high titer stock was then further concentrated using 15-25-40-54% OptiPREP (Axis-Shield USA) gradients and ultracentrifugation at 100,000xg. The virus was harvested from the gradient by puncturing the polyallomer tube with a needle and withdrawing the viral band, which was visible between the 40% and 25% OptiPREP dilutions. The virus was then diluted 1:3 in a mixture of 90% glycerol and adenovirus storage buffer (15mM Tris, pH 8.0, 150mM NaCl, 0.15% BSA, and 50% glycerol). Viral mixture was then stored in small aliquots at -80°C, leaving one aliquot for titering.

2.18.5 Virus Generation of AdX-LacZ, shLacZ, and shPKCα

AdX-LacZ was obtained from Dr. Andrew Lowy, UCSD, which is an adenovirus capable of expressing the bacterial protein, LacZ, from the AdenoX plasmid. Adenovirus capable of expressing short-hairpin sequences, shLacZ and shPKCα, were obtained from Dr. Jeffrey Matthews and Dr. Jun Tang, the University of Chicago. To generate a high titer stock of each virus, 10μl of the virus was added directly to 50-70% confluent HEK-293 cells. Once CPE was evident, generally after 1-2 days, cells were collected, lysed, and concentrated as described above. The only exception to this was the shPKCα virus, which had an exceptionally high titer without additional concentration procedures.

2.18.6 Titering of Adenoviral Stocks

Titers of adenoviral stocks were determined using the Adeno-X Rapid Titer kit (Clontech). Briefly, the concentrated adenovirus was thawed quickly in a 37°C water bath and placed on ice. The virus was diluted serially from a 10^-2 to 10^-7 in cold PBS-. Meanwhile, a subconfluent flask of HEK-293 cells was trypsinized, spun down, resuspended in HEK growth medium, and counted. Cells were diluted to 5x10^5 cells/ml, and 1ml was plated into each well of a 12 well plate. Immediately after plating, 100μl of dilutions 10^-3-10^-7 were dripped into 2 wells each. The remaining two wells were reserved as non-infected controls. Cells were incubated with virus for two days, at which time a slight CPE was typically evident in the wells treated with higher concentrations of virus. At this time, all of the medium was aspirated and the plate was left uncovered in the tissue culture hood for 5 minutes to partially dry. Cells were then fixed by slowly dripping 1ml of ice-cold methanol into each well and placing it in the freezer for 10 minutes. Methanol was then aspirated, and wells were rinsed 3X with 1%BSA/PBS-. A primary antibody solution containing 1:1000 anti-hexon in 1% BSA/PBS- was then added to the

wells and incubated with rotation at 37°C for 1hr. The plate was again washed with 1% BSA/PBS-, then incubated with an HRP conjugated secondary antibody, as described above. After antibody incubation, the plate was again washed 3X with 1% BSA/PBS-. After final wash, a mixture of DAB substrate and Stable Peroxidase Buffer (kit component) were incubated with the plate for 10 minutes. The plate was then washed one final time with PBS-, and left with 1ml PBS- in each well. Staining was quantified by counting positive "colony" staining under an inverted phase microscope using the 20X objective. Results from set A and B were averaged. To determine the viral titer, the following equation was used:

$$\text{Titer in infectious units/ml} = \frac{(\text{infected cells/field})(\text{fields/well})}{(\text{volume of virus in ml})(\text{dilution})}$$

Where the number of microscope fields per well = 573.

A viral titer of 10^9-10^10 was typically obtained.

2.18.7 Ad-shLMα3 Knockdown Procedure

MDCK stock cells, six days post-passaging, at which time they were quiescent, were trypsinized and counted. 1-1.5x10^6 cells were then plated in 60mm dishes in MDCK growth medium. Cells were incubated for 2 hrs at 37°C, 5% CO_2, which allowed them to attach, but not spread or form mature cell-cell contacts. After the incubation, cells were removed from the incubator, and washed 2X gently with PBS-. Ad-shLMα3 and control viruses were diluted to 40infU (60infU in early experiments) in 600µl of OptiMEM, and mixture was dripped onto the cells. Cells were then incubated with virus for 1hr at 37°C, 5% CO_2 to allow viral adsorption. 4ml of MDCK growth medium was then added, and cells were placed back in the tissue culture incubator and allowed to grow for another 18-24hrs. After this incubation period, infected cells were trypsinized and replated at desired experimental density. Cells were then permitted to grow for another 24hrs, then assayed. The overall time from infection to harvest was 42-46hrs.

2.19 siRNA Duplex-mediated Suppression of LMα3

2.19.1 Identification of siLMα3 RNAi Target Sequences

The target sequences for siLMα3-1, -2, -3, -4, and -5 were designed by analyzing the canine LMα3 partial coding sequence (Reference number AF236865.1) with computerized algorithms provided by Ambion, The Whitehead Institute of Biomedical Research at Massachusetts Institute of Technology (http://jura.wi.mit.edu/bioc/siRNAext), and Dharmacon (http://www.dharmacon.com/designcenter/DesignCenterPage.aspx). Potential sequences from all algorithms were mapped onto the LMα3 sequence. To ensure that potential target sequences did not align with any other gene in the canine genome, target sequences were screened against the canine genome using the blastn algorithm within the Basic Local Alignment Search Tool (BLAST) provided by the National Center for Biotechnology Information (NCBI) (www.ncbi.nlm.nih.gov/BLAST). Any sequence that generated gene matches, other than LMα3 with an e-value less than 1, was immediately eliminated from consideration. The remaining target sequences were mapped to the canine LMα3 sequences. Preference was given to target sequences that were identified by multiple algorithms. From these sequences, the final five were chosen based on optimal GC content (around 50%), low thermodynamic values, and very low e-values, which are parameters described by Elbashir, *et al* (Elbashir et al., 2001a; Elbashir et al., 2002; Elbashir et al., 2001b). The siLuc control sequence was originally identified by the Clontech Corporation. The target sequence was screened using the same parameters described above, with the exception that it did not align with the canine genome.

2.19.2 Suppression of LMα3 with siRNA Duplexes

10^6 MDCK cells were electroporated with 2μg of siRNA duplexes using the Lonza system and Lonza buffer L. Initial determination of siRNA efficacy in suppression of LMα3 was determined by qRT-PCR using primers specific for the LAMA3 gene (Qiagen) and short-term metabolic labeling following by immunoprecipitation with the 9LM5 antibody. Three target sequences were chosen. 18 hours after electroporation, cells were replated at the density required by the individual experiment, as in adenoviral shRNA experiments described above. In experiments where more than 10^6 cells were required in each parameter, duplicate samples were electroporated and then pooled at the replating step. After replating, cells were permitted an additional 24 hours to recover, and then were harvested for experimentation.

Chapter 3:
Characterization of MDCK Cell Proliferation During Formation of the Epithelium

3.1 Introduction

When MDCK cells are plated at low density, within two hours they secrete extracellular matrix proteins, and attach to this substratum. Very quickly, cells extend protrusions on the newly deposited matrix and use these protrusions to "crawl" towards neighboring cells. Within 18 hours, cells have clustered into small islands, with proliferation primarily occurring in first rows of cells from the outer edge. The outer cells additionally spread, and the island itself becomes motile to unite cells to other clusters of cells. The processes of spreading, migration, and proliferation continue until the epithelium has re-formed (Fenteany et al., 2000; Jacinto et al., 2001). Once re-formation is complete, a complex array of signaling events exit the cells from the cell cycle, and proliferation ceases. This cellular state is known as quiescence.

It is well known that MDCK cells form a quiescent epithelium at high density, but the process by which they enter and exit the cell cycle has not been broadly examined. Characterization of quiescence in other mammalian cell types has revealed many phenotypes associated with the state. For example, a G0/G1, singular 'n' DNA content is observed (Pardee, 1974), expression of the cyclins, which are required for proliferation, are lost (Afrakhte et al., 1998; Li et al., 2004), localization of the cyclin dependent kinases (cdks), is restricted to the cytoplasm, where the kinases are inactive (Yang and Kornbluth, 1999), and expression of the cell

cycle inhibitory protein, p27kip1 is enhanced (Zegers et al., 2003; Zhang et al., 2003). The purpose of the studies described here was to characterize the expression and localization of cell cycle regulatory proteins in MDCK cells as they proliferate to re-form an epithelium and confirm that MDCK cells indeed enter quiescence. These data will then serve as a platform for understanding, in future studies, how LM-332 expression or inhibition could alter the normal process by which a quiescent epithelium re-forms.

To understand how MDCK cells proliferate to re-form the epithelium, cells were plated at low density. Proliferation and the expression and localization of cell cycle proteins were then observed as the epithelium re-formed. Proliferation was analyzed by flow cytometry, BrdU incorporation, and simple counting experiments. Biochemical assays and immunofluorescence were used to elucidate protein expression and localization.

3.2 Results

3.2.1 MDCK cells Form a Quiescent Epithelium

To determine if MDCK cells at high density had a G0/G1 DNA content characteristic of quiescent cells, flow cytometry was performed. Flow cytometric analysis of DNA content is often undertaken to observe the cell cycle profile of a population of cells. The flow cytometer recognizes DNA content through propidium iodide (PI) staining of DNA. PI is a fluorescent molecule that binds to DNA, with no preferential binding for specific nucleotides. The output of data from a flow cytometer is in the form of a histogram, with the y-axis reflecting number of cells, and the x-axis reflecting fluorescence, which with PI stain, is representative of DNA content. Since each cell is read individually, and is then plotted on the histogram, a series of peaks form for cells in G0/G1, S, and G2/M phases. After the flow cytometer “reads” the fluorescence of a population of cells, analysis algorithms recognize that any single cell in G0/G1

has half the fluorescence as a cell in G2/M, because cells in G2 have two copies of DNA prior to mitosis. Cells in S phase fluoresce somewhere in the middle because DNA is undergoing replication. The flow cytometer cannot distinguish between the G0 quiescent state and G1 because both have singular DNA content and fluoresce identically. Likewise for G2 and Mitosis. Cells in quiescence display a singular peak with G0/G1 DNA content because the epithelium is a uniform body of cells that are no longer replicating or dividing.

If cells were indeed quiescent at high density, it was hypothesized that by day 6, a singular G0/G1 peak would be observed, as compared to a heterogeneous DNA content when cells were actively proliferating to re-form the epithelium. To test this hypothesis, flow cytometric analysis was performed on samples taken one day after standard tissue culture passage when cells were still subconfluent and proliferative, and again six days later when cells were at high density and the epithelium had fully re-formed (Figure 3.1). Cells were fed with fresh MDCK growth medium every two days to ensure sufficient nutrients for growth. One day after passage, FACS analysis showed that 46.2% of MDCK cells were in the G0/G1 phase of the cell cycle, 24.6% of cells were in S, and 26.6% were in G2/M. By Day 6, however, 76.9% of cells were in G0/G1, and only 2.94% of cells remained in G2/M. This singular peak observed in G0/G1 suggested that MDCK cells, upon re-formation of the epithelium, were uniformly in G0/G1, which indicated that the population was quiescent.

To characterize when proliferation of MDCK cells occurred during epithelial re-formation, growth conditions were standardized (described in 2.1.2), and cells were plated at a subconfluent density onto either coverslips to observe population density (Figure 3.2A), or onto plastic, to quantify cell number by direct counting (Figure 3.2B). At subconfluent density, MDCK cells collected into small islands, as evidenced by the observation of clustered nuclei, which increased in size over time (Figure 3.2A, days 1-2). An initial confluency was reached by

day 3, but cells continued to grow and pack tightly together until a saturation density was achieved by day 5 (Figure 3.2A, days 5-7). Cell counts were consistent with this pattern of growth (Figure 3.2B). Little proliferation was evident the first day after plating, likely because many cells had not yet entered the cell cycle from the initial quiescent state. Between days 1 and 4, however, an exponential increase in cell number was observed. After 4 days, cell number no longer increased, and appeared to level off, indicating that the logarithmic phase of growth was complete and cells were no longer proliferating.

To understand more precisely when MDCK cells ceased to proliferate, BrdU incorporation was monitored over seven days (Figure 3.3). BrdU is a synthetic thymidine analog that is incorporated into newly synthesized DNA strands during S phase and can be immunolocalized to detect proliferating cells. Based on the growth curve from Figure 3.2, it was hypothesized that the highest amount of BrdU incorporation would be observed one to two days after plating because, as determined in the previous section, this was when cells were in the logarithmic phase of growth. It was further hypothesized that a sharp reduction in BrdU incorporation would be observed after three days because growth curve analysis indicated that cell numbers were no longer rapidly increasing at this time. Consistent with growth curve analysis, BrdU was incorporated in almost 70% of cells during the first two days, which indicated that most cells were indeed passing through S phase and proliferating. By day 3, incorporation was only observed in around 15% of the population, and by day 7, less than 5% of cells were still proliferating. It was not surprising that BrdU continued to be incorporated into a small percentage of cells after 3 days, because in Figure 3.2, after 3 days, a slow population growth continued until saturation density was achieved. These data confirm that under our defined growth conditions, the logarithmic phase of MDCK cells growth occurred one to three

days after the initial plating, and that after 5 days in culture, the MDCK epithelium had re-formed and was quiescent.

3.2.2 Expression and Localization of Cell Cycle Regulators During Re-formation of the Epithelium.

Cyclin heterodimerization with cdks in the nucleus is required for cellular proliferation. For cells to enter or continue through the cell cycle, members of the cyclin family must first be expressed. In the absence of inhibitory mechanisms, cyclins next bind to their constitutively expressed cdk partners; the complex is translocated to the nucleus and activated by phosphorylation of the cdk subunit. Once the complex is activated, the cdk kinase can promote gene expression of proteins required for the next phase of the cell cycle. At the end of each phase of the cell cycle, the appropriate cyclin is phosphorylated, translocated out of the nucleus, and degraded. Failure of cyclin export and degradation can result in continuous proliferation beyond re-formation of the epithelium. Indeed, cyclins are often continuously expressed in carcinoma cells (Gong et al., 1994). In non-transformed epithelial cells, therefore, cyclins are expressed and localized to the nucleus when cells are proliferative, but are degraded and undetectable when cells are quiescent.

To first confirm that cyclins were expressed in proliferating MDCK cells, but not in quiescent cells, cells were plated in plastic dishes under standardized conditions. Lysates were generated every 24 hours for seven days, and subjected to immunoblot for cyclin D1, cdk4, cyclin E1, cdk2, cyclin B1, or cdk1 (Figure 3.4A). Based on previous growth analysis, it was hypothesized that if MDCK cells followed the cyclin expression pattern outlined above, the highest levels of cyclins would be observed the first three days after plating, but that cyclin expression would be indistinguishable by the seventh day. Indeed, cyclin D1, cyclin E, and cyclin B1 expression were the highest within the first three days after plating (Figure 3.4A, top).

Expression of cdk2 and cdk4, despite some variation in levels by day, was continuous throughout the seven-day experiment (Figure 3.4A, middle). Cdk1 expression differed from the expression of cdk2 and cdk4, in that its expression declined in parallel with cyclin B1, its cyclin partner (Figure 3.4A, right). Slight increases in expression levels were observed in cyclin B1 and cdk1 samples at day 5. This increase coincided, however, with cell medium replenishment and may have been in response to the addition of fresh growth factors. Overall, the pattern of cyclin and cdk expression followed the expected pattern and was consistent with growth and replication data described in Figures 3.1-3.3.

As described above, cyclin expression alone is not enough for cells to proliferate. Cyclin heterodimerization with cdks and their translocation to the nucleus are also required for cellular proliferation. To confirm that cyclins and cdks were nuclear during the proliferative phases of MDCK growth, cells were grown from one to seven days on glass coverslips, and localization of the cyclins and their partnering cdks was determined by immunofluorescent co-staining of cyclin D1/cdk4, cyclin E/cdk2, or cyclin B1/cdk1 (Figure 3.4B). On days 1 and 2, times when cells were the most proliferative, nuclear staining of all cyclins and cdks was observed. Some cytoplasmic staining, however, became apparent by day 2. By day 3, at a time corresponding with decreased BrdU incorporation (Figure 3.2), most of the staining was cytoplasmic, and by day 5 cyclin staining was largely undetectable and the remaining cdk staining was cytoplasmic. These data suggest that in MDCK cells, cyclins and cdks are indeed nuclear during proliferative phases of epithelial re-formation, but become cytoplasmic and the cyclins are degraded as cells enter quiescence.

In Figure 3.4A, cyclin E was detected as a doublet, and in Figure 3.4B Day 1-3 panels, some cyclin E staining was observed on the cell membrane. To determine if these abnormalities were indeed cyclin E, or were non-specific antibody binding, immunoblot and

immunofluorescence experiments were performed utilizing the cyclin E blocking peptide on Day 1 samples (Figure 3.4C). Blocking peptides are made from the epitope sequence that is recognized by a particular antibody. They bind specifically to the Fab region of the antibody. Pre-incubation of the antibody with the peptide prior to incubation with the immunoblot or slide thus prevents binding to the actual epitope. If the antibody were acting specifically in these studies, all immunofluorescent and immunoblot detection of cyclin E would be reduced or eliminated because antibody binding to cyclin E would be prevented. As depicted in Figure 3.4C, the blocking peptide completely eliminated the faster migrating band, and greatly reduced the intensity of the slower migrating band by immunoblot analysis (left), and eliminated all cyclin E staining by immunofluorescence (right). These data suggest that both bands in the doublet observed by immunoblot and the membrane staining are cyclin E.

3.2.3 Cell Cycle Inhibitory Protein p27kip1 Expression is Increased as MDCK cells Become Quiescent.

The cyclin E/cdk2 inhibitory proteins, p21waf1 and p27kip1 have been observed in quiescent cells. They regulate the activity of cyclin E/cdk2 complexes by direct binding to both subunits, which either prevents subunit dimerization, or prevents kinase activity of the complex. The inhibitory protein, p27kip1, increases as cells re-form an epithelium and enter quiescence (St Croix et al., 1998; Zegers et al., 2003). The inhibitory protein p21waf1 can compensate for p27kip1 in maintaining quiescence in the absence of p27kip1, particularly in hepatocytes (Kwon et al., 2002), and high levels of p21waf1 have been observed in quiescent fibroblasts (Itahana et al., 2002). It is unknown, however, if p21waf1 is involved in the promotion and maintenance of quiescence in MDCK cells.

To confirm that levels of p27kip1 protein increased as the MDCK epithelium re-formed, and determine if p21waf1 might also play a role in promoting the MDCK cell quiescent

phenotype, MDCK cells were plated at subconfluent density on plastic dishes and grown for seven days. Cell lysates were harvested each day, and immunoblotted for p27kip1 and p21waf1 (Figure 3.5). It was hypothesized that if either protein were involved in the initiation and promotion of quiescence, expression should be observed after 3 days, which is a time co-incident with decreased BrdU incorporation. As shown in Figure 3.5A, expression of p27kip1 was minimal the first three days after plating. By day 4 however, p27kip1 increased almost linearly until day 7 - times that corresponded to quiescence in MDCK cells. The fact that low levels of p27kip1 were apparent at day 2 was not entirely surprising. At this time, many cells have formed islands, and the cells in the center of the islands are beginning to show hallmarks of quiescence (see Figure 3.4B, Day 2: many of the interior cells have transported the cyclin and cdks out of the nucleus).

To determine if p21waf1 was also involved in the onset and maintenance of quiescence as the epithelium re-formed, lysates generated above were also immunoblotted for p21waf1. No p21waf1 expression was observed at any time during re-formation of the epithelium (Figure 3.5B). To confirm that the p21waf1 antibody indeed recognized canine p21waf1, as a positive control, MDCK cells were infected with Ad-shLMα3 (described in Chapter 4 and 5), which was known to promote p21waf1 expression. Inhibitory protein p21waf1 was observed in the positive control, but not in other samples, which indicated that p21waf1 was not expressed as normal MDCK cells proliferated to re-form the epithelium. (The issue of the p21waf1 doublet is addressed in Chapter 5.) These data further suggest that p27kip1, but not p21waf1, may aid in cell cycle arrest to promote the onset and maintenance of cellular quiescence, as was previously reported.

3.3 Discussion

3.3.1 Summary

When MDCK cells are plated from a quiescent population of cells at low density, the cell cycle is entered within 24 hours. After the initial entrance into the cell cycle, cell proliferation occurs mainly within the next two days, at which time cyclins and cdks are expressed and localized to the nucleus. As MDCK cells grow to confluence and an uninterrupted epithelium is generated, cyclins and cdks are exported out of the nucleus, and expression of the cell cycle inhibitory protein p27kip1 increases. Once cells have reached saturation density, which occurs 4-5 days after the initial plating under the described growth conditions, the cell cycle is exited, and the epithelium becomes quiescent. This is based on evidence that MDCK cell numbers plateau after four days in culture; after six days in culture, MDCK cells have a very large proportion of cells in G0/G1 phase of the cell cycle; at confluency, cyclins are no longer expressed or localized to the nucleus; p27kip1 is increasingly expressed; and, less than 10% of BrdU is incorporated into cells that have been in culture for seven days.

3.3.2 Cyclin E Membrane Staining

In Figure 3.4B, Cyclin E membrane staining was observed in proliferating cells. The reasons for this localization are unclear from the current literature. Cyclin E/cdk2 complexes have been observed in the plasma membrane of liver parenchyma (Gaulin et al., 2000), but no function was described in this report. Additionally, in HT-29 adenocarcinoma cells, cyclin E1 and cdk2 have been observed in a complex with p120 catenin (ctn), which is a protein associated with adherens junctions at cell-cell contacts in epithelial cells. In this study, however, cyclin E, cdk2 and p120ctn associated with the centrosome and were thought to participate in abnormal centrosomal amplification, which resulted in inhibition of DNA synthesis (Chartier et al., 2007).

As p120ctn and cyclin E/cdk2 association has been described, albeit under different circumstances, it is possible that in our cells, cyclin E/cdk2 are associated with p120ctn at the plasma membrane as a mechanism to maintain cyclin E outside of the nucleus prior to its degradation. This possibility was not addressed in our studies.

3.3.4 Identity of the Cyclin E Doublet

From the current literature, three possibilities exist as to the identity of the doublet observed on the cyclin E immunoblot. First, we may be detecting the phosphorylated form of Cyclin E1. Second, we may be observing a cyclin E1 splice variant, and third, we may be detecting cyclin E2. In all situations, however, expression should decline over time, and not be constitutive, as was observed in our studies. If the doublet were indeed cyclin E1, therefore, it was likely inactive. This matter remains unresolved, but does not impact the important conclusions from these studies, namely, that cyclins and cdks are localized during the proliferative stages of epithelial monolayer formation, as has been described for other epithelial and nonepithelial cell types.

Chapter 3 Figures

Figure 3.1: MDCK Cells are Growth Arrested in G0/G1 at Confluency

MDCK cells grown to confluency were split 1:5 into two T-75 tissue culture flasks. The next day, one flask was trypsinized and resuspended in 5ml MDCK growth medium. 1ml of this suspension was removed and harvested for flow cytometric analysis. Six days later, the second flask was harvested in the same manner. PI stain was used to visualize DNA content on the BD FACScan flow cytometer. Y-axis is the number of cells, and x-axis is DNA content.

Day 1 **Day 6**

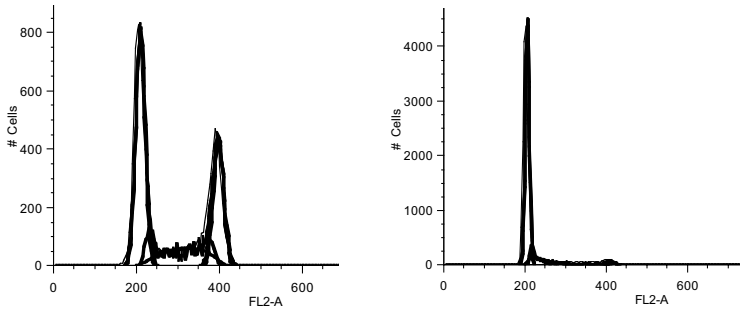

Cell Cycle Phase	*Day 1*	*Day 6*
G1	46.2%	76.9%
S	24.6%	18.6%
G2/M	26.6%	2.94%

Figure 3.2: MDCK Cells form a Quiescent Epithelium

(A) 7.5x10^5 MDCK cells were plated onto glass coverslips in MDCK growth medium and allowed to grow for one to seven days. At the same time each day coverslips were removed from growth medium, fixed with 3% PFA solution, permeabilized with .1% Triton X-100/PBS, and stained for DAPI. All samples were imaged using the Axioskip conventional fluorescence microscope, with the 63X oil immersion objective. Bars = 20μM.

(B) 8.0x10^6 MDCK cells were plated onto 10cm tissue culture treated dishes and were also allowed to grow for one to seven days. At the same time each day, one plate was removed, and was trypsinized as described in *Chapter 2.1*. Cells were then counted with a hemacytometer and total cell number was then plotted onto a graph (B). The y-axis is total cell number, and the x-axis is time in days. Results are from a single experiment.

A

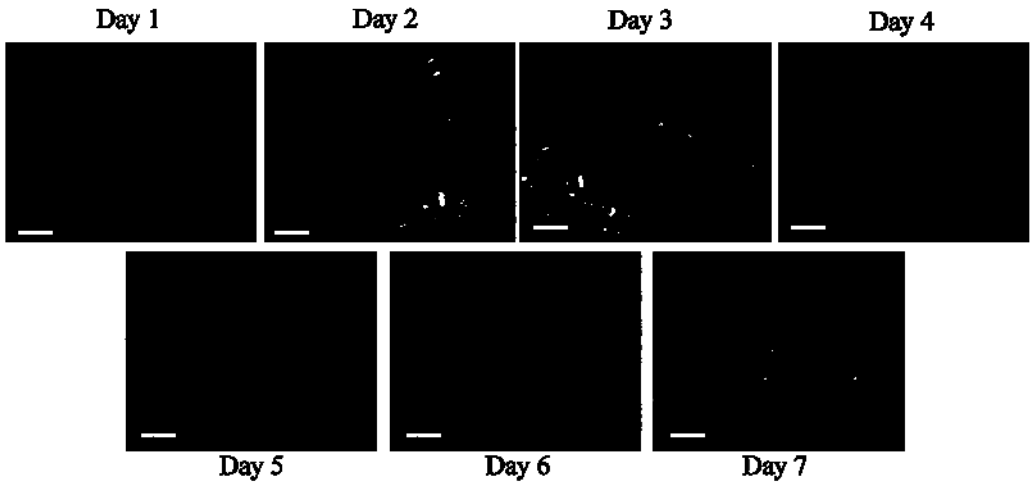
Day 1
Day 2
Day 3
Day 4
Day 5
Day 6
Day 7

B

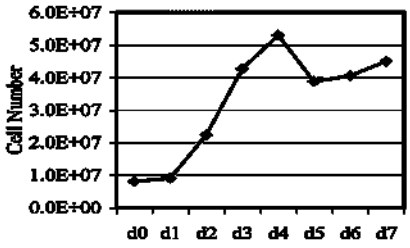
6.0E+07
5.0E+07
4.0E+07
3.0E+07
2.0E+07
1.0E+07
0.0E+00
Cell Number
d0 d1 d2 d3 d4 d5 d6 d7

Figure 3.3 MDCK cells are the Most Proliferative 24-48 hours After Plating

7.5x10^6 MDCK cells were plated onto coverslips in 7, 35mm dishes and grown for one to seven days. Six hours prior to harvest of the individual time-points, 50μM BrdU in MDCK growth medium was added to cells. After incubation, BrdU incorporation was analyzed as described in *2.7.1* using the Rat-anti-BrdU antibody (1:500). Error bars represent the standard deviation between at least three separate experiments.

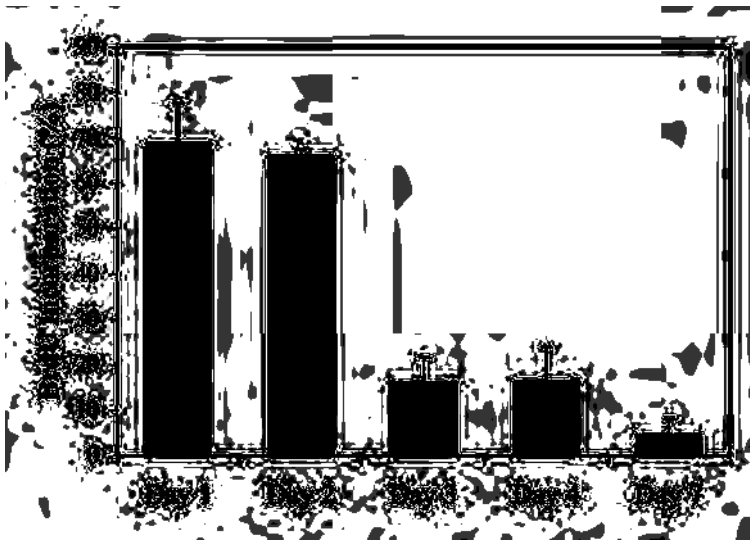

Figure 3.4: Cyclin and Cdk Localization and Expression Change as MDCK cells Become Quiescent

(A) 7.5x10^5 MDCK cells were plated onto 7, 3.5cm plates grown for one to seven days. At each time-point, cells were lysed in RIPA buffer containing protease and phosphatase inhibitors. Lysates were stored at -80'C until samples from all seven days were collected. Protein concentration was then determined, and all samples were normalized. 10-15μg of protein was loaded onto 12% polyacrylamide gels and subjected to SDS-PAGE. Gels were transferred to PVDF paper, then immunoblotted for Cyclin D1, Cdk4, Cyclin E, Cdk2, Cyclin B1, or Cdk1. All blots were stripped and reprobed two times: once for the partnering Cyclin or Cdk, and once for actin.

(B) 7.5x10^5 MDCK cells were plated onto coverslips in 7, 6 well plates and grown as described above. Cells were fixed with 3% PFA solution simultaneous to generation of the lysates above. Coverslips were stained for Cyclin D1 (green) and Cdk4 (red), Cyclin E (green) and Cdk2 (red), or Cyclin B1 (green) and Cdk1 (red). Images were taken on the Axioskop conventional fluorescence microscope using the 63X oil immersion objective. Bars, 20μM.

(C) Blocking peptide experiments were performed on extra Day 1 samples generated in (A) and (B). For immunoblot, lysates were subjected to SDS-PAGE and transferred as described above. The membrane was then split and blotted with either Rabbit anti-Cyclin E antibody (1:200), or Rabbit anti-Cyclin E antibody that was pre-incubated with Cyclin E blocking peptide (1:100). For IF, similarly, one coverslip was stained with 1:50 Rabbit anti-Cyclin E, and another was stained with Rabbit anti-Cyclin E antibody that was pre-incubated with Cyclin E blocking peptide (1:10). Cells were imaged as described above. Bars, 20μl.

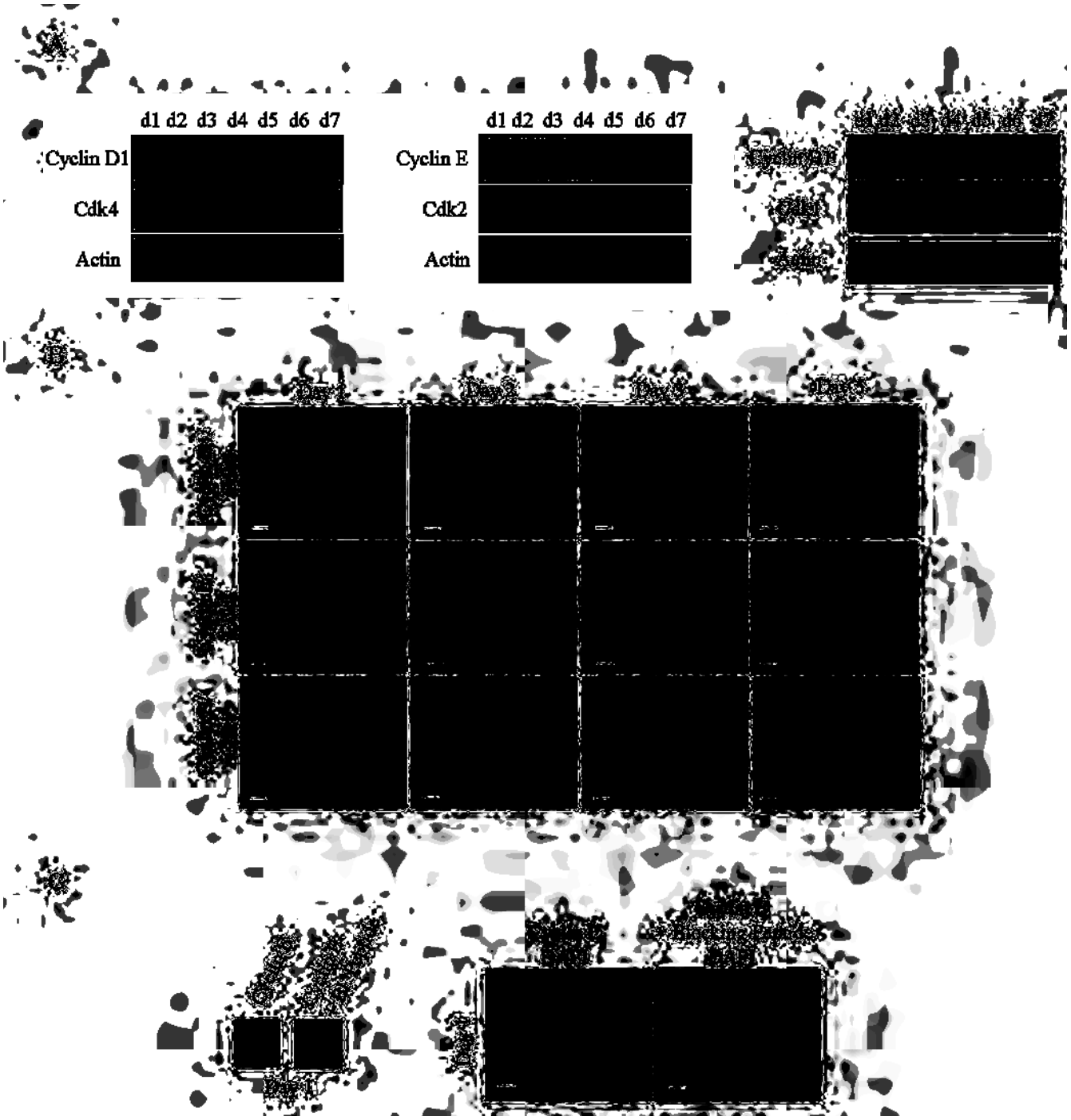
d1 d2 d3 d4 d5 d6 d7
Cyclin D1
Cdk4
Actin
d1 d2 d3 d4 d5 d6 d7
Cyclin E
Cdk2
Actin

Figure 3.5: Cell Cycle Inhibitory Protein p27kip1 Expression Increases as the Epithelium Re-forms

(A and B) 7.5x10^5 MDCK cells were plated onto 7, 3.5cm plates and grown for one to seven days. Cells were harvested from one plate each day for seven days, as in previous experiments. Cells were lysed in RIPA buffer containing protease and phosphatase inhibitors. After all samples were collected, protein concentration of the lysate was determined, and all samples were normalized. 10-15μg of protein was loaded onto 15% polyacrylamide gels and subjected to SDS-PAGE. Gels were transferred to PVDF paper, then immunoblotted for p27kip1 (A) and p21waf1 (B). All blots were stripped and reprobed for actin. (B) Lysates were run on a separate gel with the positive control and probed for p21waf1. The positive control was generated by infecting MDCK cells with the adenovirus, Ad-shLMα3 (described in *Chapters 4 and 5)*.

A

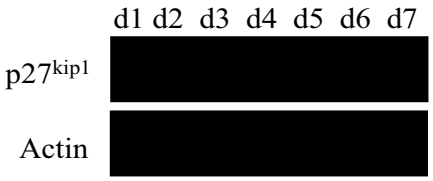
d1 d2 d3 d4 d5 d6 d7
p27kip1
Actin

B

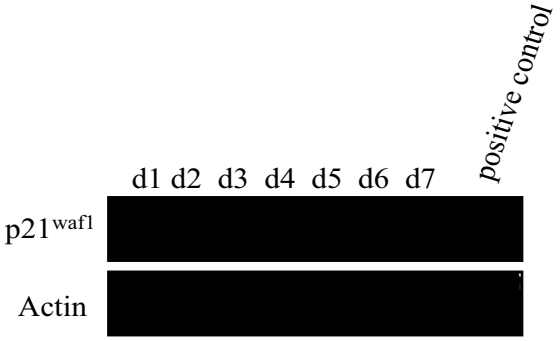
positive control
d1 d2 d3 d4 d5 d6 d7
p21waf1
Actin

Chapter 4:
Generation and Characterization of an Adenoviral shRNA Targeting LMα3

4.1 Introduction

A coordination of cellular spreading, migration, and proliferation are required for re-formation of the epithelium after injury (Jacinto et al., 2001). The basement membrane protein, LM-332 is observed at the wound edge of epithelial cells both *in vitro* and *in vivo* (Marinkovich, 2007; Nguyen et al., 2000), and is thought to support directional cellular migration into the wound (Kligys et al., 2007; Marinkovich, 2007; Sehgal et al., 2006). Additionally, LM-332 may be involved in proliferation regulation during re-formation of the epithelium, because inhibition of LM-332 results in growth arrest of mammary epithelial cells (Gonzales et al., 1999) and treatment of human kidney epithelial cells with LM-332 increases the rate of proliferation (Joly et al., 2006).

How LM-332 may be involved in formation of the renal epithelium is not well understood. Mature renal epithelia do not widely express LM-332 *in vivo*. For example, in mature adult nephrons, LMα3 and β3 have been observed in the loop of Henle, but not within the collecting ducts (Lohi et al., 1996). In developing embryonic mouse and human kidneys however, LMγ2 is observed in the basement membrane within the collecting ducts and collecting tubules in the medulla, respectively (Kallunki et al., 1992; Sugiyama et al., 1995). Also in

developing mouse kidneys, LMγ2 expression has been observed in the uteric bud and may be required for uteric bud branching morphogenesis (Zent et al., 2001). It seems LM-332 expression in adult renal tissues *in vivo*, aside from the Loop of Henle, may be limited situations when the epithelium is de-differentiated, such as following injury during epithelial repair. Indeed, in the adult rat kidney, high levels of LM-332 were observed throughout the length of the nephrons following damage by ischemic injury, but were limited prior to injury (Zuk and Matlin, 2002). Additionally, *in vitro*, LM-332 has been observed at the wound edge of MDCK cells (Moyano, unpublished). Given the role of LM-332 in epithelial re-formation in other cell types, and given that MDCK cells are derived from the canine kidney and are thought to be from the distal tubule or collecting duct, the examination of LM-332 expression and function during epithelial re-formation is of interest in this cell type.

To study the requirement of LM-332 in formation of the epithelium, LM-332 protein functionality must be inhibited. The cellular phenotypic response to LM-332 secretion and deposition is a direct result of LM-332 binding to its cellular receptors. To analyze the requirement for LM-332, cells are often treated with function blocking antibodies specific for mouse or human LM-332. LMα3 function blocking antibodies bind to the LG domain and prevent cellular adhesion to LMα3 (described in Gonzales et al., 1999). Unfortunately, despite good homology between the mouse, human, and canine LMα3, these antibodies do not recognize canine LMα3 by immunofluorescence, immunoprecipitation, or immunoblot, and are therefore unlikely to inhibit the cellular-laminin interaction. RNA interference (RNAi) technology was therefore used to suppress production of the LMα3 subunit.

RNAi technologies are based on the principle that, in normal living cells, double stranded RNA molecules can be processed into short RNA strands of around 20 nucleotides called small-

interfering RNAs (siRNA), which can promote the degradation of mRNA sequences (Fire et al., 1998; Meister and Tuschl, 2004; Montgomery et al., 1998). This method of post-transcriptional gene silencing can be exploited to suppress the protein production of nearly any target of interest. Two primary methods are used to silence genes by RNAi. First, a plasmid encoding for a short, double-stranded RNA, called a short-hairpin RNA (shRNA), which is a pre-cursor of siRNA, can be expressed; and second, siRNA duplexes can be directly transfected into the cell-line of interest.

The LMα3 subunit was chosen as a target for siRNA-mediated silencing over the LMγ2 and LMβ3 subunits because: 1) LMα3 contains the LM-332 cellular-binding domain, and 2) if the current paradigm within the laminin field is correct, assembly of all three subunits of the heterotrimeric protein within the endoplasmic reticulum is required for secretion from the cell. Suppression of one subunit therefore, should inhibit the secretion of the entire heterotrimeric protein. Short-hairpin RNAs further offered the advantage over pre-manufactured small-interfering RNAs, in that a large supply could be generated within our laboratory, and an adenovirus delivery system could be used, which is known to result in highly efficient infections and high levels of expression.

The purpose of these studies was to generate an adenovirus capable of delivering an shRNA targeted against LMα3 in MDCK cells. Adenoviral controls and adenoviral shRNA negative controls were also developed. Cells infected with the shLMα3 adenovirus and controls were then characterized for suppression of LMα3 at the protein and mRNA levels, for protein levels and localization of the LMβ3 and LMγ2 subunits, and for protein levels of LM-511 and the integrin receptors.

4.2 Results

4.2.1 Generation of Adenoviral shRNA Targeted Against LMα3

To create an adenovirus capable of delivering a shRNA against LMα3, oligonucleotides that contained the target sequence specific for canine LMα3 were designed (Figure 4.1A) (the process by which a LMα3-specific RNAi target sequence was identified is described in Chapter 2, 2.18), and cloned into the adenovirus RNAi expression system, Knockout Adenoviral RNAi System 1 (Figure 4.1 B and C). This expression system makes use of the adenoviral vector, pAdeno-X (Figure 4.1C) to generate a type 5 adenovirus that lacks the early E1 and E3 adenoviral genes, and therefore can only propagate in a packaging cell line (Mizuguchi and Kay, 1998). Upon successful cloning of the LMα3-specific shRNA target sequence into pAdeno-X, the plasmid was referred to as Ad-shLMα3. Adenovirus was generated by transfection of the Ad-shLMα3 plasmid into HEK-293 packaging cells, which are transformed with adenovirus type 5 and should contain elements of the E1 and E3 adenoviral genome (Graham et al., 1977). Adenovirus was then harvested from HEK-293 cells, purified, and titer obtained.

To infect MDCK cells with Ad-shRNAs (including adenoviral controls, described below), six days post-passage, cells were released from quiescence by plating at a subconfluent density. Cells were incubated 2hrs, which allowed them to form nascent attachments to the tissue culture plate, yet left most of the baso-lateral surface, which likely contain the adenovirus receptors, open for infection. After this incubation, cells were infected with adenovirus. As LMα3 is a subunit of a secreted, extracellular matrix protein, infected cells had to be replated after infection to remove LM-332 that may have been secreted prior to full suppression of the molecule (Figure 4.2). To accomplish this, 18 hours after the initial infection, cells were

trypsinized and replated onto new plates. Cells were allowed to grow and recover for an additional 24-48 hours, at which time they were harvested for experimentation.

4.2.2 Generation and Characterization of Adenoviral- and Adenoviral Negative shRNA Controls

To aid in phenotypic analysis in adenoviral shRNA experiments, several adenoviral controls were obtained. To control for infection by adenovirus, Ad-LacZ, which promotes expression of the LacZ protein within the same pAdeno-X expression vector as the Ad-shLMα3, was used. To control for adenoviral-mediated expression of an shRNA, two different controls were obtained. The first, Ad-shPKCα contains a short-hairpin sequence targeted against human PKCα, but not canine PKCα. The second, Ad-shLacZ, contains a target sequence specific for the bacterial LacZ gene. Both Ad-shPKCα and Ad-shLacZ drove expression of the short-hairpin through the pAd-Block-it vector. It should be noted that neither the Ad-shPKCα nor the Ad-shLacZ are ideal negative controls because adenoviruses were not generated from the same adenovirus expression system as the Ad-shLMα3. Despite multiple attempts, adequate viral titers could not be achieved when the control, Ad-shLuciferase, which uses the pAdenoX vector backbone to drive expression of a shRNA against Luciferase, was transfected into HEK-293 packaging cells.

The target sequences of both Ad-shPKCα and Ad-shLacZ were BLASTed against the canine genome and yielded no significant e-values, which indicated that they should not recognize any canine gene, and could serve as non-targeting negative adenoviral-shRNA controls. To also confirm that infection of MDCK cells with Ad-LacZ, Ad-shPKCα, and Ad-shLacZ controls did not result in major phenotypic or cytotoxic abnormalities, cells were infected and cellular morphology and proliferation were observed (Figure 4.3). Infection with

Ad-LacZ resulted in no morphological defects when compared to non-infected controls. Cells infected with the Ad-shRNAs, however, were larger, and more spread than non-infected or Ad-LacZ controls (Figure 4.3A). Many cells infected with Ad-shLacZ, detached and died after the replating step. Ad-shLacZ-mediated cell death could be remedied by infection with less adenovirus; however, infection with Ad-shLMα3 with similar concentrations was not sufficient to suppress LMα3 (data not shown). Proliferation was not significantly altered in Ad-LacZ or Ad-shPKCα infected cells when BrdU incorporation analysis was performed and samples compared to the non-infected control (Figure 4.3B). A significant decrease of proliferation was observed in Ad-shLacZ infected samples, however, which was not surprising considering the overall poor health of cells infected with this adenovirus. As proliferation was not altered in Ad-shPKCα samples, and cells appeared healthy, it last needed to be confirmed that canine PKCα protein levels were not suppressed in response to infection with this adenovirus (Figure 4.3C). No change in PKCα was observed in MDCK cells following infection of Ad-shPKCα. These data indicated that Ad-LacZ and Ad-shPKCα would serve as good controls against adenovirus infection and/or adenoviral-mediated shRNA delivery. The Ad-shLacZ control was not used due to its cytotoxic affect on cells. Ad-shPKCα was used in all studies, and referred to as shControl, except where indicated. Ad-LacZ was also used in selected studies.

4.2.3 Infection of MDCK cells with Ad-shLMα3 (D5) Suppresses LMα3

To confirm that infection of MDCK cells with Ad-shLMα3 suppressed both the production of LMα3 mRNA and protein, quantitative real-time PCR (Figure 4.4A and B), and metabolic labeling followed by immunoprecipitation of the whole LM-332 molecule, respectively, were performed. When LMα3 message levels from Ad-shLMα3 cells were

compared to non-infected controls, no significant decrease was observed (Figure 4.4A). However, LMα3 message was reduced by 70% when Ad-shLMα3 cells were compared to Ad-shControl cells (Figure 4.4B). It is unclear why LMα3 message levels were low in non-infected cells because, conversely, LMα3 protein levels were high in non-infected, Ad-shControl, and Ad-LacZ cells (Figure 4.4 C and D). Importantly, Ad-shLMα3 infection resulted in almost complete elimination of the LMα3 protein when compared to both the non-infected control and the shControl. Interestingly, an increase in LMγ2 and LMβ3 band densities were always observed in Ad-shLMα3 cells relative to the controls. The cause of this increase remains unclear, but will be addressed further in 4.3.2. These data suggest that expression of Ad-shLMα3 suppresses the production of LMα3 protein.

Morphologically, MDCK cells expressing the Ad-shLMα3 were large and flattened, with a "fried egg" appearance (Figure 4.5). This morphology was not evident in Ad-LacZ cells or non-infected controls, and was greatly exaggerated when compared to Ad-shControls (Figure 4.3A). As Ad-shControls also exhibit increased cell area as compared to non-infected and Ad-LacZ controls, it is possible that some of this morphological defect is caused by adenovirus-mediated delivery of the shRNA.

4.2.4 LMβ3 and LMγ2 are Secreted Following Suppression of LMα3

As discussed previously, the current paradigm within the laminin field is that proper assembly of all three laminin subunits is prerequisite for secretion of the heterotrimeric protein from the cell and subsequent deposition into the extracellular matrix (Matsui et al., 1995; Yurchenco et al., 1997). Data described in section 4.2.3 clearly show that the LMγ2 and LMβ3 subunits are still produced in the absence of LMα3. To confirm that LMγ2 and LMβ3 were

retained within the endoplasmic reticulum in the absence of LMα3, MDCK cells infected with Ad-shControl or Ad-shLMα3, were replated onto coverslips, and LMγ2 and LMβ3 were immunolocalized using a polyclonal antibody against the entire LM-332 molecule. Suppression of LMα3 could not be confirmed by immunofluorescence because there are no antibodies that are specific for the canine LMα3 subunit. Surprisingly, in Ad-shLMα3 cells, organized staining was observed below the cells, similar to non-infected and Ad-LacZ controls (Figure 4.5A, right), which suggested that LMβ3 and LMγ2 might also be secreted from the cell in the absence of LMα3.

The possibility existed that LMα3 might not have been fully suppressed at the time of plating, resulting in some secretion of the whole molecule and the observation of LMγ2 and LMβ3 beneath the cells. As it was not possible to determine if LMα3 was present with LMγ2 and LMβ3 in the deposited LM-332 observed in Figure 4.6A, cells infected with Ad-LacZ or Ad-shLMα3 were metabolically labeled overnight, and the culture medium and cell extracts were immunoprecipitated with the polyclonal LM-332 antibody. As shown in Figure 4.6B (left), in cellular extracts, the production of the LMα3 protein was eliminated compared to the controls. LMγ2 and LMβ3 levels were also increased following expression of Ad-shLMα3, consistent with previous observations (Figure 4.6C and D). In the medium (Figure 4.6, right), following expression of Ad-shLMα3, levels of LMα3 were slightly higher in the compared to cell lysates. However, LMα3 levels were still greatly reduced, and the LMγ2 and LMβ3 bands were also present at a greater intensity than in controls.

To further test the hypothesis that some of the apparent secretion of LMγ2 and LMβ3 was due to incomplete suppression of LMα3 at the time of the experiment, non-infected and Ad-shLMα3 cells were permitted to grow an additional 24hrs, or 66hrs after the initial infection.

Cells were again stained with the polyclonal LM-332 antibody, and were imaged at the basal and central planes by confocal microscopy (Figure 4.6C). Staining appeared less intense on the basal surface, but was still clearly in the pattern of deposited LM-332. There was an increase in the amount of cellular staining, which was believed to correspond to LMβ3 and LMγ2 retained within the endoplasmic reticulum. These data suggested that incomplete suppression of LMα3 may be partially to blame for the secreted LMγ2 and LMβ3, and, that given more time, LMβ3 and LMγ2 would be retained within the endoplasmic reticulum. However, at the time in which cells are normally harvested for experimentation (42 hours after infection), LMβ3 and LMγ2 are deposited, despite low levels of the LMα3 chain.

4.2.5 Suppression of LMα3 does not Alter Protein Levels of LM-511 or Integrin α6 and β1

MDCK cells, in addition to expressing LM-332, express another laminin, LM-511. Although structurally, these molecules are very different, they use the same integrin receptors to mediate cellular function, integrins α3β1 and α6β4. It is unknown how expression of one laminin family member may alter the expression of other laminin family members, or their integrin receptors. Expression of the α6 integrin receptor, however, seems to affect expression of the laminin receptors, as studies in α6 integrin deficient primary keratinocytes showed a significant reduction in protein levels of both LM-332 and LM-511 (Rodius et al., 2007). To determine if protein levels of LM-511 or integrins receptors, α6 and β1 were altered in the absence of LMα3, LM-511 and integrin α6 were immunoprecipitated from metabolically labeled cells, and cell extracts were immunoblotted for integrin β1 in non-infected, Ad-LacZ, and Ad-shLMα3 cells (Figure 4.7). LM-511 was immunoprecipitated using a polyclonal LM-1 antibody (Sigma). It should be noted that this antibody was originally made from laminin isolated from the

basement membrane of Englebreth Holm-Swarm (EHS) mouse sarcoma, which is rich in LM-111. As LMα1 has never been detected in MDCK cells at the mRNA level, and LMα5 has, this antibody is believed to immunoprecipitate LM-511. As shown in Figure 4.7A, no alterations in the protein levels of any LM-511 subunit were observed following expression of Ad-shLMα3 compared to the non-infected or Ad-LacZ controls. Additionally, the immunoprecipitation of integrin α6 yielded no differences in integrin α6 protein levels (Figure 4.7B). Two slower migrating bands were precipitated with integrin α6. The identity of these bands is unresolved, but because integrin α6 heterodimerizes with integrin β4, these bands may be the integrin β4 protein and its precursor. Lastly, immunoblot analysis of integrin β1 showed no changes in protein levels when Ad-shLMα3 cells were compared to controls (Figure 4.7C). These data suggest that suppression of LMα3 does not alter protein levels of LM-511 or the integrin receptors.

4.3 Discussion

4.3.1 Summary

An adenovirus capable of expressing a shRNA targeted against LMα3, Ad-shLMα3, was generated and used to infect MDCK cells. Infection with Ad-shLMα3 suppressed the production of LMα3 protein but, despite the absence of LMα3, LMβ3 and LMγ2 continued to be produced and secreted. Suppression of LMα3 also did not alter protein levels of LM-511 or the integrin receptors, α6 and β1. These results indicate that the adenoviral shLMα3 can be used for future studies to assess the function of LM-332 in MDCK cells.

4.3.2 Possible Causes of Increased LMγ2 and LMβ3 Protein Levels Induced by Ad-shLMα3

Expression of Ad-shLMα3 reduces protein levels of the LMα3 protein, but at the same time, production of LMγ2 and LMβ3 appear to increase, as observed by short-term metabolic labeling. How LMγ2 and LMβ3 expression are regulated is largely unknown, therefore, understanding how the suppression of LMα3 may disregulate the production of LMγ2 and LMβ3 is difficult to discern. The LAMC2 gene, which codes for LMγ2, has two AP1 elements, and a TGFβ response element in its promoter. In HT29mtx cells, which are human carcinoma cells, JunD containing AP-1 dimers promoted an increase in LAMC2 promoter activity (Olsen et al., 2000). In this same study, LAMC2 promoter activity was unchanged in response to TGF-β stimulation. Conversely, in SW480 and BxPC3, which are human colorectal and pancreatic carcinoma cells lines, respectively, treatment with TGFβ resulted in increased promoter activity of both LAMC2 and LAMB3 (Zboralski et al., 2008). As understanding the transcriptional regulation of LAMB3 and LAMC2 are outside of the scope of these studies, the potential role of TGFβ signaling will not be addressed.

Chapter 4 Figures

Figure 4.1 Generation of Ad-shLMα3 (D5)

Two oligonucleotide sequences that contained the shRNA sequence targeted against canine LMα3 were designed (A). The first, in the direction of 5' to 3' contained a *BamHI* restriction site, followed by the LMα3 target sense sequence, a hairpin sequence, the LMα3 target antisense sequence, the terminator sequence, and a unique *KpnI* restriction site. The second was the complement to the first strand, with the exception that it contained an *EcoRI* at the 5' end, and no *BamH1* site at the 3'end. The two oligonucleotide strands were annealed, ligated into the pSIREN-Shuttle vector (B) with the *BamHI* and *EcoRI* overhangs, and transformed into DH5α *E. coli* competent cells. A pUC origin within the pSIREN-Shuttle vector backbone allowed for propagation within *E. coli* competent cells, and a kanamycin resistance sequence ensured selection of bacteria that carried the vector. After transformation, the bacterial culture was amplified by Maxi-prep (Qiagen), and positive insertion of the short-hairpin was confirmed by restriction digest with the enzyme *KpnI*. Two positive shLMα3 clones, named D4 and D5, were then digested out of the pSIREN backbone at *I-CeuI* and *PI-SceI.* This created overhangs that were used to next insert the hairpin sequence and a unique *SwaI* site into the pre-linearized pAdeno-X vector (Clontech). The vector was amplified in the same manner as before. Positive ligation was confirmed by restriction digest with the *SwaI* restriction enzyme, and also by PCR. To generate adenovirus capable of infection and expression of the shLMα3 in MDCK cells, pAd-shLMα3 was last digested with *PacI* to expose the inverted terminal repeats, which contained the adenovirus origin of replication. The D5 clone was used for all studies.

A

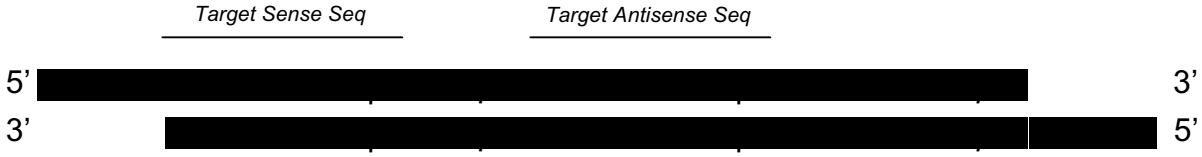

B[1]

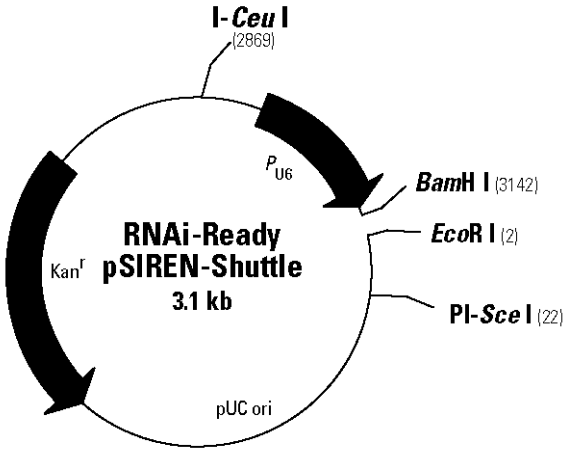

C[2]

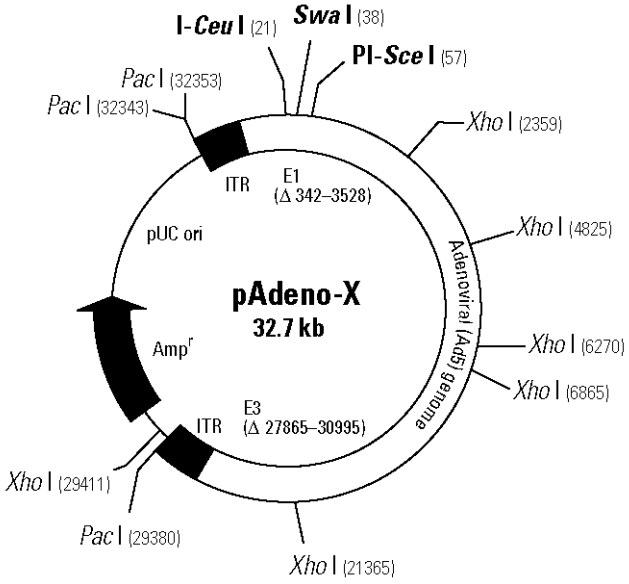

---

[1]: Image is a reproduction from BD Biosciences Clontech's Protocol. Protocol number PT3739-1. Version number PR42756. Published 12 February 2004. © 2004 Becton, Dickinson, and Company.
[2]: Image is a reproduction from BD Biosciences Clontech's Protocol. Protocol number PT3414-1. Version number PR3X481. Published 28 October 2003. © 2003 Becton, Dickinson, and Company.

Figure 4.2 Infection of MDCK Cells with Ad-Controls and Ad-shLMα3

MDCK cells, six days post-passage, were released from quiescence by plating at a subconfluent density. Cells were incubated 2hrs, which allowed them to loosely attach to the tissue culture plate, yet left most of the basolateral surface available for adenovirus infection. After this incubation, cells were infected with 40infU of Ad-LacZ, Ad-shControls, or Ad-shLMα3. To remove any LM-332 that may have been secreted prior to full suppression of the LMα3 molecule, infected cells were trypsinized and replated onto tissue culture plates or coverslips at the density required for individual experiments. Cells were then allowed to grow and recover for an additional 24 hours, which was 42 hours after the initial infection. Cells were then harvested for experimentation.

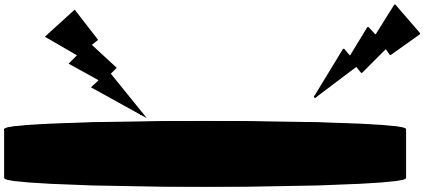

Release cells from quiescence by re-plating. Infect with Ad-shLNα3, Ad-LacZ or Ad-shRNA control

18hrs

Re-plate

42h

Harvest for experiments

Figure 4.3 Characterization of Adenoviral Controls

(A) MDCK cells were infected with adenovirus capable of expressing LacZ (Ad-LacZ), an shRNA targeted against human PKCα (Ad-shPKCα), or an shRNA targeted against LacZ (Ad-shLacZ) After 18hrs, .25x10^6 cells were replated onto two sets of glass coverslips. The first set was fixed with 3% PFA, and stained for either actin with phalloidin488 (green) or total nuclei with DAPI (blue). Images were taken on the Axioskop conventional fluorescent microscope, using the 40X oil immersion objective.

(B) Six hours before the second set was harvested, BrdU was diluted to 50μM in MDCK growth medium and added to cells. After 6hr BrdU incubation, cells were fixed with 3% PFA and stained for BrdU with a rat-anti-BrdU antibody (1:500), and nuclei, with DAPI. Percent BrdU incorporation was first determined. Fold change in percent BrdU incorporation compared to non-infected controls was then determined. Results from three experiments were averaged. Error bars represent the standard deviation between experiments. P-value = .0027 was determined by two-tailed student's *t-test.*

(C) To confirm that the shRNA targeted against human PKCα did not also suppress canine PKCα, MDCK cells were infected with either Ad-shPKCα or Ad-shLMα3. After 18hrs, 10^6 cells were replated into 60mm tissue culture plates, then 24 hours later, were extracted with SDS extraction buffer. Protein concentration was determined and samples were normalized. Following sample denaturization and alkylation, samples were loaded onto a 12% polyacrylamide gel and subjected to SDS-PAGE. Gels were then transferred to PVDF membrane, and immunoblotted for PKCα with a rabbit anti-PKCα antibody (1:500). Blots were then stripped and reprobed for total actin.

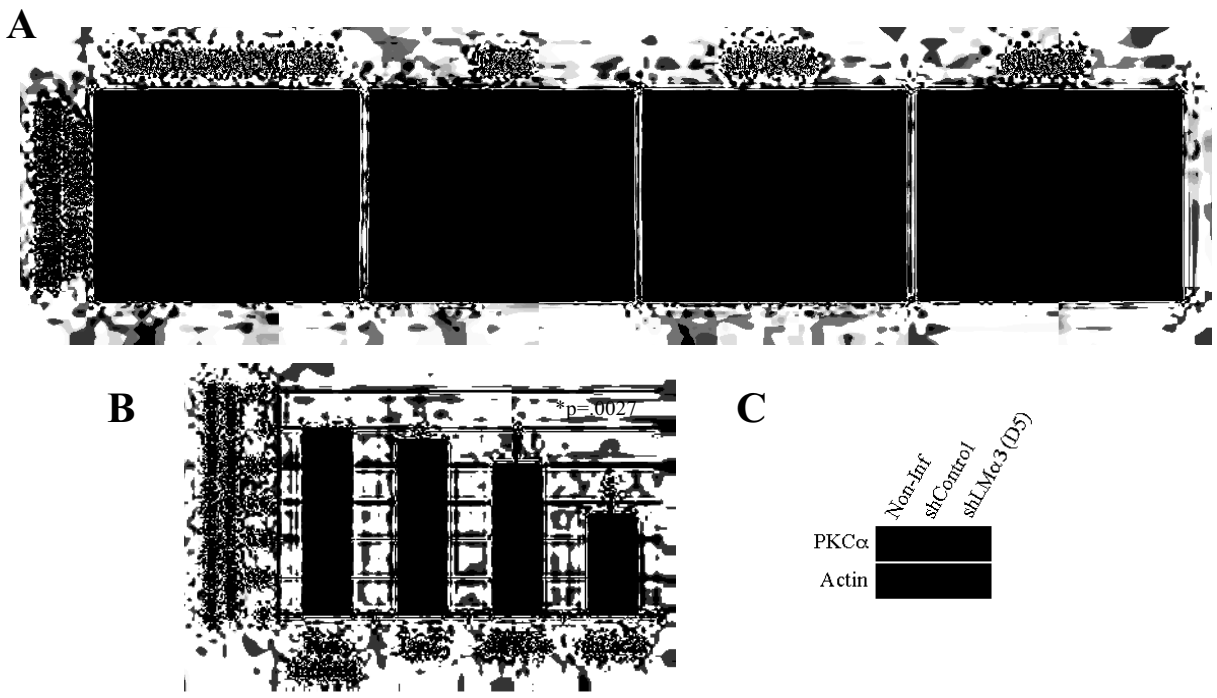
A
B
*p=.0027
C
Non-Inf
shControl
shLMα3 (D5)
PKCα
Actin

Figure 4.4 Expression of Ad-shLMα3 Suppresses LMα3 RNA and Protein Production.

(A and B) MDCK cells were infected with Ad-shControl (shPKCα) or Ad-shLMα3. 18hrs after infection, .75x10^6 cells were replated into 35mm dishes. Total RNA was extracted with the Qiagen RNeasy kit, and LAMA3 gene expression was analyzed with LAMA3 primers (Qiagen) by quantitative real-time PCR. C(t) values were generated, and then analyzed against a standard curve to calculate total nanogram (ng) expression of LMα3. LMα3 amounts were then compared to non-infected ng values, to determine the fold change of LMα3 expression in all samples (A). Figure 4.5B compares ng values of shLMα3 samples to the shControl. Graph depicts the average of three experiments. Error bars represent sample standard deviation. P-value was determined by two-tailed student's *t-test*.

MDCK cells were infected with Ad-shControl and Ad-shLMα3 (C) or Ad-LacZ and Ad-shLMα3 (D), and 18hrs later, 10^6 cells were replated into 60mm dishes. Around 20 hours after replating, MDCK growth medium was replaced with 2ml of Labeling medium that contained 50μCi/ml ^{35}S Methionine/Cysteine, and cells were subjected to a 4hr short-term label. Samples were then lysed with RIPA buffer, protein concentration determined, normalized, and subjected to immunoprecipitation with 5μg of the 8LN5 rabbit anti-LM-332 antibody. LM-332 was analyzed by SDS-PAGE and fluorography. * indicates the presumed LMα3B (top) and LMα3A (bottom) bands.

A

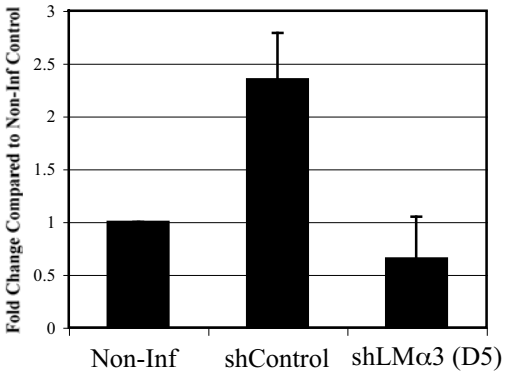
Fold Change Compared to Non-Inf Control
3
2.5
2
1.5
1
0.5
0
Non-Inf
shControl
shLMα3 (D5)

B

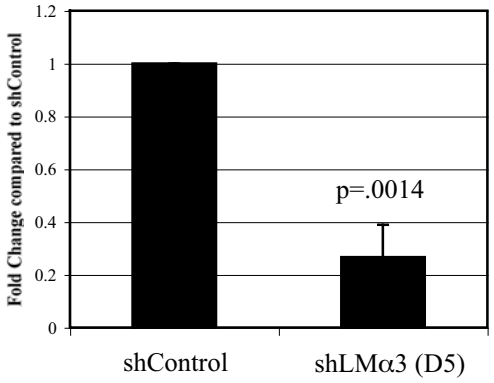
Fold Change compared to shControl
1.2
1
0.8
0.6
0.4
0.2
0
p=.0014
shControl
shLMα3 (D5)

C

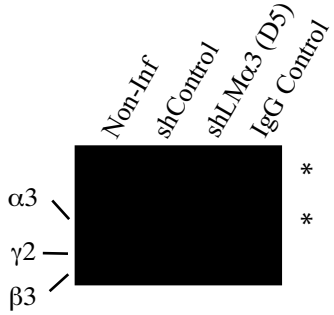
Non-Inf
shControl
shLMα3 (D5)
IgG Control
α3
γ2
β3
*
*

D

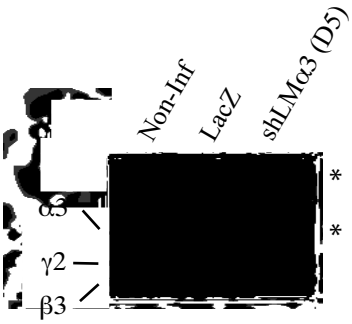
Non-Inf
LacZ
shLMα3 (D5)
α3
γ2
β3
*
*

Figure 4.5 Expression of Ad-shLMα3 Alters the Morphology of MDCK Cells

MDCK cells were infected with Ad-LacZ or Ad-shLMα3 (D5). 18hrs later, cells were replated at low density onto glass coverslips. 24hrs later, cells were fixed with 3% PFA and stained for actin (green) with phalloidin488 and nuclei (blue). Arrows indicate bundles of actin filaments and actin stress fibers. Bar, 20μM. (Inset) Cell-cell contacts appear to form. Bar, 20μM. (Mak et al., 2006)

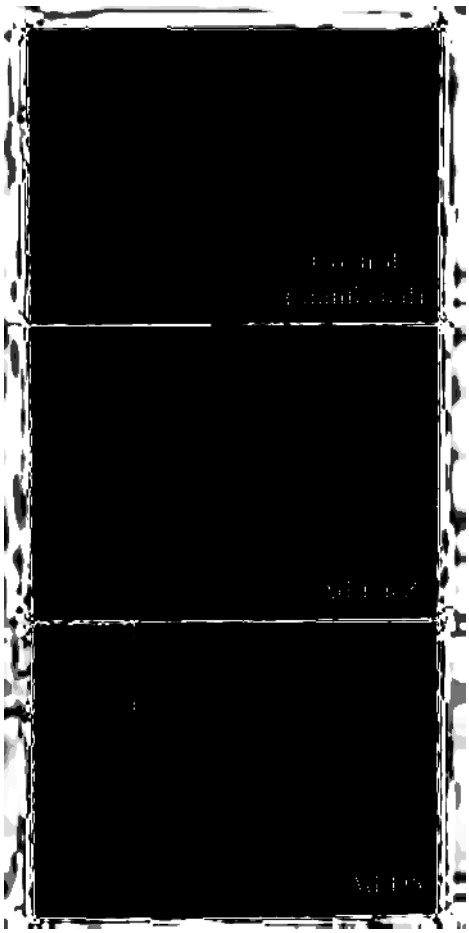

Figure 4.6 LMβ3 and LMγ2 are Secreted Following Expression of Ad-shLMα3

(A and C) MDCK cells were infected with either Ad-LacZ or Ad-shLMα3(D5). After 18hrs, cells were replated at low density onto glass coverslips, and then allowed to grow for another 24hrs. Cells were fixed with 3% PFA, then stained for LM-332 with the 8LN5 polyclonal rabbit anti-LM-332 antibody (10μg/ml) (red), actin, with phalloidin488 (green), and DAPI (blue). Staining was observed by either conventional fluorescence microscopy, bar, 20μM (A), or by confocal microscopy of the basal and central planes, bar, 10μM (C) Arrow indicates higher intensity staining of LM-332 within the presumptive endoplasmic reticulum.

(B) MDCK cells were infected as above. Cells were replated onto 35mm tissue culture dishes into labeling medium containing 100μCi ^{35}S Methionine/Cysteine, and were incubated overnight (18-24hrs). Cells were extracted with RIPA buffer. Extracts (left) and tissue culture medium (right) were immunoprecipitated with the 8LN5 polyclonal rabbit anti-LM-332 antibody (5μg). Samples were then denatured and subjected to SDS-PAGE on 6% polyacrylamide gels. Bands were visualized by fluorography. (Mak et al., 2006)

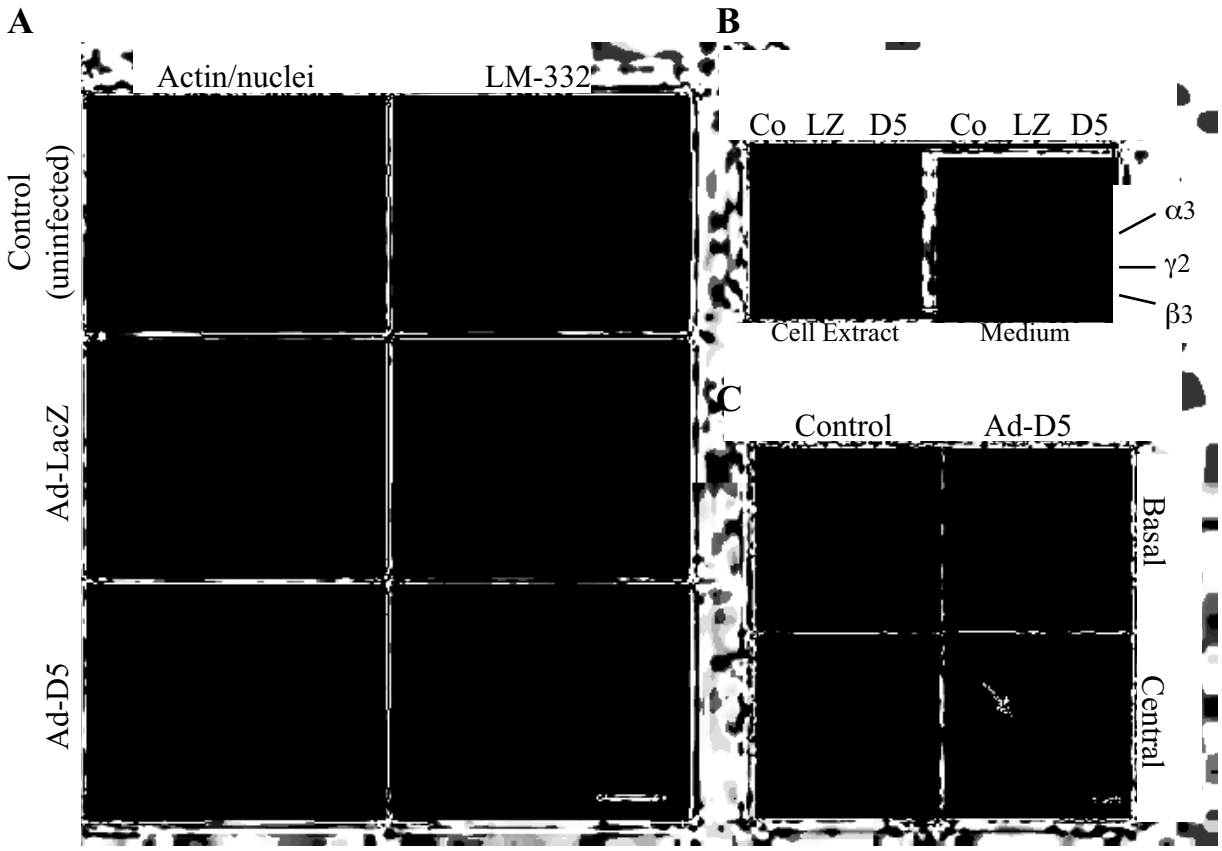
A
Actin/nuclei
LM-332
Control (uninfected)
Ad-LacZ
Ad-D5
B
Co LZ D5 Co LZ D5
α3
γ2
β3
Cell Extract
Medium
C
Control
Ad-D5
Basal
Central

Figure 4.7 Expression of Ad-shLMα3 does not Alter LM-511, Integrin α6, or Integrin β1 Protein Levels

Following immunoprecipitation of samples in Figure 4.5D, lysates were re-precipitated for first, LM1 (presumed LM-511) with rabbit anti-LM1 antibody (A), then integrin α6 (B). *Immunoprecipitation of integrin α6 also pulled down two slower migrating proteins. These proteins may be integrin β4 and the integrin β4 pre-cursor, but this was not tested in these studies.

(C) SDS extracts generated from non-infected, Ad-LacZ, and Ad-shLMα3 infected cells were immunoblotted with rabbit anti-Integrin β1 (1:1000). The antibody recognized two bands. The faster migrating band was believed to be the integrin β1 precursor. (Mak et al., 2006)

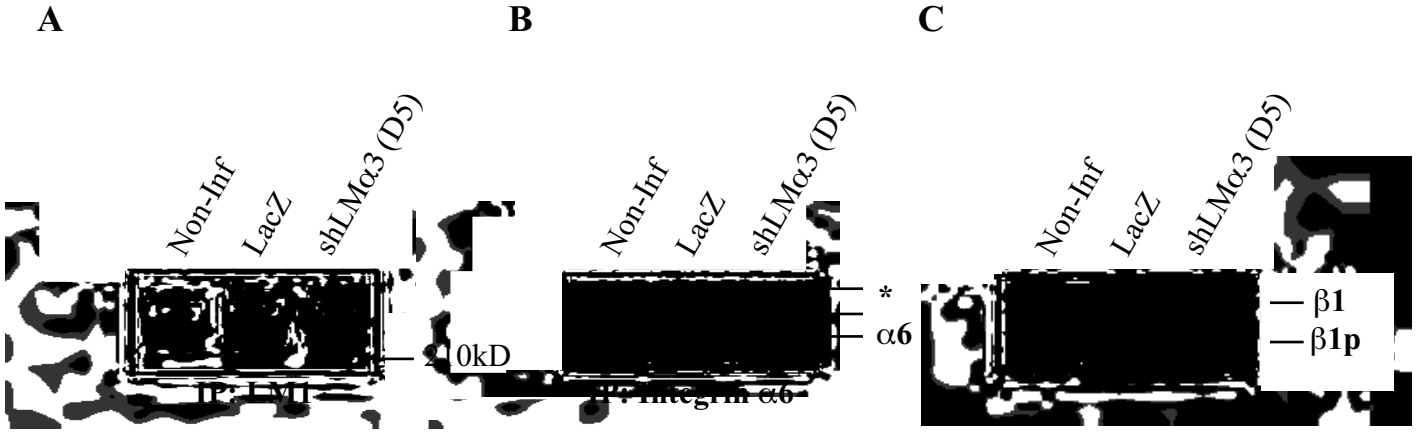
A
B
C
Non-Inf
LacZ
shLMα3 (D5)
Non-Inf
LacZ
shLMα3 (D5)
Non-Inf
LacZ
shLMα3 (D5)
200kD
IP: LM1
IP: Integrin α6
*
α6
β1
β1p

Chapter 5:
Laminin-332-Mediated Control of MDCK Proliferation

5.1 Introduction

LM-332 has been implicated in proliferation control of both normal and diseased cells. During re-formation of the epithelium, the full-length, pre-LM-332 is expressed at the leading edge in multiple cell types including keratinocytes and MDCK cells, at roughly the same geographical location where cellular proliferation is occurring (Matoltsy and Viziam, 1970; Nguyen et al., 2000) Moyano, unpublished). Overexpression of LM-332 has also been shown to accelerate the proliferation rate of fibrosarcomas (Mizushima et al., 2002), as has exogenous exposure of LM-332 to kidney epithelial cells and mesenchymal stem cells (Hashimoto et al., 2006; Joly et al., 2006). Finally, inhibition of the LM-332-cellular interaction in both MCF-10A mammary epithelial cells and 804G rat bladder carcinoma cells results in decreased proliferation and downregulation of the ERK signaling pathway (Gonzales et al., 1999). Despite an obvious role of LM-332 in proliferation regulation, the mechanism for this control is still largely unknown.

The purposes of the studies presented in this chapter were, first, to determine if a

relationship existed between LM-332 synthesis and deposition, and epithelial re-formation in MDCK cells, second, to use the adenoviral shRNA targeted against LMα3 (Chapter 4) to identify if LM-332 was required for MDCK proliferation, and last, to understand the mechanism by which loss of LM-332 may lead to proliferative arrest.

5.2 Results

5.2.1 LM-332 Deposition and Proliferation Correlate

In vivo, it appears that LM-332 expression is limited to when the epithelium is forming, therefore, LM-332 was hypothesized to be present when cells were subconfluent, which is a time that MDCK cells resemble developing renal epithelia, but, that the protein would no longer be evident once the mature epithelium had re-formed. To first determine when LM-332 is expressed as the MDCK epithelium formed, cells were plated onto coverslips at low density and LM-332 protein expression was monitored over 7 days by immunofluorescence. Immunofluorescent staining showed that LM-332 was present on the basal surface when cultures were subconfluent, but was absent when the epithelium had re-formed (Figure 5.1A, compare days 1-3 to days 4 and 7). To confirm, more precisely the levels of LM-332 that were deposited into the extracellular matrix, MDCK cells were grown as above on plastic dishes. Cells were removed from the underlying matrix by treatment with dilute ammonium hydroxide (Michelson et al., 2000). The residual matrix proteins in the dish were then extracted with SDS-containing buffer and analyzed by immunoblot with an antibody against LMβ3. As in Figure 5.1A, LM-332 was deposited from days 1-3 as the cells reached initial confluency, but then declined sharply at day 5, and became undetectable by day 7 (Figure 5.1B). The failure to detect LMβ3 that was previously deposited, may suggest that LM-332 was degraded as cells reached a saturating density.

These results were also confirmed by examining the biosynthesis of LM-332. Cells were

pulse labeled and LM-332 was immunoprecipitated from extracts using an antibody against the entire LM-332 molecule (Figure 5.1C). On day 1, synthesis of all three chains was evident. By day 3, however, synthesis of both LMα3 and LMγ2 decline, while synthesis of LMβ3 continued. As deposited LMβ3 was not observed at times when cells were at high density (Figure 5.1A and B, day 5-7), the newly synthesized LMβ3 that was observed in Figure 5.1C day 7, was likely not secreted, but was retained within the endoplasmic reticulum and degraded without significant accumulation. Overall, these data suggest that LM-332 is produced and secreted when cells are subconfluent, but is no longer produced and possibly degraded once the epithelium has re-formed. These results are consistent with the observations *in vivo* that LM-332 is only expressed in developing renal epithelia.

If LM-332 is indeed required for proliferation to re-form an epithelium in MDCK cells similar to other cell types (Gonzales et al., 1999), a correlation should exist between the timing when LM-332 is deposited and when cells were the most proliferative. As the time-course and experimental set-up of the LM-332 studies described above was identical to that described in Chapter 3, it was possible to compare LM-332 synthesis and deposition to the timing of proliferation, as assessed by the BrdU time-course (Figure 3.3). LM-332 synthesis and deposition was the highest 24-48 hours after plating, which is exactly when cells were the most proliferative. Likewise, the absence of LM-332 at day 6-7 was consistent with absence of proliferation at day 7. These results suggest that there may be a relationship between LM-332 expression and proliferation to re-form the epithelium, and raise the possibility that LM-332 may, in some way, regulate proliferation in MDCK cells.

5.2.2 MDCK Proliferation is Inhibited Following Ad-shLMα3 Expression

Based upon the arguments and results described above, it was hypothesized, that LM-332 is required for MDCK proliferation. To test this hypothesis, synthesis of LM-332 was suppressed by expression of a shRNA targeted to the LMα3 subunit, as described previously (Chapter 4). Cells were infected with either Ad-shControl or Ad-shLMα3, and proliferation was analyzed by BrdU incorporation (Figure 5.2). Almost 60% of non-infected cells, and almost 50% of shControl infected cells incorporated BrdU, which was consistent with BrdU incorporation percentages previously observed in proliferating MDCK cells. In contrast, only 12% of MDCK cells infected with Ad-shLMα3 incorporated BrdU, which was significant at p-value<.001, indicating that these cells were essentially non-proliferative.

As proliferative arrest prevents progression through restriction points within the cell cycle, cells will accumulate in the phase of the cell cycle where arrest occurs. To determine where in the cell cycle proliferative arrest was occurring following expression of Ad-shLMα3, flow cytometric analysis of DNA content was performed (Figure 5.3A). Control cells had cell cycle profiles similar to what was expected for proliferative cells, that is, DNA content was divided among all three phases of the cell cycle. Specifically, in both non-infected and Ad-shControl cells, roughly 30% of cells were in G0/G1, 40% were in S phase, and around 20% were in G2/M. Oddly, most Ad-shLMα3 cells had very few cells in S-phase, but had over 40% of cells in both G1 and G2/M phases, which indicated that Ad-shLMα3 cells were potentially arresting in both G1 and G2/M. It should be noted that 36% of Ad-shLMα3 cells had two or more nuclei, which was never observed in the non-infected controls (Figure 5.3B). Based on the observed binucleation, and based on the fact that flow cytometry, when staining for DNA content cannot distinguish between one cell in G2/M of the cell cycle with 2n DNA content, versus one

cell with two nuclei with G1 DNA content, it was possible that Ad-shLMα3 cells may be arrested in solely in G1. Based on this data alone however, the possibility that these cells are arrested in both G1 and G2/M cannot be ruled out. The next section, therefore, will further address both G1 and G2/M arrest mechanisms.

5.2.3 Cyclin and Cdk Expression Following Expression of Ad-shLMα3

The LM-332 integrin receptors are coupled to growth factor receptors and can promote growth factor signaling. Cyclin D1 is expressed downstream of growth factor signaling pathways and initiates entry into the cell cycle in G1 (Fu et al., 2004). It was hypothesized that Ad-shLMα3-mediated proliferation arrest may, because of ligand loss, inhibit integrin-mediated growth factor signaling and, subsequently, prevent cyclin D1 expression. To test this hypothesis, cellular extracts from non-infected, Ad-shControl, or Ad-shLMα3 were immunoblotted for cyclin D1 and cdk4 (Figure 5.4 A-C). Surprisingly, expression of Ad-shLMα3 resulted in a five-fold increase in cyclin D1 relative to non-infected controls, and three-fold increase when compared to the Ad-shControl, which suggested that cell cycle inhibition in Ad-shLMα3 cells was not due to loss of cyclin D1 expression. As activity of the cyclin D1/cdk4 complex is prerequisite for expression of the second G1 cyclin, cyclin E (Zhang et al., 2000), it was also of interest to determine if cyclin E was expressed following expression of Ad-shLMα3. To determine if cyclin E was expressed, immunoblot analysis was again performed, analyzing for cyclin E and cdk2 in non-infected, Ad-shControl, and Ad-shLMα3 cells. As depicted in Figure 5.4D-F, comparison of non-infected and Ad-shControl to Ad-shLMα3 did not result in significant alteration of expression levels of cyclin E and cdk2. As cyclin E and cdk2 protein levels were similar to those observed in proliferating MDCK cells, cyclin E expression is likely

not influenced by suppression of LMα3.

In the previous flow cytometric studies, accumulations of cells in both G1 and G2/M were observed following suppression of LMα3. Normal cells at the G2/M transition increase cyclin B1 levels greater than four fold in comparison to G1/S (Hwang et al., 1995; Pines and Hunter, 1989). Additionally, cyclin B1 expression is regulated downstream of E2F (Lukas et al., 1999). Therefore, cells that have passed the pRB, G1 restriction point, should express cyclin B1, whereas those that are arrested at G1/S, should not. Cdk1, whose binding to cyclin B1 and is required for cdk1 kinase activity, is also regulated by E2F downstream of cyclin E/cdk2. To determine if Ad-shLMα3 cells were, in fact, progressing through the G1/S checkpoint, immunoblots were performed to analyze cyclin B1 and cdk1 expression (Figure 5.4 G-I). A significant decrease in expression was observed for both cyclin B1 and cdk1 following expression of Ad-shLMα3, which suggested that these cells were not progressing to G2/M, and were likely arrested in the G1 phase of the cell cycle.

5.2.4 The Cyclin E/Cdk2 Complex is Inactivated Following Expression of Ad-shLMα3

To determine which G1 cyclin/cdk complex was inactivated following suppression of LMα3, *in vitro* kinase assays were performed for cyclin D1/cdk4 (Figure 5.5A) and cyclin E/cdk2 (Figure 5.5B). To first assess the activity of cyclin D1/cdk4, an immunoprecipitation was first performed for cdk4. The precipitate was then incubated with ^{32}PγATP and the pRB substrate. Phosphorylation of pRB was then determined by SDS-PAGE and fluorography. As expected based on data described in the previous section, no difference in the ability of cyclin D1/cdk4 to phosphorylate its substrate was observed following expression of Ad-shLMα3, compared to non-infected and Ad-shControl cells (Figure 5.5A). These data suggested that the

cyclin D1/cdk4 complex was active, and was not responsible for proliferative arrest in the absence of LMα3.

To next assess the activity of the second G1 cyclin/cdk complex, cyclin E/cdk2, a similar kinase reaction was performed as described above, with the exception that cdk2 was immunoprecipitated, followed by a kinase reaction with the Histone H1 substrate. In non-infected and Ad-shControl cells, cdk2 complexes phosphorylated the Histone H1 substrate (Figure 5.5B). However, expression of Ad-shLMα3 completely eliminated the kinase activity of cyclin E/cdk2, as a phospho-histone band was not evident. These data suggest that it was the cyclin E/cdk2 complex that was inactivated following suppression of LMα3, and not cyclin D1/cdk2.

5.2.5 Cdk2 Inhibitory Proteins p21waf1 and p27kip1 are Expressed and Bound to Cdk2

Two inhibitory proteins are primarily responsible for the inactivation of cyclin E/cdk2 complexes: p21waf1 and p27kip1. As cdk2 was inactivated in Ad-shLMα3 cells, it was hypothesized that loss of LMα3 might result in expression of p21waf1 and/or p27kip1. To test this, immunoblot analysis for both p21waf1 and p27kip1 was performed on non-infected, Ad-shControl, and Ad-shLMα3 cells. As shown in Figure 5.6A, p21waf1 was not detected in non-infected or Ad-shControl cells. However, following expression of Ad-shLMα3, a dense p21waf1 doublet was observed. To confirm that both bands of the doublet were p21waf1, p21waf1 primary antibody and the p21waf1 blocking peptide associated with this antibody were incubated with the blot at the primary incubation step. Treatment with the blocking peptide eliminated both bands of p21waf1, which suggested that both bands were p21waf1.

To assess if the second cdk2 inhibitory protein, p27waf1 was also expressed following

expression of Ad-shLMα3, lysates generated above were reprobed for p27waf1. Inhibitory protein p27kip1 was expressed at very low levels in the non-infected control, slightly more was observed in Ad-shControl cells, and even more was evident in Ad-shLMα3 cells (Figure 5.6B). These data indicated that adenovirus expression alone might promote some increase in p27kip1 levels, although, not to the same extent as expression of Ad-shLMα3.

The inhibitory proteins p21waf1 and p27kip1 inhibit the activity of cdk2 by directly binding to the kinase. As high levels of p21waf1 and p27kip1 were observed and the cdk2 kinase was inactive, it was hypothesized that not only were p21waf1 and p27kip1 expressed following suppression of LMα3, but that they were bound to cdk2. To first confirm p21waf1 binding to cdk2, immunoprecipitations were performed using an antibody against cdk2 or p21waf1, followed by immunoblot of p21waf1 and cdk2, respectively (Figure 5.6 C and D). As shown in Figure 5.6 C and D, inhibitory protein p21waf1 only precipitated with cdk2 in Ad-shLMα3 cells. To next confirm p27kip1 binding to cdk2, an immunoprecipitation was performed using an antibody against cdk2, followed by immunoblot of p27kip1 (Figure 5.6E). A small amount of p27kip1 precipitated with cdk2 in non-infected controls. Equal levels were precipitated in Ad-shControl compared to Ad-shLMα3. As Ad-shControl cells are proliferative, yet levels of p27kip1 are observed in association with cdk2 at equal levels to Ad-shLMα3 cells, these results suggest that p21waf1 likely is more responsible for the promotion of cell cycle arrest following suppression of LMα3.

5.2.6 JNK and Akt are Phosphorylated Following Expression of Ad-shLMα3

To determine how p21waf1 expression might be regulated, it was next of interest to examine signaling pathways upstream of p21waf1 that may be altered in the absence of LMα3.

The MAPK and PI3K/Akt signaling pathways, although traditionally thought of as "stimulators" of cellular proliferation, have been shown to promote the expression of p21waf1. Activation of the ERK1/2 and p38 MAPK pathways can coordinately activate expression of p21waf1 in fibroblasts (Todd et al., 2004). JNK activity, specifically, activates c-jun, which in combination with c-Fos forms the transcription factor, AP-1, and c-jun activity has been shown to increase the expression of p21waf1 (Kardassis et al., 1999). Last, activation of the PI3K/Akt signaling pathway may also promote p21waf1 expression, as inhibition of this pathway by treatment with a PI3K inhibitor, prevented p21waf1 expression following treatment the DNA damaging drugs (Mitsuuchi et al., 2000).

To determine how the activity of the MAPK and PI3K pathways were altered following expression of Ad-shLMα3, cell extracts were generated from non-infected, Ad-LacZ, and Ad-shLMα3 cells, and immunoblotted for ERK and pERK, p38 and pp38, JNK and pJNK, and Akt and pAkt (Figure 5.7A). Phosphorylation of ERK and p38 were unaltered in Ad-shLMα3 cells when compared to controls. Phospho-JNK was not observed in non-infected or Ad-LacZ cells, but was hyper-phosphorylated in Ad-shLMα3 cells. Phospho-Akt was observed in non-infected and Ad-LacZ cells, but Akt was hyper-phosphorylated in Ad-shLMα3 cells. These data suggest that suppression of LMα3 results in increased phosphorylation of JNK and Akt.

To next determine if the high levels of phosphorylated JNK was responsible for the increased p21waf1, p21waf1 expression was observed in non-infected, Ad-shControl, or Ad-shLMα3 cells treated with 30μM of the JNK inhibitor, SP600125 or DMSO vehicle control. SP600125 is an ATP competitive inhibitor that blocks the downstream activation of JNK substrates, such as c-jun. As depicted in Figure 5.7B, in DMSO treated control cells, expression of Ad-shLMα3 continued to promote expression of p21waf1, consistent with previous

observations. In Ad-shLMα3 cells, the treatment with SP600125 did not eliminate expression of the p21waf1 protein, but it did eliminate the faster migrating p21waf1 band of the p21waf1 doublet. This suggests that JNK activity may be at least partially responsible for the observed p21waf1 doublet, although, at this time it is unclear how JNK-mediated p21waf1 doublet formation may affect cellular proliferation in Ad-shLMα3 cells.

5.3 Discussion

5.3.1 Summary

LM-332 is produced and secreted in subconfluent MDCK cells, but it is no longer produced once the epithelium is re-formed. LM-332 production coincides with cell proliferation during epithelial re-formation, and LM-332 degradation correlates with the onset of cellular quiescence. Suppression of LMα3 with Ad-shLMα3 results in proliferative arrest, which is likely due to increased levels of p21waf1, and possibly p27kip1 that associate with, and inactivate cyclin E/cdk2. The kinases, JNK and Akt are hyper-phosphorylated following expression of Ad-shLMα3, and inhibition of JNK eliminates the appearance of the faster migrating p21waf1 polypeptide.

5.3.2 Regulation of p21waf1: Are the Integrins Involved?

Following the loss of laminin-integrin interactions, could integrin signaling promote the expression of p21waf1 and lead to cell cycle arrest? As described in the introduction, the cytoplasmic domain of integrin β4 contains many phosphorylation sites, which are differentially regulated ligand binding and cross-talk with growth factor receptors. Ligand binding of integrin α6β4 results in tyrosine phosphorylation of the β4 subunit on Tyr1526 and Tyr1494, and

subsequent signaling through the Shc and PI3K pathways, respectively (Dans et al., 2001; Shaw, 2001). The phosphorylation of integrin β4 can also result in phosphorylation of the EGF receptor (Moro et al., 2002). These events are thought to be required for proliferation because cells that are treated with β4 integrin function blocking antibodies, as well as cells expressing mutant forms of integrin β4 do not proliferate (Mainiero et al., 1997; Nikolopoulos et al., 2005). A series of studies suggest that ligand may not be required for integrin β4 signaling. Expression of a mutant β4 integrin that had no extracellular domain, and was therefore unable to associate with ligand, continued to be associated with the Met receptor, and resulted in phosphorylation of β4 integrin (Trusolino et al., 2001). Using these same mutants, Gamballeta, *et al* showed that the mutant β4 integrin continued to associate with ErbB2, which resulted in PI3K signaling (Gambaletta et al., 2000). In the latter study, a region of the β4 cytoplasmic domain between amino acids 854 and 1183 was important to promote PI3K signaling. This is a different region of the β4 subunit that promotes PI3K signaling after ligand binding. The ability of β4 integrin, in the absence of ligand binding, to promote or prevent cellular proliferation was not assessed in these studies. In the rectal carcinoma cell line, RKO, however, cells that expressed a full-length integrin β4 promoted expression of p21waf1, whereas mutant forms lacking the cytoplasmic domain did not (Clarke et al., 1995). In these studies, it was not determined if p21waf1 expression was mediated by interaction with LM-332, and it was unclear if the RKO cell line endogenously expressed the laminin. Therefore, when results of the described studies are taken together, it seems possible that the integrin β4 subunit may be capable of signaling p21waf1 expression and cell cycle arrest in absence of ligand, but in the presence of growth factor receptor association.

It is unclear if integrin α3β1 signals in the absence of ligand. β1 integrins can also associate with growth factor receptors, but only in adherent cells (Legate et al., 2009). In the absence of the β1 integrin-growth factor receptor interaction, prostate cancer cells do not proliferate, suggesting that the growth factor receptor is only fully activated to promote proliferation following adhesion (Goel et al., 2005). The disruption of integrin-ligand binding therefore may prevent proliferation and signal p21waf1 expression through the partially activated growth factor receptor and not the integrin.

5.3.3 Cyclin D1 Expression Following Expression of Ad-shLMα3

Integrin signaling following adhesion is most commonly connected with expression of cyclin D1 and cellular proliferation. Unexpectedly, following expression of Ad-shLMα3, a five-fold increase in Cyclin D1 protein levels AND failure to proliferate were observed (Figure 5.5 A-C). Similar to our observations, high levels of cyclin D1 are often concomitant with G1 cell cycle arrest and have been observed in senescent cells (Atadja et al., 1995; Han et al., 1999; Lucibello et al., 1993). Very little is known about the relationship between cyclin D1 expression and the promotion of proliferative arrest. Increasing evidence suggests that an intricate and delicate relationship exists between cyclin D1 and the cell cycle inhibitory proteins, p21waf1 and p27kip1. Oddly, p21waf1 and p27kip1 association with the cyclin D1/cdk4 complex seems to be required for stability and assembly of the kinase. Indeed, in primary mouse embryonic fibroblasts that lack p21waf1 and p27kip1, cyclin D1 and cdk4 complexes do not assemble, but adding the proteins back restores complex assembly (Cheng et al., 1999). Additionally, p21waf1, upon binding to the complex, provides a localization signal for their nuclear import (LaBaer et al., 1997) and inhibits GSK3β phosphorylation of cyclin D1, which retains it in the nucleus (Alt

et al., 2002). Increases in cyclin D1 also seem to stabilize p21waf1 by inhibiting its degradation (Coleman et al., 2003). It would seem contradictory that increased p21waf1 and p27kip1 in association with cyclin D1/cdk4 are required for proliferation, but that the same inhibitory proteins in association with cyclin E/cdk2 lead to cell cycle arrest. It is possible that p21waf1, at low levels promotes proliferation by aiding in cyclin D1/cdk4 assembly, nuclear import, and activity, but when the cdk4 kinase is super-saturated, excess p21waf1 or p27kip1 are free to bind to, and inactivate cdk2, which would promote cell cycle arrest. In these studies, low levels of p27kip1, but not p21waf1 were detected in proliferating cells (Figures 5.6 and Chapter 3, Figure 3.5). It is possible, however, that the p21waf1 antibody was not sensitive enough to detect low levels of p21waf1 protein.

5.3.4 p21waf1 Doublets: Causes and Consequences

Others have often observed p21waf1 as a doublet by immunoblot, which is consistent with the results described in Section 5.2.5, Figure 5.6. Inhibitory protein p21waf1 is observed as a doublet for two reasons: proteolytic cleavage of the C-terminus, or phosphorylation. Inhibitory protein p21waf1 is cleaved at the C-terminus, which results in two 20-21kD peptides. The first is full length, but the second lacks several phosphorylation sites and the NLS, but retains the ability to interact with cyclins and cdks. Although one could imagine that the faster migrating p21waf1 would be unable to function as a cell cycle inhibitor due to loss of its NLS, existing data on the topic are contradictory. In one study, the faster migrating form seems to preferentially bind to and inactivate cyclin B1 (Tchou et al., 1996), but in another, the cleaved p21waf1 was mainly localized to the cytoplasm (Poon and Hunter, 1998).

Phosphorylation of p21waf1 occurs on six different sites on the molecule (Child and Mann, 2006), which differentially prevents p21waf1 association to its targets (i.e. cyclins, cdks,

PCNA). Unbound p21waf1 has a short half-life (Gartel and Radhakrishnan, 2005); hence phosphorylation of p21waf1 typically results in rapid degradation of the protein. As stable p21waf1, which was bound to cdk2 was observed; it would seem unlikely that the p21waf1 doublet was caused by phosphorylation.

5.3.5 Does Loss of LMα3 Result in Cell Senescence?

MDCK cells, following expression of Ad-shLMα3 exhibited many phenotypes that are commonly observed in senescent cells. Cellular senescence is a non-proliferative cellular state, activated by cellular stresses such as DNA damage, oxidative stress, telomere uncapping, and oncogene activation (Ben-Porath and Weinberg, 2005). Hallmarks of senescent cells, among other factors, are G1 cell cycle arrest, high levels of p21waf1 (Kagawa et al., 1999) hypo-phosphorylated pRB, and increased levels of cyclin D1 (Han et al., 1999). Senescent cells are also flattened and enlarged, unresponsive to growth factors, and have cytochemically detectable β-galactosidase (β-gal). As β-gal expression is a marker for cellular senescence, a common β-gal staining procedure is used to determine if cells are, or are not senescent (Severino et al., 2000). This procedure was unsuccessfully attempted many times on Ad-shLMα3 cells, but β-gal staining was never detected in these, or in supposed "positive" controls (MDCK cells treated with bleomycin (Aoshiba et al., 2003) or camptothecin (recommended by Dr. Kay Macleod, the University of Chicago to promote DNA damage)). It was therefore unclear if expression of Ad-shLMα3 resulted in cellular senescence, despite the fact that these cells had many hallmarks of senescent cells.

5.3.6 Model for LM-332 Involvement in Proliferation Control

The literature suggests that LM-332 signaling, likely through integrins, positively signals through MAPK to promote proliferation. Based on our studies, and those described in 5.3.2, we could hypothesize an addition to this model: in the absence of LM-332, integrin α6β4 is still phosphorylated and participates in growth factor receptor signaling cross-talk, resulting in phosphorylation events within the long integrin β4 subunit, that promote expression of p21waf1, inactivation of cyclin E/cdk2, and subsequent G1 arrest (Figure 5.8). Further studies are required to validate the requirement for LM-332 and confirm the involvement of the integrins in this model, which will be addressed in Chapter 6.

Chapter 5 Figures

Figure 5.1: LM-332 is Produced and Deposited in Subconfluent Cells

(A) 7.5x10^5 MDCK cells were plated onto coverslips in 7, 35mm dishes and grown as described previously (Chapter 2, 2.1.2). Cells were fixed with 3% PFA solution and IF was performed. Coverslips were stained for LM-332 (red) with the 8LN5 rabbit anti-LM-332 polyclonal antibody (1:200), actin (green) with phalloidin488 (1:100), and DAPI (blue). Images were taken on the Axioskop conventional fluorescence microscope using the 63X oil immersion objective. Bars, 20μM.

(B) 7.5x10^6 MDCK cells were plated into 7, 35mm dishes and grown as described above. At appropriate time-points, endogenous matrix was extracted as described in *2.8.2*. The protein concentration of the extracts was determined and samples were normalized. Samples were subjected to SDS-PAGE on a 6% gel, and immunoblotted for LMβ3, with a mouse anti-LMβ3 antibody (1:1000).

(C) 7.5x10^5 MDCK cells were plated into 4, 35mm dishes, and allowed to grow for one, three, four, and seven days, respectively. Prior to time-point harvest, cells were pulsed for 40 minutes with ^{35}S Methionine/Cysteine labeling medium. Cells were then lysed with RIPA buffer, stored at -80°C until all samples were ready, then subjected to IP with 5μg Rabbit-anti-LM-332 antibody. Samples were run on a 6% polyacrylamide gel, and bands visualized by fluorography.

A

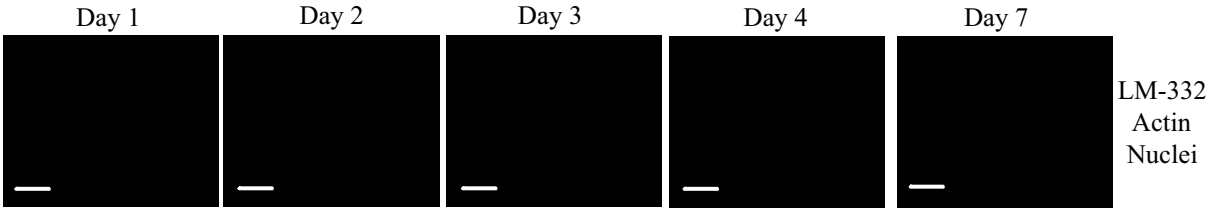
Day 1
Day 2
Day 3
Day 4
Day 7
LM-332
Actin
Nuclei

B

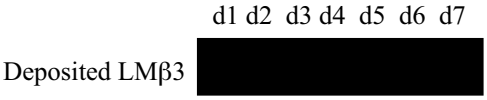
d1 d2 d3 d4 d5 d6 d7
Deposited LMβ3

C

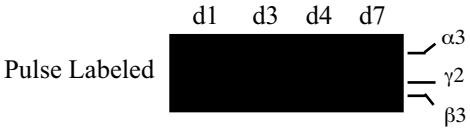
d1 d3 d4 d7
Pulse Labeled
α3
γ2
β3

Figure 5.2 Expression of Ad-shLMα3 Inhibits MDCK Proliferation

MDCK cells were infected with either Ad-shControl (shPKCα) or Ad-shLMα3. After 18hrs, .25x10^6 cells were replated onto glass coverslips and allowed to grow for another 24hrs. Six hours before harvest, 50μM BrdU in MDCK growth medium was added to cells. After 6hr incubation, cells were fixed with 3% PFA and stained for BrdU with the rat anti-BrdU antibody (1:500) and total nuclei (DAPI). Samples were imaged by conventional fluorescence microscopy and images quantified for BrdU incorporation and total nuclei. Graph depicts the average percent BrdU incorporation from three experiments, and error bars are the standard deviation between experiments. P-value was determined by two-tailed student's *t-test,* comparing the shControl and shLMα3 groups to the non-infected control group.

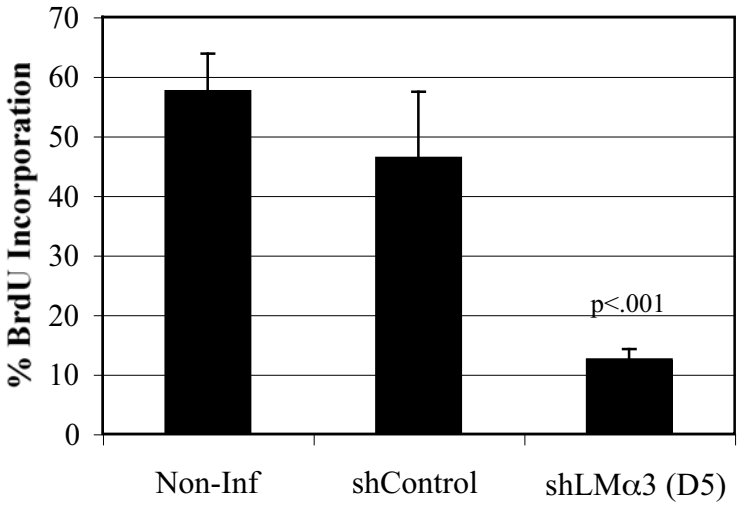
% BrdU Incorporation
70
60
50
40
30
20
10
0
p<.001
Non-Inf
shControl
shLMα3 (D5)

Figure 5.3 Ad-shLMα3 Cells have an Accumulation of DNA Content in G1 and G2/M of the Cell Cycle and are Bi-nucleated

(A) MDCK cells were infected with Ad-shControl (shPKCα) or Ad-shLMα3 (D5). 18hrs after infection, 10^6 cells were replated into 60mm tissue culture dishes, and allowed to grow for another 24hrs. Cells were fixed in 70% EtOH and stained with 1X PI stain. Samples were subjected to flow cytometry, and analyzed with FlowJo software, gating for the single-cell population. The x-axis is DNA content, and the y-axis is number of cells. The data table depicts average percentage of cells in G1, S, or G2/M phases, as determined by the Watson algorithm within FlowJo, from three or more experiments, and ± represents the standard deviation between experiments.

(B) Prior to fixation in (A), living cells were imaged by phase-contrast microscopy with an inverted microscope using the 40X objective. Five fields were imaged, and total and bi-nucleated cells were counted. Percentage is the average number of bi-nucleated cells between fields. ± represents standard deviation between fields.

A

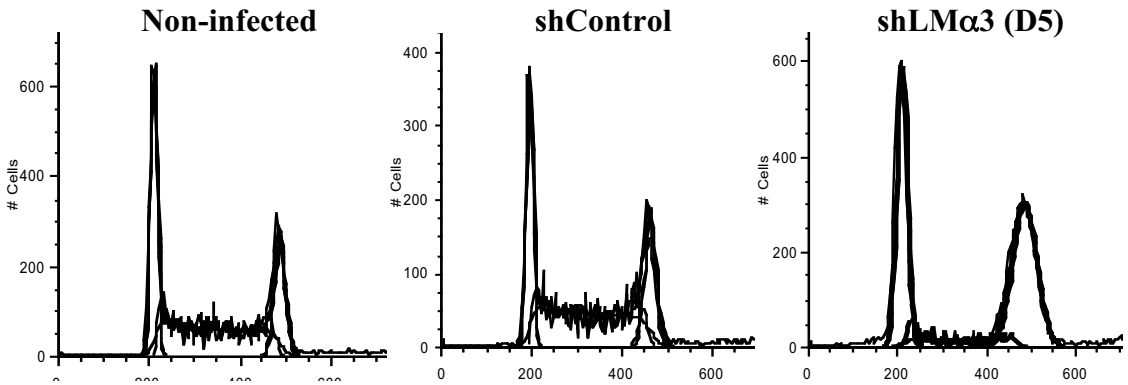

Cell Cycle Phase	Non-Infected	shControl	shLMα3 (D5)
G1	31.68± 4.04%	26.55±4.74%	46.87 ± 9.27%
S	41.47 ± 6.90%	42±7.35%	8.09 ± 4.30%
G2/M	23.12 ± 6.56%	17.3±1.98%	40.14 ± 4.29%

B

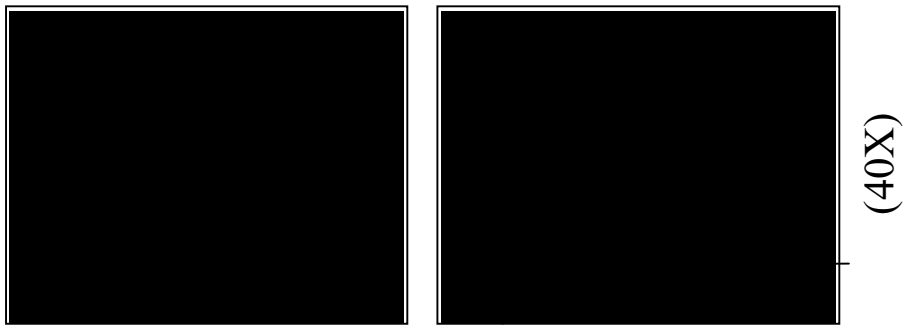

0%±0% 2+ Nuclei

36.2%±16.1% 2+ Nuclei

Figure 5.4 Cyclins and Cdks are Expressed Following Expression of Ad-shLMα3

MDCK cells were infected with Ad-shControl (Ad-PKCα), or Ad-shLMα3. After 18hrs, 2x10^6 cells were replated into 60mm tissue culture dishes. SDS cellular extracts were made, protein concentration were determined, and samples were normalized. Proteins were separated by SDS-PAGE on 15% polyacrylamide gels, and immunoblotted for (A) cyclin D1 and cdk4, (D) cyclin E and cdk2, or (E) cyclin B1 and cdk1. Each blot was stripped and re-probed two times: once for the partnering cyclin or cdk, and once for actin. Densitometric analysis (B-C; E-F; H-I) was performed by first normalizing each band to its actin counterpart, then averaging band density from three experiments. Fold change for all parameters was computed by comparing shControl and shLMα3 samples to non-infected control samples. *p-value<.05, **p-value<.005 was determined by two-tailed student's *t-test.* Experiments were repeated with Ad-LacZ and Ad-shLacZ controls, and yielded the same results (data not shown).

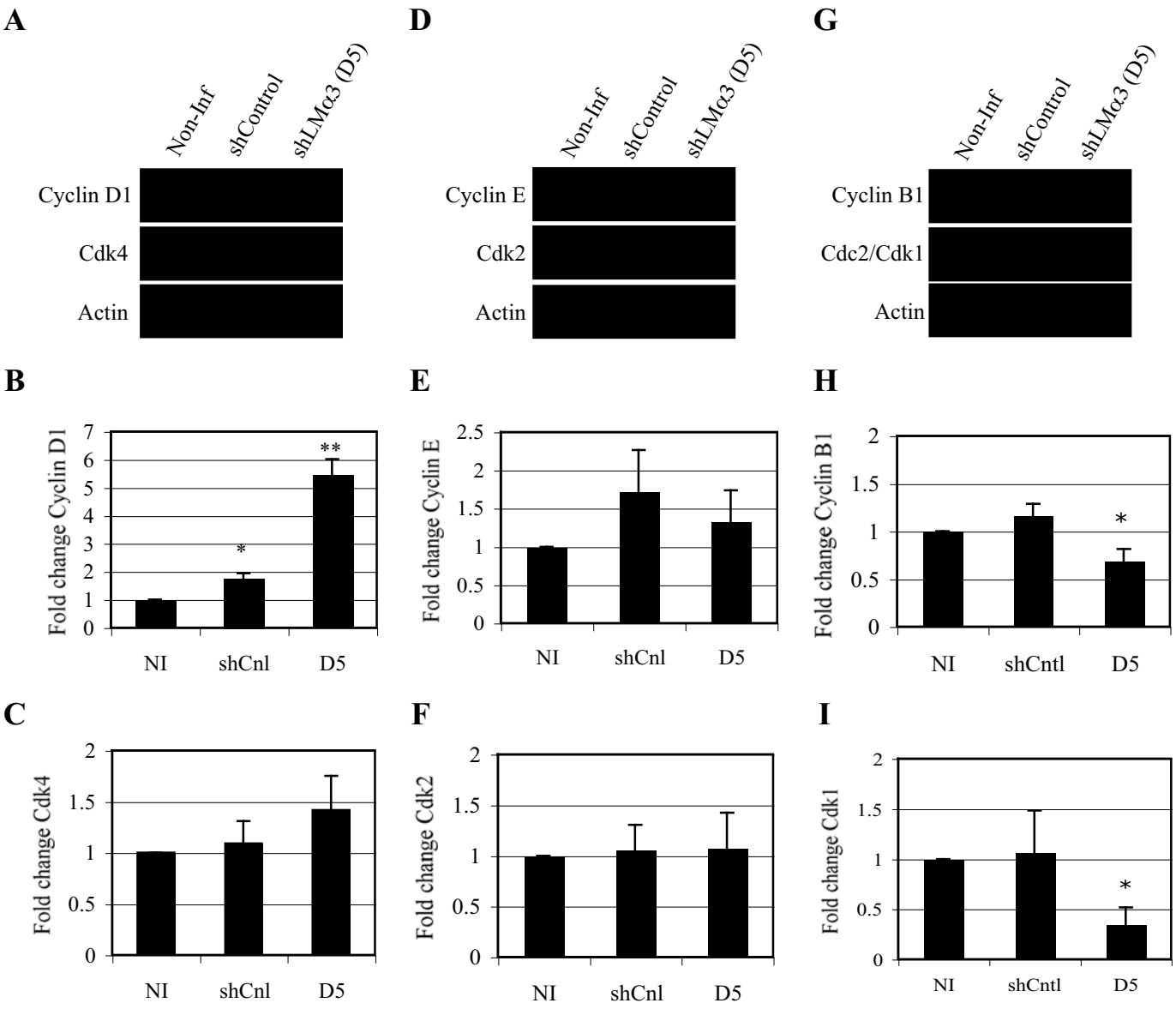
A
Non-Inf
shControl
shLMc3 (D5)
Cyclin D1
Cdk4
Actin
D
Non-Inf
shControl
shLMc3 (D5)
Cyclin E
Cdk2
Actin
G
Non-Inf
shControl
shLMc3 (D5)
Cyclin B1
Cdc2/Cdk1
Actin
B
Fold change Cyclin D1
NI
shCnl
D5
E
Fold change Cyclin E
NI
shCnl
D5
H
Fold change Cyclin B1
NI
shCntl
D5
C
Fold change Cdk4
NI
shCnl
D5
F
Fold change Cdk2
NI
shCnl
D5
I
Fold change Cdk1
NI
shCntl
D5

Figure 5.5 The Cyclin E/Cdk2 Complex is Inactive Following Expression of Ad-shLMα3

(A) MDCK cells were infected with Ad-shControl (shPKCα) or Ad-shLMα3. Two extra plates of non-infected cells were created for use as kinase assay controls. 18hrs after infection, 1.25x10^6 cells were replated into 60mm tissue culture dishes. Cells were extracted with Cdk4 kinase assay buffer, and cdk4 from lysates was immunoprecipitated with 7.5μg rabbit anti-cdk4 antibody and protein A trisacryl beads. Rabbit IgG (7.5μg) was used in a control IP. Precipitates were then incubated with 5μCi ^{32}PγATP and 2μg recombinant C-terminal pRB peptide. Simultaneously, a control with no pRB was also incubated with 5μCi ^{32}PγATP. After kinase reaction, samples were denatured and subjected to SDS-PAGE on a 12% polyacrylamide gel, then transferred onto a PVDF membrane. Bands were visualized by fluorography. PVDF membrane was then immunoblotted for total cdk4.

(B) MDCK cells were infected as above. 18 hours after infection, 2.25x10^6 cells were replated into 10cm tissue culture dishes. Cells were extracted in Cdk2 kinase assay buffer, and cdk2 from lysates was immunoprecipitated with 5μg rabbit anti-cdk2 antibody and protein A trisacryl beads. Rabbit IgG (5μg) was used in a control IP. Precipitates were then incubated with 25μCi ^{32}PγATP and 1.5μg Histone H1 protein (His-H1). Simultaneously, a control with no His-H1 was also incubated with 25μCi ^{32}PγATP. Kinase activity was observed as above. PVDF membrane was then immunoblotted for total cdk2.

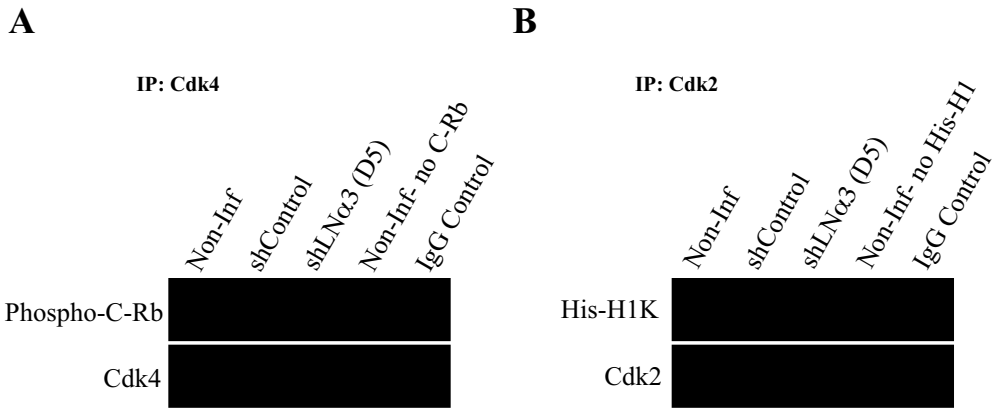
A
IP: Cdk4
Non-Inf
shControl
shLNα3 (D5)
Non-Inf- no C-Rb
IgG Control
Phospho-C-Rb
Cdk4
B
IP: Cdk2
Non-Inf
shControl
shLNα3 (D5)
Non-Inf- no His-H1
IgG Control
His-H1K
Cdk2

Figure 5.6 Cell cycle Inhibitory Protein p21waf1 is Expressed and Bound to Cdk2 Following Expression of Ad-shLMα3

(A and B) MDCK cells were infected with Ad-shControl (Ad-shPKCα), or Ad-shLMα3. After 18hrs, 2x10^6 cells were replated into 60mm tissue culture dishes, then incubated another 24hrs. Cells were extracted in SDS extraction buffer, protein concentration determined, and normalized. Samples were subjected to SDS-PAGE on 15% polyacrylamide gels, then immunoblotted with rabbit anti-p21waf1 (1:1000) or rabbit anti-p21 pre-incubated with p21waf` blocking peptide (1:500) (A), or mouse anti-p27kip1 (1:1000) (B). Blots were stripped and reprobed two times, once for the opposite (p21waf1 versus blocking peptide, etc), and once for actin.

(C and D) MDCK cells were infected and replated as described above. Cells were extracted with RIPA buffer, protein concentration determined, and normalized. Samples were IP'd with either rabbit anti-cdk2 (5μg) (C), rabbit anti-p21 (5μg) (D), or rabbit IgG (5μg), subjected to SDS-PAGE on a 15% polyacrylamide gel, and then transferred to PVDF membrane. Membranes were immunoblotted for either p21waf1 or cdk2, then stripped and re-probed for the opposite protein. In (D), a different lot number of the p21waf1 antibody was used, and resulted in three bands in the shLMα3 sample. The bottom two bands were p21waf1 (brackets). The top band, present in all samples including the IgG control, was believed to be non-specific binding by the p21 antibody.

(E) MDCK cells were infected, replated, and harvested as in C and D. A small amount of lysate was reserved from each sample as 'Pre-IP' control. The remainder was immunoprecipitated with 5μg of rabbit anti-Cdk2 primary antibody, or 5μg rabbit IgG. Precipitates were subjected to SDS-PAGE on a 12% gel, and immunoblotted for p27kip1 with a mouse anti-p27kip1 antibody (1:1000).

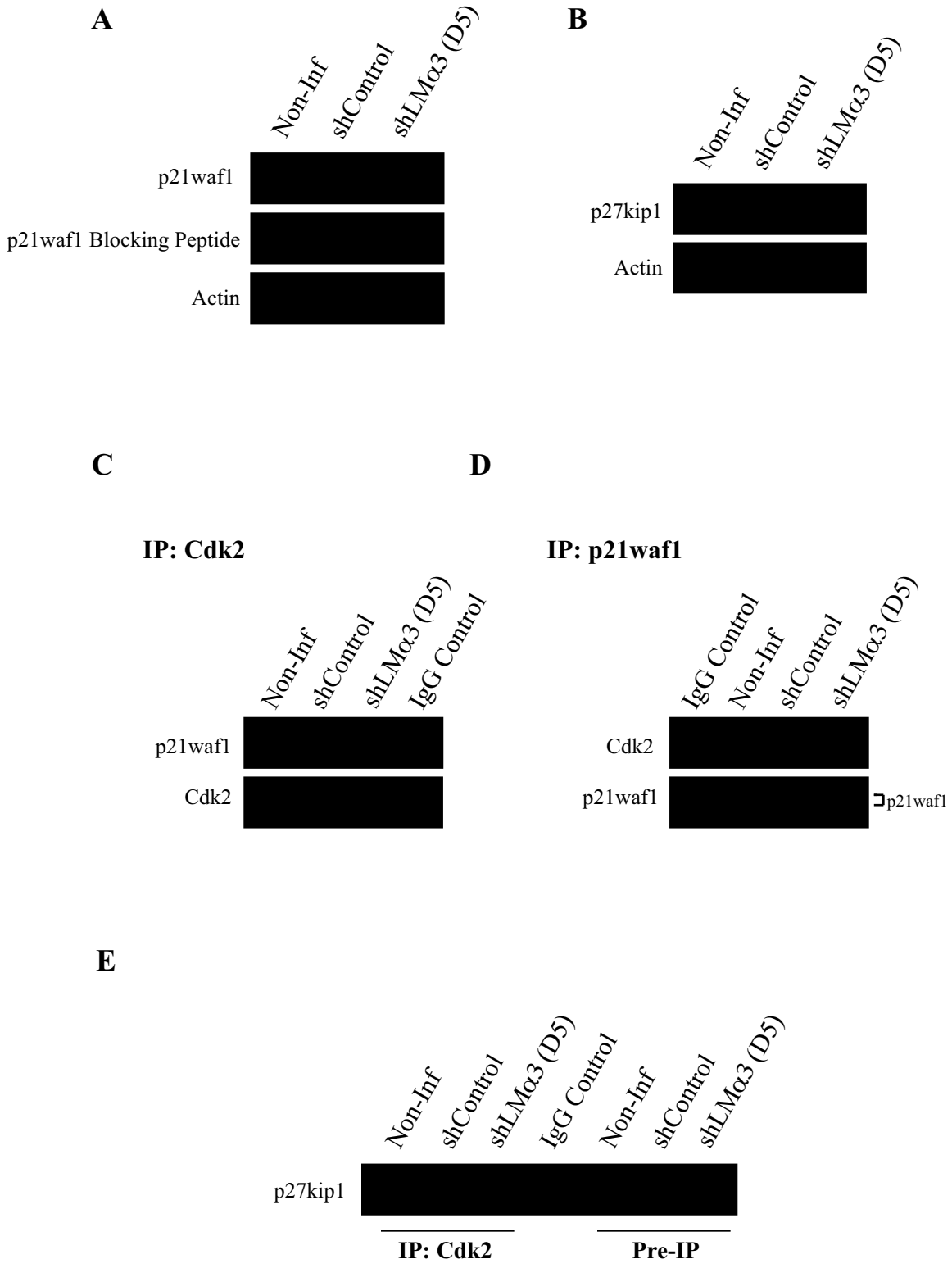
A
Non-Inf
shControl
shLMα3 (D5)
p21waf1
p21waf1 Blocking Peptide
Actin
B
Non-Inf
shControl
shLMα3 (D5)
p27kip1
Actin
C
IP: Cdk2
Non-Inf
shControl
shLMα3 (D5)
IgG Control
p21waf1
Cdk2
D
IP: p21waf1
IgG Control
Non-Inf
shControl
shLMα3 (D5)
Cdk2
p21waf1
p21waf1
E
Non-Inf
shControl
shLMα3 (D5)
IgG Control
Non-Inf
shControl
shLMα3 (D5)
p27kip1
IP: Cdk2
Pre-IP

Figure 5.7 JNK1/2 and Akt are Hyper-Phosphorylated Following Ad-shLMα3 Expression.

(A) MDCK cells were infected with Ad-LacZ or Ad-shLMα3. Cells were extracted in Rho-binding lysis buffer, protein concentration determined, and samples normalized. Samples were subjected to SDS-PAGE on 15% polyacrylamide gels, then immunoblotted with rabbit anti-ppERK (1:2000), rabbit anti-pp38 (1:1000), rabbit anti-pJNK (1:1000), or rabbit anti-pAkt (1:1000). Blots were stripped and reprobed for total ERK (1:200), total p38 (1:1000), total JNK (1:200), or total Akt (1:1000), respectively.

(B) MDCK cells were infected with Ad-shControl (shPKCα) or Ad-shLMα3. After 18hrs, cells were divided into two sets containing .5x10^6 cells, each, and were replated into 35mm dishes. 5 hours after replating, JNK inhibitor, SP600125 (Calbiochem) was diluted to $[30\mu M]_f$ in MDCK growth medium and added to one set of samples. The "untreated" samples were incubated with DMSO in MDCK growth medium (1: 350). 19hrs later, cells were extracted with SDS extraction buffer, protein concentration was determined, and samples were normalized. Samples were denatured and alklyated, then subjected to SDS-PAGE on a 12% gels. Gels were transferred to a PVDF membrane and immunoblotted for p21waf1, using a rabbit anti-p21waf1 antibody (1:750) (C). Membrane was then stripped and reprobed for actin.

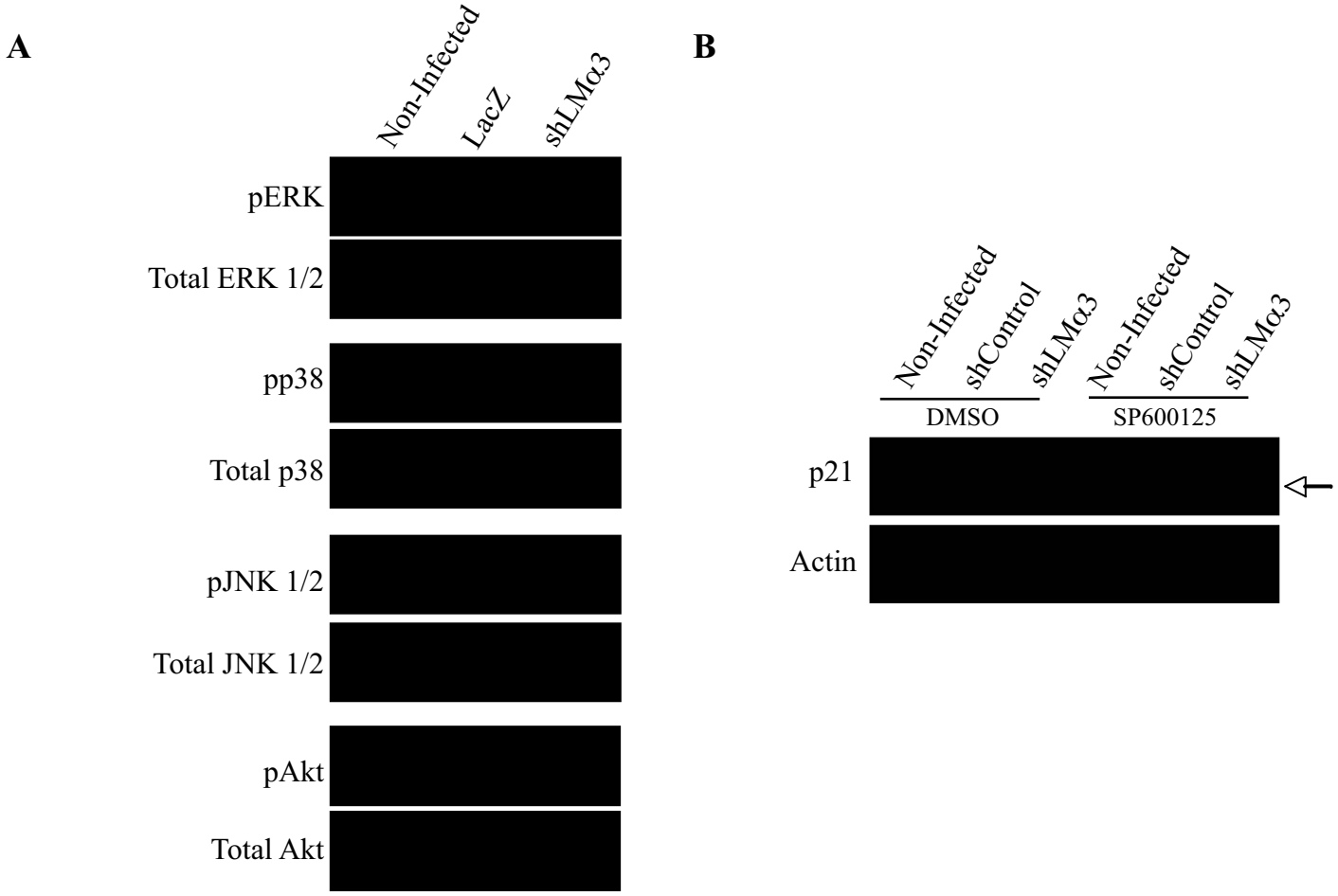
A
Non-Infected
LacZ
shLMα3
pERK
Total ERK 1/2
pp38
Total p38
pJNK 1/2
Total JNK 1/2
pAkt
Total Akt
B
Non-Infected
shControl
shLMα3
Non-Infected
shControl
shLMα3
DMSO
SP600125
p21
Actin

5.8 Model for LM-332-Mediated Cell Cycle Arrest

Based on our studies, and the studies described by others (Clarke et al., 1995; Nikolopoulos et al., 2005; Trusolino et al., 2001), we propose that in the absence of LM-332, integrin α6β4 continues to be phosphorylated by cross-talk with growth factor receptors. However, in the absence of ligand binding, integrin β4 signals through JNK and/or Akt, resulting in expression of p21waf1, which inactivates the cyclin E/cdk2 complex, and results in G1 cell cycle arrest.

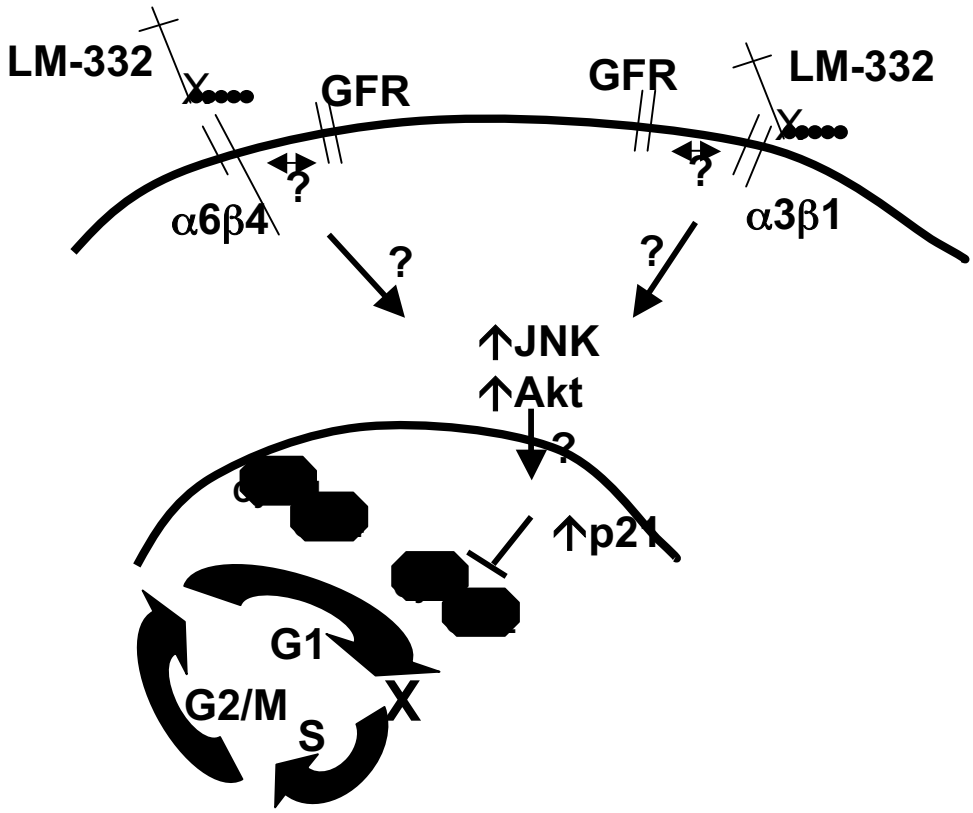
LM-332
GFR
GFR
LM-332
?
?
α6β4
α3β1
?
?
↑JNK
↑Akt
?
↑p21
G1
G2/M
S
X

Chapter 6:
Validation of the Ad-shLMα3-Mediated Proliferation Defect

6.1 Introduction

Data described in the previous chapter showed that expression of an adenoviral-shRNA targeted against LMα3 arrested proliferation, which was likely caused by the cell cycle inhibitory protein, p21waf1. Although these data were consistent with other studies that describe a requirement for LM-332 in epithelial proliferation control (Gonzales et al., 1999; Joly et al., 2006), they were obtained using only one shRNA target sequence. The results, therefore, must be validated using additional target sequences and alternate methods of inhibiting the LM-332-mediated signaling pathways.

The most important reason to validate data obtained using RNAi expression systems is the numerous off-target effects generated by RNAi target sequences. RNAi off-targeting is defined as the suppression of genes that are unrelated to the target gene, in more than one functional RNAi replicate (Echeverri et al., 2006). Off-target effects can result in 1.5 to 4-fold changes in the expression of up to hundreds of genes (Jackson et al., 2003). In one study, for example, when expression signatures by microarray analysis were performed from cells

transfected with 12 different siRNAs targeting three different genes, suppression of 347 off-targeted genes were observed (Birmingham et al., 2006). In some cell types, off-target effects have been linked to the method of delivery, concentration of the siRNA, or even the cell type in which studies were performed (Fedorov et al., 2006; Fedorov et al., 2005). Off-target effects, however, are thought to largely result from perfect RNAi matches to the 3' untranslated region (UTR) of one or more mRNA sequences (Birmingham et al., 2006; Lin et al., 2005b).

The phenotypic outcomes of off-target effects are potentially numerous depending on the genes that are non-specifically altered. Eliminating off-target effects by changing RNAi design is currently impossible. Controlling for off-target effects, therefore, is crucial to understand if, and how, suppression of a gene may result in phenotypic alterations within the cell. 'Rescue' and 'redundancy' experiments are the best ways to confirm RNAi specificity against a particular target. Rescue experiments are performed by co-expression of a functional version of the targeted gene that is resistant to RNAi-mediated suppression. Alternatively, a plasmid encoding for the same protein, but from a different mammalian species can be expressed as long as the target sites are not identical. In both scenarios, if the RNAi-mediated phenotype is specific, and not an off-target effect, the phenotype will be reversed.

In addition to rescue experiments, redundancy experiments are also necessary to confirm RNAi target specificity. In this case, redundancy refers to the use of multiple target sequences against the gene of interest. A debate currently exists as to the optimal number of target sequences necessary to confirm a phenotype. The general thought is that two RNAi target sequences are sufficient if other controls are in place, for example, rescue controls, and negative, non-targetting RNAi controls. In the absence of either control, more RNAi target sequences are required (Echeverri et al., 2006).

The purpose of these studies therefore, was, to use rescue and redundancy experiments to validate that the observed proliferative defect was due to the suppression of LMα3. Several approaches were taken to confirm the requirement for LMα3 in the control of MDCK proliferation. First, Ad-shLMα3 cells were either replated in the presence of endogenous MDCK LM-332, or Ad-shLMα3 was infected into a stable, human LMα3-expressing cell line. In both cases, proliferation and/or p21waf1 expression was analyzed. Second, the requirement for the LM-332 integrin receptors, α3β1 and α6β4 in LM-332-mediated proliferation control was analyzed; finally, five more siRNA target sequences specific for LMα3 were generated and proliferation was analyzed following the suppression of LMα3.

6.2 Results

6.2.1 Characterization of MDCK Endogenous Matrix to be used for Ad-shLMα3 Rescue Experiments.

Subconfluent MDCK cells secrete LM-332 and deposit it into the extracellular matrix (Figure 5.1). Previous reports from other laboratories have indicated that it is possible to remove cells from a LM-332 rich matrix, and use the matrix as a substratum on which to grow cells The matrix is thought to be functional because the epitope required for LMα3 antibody binding is preserved, and cells attach to it and form stable adhesions (Langhofer et al., 1993) (Plopper et al., 1996). Typical RNAi rescue experiments require co-expression of the functional protein. In our studies, an extracellular matrix protein had been suppressed, and not an intracellular protein. The functional LMα3 protein could therefore be re-introduced by plating Ad-shLMα3 cells onto a LM-332 rich matrix previously deposited by normal MDCK cells.

To ‘coat’ plates with a LM-332 rich matrix on which to re-plate Ad-shLMα3 cells, non-infected MDCK cells were grown to 90-95% confluency. At this time, based on studies

described in Figure 5.1, it was thought that LM-332 would still be present, and since cells were almost confluent, the protein would be uniformly distributed on the plate. Cells were removed from the matrix by treatment with sterile dilute ammonium hydroxide, followed by several washes with sterile de-ionized water. As a negative control, plates were coated with rat collagen I. Collagen I was chosen for several reasons. First, commercially available collagen I is a pure substratum and contains no LM-332 or other laminin isoforms, and second, MDCK cells attach well to it. Endogenous matrix from Ad-shLMα3 cells was not used as a negative control because how the structure and function of the endogenous matrix of Ad-shLMα3 cells might be altered in the absence of LMα3 has not been tested and therefore could introduce uncontrolled variances. Likewise, the matrix of quiescent MDCK cells was not used as a negative control because compositional and structural changes of the MDCK endogenous matrix over time are not well understood.

To confirm that the matrix prepared from MDCK cells grown to 90-95% confluency was rich in LM-332 and that plates coated with collagen I contained no LM-332, endogenous matrix or collagen I were extracted with an SDS buffer and immunoblotted for LMβ3 (Figure 6.1A). As expected, the endogenous matrix from MDCK cells was rich in LMβ3 and the collagen I contained no LMβ3. It should be noted that, in addition to LM-332, MDCK cells express LM-511, fibronectin, and collagen IV, therefore, these components were also likely in this matrix. Next, to ensure that MDCK cells could attach to the harvested endogenous matrix, endogenous matrix was prepared on 96 well plates as described above, and as controls, additional wells were coated collagen I, or BSA, and adhesion assays were performed over one hour (Figure 6.1B). One hour after plating, MDCK cells plated onto collagen I or endogenous matrix adhered to a much greater extent than MDCK cells plated onto BSA alone. More cells attached to collagen I

than endogenous matrix, but this difference was not statistically significant (p=.061). To last confirm there was no evidence of MDCK cytotoxicity in cells grown on endogenous matrix, cells were plated onto plastic, collagen I, or endogenous matrix. Cells were allowed to grow for 24 hours and imaged by phase-contrast microscopy. After 24 hours, under all conditions, cells had formed islands and exhibited some spreading, which indicated that cells behaved similarly on endogenous matrix coating compared to collagen I and uncoated plates (Figure 6.1C). These data suggested that MDCK cells, when grown to 90-95% confluency, produced matrices rich in LM-332 that could be prepared, and used for Ad-shLMα3 rescue studies.

6.2.2 Plating Ad-shLMα3 cells Onto LM-332-Rich Endogenous Matrix and Exposure of Ad-shLMα3 cells to LM-332-Rich Conditioned Medium does not Rescue Proliferation or p21waf1 expression

As described in Chapter 4, Ad-shLMα3-mediated proliferative arrest was believed to be due to high levels of p21waf1 that bound to and inhibited cdk2. It was therefore hypothesized that if this proliferative defect were specific to loss of LMα3, p21waf1 expression should be eliminated and proliferation rescued by plating Ad-shLMα3 cells on LM-332-rich endogenous matrix. To test this hypothesis, MDCK cells alone, and MDCK cells infected with Ad-shLMα3 were replated onto either LM-332 rich endogenous matrix, or onto collagen-coated plates, and immunoblotted for p21waf1. As shown in Figure 6.2A, expression of p21waf1 was not observed in non-infected MDCK cells plated on either collagen I or endogenous matrix coated surfaces. The p21waf1 doublet was observed in Ad-shLMα3 cells plated on both collagen I and endogenous matrix. Oddly, p21waf1 was present in greater amounts in Ad-shLMα3 cells adherent to endogenous matrix coated plates than in those adherent to collagen I. These data

suggest that plating Ad-shLMα3 cells on LM-332-rich endogenous matrix cannot reverse p21waf1 expression.

To determine if the continued and enhanced expression of p21waf1 in Ad-shLMα3 cells replated onto endogenous matrix correlated with the inability of endogenous matrix to rescue the Ad-shLMα3-mediated proliferation defect, non-infected and Ad-shLMα3 cells were plated onto endogenous matrix or collagen I, and analyzed for BrdU incorporation (Figure 6.2B). Consistent with the observation of continued p21waf1 expression, re-plating MDCK cells onto endogenous matrix did not rescue the Ad-shLMα3 proliferation defect, as only 15 to 20 percent of Ad-shLMα3 cells on both collagen I and endogenous matrix incorporated BrdU, compared to almost 70 percent of the non-infected controls.

It was unclear why replating Ad-shLMα3 cells onto MDCK, LM-332-rich, endogenous matrix could not rescue the Ad-shLMα3 proliferative defect. It was possible that the harsh processing involved in extracting cells off the matrix and the additional wash steps somehow altered the LM-332 within the matrix in a way that prevented the protein from rescuing proliferation. Instead of plating Ad-shLMα3 cells onto a LM-332 rich substratum, therefore, cells were plated in a LM-332-rich conditioned medium. To generate conditioned medium, MDCK cells were plated at a subconfluent density and allowed to grow for two days. Medium was then collected from the cells. To first confirm that LM-332 was present in the conditioned medium, LM-332 conditioned medium was collected and analyzed for LMβ3 by immunoblot. As a negative control MDCK growth medium was taken directly from the bottle and blotted. Immunoblot analysis confirmed that conditioned medium was rich in LMβ3, but that MDCK growth medium did not contain the protein (Figure 6.3A).

To determine if exposure of Ad-shLMα3 cells to conditioned medium could rescue proliferation, non-infected and Ad-shLMα3 cells were replated onto Transwell® filters with either conditioned medium, or MDCK growth medium in both the apical and basal chambers of the filter unit. This method allowed Ad-shLMα3 cells to be exposed to endogenous LM-332 on all surfaces. As a marker for proliferative arrest, expression of p21waf1 was again analyzed. As shown in Figure 6.3B, p21waf1 was not expressed in non-infected cells treated with MDCK growth medium or conditioned medium. Upon infection with Ad-shLMα3 however, p21waf1 continued to be expressed as a doublet, regardless of treatment with LM-332-rich conditioned medium. A reduction in the top band of the p21waf1 doublet was observed in the conditioned medium sample, as compared to the MDCK growth medium samples. This was not believed to indicate a proliferative rescue, however, because the p21waf1 band density in Ad-shLMα3 cells from conditioned medium samples was similar to the p21waf1 band density in Figure 6.2B after plating Ad-shLMα3 cells on endogenous matrix. When taken together, these data indicate that treatment of Ad-shLMα3 with medium rich in endogenously expressed LM-332 cannot rescue the Ad-shLMα3-mediated proliferation defect.

6.2.3 Co-expression of Human LMα3 does not Rescue the Ad-shLMα3 Proliferation Defect

One explanation for the failure of exogenous LM-332 to rescue the Ad-shLMα3-mediated proliferation defect is that cells may have to synthesize and deposit LM-332 themselves to signal proliferation. Indeed, in studies using primary keratinocytes derived from a LMα3-/- mouse, proliferation of cells was only rescued by co-expressing human LMα3 (Sigle et al., 2004). Furthermore, the LM-332 integrin receptor, α3β1, seems to preferentially localize to secreted LM-332 over endogenous matrix (Carter et al., 1990), suggesting that LM-332 receptors

require nascently secreted LM-332 for activity. It was therefore hypothesized that if the Ad-shLMα3 proliferation defect were due to the suppression of LMα3, stable expression of human LMα3 in MDCK cells prior to infection with Ad-shLMα3 would rescue the Ad-shLMα3 proliferative defect.

Before human LMα3 (hLMα3) expressing MDCK cells could be generated, the specificity of Ad-shLMα3 for canine and not human LMα3 had to be determined. The shLMα3 target sequence aligns with the human LMα3 gene with the exception of one nucleotide and it was unclear if one mismatch would prevent recognition and subsequent degradation of the hLMα3 mRNA. To test this, the human colon carcinoma cell line, Caco-2, which is known to produce LM-332 (Pyke et al., 1995), was infected with Ad-shLMα3, and the synthesis of LM-332 was monitored by metabolic labeling and immunoprecipitation with a polyclonal anti-LM-332 antibody. Immunoprecipitation of LM-332 resulted in four bands in both non-infected and Ad-shLMα3 cells (Figure 6.4). The two slowest migrating bands were potentially LMα3. The slower migrating of the two is likely the higher molecular weight LMα3B protein. The next band, which migrated slightly slower than the 130kD ladder, was probably the processed form of LMα3A, which is 165kD. Regardless, no differences in protein levels were observed in either of the potential LMα3 bands when non-infected control and Ad-shLMα3 samples were compared. These results suggest that the canine-specific, Ad-shLMα3 cannot suppress human LMα3 mRNA and that expression of Ad-shLMα3 in hLMα3 cells was a reasonable approach to rescue the Ad-shLMα3 proliferation defect.

To generate a MDCK cell line stably expressing hLMα3, a construct coding for the full-length hLMα3 contained within a pcDNA3.1*Hygro* vector was obtained. The hLMα3 construct and the empty pcDNA3.1*Hygro* vector were transfected into MDCK cells using a calcium

phosphate transfection procedure. Stable hLMα3 expressing MDCK clones were then selected by treatment with hygromycin. Clones were then screened for expression of hLMα3 with an antibody that recognized human, but not canine LMα3. Clones 5 and 12 had the highest levels of hLMα3 expression and were therefore selected for studies (Figure 6.5 bottom two panels). Importantly, hLMα3 appeared to be secreted from these cells as staining was evident below the epithelium. The absence of LMα3 staining in the vector control further indicated that the observed LMα3 staining in stable clones was hLMα3 and not endogenous canine LMα3 (Figure 6.5 top panels).

To determine if co-expression of hLMα3 could rescue the Ad-shLMα3-mediated proliferation defect, vector expressing or hLMα3 expressing clones 5 and 12 were infected with Ad-shControl and Ad-shLMα3, and proliferation was analyzed by the Click-iT® EdU incorporation assay. This assay is similar to the BrdU incorporation assay in that cells are treated with a synthetic nucleoside analog, in this case 5-ethynyl-2'-deoxyuridine (EdU). The advantage of the Click-iT assay is that it allows EdU incorporation to be analyzed with high sensitivity on a plate reader, which was desirable because these rescue experiments involved a large number of samples that required simultaneous analysis. As shown in Figure 6.6A, non-infected and Ad-shControl cells incorporated EdU to a similar extent in vector expressing and hLMα3 clone 5 and clone 12 cells, as EdU absorbance values were similar. All cells, whether vector expressing or hLMα3 expressing, that were infected with Ad-shLMα3 failed to incorporate EdU at levels higher than background, which suggested that Ad-shLMα3 continued to arrest prior to S phase. To ensure that the failure of hLMα3 cells to rescue the Ad-shLMα3-mediated proliferative arrest was not due to suppression of the hLMα3 by Ad-shLMα3, at the replating step from experiments above, remaining Ad-shLMα3 samples were replated onto coverslips and stained for hLMα3

(Figure 6.6B). Intense staining in the pattern typical of secreted LMα3 was observed below the cells. Additionally, cells infected with Ad-shLMα3 continue to display the "large, flattened cell" phenotype, which was characteristic of MDCK cells following expression of the Ad-shLMα3. The presence of hLMα3 staining supports the data from Caco-2 cells, and suggests that the Ad-shLMα3 cannot suppress hLMα3. These data together suggest that expression of hLMα3 cannot rescue the Ad-shLMα3 proliferation defect.

6.2.4 Treatment with Integrin Inhibitory Antibodies Cannot Validate the Ad-shLMα3-mediated Proliferation Defect

The Ad-shLMα3 proliferation defect could not be rescued by replating cells onto endogenous, LM-332 rich matrix, or by co-expressing hLMα3. These results suggest that either, 1) the LMα3 was not being introduced in a way that was permissive of MDCK cell recognition and signaling, resulting in a failure to rescue the Ad-shLMα3-mediated proliferation defect, or 2) the Ad-shLMα3-mediated proliferation defect is caused by an RNAi off-target effect. To gain more confidence that the results with Ad-shLMα3 were in fact, specific, integrin inhibitory studies were performed. The integrin receptors, α6β4 and α3β1, bind to LM-332, and the interaction is thought to be required for cell proliferation. It is likely that LM-332, if truly required for proliferation in MDCK cells, would also use these integrin receptors to promote proliferation. Inhibition of the integrin receptor required for proliferation should therefore cause a G1 proliferative arrest similar as suppression of LMα3.

The activity of integrin receptors can be inhibited by treatment with integrin function blocking antibodies. Specifically, antibodies AIIB2 (Hall et al., 1990) and GOH3 (Sonnenberg et al., 1986), which recognize integrin β1 and α6, respectively, prevent the integrin interaction with

their laminin receptors (Hall et al., 1990). The inhibitory antibodies are thought to function by binding to the integrin in the extracellular domain, which generates a conformational change such that the ligand can no longer bind to the integrin receptor (Humphries, 1996; Takada and Puzon, 1993).

To determine if the integrin α3β1 or α6β4 receptors were required downstream of LM-332 for proliferation, cells were treated with the function blocking antibodies, plated onto endogenous matrix coated plates, and incubated for 20 hours, with BrdU being added in the final six hours of the incubation. Neither AIIB2, nor GOH3 antibodies were internalized during this 20-hour incubation (Figure 6.7A) and qualitative assessment of the medium suggested that antibody treatment did not result in decreased cell adhesion, as very few cells were floating in the medium of untreated or treated cells (data not shown). As shown in Figure 6.7B, treatment of MDCK cells with AIIB2 and GOH3 resulted in an almost 20 percent reduction in proliferation as compared to untreated controls (Figure 6.7B, left), which was statistically significant. Although treatment with these inhibitory proteins reduced proliferation, proliferation was not reduced to the same extent as in Ad-shLMα3 cells (Ad-shLMα3 was reduced by around 80 percent when compared to non-infected controls, Figure 5.2).

MDCK cells express another integrin receptor, the fibronectin and vitronectin binding integrin, αvβ3 (Schoenenberger et al., 1994). Ligation of αvβ3 integrin has been shown to affect the function of β1 integrins, and vice versa through cross-talk (Blystone et al., 1999) (Retta et al., 2001). Integrin αvβ3 has also been implicated in proliferation control (Cruet-Hennequart et al., 2003; Schwartz and Ginsberg, 2002), and as proliferation was only slightly altered by treatment with integrin β1 and α6 function blocking antibodies, it was hypothesized that activity of integrin αvβ3 may additionally be involved in proliferation control in MDCK cells. To test this

hypothesis, MDCK cells were treated with Arginine-Glycine-Aspartic Acid (RGD) peptides, and proliferation was again assessed by BrdU incorporation. RGD peptides mimic the integrin αvβ3 integrin binding site of fibronectin and vitronectin. In the presence of RGD peptides in solution, αvβ3 integrins bind to the peptide, which prevents interaction with its ligands (Ruoslahti, 1996) and interferes with integrin αvβ3-mediated cellular processes, such as migration (Kim et al., 1992). As shown in Figure 6.7B, treatment with RGD peptides did not alter BrdU incorporation as compared to the untreated control, or the RGD peptide negative control, Arginine-Glycine-Glutamate (RGE). These data suggest that the integrin αvβ3 is not responsible for proliferation in MDCK cells.

Treatment of LM-332 integrin receptors with function blocking antibodies did not reduce proliferation to the same extent as suppression of LMα3 by Ad-shLMα3. As LM-332 interacts with both integrin α6β4 and α3β1, and in these studies only one integrin was inhibited at a time, it was hypothesized that the activity of the uninhibited integrin might be compensating for the loss of activity in the other. It was also hypothesized that cross-talk with the integrin αvβ3 receptor might be further enhancing cellular proliferation. To determine, therefore, if simultaneous inhibition of the integrin receptors was required to reduce proliferation similar to the Ad-shLMα3 cells, cells were treated with integrin inhibitory antibodies or RGD in combination. As shown in Figure 6.7B (left), treatment of cells with the antibodies or peptides in combination only reduced BrdU incorporation by an additional 5 percent over treatment with AIIB2, GOH3, or RGD alone. Furthermore, this reduction was only observed in cells treated with an antibody combination including AIIB2. The combination of GOH3 and RGD did not result in a further decrease in BrdU incorporation. These results indicated that integrin β1 was

important for proliferation, but that other factors likely compensate for loss of β1 activity, such as growth factor receptor signaling, or signaling from other non-integrin, LM-332 receptors.

6.2.5 Design of Five Additional siRNAs Targeted Against Canine LMα3

Based on studies described thus far, the proliferative defect observed in Ad-shLMα3 cells could not be directly linked to the suppression of LMα3. In a final effort to determine the requirement for LM-332 in MDCK proliferation, five additional siRNAs targeted against the LMα3 subunit were designed (Figure 6.8). siRNA target sequences were identified at varying places along the length of the canine LMα3 coding sequence. LMα3-specific siRNA target sequences (named siLMα3-1 to -5) were chosen using siRNA target identification software (described in *2.19.1*), which selected targets based on thermodynamic value, GC content, and BLAST analysis. Synthetic siRNA duplexes were commercially obtained. As controls, the Ad-shLMα3 target sequence (named siLMα3-D5) was obtained for use as a positive RNAi-mediated suppression control, and a siRNA targeted against Luciferase within the firefly genome was obtained for use as a negative siRNA control (named siLuc). To determine the efficacy of the siRNA duplexes, siLuc, siLMα3-1 to -5, and siLMα3-D5 were electroporated into MDCK cells. LMα3 protein and mRNA levels were analyzed by short-term labeling followed by immunoprecipitation of LM-332 and quantitative real-time PCR with primers specific for the LAMA3 gene, respectively. Electroporation efficiency was monitored using a plasmid that codes for expression of GFP. As shown in Figure 6.9A, short-term metabolic labeling and immunoprecipitation of these samples showed that expression of the siLMα3-1 to -5 resulted in an almost complete elimination of the LMα3 protein. Consistent with these observations, all five of the designed siRNAs against LMα3 also resulted in significant reduction of LMα3 mRNA

compared to both the 'No siRNA' and the siLuc controls (Figure 6.9B). Surprisingly, the siRNA designed with the same target sequence as the Ad-shLMα3 shRNA, did not result in a significant reduction of LMα3 mRNA or protein when compared to the siLuc control. The failure of siLMα3-D5 to suppress LMα3 was not dependent on siRNA concentration because lowering and increasing the concentration of the siLMα3-D5 duplex electroporated into MDCK cells did not result in suppression of LMα3 mRNA (data not shown). Nevertheless, it is possible that electroporation of RNA duplexes is not able to reach the efficiency and level of RNA expression achievable by adenoviral vector mediated suppression. In any case, it was apparent that the siLMα3-D5 duplex was not as efficient as the new siRNAs in suppression LMα3 expression under these conditions. Three siRNA sequences, siLMα3-2, siLMα3-3, and siLMα3-5, were chosen for future experiments.

6.2.6 LMα3 Protein Expression Continues to be Suppressed 48 hours after Expression of LMα3 siRNAs

In previous studies using the adenoviral Ad-shLMα3, cells were replated 18 hours after infection to remove any LMα3 that was secreted prior to full suppression of the protein, and then cells were given an additional 24 hours to recover prior to experimentation (Figure 4.2). Use of this replating scheme was also necessary for studies with the new siRNAs. As this approach requires siRNA expression for 42 to 48 hours, it was first necessary to confirm that LMα3 protein continued to be suppressed 48 hours after the original electroporation. MDCK cells were electroporated with siRNA controls and siLMα3-2, -3, and -5, replated after 18 hours to eliminate residual LM-332, and incubated another 24 hours. To determine if LMα3 protein was continuously suppressed during this time, cells were subjected to a short-term metabolic labeling at two different points within the experiment: first, shortly after replating (24 hours after

electroporation), or 48 hours after electroporation. Metabolically labeled cells were extracted, and the lysates were immunoprecipitated with a polyclonal antibody against LM-332. As shown in Figure 6.10A (left), at 24 hours, LMα3 protein was almost entirely eliminated compared to the siLuc control, as was previously observed (Figure 6.9) Additionally, in siLMα3 cells, LMγ2 and LMβ3 band density was increased compared to the siLuc control, which also observed in Ad-shLMα3 cells (Figure 4.4). LMα3 was still suppressed 48 hours after the initial expression of siRNAs relative to the siLuc control; however, the accumulation of the bands representative of LMγ2 and LMβ3 was no longer evident (Figure 6.10A, right).

To determine if LMα3 mRNA was also still suppressed 48 hours after expression of the siRNAs, controls and siLMα3 expressing cells were generated as above. At 24, and 48 hours, RNA was harvested, cDNA was generated, and quantitative real-time PCR was performed using primers specific for the LAMA3 gene. At 24 hours, in siLMα3 samples, LMα3 was suppressed to a similar extent as was observed in Figure 6.9, and LMα3 mRNA continued to be expressed in the 'No siRNA' and siLuc controls (Figure 6.10B, black bars). At 48 hours, however, LMα3 mRNA expression was low in all samples, including controls. Previous data suggests that cellular density impacts LMα3 protein levels (Figure 5.1). However, siLMα3 cells were replated at a subconfluent density, and remained subconfluent at harvest (data not shown). Therefore, it is unknown why LMα3 expression is turned off in the control samples at 48 hours. Since LMα3 mRNA was so low in the control cells, it was impossible to decipher the siRNA efficacy by qPCR alone. Importantly, based strictly on the protein data (Figure 6.10A), these data suggested that LMα3 protein was still suppressed 48 hours after electroporation of the siRNAs, and that the same expression and replating scheme could be followed for siRNAs as previous Ad-shRNA experiments.

6.2.7 Expression of LMα3-specific siRNAs does not Alter MDCK Proliferation

Studies described thus far have not resolved the issue of specificity of the Ad-shLMα3 proliferation defect. It was therefore hypothesized that if the Ad-shLMα3 proliferation defect was caused by the specific suppression of LMα3, expression of the three new siRNAs targeted against LMα3 should also result in proliferative arrest. To determine, therefore, if LMα3 was required for MDCK proliferation, BrdU incorporation analysis was performed in 'No siRNA', siLuc, siLMα3-2, siLMα3-3, and siLMα3-5 expressing cells. 'No siRNA' and siLuc control cells incorporated BrdU in around 55 percent of cells. This percentage was consistent with what had previously been observed in our studies of proliferating MDCK cells. Suppression of LMα3 by three different siRNAs, however, did not alter BrdU incorporation as compared to the controls, as roughly 55 percent of cells continued to incorporate BrdU. These data indicated that the suppression of LMα3 by expression of three different siRNA duplexes did not alter cellular proliferation.

6.2.8 Suppression of LMα3 Reduces MDCK Cell Area and Morphologically Alters the Epithelium

It was previously shown in these studies that LM-332 is produced and degraded in a regulated fashion corresponding to re-formation of the epithelium. As expression of three different siRNAs targeted against LMα3 suggested that LM-332 might not be required for MDCK proliferation, we wondered if suppression of LMα3 altered other processes that are required for re-formation of the epithelium. Cell spreading is an important event that occurs at the leading edge and is pre-requisite for cell migration and hence, formation of the epithelium (DeMali and Burridge, 2003; Jacinto et al., 2001; Price et al., 1998). Cells spread by first putting

out cell membrane protrusions, such as lamellipodia and filopodia that contact and attach firmly to the substratum. LM-332 has been implicated in the regulation of cellular spreading in many cell types, including keratinocytes, rat bladder carcinoma cells, and MDCK cells (Hormia et al., 1995; Mak et al., 2006; Shang et al., 2001). It was therefore hypothesized that loss of LMα3 would reduce MDCK cell spreading, as evident by a reduction in total cellular area compared to controls. To test this hypothesis, 'No siRNA', siLuc, siLMα3-2, siLMα3-3 and siLMα3 were electroporated into MDCK cells. 18 hours after electroporation, cells were replated, and actin and nuclei stained the next day. Cells were imaged by conventional fluorescence, and the actin outline of the cell was used to estimate the total cell area with image analysis software. Total cell area was then compared to total nuclei to generated a total area per cell value. As shown in Figure 6.12A, in all cells, islands continued to form, as is typical for MDCK cells at low density. However, islands in 'No siRNA' and siLuc controls were much larger than islands in siLMα3 cells even though all islands contained similar numbers of cells. Additionally, control cells appeared to have larger lamellopodia extending from the periphery of the islands than siLMα3 cells. When total area per cell was quantified (Figure 6.12B), cell area of siLMα3 cells was significantly reduced compared to the controls. Overall, the apparent inhibition of lamellopodia formation and reduced area per cell indicates that LM-332 is important for MDCK cell spreading, which is consistent with observations in other cell types.

Inhibition of the laminin interaction with epithelial cells has been shown to alter epithelial polarity both *in vivo* and *in vitro* (Klein et al., 1988; Zinkl et al., 1996). Furthermore, mammary epithelial cells expressing a mutant of the LM-332 receptor, integrin β4, failed to form polarized cysts (Weaver et al., 2002). To determine if suppression of LMα3 altered the ability of MDCK cells to form a polarized epithelium at high density, 'No siRNA', siLuc, siLMα3-2,

siLMα3-3 or siLMα3-5 expressing cells were replated at high density onto permeable supports. The next day, cells were stained for the apical protein, podocalyxin and filamentous actin, and imaged by confocal microscopy (Meder et al., 2005). As shown in Figure 6.13A, podocalyxin was localized apically in all samples, including the siLMα3 cells, suggesting that proper apical polarization was occurring. The epithelium however, was morphologically altered in siLMα3 expressing cells. The epithelium was not of uniform height, but contained some cells that appeared taller than others. In several fields, the taller parts of the epithelium were clearly single cells (Figure 6.13A, middle panel). In other fields however, it was difficult to discern whether cells were forming more than one layer, or were simply taller than surrounding cells (Figure 6.13A, right panel). By both confocal and conventional fluorescence microscopy, the taller areas were visible as clusters of cells surrounded by a ring of podocalyxin staining. To quantify this morphological defect, fields were counted as either containing, or not containing these raised areas (Figure 6.13B). The morphological defect was seldom observed in 'No siRNA' or siLuc cells, as less than 18% of fields contained the abnormality. Conversely, in cells expressing the siLMα3 siRNAs, roughly 65-75% of fields contained the morphological defect. Although these data are preliminary, they suggest that LM-332 may be required for proper morphogenesis of the epithelium.

6.3 Discussion

6.3.1 Summary

The G1 proliferation defect observed following suppression of LMα3, mediated by expression of Ad-shLMα3, could not be rescued by exposure of the cells to exogenous LM-332 or by co-expression of hLMα3. Additionally, inhibition of β1 and α6 integrins by treatment with

integrin inhibitory antibodies did not cause proliferative arrest to a similar extent as in Ad-shLMα3 cells. Last, expression of three additional siRNAs specific for LMα3 did not alter proliferation. The Ad-shLMα3-mediated proliferation defect could therefore not be validated. Expression of the new siLMα3 siRNAs indicates that instead, LM-332 is important for cellular spreading, and perhaps morphology of the re-formed epithelium.

6.3.2 The Requirement for LM-332 in Epithelial Morphogenesis

The development of an epithelium that is properly apically and basolaterally polarized is vital for proper tissue functionality. The finding that suppression of LMα3 altered the morphology of the MDCK epithelium is therefore of great interest. In the studies described in *6.2.8*, cells expressing the siRNA against LMα3 were taller than other cells within the epithelium. One process that increases the height of epithelial cells is columnarization (Schock and Perrimon, 2002). MDCK cells are normally columnar after the epithelium has re-formed when cells are terminally differentiated. It is interesting therefore; that the LM-332 protein, which is normally shut off and degraded at confluence, might somehow promote the morphogenesis of this terminally differentiated phenotype when it is artificially suppressed at high density. The mechanisms that regulate the actin cytoskeletal rearrangements required for columnarization are not known, therefore determining how the loss of LM-332 might promote this phenotype may be difficult to discern. The role for LM-332 in morphogenesis however, may become clearer upon further characterization of other apical and basolateral markers and known polarity complexes.

6.3.3 Alternate Explanations for the Failure to Validate the Ad-shLMα3 Proliferation Defect

Within each of the Ad-shLMα3 rescue experiments, pitfalls were present that may have prohibited proliferation rescue. First, as described in *6.2.3,* one explanation for the failure of exogenous LM-332 to rescue the Ad-shLMα3-mediated proliferation defect is that cells may need to synthesize and deposit LM-332 themselves to signal proliferation. This idea is supported by studies using primary keratinocytes derived from a LMα3-/- mouse, in which proliferation of cells was only rescued by co-expressing human LMα3 (Sigle et al., 2004). In our studies, when hLMα3 was co-expressed with Ad-shLMα3 however, stable overexpression of the untargeted hLMα3 was not sufficient to rescue the Ad-shLMα3 proliferation defect. Although we confirmed that Ad-shLMα3 could not suppress the hLMα3 protein, we did not confirm that the hLMα3 properly heterotrimerized with canine LMβ3 and LMγ2 because we do not have an antibody against the hLMα3 to immunoprecipitate the complex. We did observe that the hLMα3 was continuously deposited and was in the rosette pattern, which suggests that the hLMα3 was secreted. The observation of deposited hLMα3 does not necessarily indicate, however, that it is secreted as a heterotrimer with LMβ3 and LMγ2. Studies by Yurchenco *et al* have reported that LMα3 can be deposited from the cell in the monomeric form (Yurchenco et al., 1997). Additionally, adhesion assays were not performed using the endogenous matrix from hLMα3 overexpressing cells, so it is also unclear if the canine receptors on MDCK cells could adhere to, or signal through the hLMα3 protein.

In the second set of validation studies, we hypothesized that if LM-332 were indeed required for MDCK proliferation, inhibition of its integrin receptors should result in the same proliferation defect. When α6 and β1 integrins were inhibited by treatment with function blocking antibodies, however, proliferation was only slightly reduced, which did not recapitulate

the Ad-shLMα3 defect. The best, and perhaps most likely explanation for this is that we may have been examining the wrong LM-332 receptors. We had long assumed that the integrins were required for LM-332-mediated proliferation control, as a vast amount of literature suggests that this is the case. Indeed, our integrin inhibition studies were modeled after those described in Gonzales, *et al,* who clearly indicated that inhibition of α3β1 prevented proliferation downstream of LM-332 (Gonzales et al., 1999). As described in the introduction, however, the syndecan and dystroglycan receptors could be required for cell proliferation within the kidney. Nevertheless, it still remains possible that the LM-332 integrin receptors are required for proliferation, but that the antibody treatment did not sufficiently inhibit the function of these receptors.

In the last set of validation studies, we transiently expressed three additional siRNA duplexes targeting the LMα3 subunit and analyzed proliferation. To our surprise, absolutely no change in proliferation was observed between siLMα3 and control cells. Although these proliferation results using the siLMα3 cells are seemingly definitive, when comparing the siRNA system to the Ad-shRNA system, it is important to recognize that the duration of LMα3 suppression is very different. Using the adenoviral system, LMα3 can be suppressed continuously for at least 66 hours (data not shown), whereas in the siLMα3 system, protein production of the LMα3 subunit was beginning to return by 48 hours. It is unclear however, if this low level of LMα3 protein that were present at the time of the experimentation would be sufficient to drive proliferation. In future studies, as will be discussed in the next chapter, it will be important to generate retroviral shRNA knockdowns with the new LMα3 target sequences. Importantly, if LMα3 is required for proliferation as the literature suggests, we will be unable to

generate stable cell lines, but at least would have a system in which longer-term suppression of LMα3 can be achieved.

6.3.4 Is the Ad-shLMα3-mediated Proliferation Defect Caused by Off-targeting of the shRNA?

The phenotypic consequences of siRNA off-targeting caused by design of the siRNA alone have not been well studied. Specifically, no studies have reported proliferative defects caused solely by off-targeting effects of siRNA. One study has reported a strong correlation between apoptosis and expression of siRNAs containing a 5'-UGGC-3' sequence in the RISC entering, guide strand (Fedorov et al., 2006). The guide strand is the strand whose 5' end is the least paired to its complement (Schwarz et al., 2003). It should be noted that the 5'–UGGC-3' sequence is present in the anti-sense strand of the Ad-shLMα3 target sequence. What is unclear is if in the Ad-shLMα3, the sense or the anti-sense strand is the guide strand. Ad-shLMα3 cells, however, displayed no evidence of apoptosis (i.e there was no peak prior to the G1 by flow cytometric analysis, or blebbing nuclei). Importantly, the study by Federov, *et al* suggests that RNAi containing specific sequences alone may result in off-target effects. As BLAST analysis yielded no significant matches of the Ad-shLMα3 target sequence within the canine or human genomes other than LMα3, it is possible that an Ad-shLMα3-mediated proliferative effect may have been caused by an element of the sequence or design of the Ad-shLMα3, which, as of yet has not been connected to proliferative defects.

Failure of BLAST analysis to accurately predict all matches of the Ad-shLMα3 sequence to the entire canine genome also may hide the true cause of the Ad-shLMα3-mediated off-target proliferative defect. One important pitfall of BLAST analysis is that the software only searches for matching sequences within the NCBI sequence database for a particular species (Pertsemlidis

and Fondon, 2001). If the database is incomplete pertaining to either coding or non-coding regions, or contains a large number of "predicted" sequences that have not been confirmed (as the *Canis familiaris* genome does), the predicted matches between target sequences and the rest of the genome may be incomplete. It is possible, therefore, that the shLMα3 shRNA may, in addition to LMα3, target a gene that is required for proliferation, but that was not identified by BLAST analysis.

6.3.5 Potential Contribution of the Adenovirus to the Observed Ad-shLMα3 Proliferative Defect

Normal adenovirus, upon infection of the host cell, rapidly replicates its genome, and then causes cytotoxicity and lysis of the host cell as a means to spread to neighboring cells and propagate further (Goncalves and de Vries, 2006). Expression of the early genes, E1 and E3 are required for adenoviral propagation. The adenovirus vector used in our studies to deliver a shRNA did not contain the E1 and E3 regions of the adenoviral genome. Infecting host cells with adenovirus lacking the E1 and E3 genes has proven to promote expression of desired genes, without altering the proliferation of the host cell (Scibetta et al., 2005). These E1 deficient adenoviruses have, however, been reported to alter microtubule dynamics in human lung carcinoma cells (Warren et al., 2006). There have also been reports that E1 and E3 deficient adenoviruses may re-acquire the E1 and E3 regions from homologous recombinations with the genome of the packaging cell line (Lochmuller et al., 1994). Importantly, the common trademarks associated with adenovirus propagation, cellular rounding and lysis, were not present following infection of MDCK cells with Ad-shLMα3. Additionally, no cytotoxic, proliferative, or morphological defect was observed following adenoviral expression of the LacZ protein using

a closely-related vector, which suggests that the proliferative defect was not vector-mediated (Figures 4.3 and 4.4).

Nevertheless, the possibility that adenoviral-mediated shRNA delivery may promote a proliferative defect in our cells cannot be entirely ruled out. Expression of all of the adenoviral shRNA controls alone was capable of altering MDCK morphology, which suggested that virus-mediated shRNA expression alone could somehow alter normal cell phenotypes. In the proliferation analysis of the shRNA negative control, Ad-shPKCα however, a proliferative defect similar to the Ad-shLMα3 was not observed. Some cytotoxic and proliferative defects were observed in the Ad-shLacZ cells. The proliferative defect was not as pronounced as that caused by Ad-shLMα3 expression, and may be related to the cytotoxic phenotype of the Ad-shLacZ cells. It should also be noted that no reports could be found in the literature describing phenotypic alterations of host cells that had been infected with an adenovirus capable of delivering shRNA. Overall, effects of the adenoviral vector on proliferation cannot be ruled out, but seem unlikely considering the various controls utilized in our experiments.

Chapter 6 Figures

Figure 6.1 Characterization of the MDCK LM-332-Rich Endogenous Matrix

(A) 35mm plates containing MDCK endogenous matrix (described in Chapter 2 Materials and Methods) or coated with 10μg/cm^2 collagen Type I were extracted with SDS extraction buffer. Samples were denatured, alklyated, and subjected to SDS-PAGE. Immunoblot was then performed for LMβ3 using the mouse anti-LMβ3 antibody (1:1000).

(B) 96 well plates were coated with 1%BSA in PBS, collagen I or MDCK endogenous matrix. For the adhesion assay, subconfluent MDCK cells were harvested by treatment with 4mm EDTA/1mM EGTA in PBS. Cells were collected by centrifugation, and resuspended in serum free MDCK growth medium. 10^5 cells in 100μl was added to pre-coated wells. Four wells of each coating condition were used per experiment. Cells were given 1hr to attach. Plate was then fixed with methanol and stained with crystal violet. Absorbance was read at 590nm. Experiment was repeated three times. Graph represents the average between experiments. Error bars represent the standard deviation between experiments.

(C) MDCK stock cells were harvested by trypsinization and .75x10^6 were plated onto 35mm tissue culture plates containing MDCK endogenous matrix. Cells were allowed to grow for 18hrs and then were imaged on an inverted phase contrast microscope using the 20X objective.

A

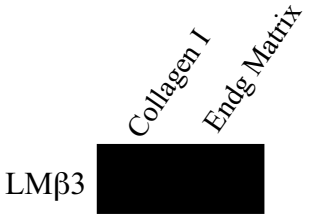
Collagen I
Endg Matrix
LMβ3

B

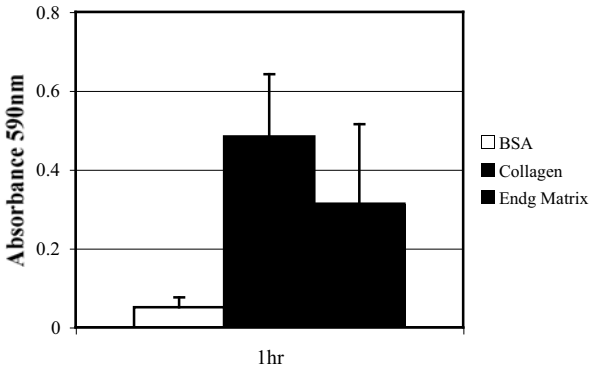
0.8
0.6
0.4
0.2
0
Absorbance 590nm
1hr
BSA
Collagen
Endg Matrix

C

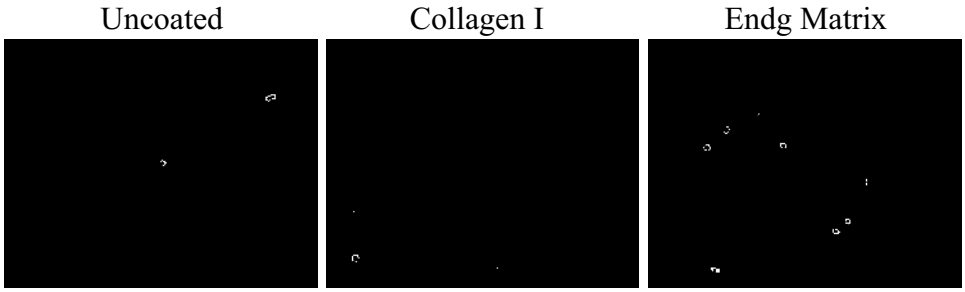
Uncoated
Collagen I
Endg Matrix

Figure 6.2 Ad-shLMα3 Proliferation and p21waf1 Expression cannot be Rescued by Plating on Endogenous Matrix

(A) To generate plates coated with MDCK endogenous matrix, 1.5x10^6 cells were plated into 35mm dishes. Alternately, dishes were coated with 10μg/cm^2 Collagen Type I. 24 hours after dishes were coated or cells were plated, cells were removed by treatment with 20mM NH_4OH. The remaining extracellular matrix from the first dish and the collagen I from the other dish were extracted with SDS extraction buffer. Samples were denatured, alklyated, and subjected to SDS-PAGE. Immunoblot was then performed for LMβ3 using the mouse anti-LMβ3 antibody (1:1000).

(B) Four 35mm plates were coated with either Collagen I or prepared with endogenous matrix, as described previosly. MDCK cells were infected with Ad-shLMα3, as previously described. 18 hours after the initial infection, .83x10^6 cells were replated onto either collagen I or endogenous matrix. 24 hours after replating, cells were extracted with RIPA buffer, protein concentration determined, samples normalized, denatured, and alklyated, and subjected to SDS-PAGE. Immunoblot analysis was performed for p21waf1. Membranes were then stripped and re-probed for actin.

(C) Plates and samples were prepared simultaneously with (B), except plates were prepared with coverslips. 18 hours after replating, 50μM BrdU in MDCK growth medium was added to cells. After a 6 hour incubation with BrdU, cells were fixed with 3% PFA and stained for BrdU with a rat anti-BrdU antibody (1:500) and DAPI. Cells positively stained for BrdU were counted and compared to the total number of nuclei.

A

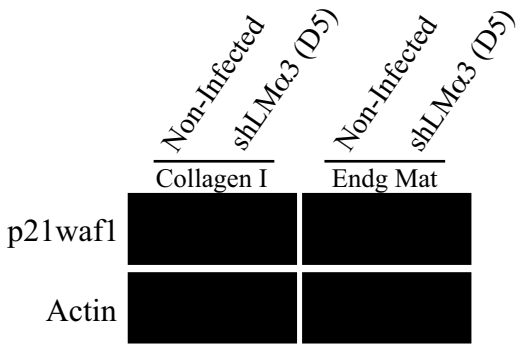
Non-Infected
shLMα3 (D5)
Non-Infected
shLMα3 (D5)
Collagen I
Endg Mat
p21waf1
Actin

B

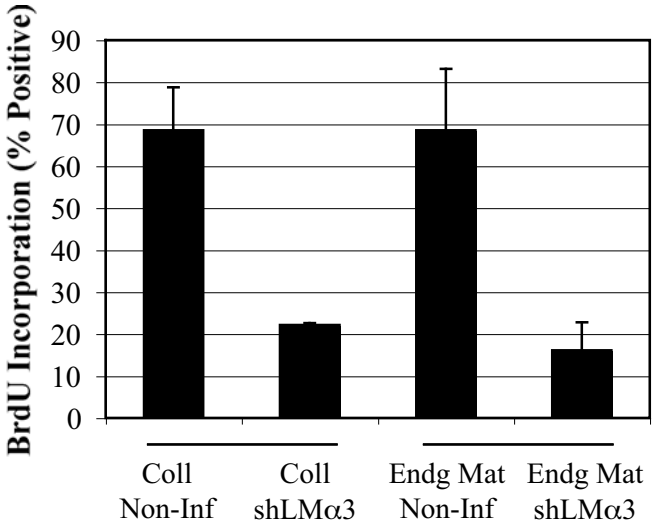
BrdU Incorporation (% Positive)
90
80
70
60
50
40
30
20
10
0
Coll Non-Inf
Coll shLMα3
Endg Mat Non-Inf
Endg Mat shLMα3

Figure 6.3 Ad-shLMα3-mediated p21waf1 Expression cannot be Rescued by Treatment with MDCK-LM-332 Conditioned Medium

(A) A T-75 flask of confluent MDCK cells was split 1:5 and allowed to grow for two days. Medium was then collected from cells, and was referred to as "Conditioned Medium". 100μl of conditioned medium was removed, and 100μl of MDCK growth medium was taken directly from the bottle. Sample buffer was added to the medium in 1.5ml microcentrifuge tubes, and samples were boiled to denature. Samples were then subjected to SDS-PAGE and immunoblotted for LMβ3 with a mouse anti LM-β3 antibody (1:1000).

(B) MDCK cells were infected with Ad-shLMα3. 18 hours later, cells were collected by trypsinization, and then spun down. Cell pellets were then resuspended in either Conditioned Medium or MDCK growth medium. .83x10^6 cells were then replated onto transwell filters. 24 hours later, cells were extracted with RIPA buffer. A protein assay was performed and samples were normalized. SDS-PAGE was performed followed by immunoblot for p21waf1. Membrane was then stripped and re-probed for actin.

A

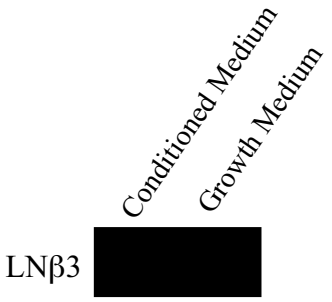
Conditioned Medium
Growth Medium
LNβ3

B

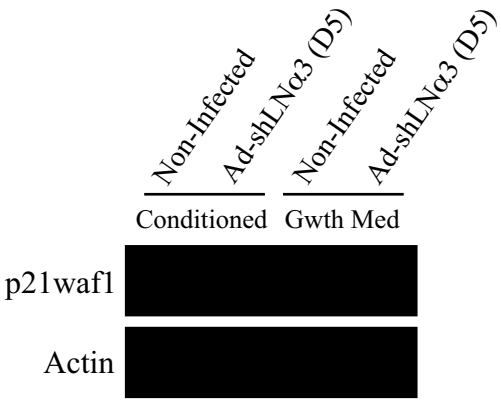
Non-Infected
Ad-shLNα3 (D5)
Non-Infected
Ad-shLNα3 (D5)
Conditioned
Gwth Med
p21waf1
Actin

Figure 6.4 Canine Specific Ad-shLMα3 does not Suppress LMα3 in Caco-2 Cells

(A) Caco-2 cells were infected with Ad-shLMα3, in exactly the same manner as in experiments with MDCK cells (Figure 4.3). After 18hrs, 10^6 cells were re-plated. The next day growth medium was replaced with Labeling medium containing 50μCi/ml ^{35}S Methionine/Cysteine. Cells were pulse labeled for 30 minutes, and then extracted. Extracts were immunoprecipitated for LM-332 using 5μg of the rabbit anti-LM-332 (8LN5) antibody. Additionally, one non-infected sample was immunoprecipitated for LMα3 using the mouse anti-LMα3 antibody, RG13 (1:5), and beads alone were added to one, non-infected sample. Samples were denatured and alklyated, then subjected to SDS-PAGE on a 6% polyacrylamide gel. Bands were visualized by fluorography.

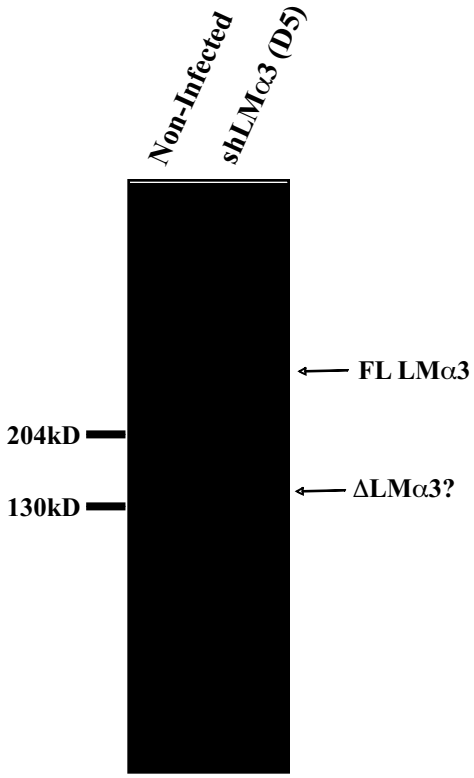
Non-Infected
shLMα3 (D5)
FL LMα3
204kD
130kD
ΔLMα3?

Figure 6.5 Generation of Stable Clones Expressing Human LMα3 in MDCK Cells

MDCK cells were transfected with empty pcDNA3.1Hygro vector (Invitrogen) or hLMα3 within the pcDNA3.1Hygro vector (J. Jones, Northwestern University) by the calcium phosphate transfection procedure. After three days, cells were diluted into 300μg/ml Hygromycin and allowed to grow until colonies were well defined. Colonies were then selected, then grown up in 24 well plates.

To select positive clones, 24 different clones were plated onto glass coverslips and allowed to grow overnight. Clones were fixed in cold acetone and then stained for hLMα3 with the mouse anti-hLMα3 antibody, RG13 (used straight) (red) and actin with phalloidin 488 (1:100) (green). Samples were imaged on a conventional fluorescence microscope with the 40X oil immersion objective. RG13 does not recognize canine LMα3, as no staining was observed in the vector control (top). Six clones stained positive for expression of hLMα3. The two clones with the most intense staining, clones 5 and 12, were selected for all studies (bottom).

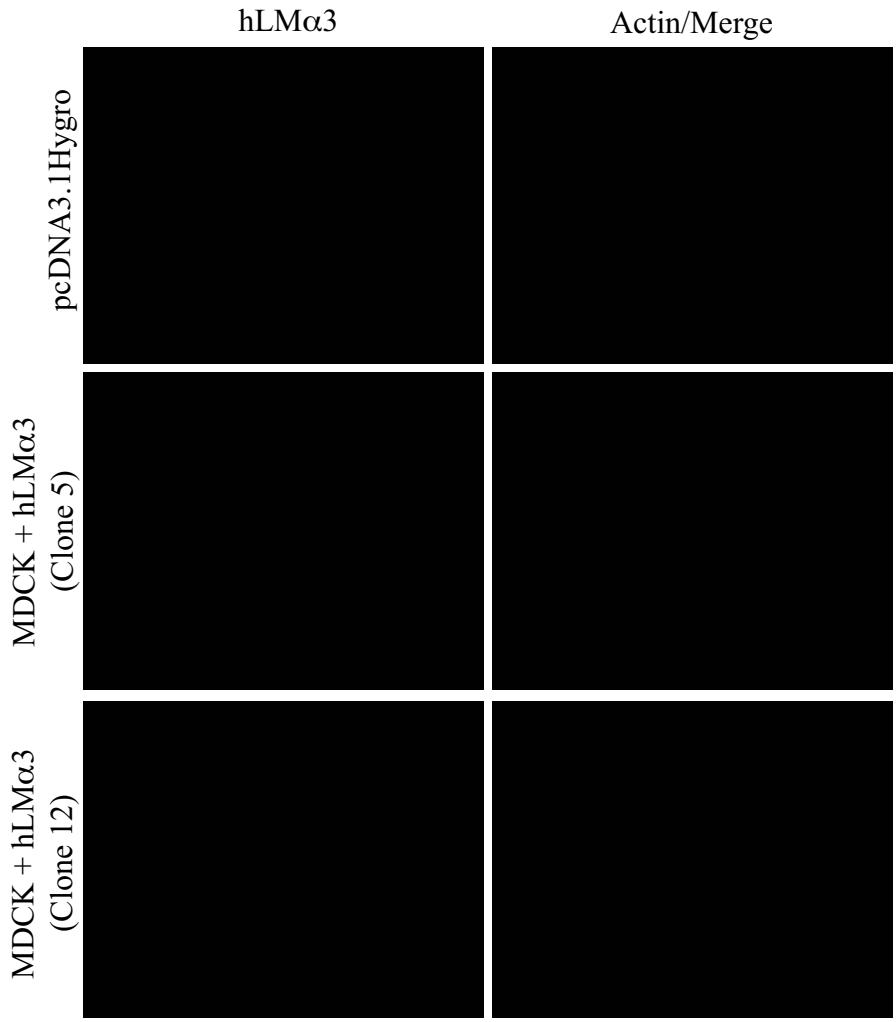
hLMα3
Actin/Merge
pcDNA3.1Hygro
MDCK + hLMα3 (Clone 5)
MDCK + hLMα3 (Clone 12)

Figure 6.6 Infecting hLMα3 Cells with Ad-shLMα3 does not Rescue the Ad-shLMα3 Proliferation Defect

(A and B) Vector, hLMα3 (clone 5), and hLMα3 (clone 12) cells were infected with Ad-shControl or Ad-shLMα3. After 18hrs, 8,000 cells were replated into wells of a black, clear bottom, 96 well plate, with three wells per parameter. The remaining Ad-shLMα3 cells were plated onto coverslips in 35mm dishes (A). After 24 hours, cells were fixed with cold acetone and stained for human LMα3 with the mouse anti-hLMα3 antibody, RG13 (used straight) (red) and actin with phalloidin488 (1:100). Cells were imaged with the 63X oil immersion objective on a conventional fluorescence microscope. Bar, 20μM.

(B) For analysis of proliferation, 18 hours after cells were replated into the black clear bottom plate, 30μM of the nucleoside analog, EdU was added to the cells in 100μl MDCK growth medium (Click-it Proliferation Assay, Invitrogen), and incubated for 6 hours. Cells were then harvested and analyzed for EdU incorporation, as per the manufacturer's protocol. EdU contains an alkyne group that reacts with an azide group on a HRP-conjugated secondary antibody via a copper catalyzed reaction. The HRP then reacts with an Amplex ® UltraRed substrate (Invitrogen) to produce a red fluorescence product. EdU incorporation was analyzed on a plate reader, which read the excitation/emission at 568 and 585nm. Absorbance data was then exported into Excel (Microsoft). Bars represent the average of six wells from two experiments, and the error bars are the standard deviation of the absorbance between wells.

A

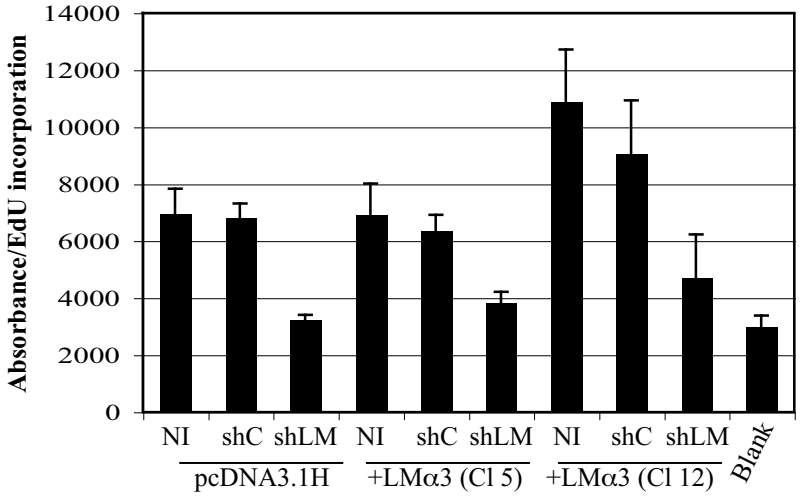
Absorbance/EdU incorporation
14000
12000
10000
8000
6000
4000
2000
0
NI
shC
shLM
NI
shC
shLM
NI
shC
shLM
Blank
pcDNA3.1H
+LMα3 (Cl 5)
+LMα3 (Cl 12)

B

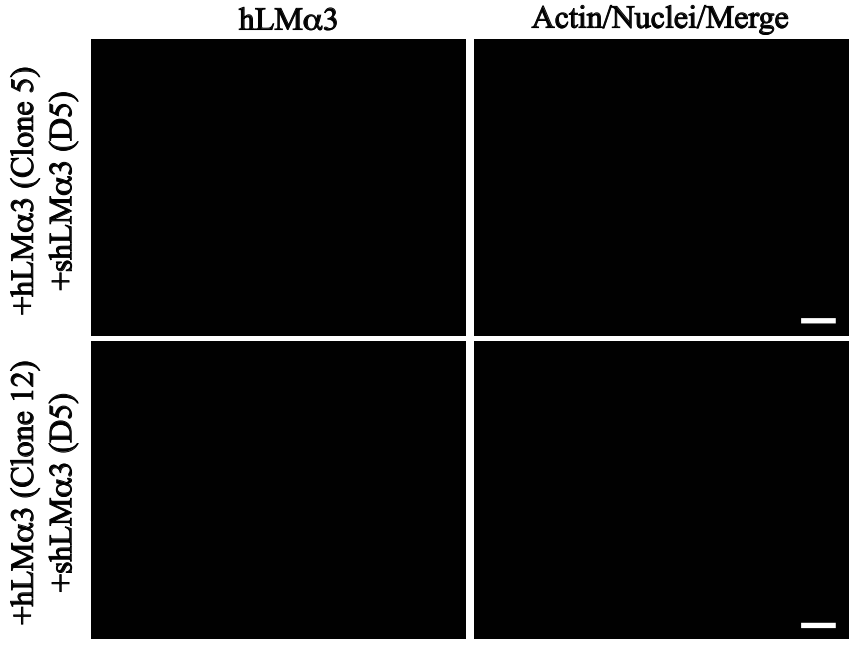
hLMα3
Actin/Nuclei/Merge
+hLMα3 (Clone 5)
+shLMα3 (D5)
+hLMα3 (Clone 12)
+shLMα3 (D5)

Figure 6.7 Treatment of MDCK Cells with Integrin β1 and Integrin α6 Inhibitory Antibodies does not Reduce Proliferation to the Same Extent as Ad-shLMα3 Expression.

(A) Quiescent MDCK cells were split 1:10 two days prior to the experiment. After two days, a single cell suspension was made by releasing cells from the tissue culture plate by EDTA/EGTA treatment. 100,000 MDCK cells were incubated with 10μg/ml Rat anti-β1 integrin, AIIB2, or 5μg/ml rat anti-α6 integrin, GOH3 for 30 minutes. Treated cells were then plated onto coverslips and incubated for 19hrs. After incubation, cells were fixed with 3% PFA and permeabilized with .1% Triton X-100 in PBS-. To detect AIIB2 or GOH3, cells were stained with goat anti-rat555 and observed with a 63X oil immersion objective on a conventional fluorescence microscope. Bar, 20μM.

(B) A single-cell suspension of MDCK cells was prepared as above. .25x10^6 cells were then incubated for 30 minutes with 10μg/ml AIIB2, 5μg/ml GOH3, 150μg/ml RGD, 150μg/ml RGE, or combinations of the like in serum free medium. Cells were then plated onto coverslips coated with MDCK endogenous matrix in 35mm dishes containing MDCK growth medium. Cells were incubated for 16 hours, then 50μM BrdU was added to the growth medium, and incubated another 6 hours. Cells were then fixed with 3% PFA and stained for BrdU incorporation with a mouse anti-BrdU antibody (1:500) and total nuclei with DAPI. Cells positive for BrdU incorporation were counted and compared to total nuclei for each sample. Fold change was determined by comparing the percent BrdU incorporation for all samples to the Untreated control. Bars represent the average between three or more experiments, and the error bars represent the standard deviation between experiments.

** $p<.001$, * $p<.05$ as determined by two-tailed student's *t-test*.

A

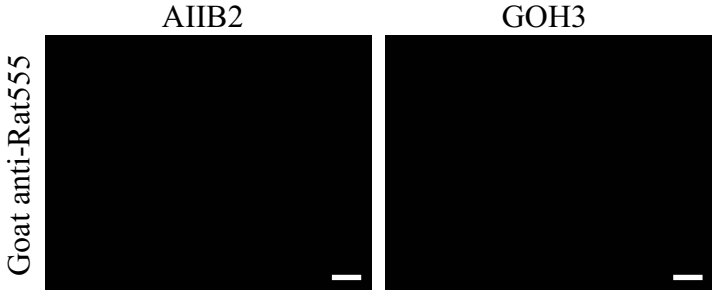
AIIB2
GOH3
Goat anti-Rat555

B

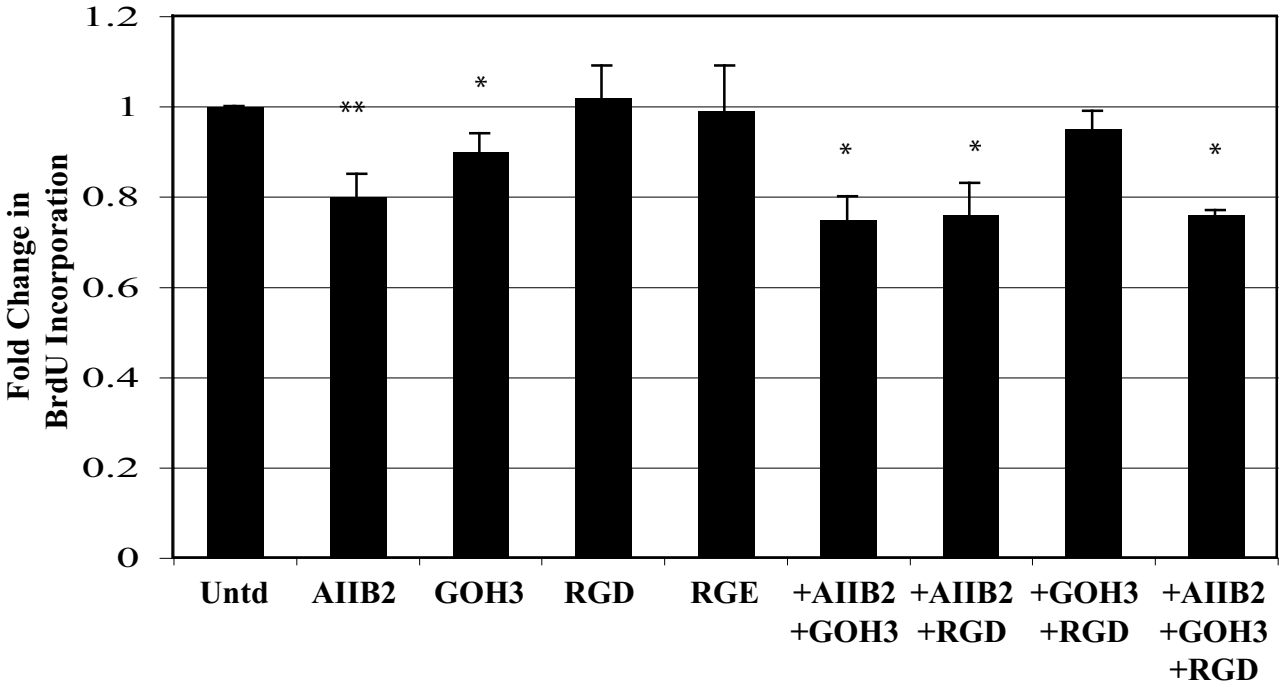
Fold Change in BrdU Incorporation
1.2
1
0.8
0.6
0.4
0.2
0
**
*
*
*
*
*
Untd
AIIB2
GOH3
RGD
RGE
+AIIB2 +GOH3
+AIIB2 +RGD
+GOH3 +RGD
+AIIB2 +GOH3 +RGD

Figure 6.8 Target Sites for Canine LMα3-Specific siRNAs

RNAi target sites along the Canis familiaris partial coding sequence of LMα3 were generated using four different algorithms. The siRNAs were mapped to the LMα3 sequence, and the siRNA target sequences that overlapped between algorithms, but did not align with any other genes in the canine genome by BLAST analysis, were chosen (blue bars). siRNAs were synthesized by ThermoFisher. As a positive control for LMα3 suppression, the siRNA target sequence from Ad-shLMα3 named siLMα3-D5, was obtained (red bar). As a negative control, a siRNA specific for the Luciferase gene within the firefly genome was also obtained (not shown). This figure displays where the siLMα3 target sites map to the Canis famiaris LMα3 sequence.

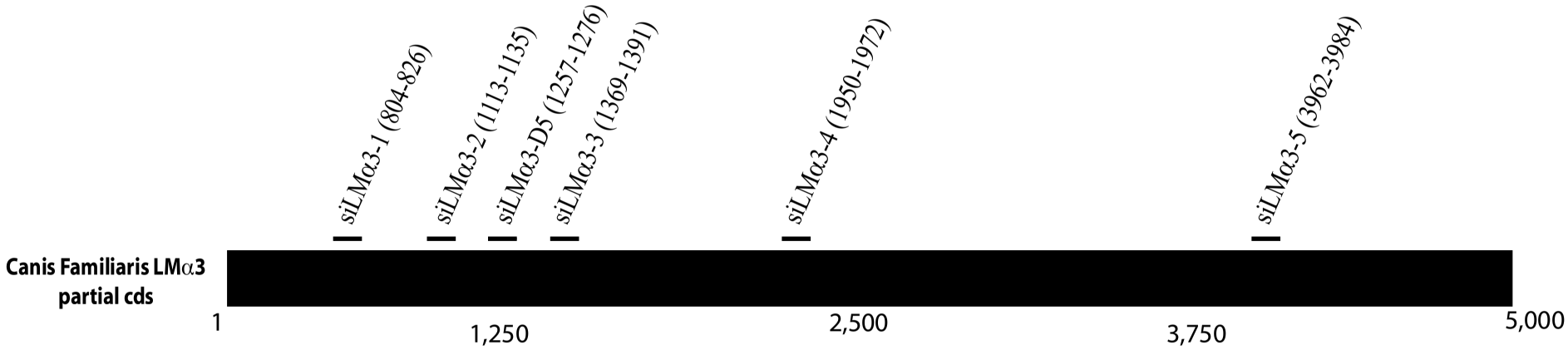
siLMα3-1 (804-826)
siLMα3-2 (1113-1135)
siLMα3-D5 (1257-1276)
siLMα3-3 (1369-1391)
siLMα3-4 (1950-1972)
siLMα3-5 (3962-3984)
Canis Familiaris LMα3
partial cds
1
1,250
2,500
3,750
5,000

Figure 6.9 Transient Expression of LMα3 siRNAs Suppresses LMα3 RNA and Protein Production.

(A) 10^6 MDCK cells were electroporated with electroporation buffer alone (No siRNA), a GFP positive control, siLuc siRNA control, and different siRNAs against LMα3 (siLMα3-1-5 and siLMα3-D5). Cells were then split 1:1 with 500,000 cell plated into 35mm dishes for qPCR analysis of the LAMA3 gene. Cells were allowed to grow for 24 hours. RNA was then isolated using the Qiagen RNeasy kit, and concentration determined. RNA was normalized and integrity of the RNA confirmed by agarose gel electrophoresis. RNA was then treated with DNase to remove any contaminating DNA. RT-PCR was performed to generate cDNA using primers against random hexomers. The resulting cDNA was then analyzed for LAMA3 expression using primers against the LAMA3 gene. Concentration in nanograms was determined by comparing LAMA3 values to a LAMA3 standard curve. Each experiment contained samples in triplicate, and experiment was repeated two times. Bars on the graph represent average LAMA3 values between all wells in both experiments, and error bars are the standard deviation between the wells. **p<.005, *p<.05 as determined by two-tailed student's *t-test*, comparing the values of siLMα3 to the siLuc values.

(B) Following electroporation of samples (above), the remaining 500,000 cells were plated into separate 35mm dishes and allowed to grow for 24 hours. The next day, MDCK growth medium was replaced with Labeling Medium containing 50μCi/ml ^{35}S Methionine Cysteine, and cells were labeled for four hours. Cells were then extracted with RIPA buffer and a protein assay performed. Lysates were normalized and subjected to IP with a rabbit anti-LM332 antibody (1:100) or 5μg IgG, respectively. Samples were denatured and alklylated, then subjected to SDS-PAGE on a 6% polyacrylamide gel. Bands were visualized by fluorography.

A

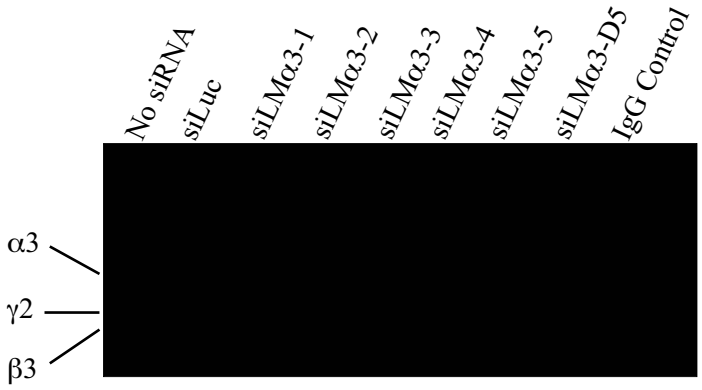
No siRNA
siLuc
siLMα3-1
siLMα3-2
siLMα3-3
siLMα3-4
siLMα3-5
siLMα3-D5
IgG Control
α3
γ2
β3

B

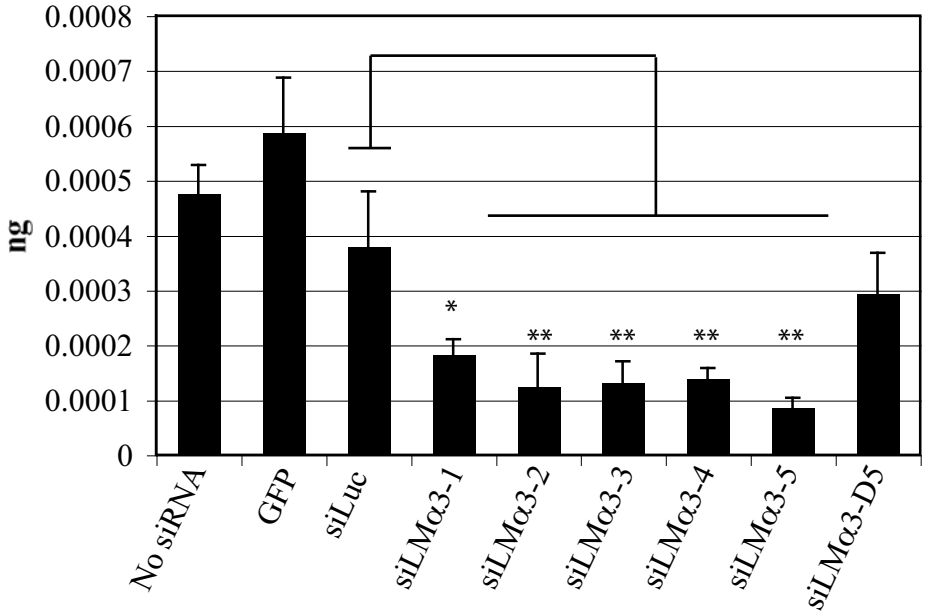
ng
0.0008
0.0007
0.0006
0.0005
0.0004
0.0003
0.0002
0.0001
0
*
**
**
**
**
No siRNA
GFP
siLuc
siLMα3-1
siLMα3-2
siLMα3-3
siLMα3-4
siLMα3-5
siLMα3-D5

Figure 6.10 LMα3 Protein Remains Suppressed 48 hours After Expression of LMα3 siRNAs

(A) 10^6 MDCK cells were electroporated with siLuc, siLMα3-2, siLMα3-3, and siLMα3-5 in two sets. Sets were pooled and 10^6 cells were plated into 2- 35mm dishes per parameter. After 18hrs, 500,000 cells were replated into 4-35mm dishes, as in Ad-shLMα3 experiments. After 24 hours, two plates were removed and either labeled with 50μCi/ml ^{35}S Methionine/Cysteine for four hours (A), or harvested for RNA (B). After protein label, cells were extracted with RIPA buffer and were stored at -80°C until remaining samples were ready. 24 hours later, or 48 hours after the initial electroporation, the second set was either metabolically labeled or RNA harvested, as above. Extracts from the day prior were removed from the freezer, a protein assay was performed on all samples, and samples were normalized. LM-332 was immunoprecipitated from the lysates with either rabbit anti-LM-332 antibody 9LN5 (1:150), or 5μg IgG. Samples were denatured, alklyated, and subjected to SDS-PAGE on a 6% polyacrylamide gel. Bands were visualized by fluorography.

(B) RNA was harvested from the second set of plates and qPCR performed on both sets as described in Figure 5.8. In each experiment, samples were analyzed in triplicate. The experiment was repeated two times. The bars in the graph represent the average LAMA3 ng values of all wells from both experiments, and error bars represent the standard deviation between wells.

A

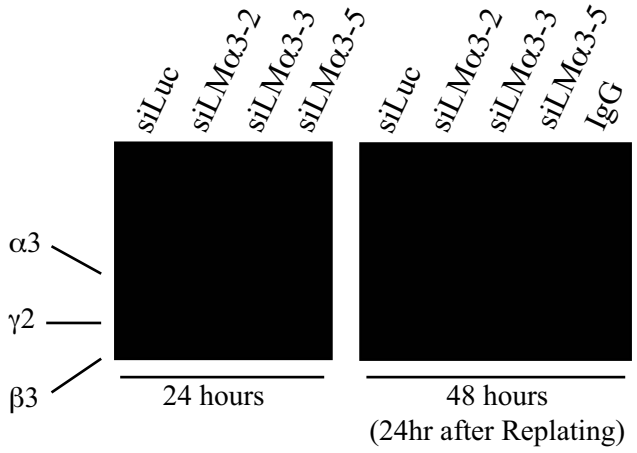
siLuc
siLMα3-2
siLMα3-3
siLMα3-5
siLuc
siLMα3-2
siLMα3-3
siLMα3-5
IgG
α3
γ2
β3
24 hours
48 hours
(24hr after Replating)

B

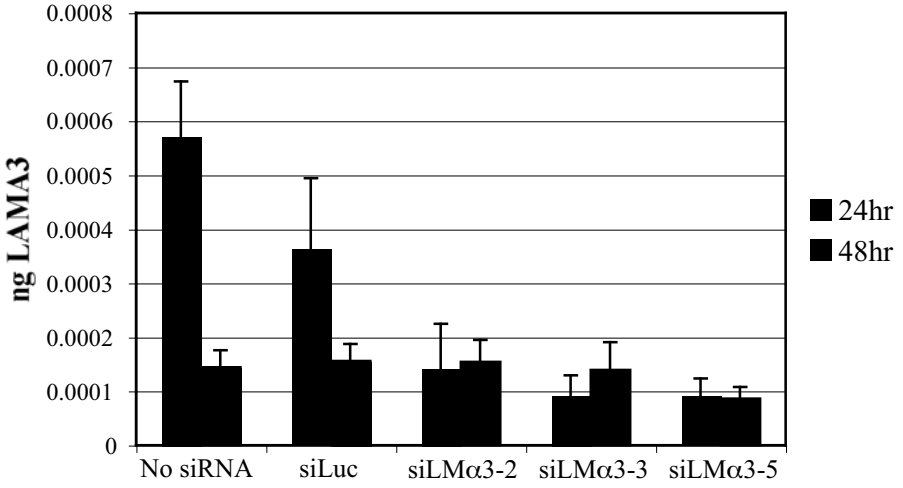
0.0008
0.0007
0.0006
0.0005
0.0004
0.0003
0.0002
0.0001
0
ng LAMA3
No siRNA
siLuc
siLMα3-2
siLMα3-3
siLMα3-5
24hr
48hr

Figure 6.11 Suppression of LMα3 by Expression of siRNAs does not Alter MDCK Proliferation

10^6 MDCK cells were electroporated with electroporation buffer alone (No siRNA), siLuc, siLMα3-2, siLMα3-3, and siLMα3-5. 18 hours later, .25x10^6 cells were replated onto glass coverslips in 35mm dishes. 18 hours later, 50μM BrdU in MDCK growth medium was added to cells and incubated for an additional 6 hours. After BrdU label, cells were fixed with 3% PFA, DNA was denatured with HCl, and incorporated BrdU was stained with a rat anti-BrdU antibody (1:500) and total nuclei were stained with DAPI. Coverslips were imaged by conventional fluorescence microscopy and were quantified for positive BrdU incorporation and total nuclei. Experiment was repeated three times. The graph represents the average percent BrdU incorporation between experiments, and the error bars represent the standard deviation between experiments.

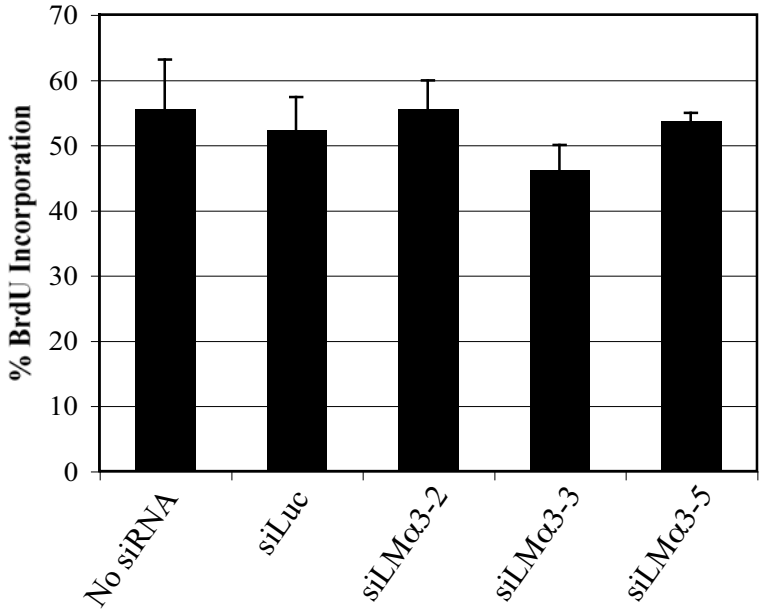
% BrdU Incorporation
70
60
50
40
30
20
10
0
No siRNA
siLuc
siLMα3-2
siLMα3-3
siLMα3-5

Figure 6.12 Suppression of LMα3 by Expression of siRNAs Reduces MDCK Cell Area

10^6 MDCK cells were electroporated with electroporation buffer alone (No siRNA), siLuc, siLMα3-2, siLMα3-3, and siLMα3-5. 18 hours later, .1x10^6 cells were replated onto glass coverslips in 35mm dishes. 24 hours later, cells were fixed with 3% PFA, permeabilized, and actin (green) and nuclei (blue) were stained with phalloidin488 (1:100) and DAPI, respectively. Cells were imaged on a conventional microscope using the 63X oil immersion objective (A). Images were analyzed for total cell area using ImageJ software. Nuclei were then counted. Total area per cell was determined for each parameter and then normalized to siLuc samples. Graph depicts the average fold change compared to siLuc between three separate experiments. Error bars represent the standard deviation between experiments. **p<.005, *p<.05 were determined by two-tailed student's *t-test*, comparing the values of siLMα3 to the siLuc values.

A

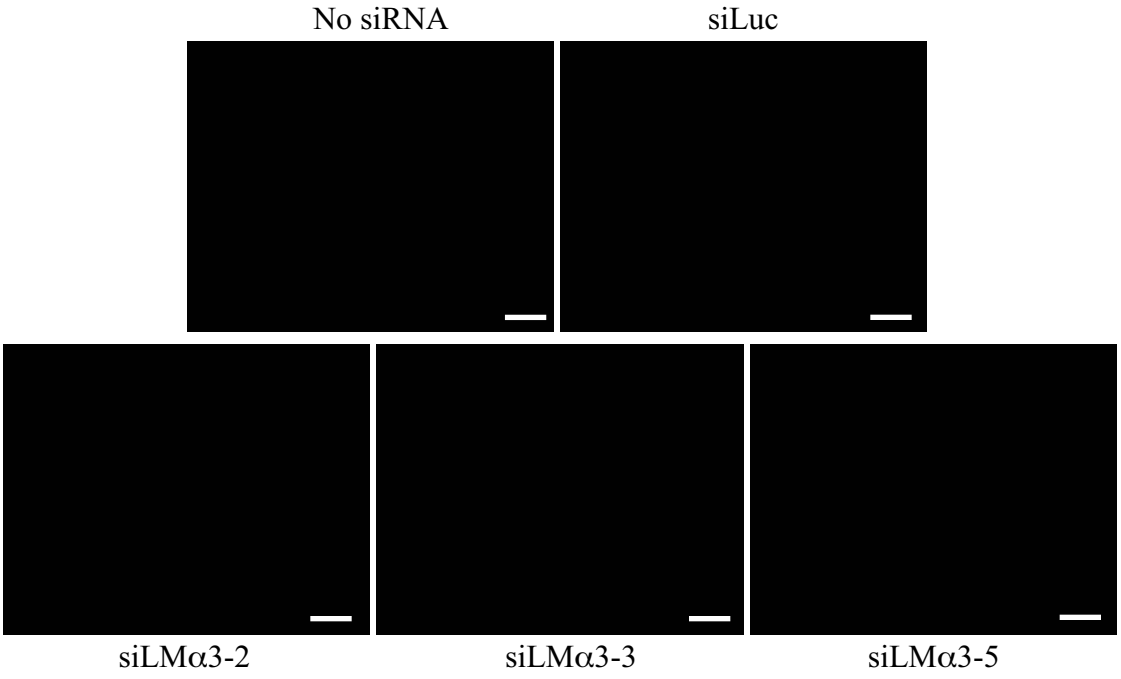
No siRNA
siLuc
siLMα3-2
siLMα3-3
siLMα3-5

B

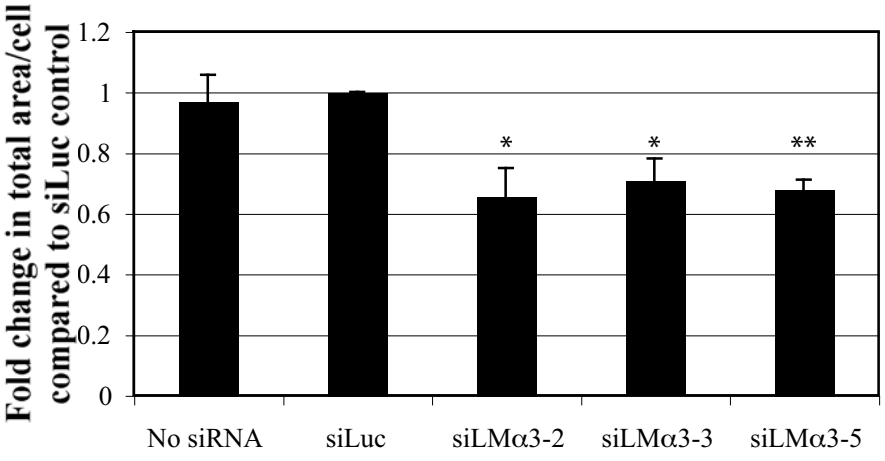
Fold change in total area/cell compared to siLuc control
1.2
1
0.8
0.6
0.4
0.2
0
*
*
**
No siRNA
siLuc
siLMα3-2
siLMα3-3
siLMα3-5

Figure 6.13: Suppression of LMα3 by Expression of siRNAs Morphologically Alters the Epithelial Monolayer

(A) To determine if MDCK cells at high density could form polarized epithelial monolayers, electroporation buffer alone, siLuc, siLMα3-2, siLMα3-3, and siLMα3-5 were electroporated into 2.0x10^6 cells. After 18 hours, 1.5x10^6 cells were replated onto 2.4cm transwells filters, pore size .4μm. After an additional 24 hours, cells were fixed with 3% PFA, permeabilized with .1% triton X-100/PBS, and stained for the apical marker, gp-135 (hybridoma supernatant, used straight) (red), actin (phalloidin488 1:100) (green), or nuclei (DAPI). Filters were imaged by confocal microscopy with the 63X oil immersion objective. A z-series was generated (top). Figure shows representative images from the apical and mid-planes, and, as shown in the bottom panel, an overlay of the two optical slices.

(B) To quantify the presence of "raised" areas in any given field, samples were observed on the conventional fluorescence microscope using the 63X oil immersion objective and were scored field-by-field for appearance of these "raised" areas, '0' for no raised areas, '1' for raised areas. The number of fields with raised areas was then compared to total fields, to generate a percentage, which was then plotted. These results are from a single experiment.

A

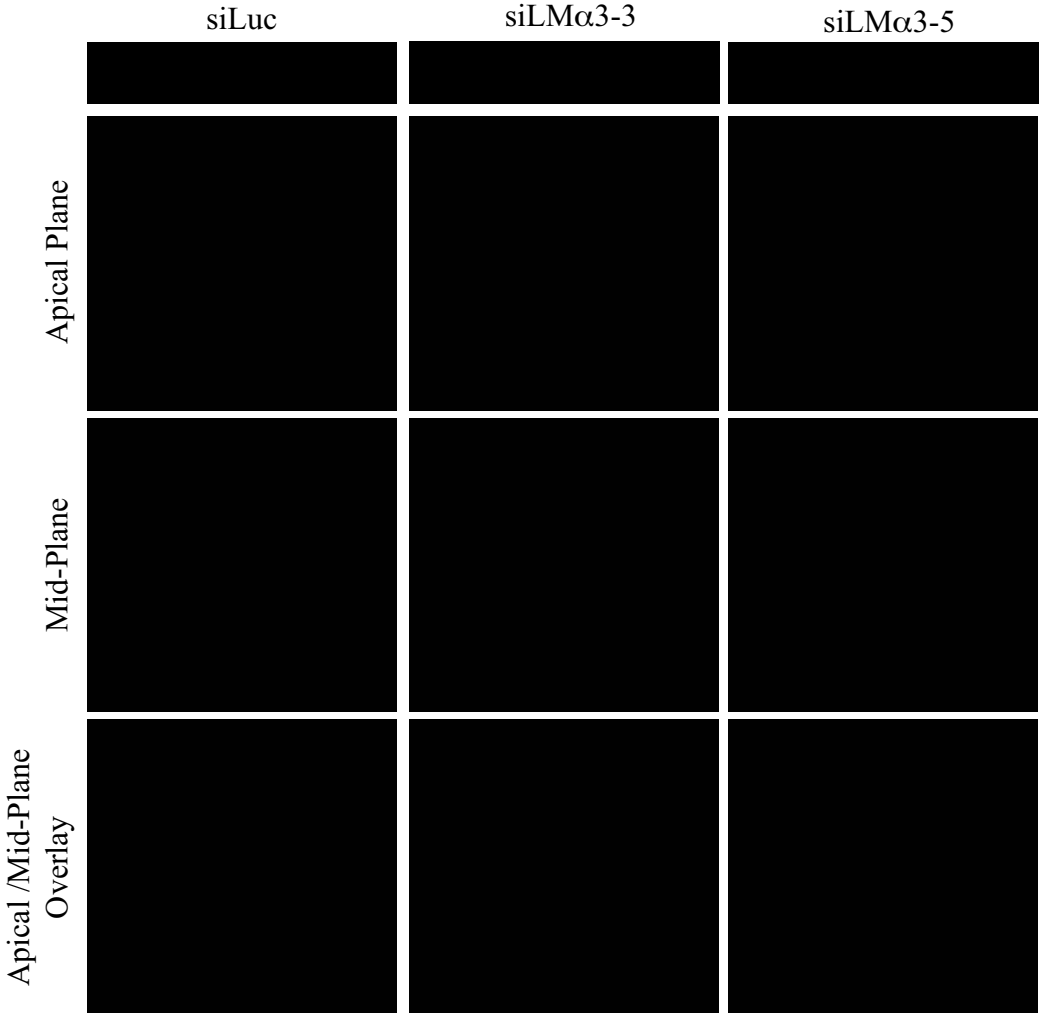
siLuc
siLMα3-3
siLMα3-5
Apical Plane
Mid-Plane
Apical /Mid-Plane Overlay

B

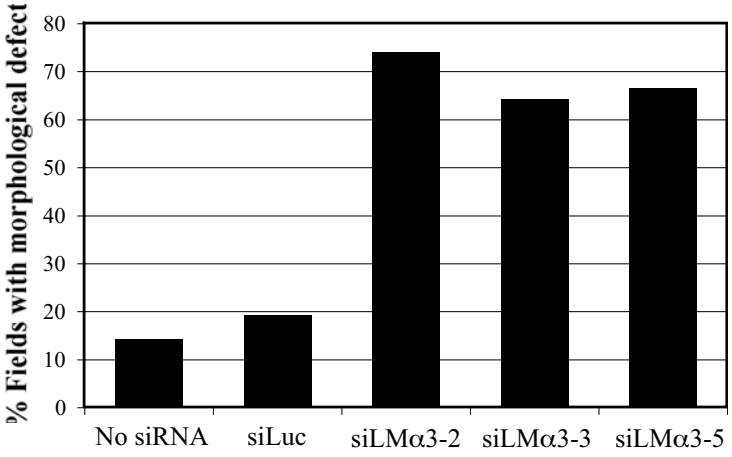
% Fields with morphological defect
80
70
60
50
40
30
20
10
0
No siRNA
siLuc
siLMα3-2
siLMα3-3
siLMα3-5

Chapter 7:
Discussion and Future Directions

7.1 Summary

The studies described in this work tested the hypothesis that LM-332 regulates proliferation of MDCK cells through interaction with α6β4 and α3β1 integrins and subsequent signaling to G1 cell cycle regulatory proteins. The overall goal was to understand the requirement for LM-332 in proliferation control to form a polarized epithelium using the Madin Darby Canine Kidney (MDCK) cell model system. LM-332 expression was turned on at low cell density when cells were proliferative, and turned off and degraded upon re-formation of the epithelium. Furthermore, the suppression of LM-332 by expression of an shRNA targeted against the LMα3 subunit induced a G1 cell cycle arrest, likely through a mechanism involving p21waf1-mediated inhibition of the cyclin E/cdk2 complex. The LMα3 shRNA-mediated proliferation arrest, however could not be validated, as proliferation arrest could not be rescued by plating cells on, or exposing cells to endogenous LM-332, or by co-expression of human LMα3. Also, inhibition of the LM-332 receptors, integrins α3β1 and α6β4, did not cause proliferative arrest to a similar extent as cell expressing the shRNA, and last, expression of three additional siRNAs specific for the LMα3 chain did not alter proliferation. Studies using the new siRNAs instead indicated that LM-332 is important for cell spreading and morphogenesis of the

epithelium. All of these studies collectively suggest that deposition of LM-332 plays an important role in the regulation of cell spreading, morphogenesis, and possibly proliferation, to establish a polarized epithelium.

7.2 MDCK Proliferation to Re-form the Epithelium

To test our hypothesis, it was first necessary to have an understanding of the regulatory mechanisms that control proliferation to form the epithelium in MDCK cells. Based on the studies described in Chapter 3, cells plated at low density enter S phase within 24 hours, and cell proliferation continues over the next two days (Figure 3.2 and 3.3). During this time, cyclin D1, cdk4, cyclin E, cdk2, cyclin B1, and cdk2 are expressed and localized to the nucleus (Figure 3.4). As cells grow to confluence, cyclins and cdks are exported to the cytoplasm, and expression of p27kip1 increases (Figure 3.5). Cells reach saturation density 4-5 days after plating, at which time the cell cycle is exited, and the epithelium is quiescent. The conclusion that MDCK epithelia are quiescent at high density is based on the observations that: 1) Greater than 70% of cells grown for 6 days have a G1 DNA content (Figure 3.1), 2) MDCK cell numbers plateau after four days in culture (Figure 3.2), and 3) After 7 days in culture, BrdU is incorporated into less than 10% of cells (Figure 3.3).

Based on our studies, the mechanisms that control MDCK proliferation during re-formation of the epithelium are consistent with the mechanisms described in other cell types and studies. For example, Matoltsy *et al* describe a proliferative "burst" at the leading edge of epidermal wounds 24 hours after wounding, which is the same time that we observed proliferation of MDCK cells after releasing from quiescence (Matoltsy and Viziam, 1970); the nuclear import and export of cyclin D1, cdk4, cyclin E, cdk2, cyclin B1, and cdk1 correlated with the times of proliferation and quiescence, respectively, which is consistent with the

paradigm that the nuclear localization of these cyclins and cdks is required for proliferation (Gladden and Diehl, 2005; Yang and Kornbluth, 1999); and last, the increase in p27kip1 expression as the epithelium formed is consistent with the observations of Zhang, et al, and Zegers, et al, who describe an increase in p27kip1 in quiescent cells (Zegers et al., 2003; Zhang et al., 2003). Prior to these studies, the mechanisms controlling MDCK proliferation were not well defined. As MDCK cells are one of the most broadly used systems for understanding epithelial biology, these data, in addition to being necessary for our studies, can also serve as a platform for understanding how other factors might promote or prevent proliferation in this cell type.

7.3 Suppression of LM-332 by Expression of an shRNA Targeted Against LMα3

7.3.1 Summary

LM-332 expression is observed following wounding of an epithelium both *in vitro* and *in vivo*, and has been connected with cell spreading, migration, and proliferation (described in Chapter 4, section 4.1). The goal of studies described in Chapter 4 was to generate and characterize an adenoviral shRNA targeted against the LMα3 subunit (Ad-shLMα3), so that the requirement for LM-332 in formation of the epithelium could be assessed. Expression of Ad-shLMα3 effectively suppresses the LMα3 protein compared to non-infected and non-canine targeting Ad-Controls (Figure 4.4), without altering the expression of LM-511, or the integrin receptors, α6 and β1 (Figure 4.7). In the absence of the LMα3 subunit however, levels of the LMβ3 and γ2 chains seem to increase, and are deposited from the cell (Figures 4.4 and 4.6).

7.3.2 The Regulation of LMα3, LMβ3, and LMγ2 Chain Expression

Our studies have been the first to report the impact of shRNA-mediated LMα3 suppression on the protein levels of the other LM-332 chains, LMβ3 and LNγ2 (Mak et al., 2006). The finding that loss of LMα3 seemingly increased LMβ3 and LMγ2 protein levels was therefore novel and interesting. It is unclear if the increases in LMβ3 or LMγ2 are due to delayed secretion and cellular retention of these chains in the absence of the LMα3 subunit, or if the chains are transcriptionally upregulated, as qPCR studies examining LMβ3 and LNγ2 have not yet been performed. Pulse-labeling studies, in which the new production of the LM-332 chains in Ad-shLMα3 cells was monitored following a 30 minute pulse, may indicate a transcriptional regulation, because an increase in LMγ2, and possibly LMβ3 protein levels were observed compared to the non-infected and Ad-shControl cells (data not shown).

Very few studies describe the transcriptional regulation of the LM-332 chains, and those that do are often inconsistent between cell types (Olsen et al., 2000; Zboralski et al., 2008). Regardless, it seems that expression of the individual LM-332 chains impacts the expressions of the others. Indeed, recent studies by Liu *et al* show that RNAi-mediated suppression of LMγ2 eliminated the expressions of LMα3 and LMβ3 in rat bladder carcinoma cells (Liu et al., 2010). Considering our findings with those of Liu *et al*, a feedback loop may regulate expression of the LMα3 chain, in which the decrease in LMα3 expression promotes cell signaling to drive expression of first the LMγ2 and then LMβ3 chains, which then in turn, drive expression of LMα3. This mechanism is appealing because the regulation one subunit, in this case LMγ2, could initiate a signaling cascade to promote the expressions of the other two. Understanding these mechanisms will be important in future studies to determine the precise controls of LM-332 expression during re-formation of the epithelium.

7.3.3 Biological Activity of LMβ3 and LMγ2 in the Absence of LMα3

The finding that MDCK cells continue to secrete LMβ3 and LMγ2 in the absence of the LMα3 chain was unexpected, as the current paradigm is that assembly of all three chains is required for secretion of the heterotrimeric molecule (Matsui et al., 1995; Yurchenco et al., 1997). It is unclear to what extent the cell or other matrix proteins may interact with the LMβ3 and LMγ2 chains in the absence of the entire LM-332 molecule and how these interactions might promote or inhibit cell functions such as migration or proliferation. It is known however, that the LMγ2 and LMβ3 chains interact with other matrix proteins and cell receptors. LMγ2 can bind to the integrin α2β1 in keratinocytes to promote adhesion and prevent migration (Decline and Rousselle, 2001). LMγ2 can also interact with the receptor tyrosine kinase, EGFR in mammary epithelial cells to promote migration (Schenk et al., 2003). The LMγ2 chain, unlike the LMγ1 chain, may not interact well with other BM proteins, specifically collagen IV, as LMγ2 interacts with very low affinity to the linker protein, nidogen/entactin (Mayer et al., 1995). Conversely, LMβ3 can interact directly with the BM protein collagen VII (Rousselle et al., 1997; Waterman et al., 2007) and this interaction in keratinocytes promotes tumorigenesis (Waterman et al., 2007). It is unknown however, if these interactions 1) can occur in MDCK cells, 2) could occur in the absence of heterotrimerization with LMα3, and 3) could promote or inhibit cell processes such as adhesion, migration, and proliferation in MDCK cells.

7.4 The Requirement for LM-332 in MDCK Proliferation Control

The goal of studies described in Chapter 5 was to determine if a relationship existed between LM-332 synthesis, deposition, and epithelial re-formation, to identify if LM-332 was required for proliferation, and to understand the mechanism by which loss of LM-332 could lead

to proliferative arrest. We determined that LM-332 production positively correlates with proliferation as the epithelium forms (Figure 5.1), and that LM-332 is likely required for this process as suppression of LMα3 results in a G1 proliferative arrest. This arrest is likely due to p21waf1, and possibly p27kip1, association and inactivation of the cdk2 kinase (Figures 5.2-5.6). Additionally, the JNK and Akt kinases are hyper-phosphorylated following suppression of LMα3, but their involvement in promoting cell cycle arrest is unclear, as inhibition of JNK did not fully reverse p21waf1 expression (Figure 5.7).

Our studies describing the requirement and mechanism for LM-332-mediated progression through G1 phase of the cell cycle in MDCK cells are consistent with studies by others suggesting that LM-332 is required for proliferation (Gonzales et al., 1999; Hashimoto et al., 2006; Joly et al., 2006; Mizushima et al., 2002; Tran et al., 2008). Prior to our studies, a mechanism linking LM-332 to the cell cycle machinery had not been defined. Although we did not examine the requirement for the integrin receptors in this chapter, the observation that p21waf1 expression is increased in the absence of LMα3 is also consistent with the observations that inhibition of β1 integrin, a subunit of the LM-332 receptor, α3β1 integrin, promotes expression of p21waf1 (Li et al., 2005a), and; that p21waf1 can be expressed downstream of integrin α6β4 (Clarke et al., 1995).

7.5 Validation of the Ad-shLMα3 proliferation defect

7.5.1 Summary

The data described in Chapter 5 were consistent with studies from other laboratories that suggested a requirement for LM-332 in proliferation control. Our data, however, were obtained using only one shRNA target sequence and therefore required validation, as the expression of

RNAi target sequences are known to generate a large number of off-target effects (Echeverri et al., 2006; Jackson et al., 2003). Plating Ad-shLMα3 cells on, or exposing cells to endogenous LM-332, and co-expression of hLMα3 did not rescue the proliferation defect and/or p21waf1 expression (Figure 6.2, 6.3, and 6.6). Additionally, inhibition of the LM-332 receptors, integrin α6β4 and α3β1, did not cause proliferative arrest to a similar extent as in Ad-shLMα3 cells. Specifically, treatment with integrin inhibitory antibodies only reduce S phase progression in 20% of the population, compared to the 80% reduction observed in Ad-shLMα3 cells (Figure 6.10). Last, expression of three additional siRNAs specific for LMα3 did not alter proliferation compared to 'No siRNA' and cells expressing a negative control siRNA (Figure 6.11). The Ad-shLMα3-mediated proliferation defect, therefore, could not be validated. Instead, studies using the new LMα3 siRNAs indicate that LM-332 is important for MDCK spreading (Figure 6.12) and morphogenesis of the epithelium (Figure 6.13).

7.5.2 LM-332 in Epithelial Proliferation Control: Contradictions Between Cell Types

If the Ad-shLMα3-mediated G1 proliferation arrest is indeed caused by an off-target effect, and LM-332 is not required for proliferation of MDCK cells, this finding would be in direct conflict with studies described by Gonzales, *et al*, Joly, *et al*, and Tran, *et al* (Gonzales et al., 1999; Joly et al., 2006; Tran et al., 2008). The differences between our studies and theirs could be reconciled by the fact that their studies were performed in mammary epithelial and rat bladder carcinoma cells, kidney epithelial cells derived from a polycystic kidney, and keratinocytes, respectively. The full extent of differences in LM-332 receptor expression, the expressions of other laminins, and the functions mediated by LM-332 between the above mentioned cell types and MDCK cells have not been assessed. One of the biggest differences

between mammary epithelial cells, rat bladder carcinoma cells, and keratinocytes compared to MDCK cells, is the ability of the LMα3 chain to be proteolytically cleaved within the LG domain to release the LG4-5 modules. In MDCK cells, LMα3 is observed at ~190kD when cells are subconfluent, which is the size of the full-length LMα3 chain, and is never observed as the ~165kD, cleaved form (Figure 5.1; (Mak et al., 2006). Studies by Tran *et al*, however, suggest that the proliferation contradiction between MDCK cells and keratinocytes is not due to a difference in LMα3 chain cleavage (Tran et al., 2008). Specifically, in their studies, a LMα3 lacking the LG4-5 domain (LMα3ΔLG4-5) was expressed in primary keratinocytes derived from a patient with junctional dystrophic epidermolysis bullosa; that is, in primary keratinocytes normally lacking LMα3 expression; or a Ras transformed cell line that expressed high levels of full-length LMα3 was treated with function blocking antibodies against the LG4-5 domain. In both cases, cells were not proliferative. These results suggest that the full-length LMα3 is required for proliferation, but the cleaved form is not. Therefore, if LM-332 is not required for proliferation in MDCK cells, the disparity is more likely due to a difference in receptor distribution, expression, and signaling.

7.5.3 The Requirement for LM-332 Integrin Receptors in MDCK Proliferation Control

The finding that the LM-332 integrin receptors were only partially required for progression into S phase in MDCK cells also contradicts studies by Gonzales *et al,* Nikolopoulos *et al*, Murgia *et al*, Li *et al*, and Raghavan *et al,* who individually reported a more significant requirement for either α6β4 or α3β1 integrins in cell proliferation. The discrepancy between our results and theirs, similar to the requirement for LM-332, could be explained by differences in the cell type, expression of cell receptors, or the methods by which studies were performed.

Although it is possible that our integrin studies were not entirely accurate for various reasons (see 6.3.3), studies by Yu *et al* hint that they may be correct (Yu et al., 2005). In this report, the authors were examining the requirement for β1 and α6 integrins in MDCK morphogenesis. They did this by treating MDCK cells with AIIB2 and GOH3 function blocking antibodies (the same that were used in our studies), and then allowing cells to form epithelia on filters, or cysts in 3D. Cell proliferation is also prerequisite for cyst formation, as cells are initially plated in a collagen suspension, and then coordinately proliferate and polarize to form a highly organized, hallow ball of cells. Although the polarity was altered in cells treated with β1 function blocking antibodies, cells were capable of multiplying to form both cysts in 3D, and an uninterrupted epithelium on filters. Assuming that treatment with integrin inhibitory antibodies is sufficient to inhibit integrin function, these data in conjunction with our own suggest that if LM-332 is required for proliferation, it is also using non-integrin receptors, such as the syndecans, to regulate proliferation. Indeed, members of the syndecan family are expressed in MDCK cells, and have been implicated in proliferation control in the epidermis and in corneal epithelial cells (Erickson and Couchman, 2001; Ojeh et al., 2008; Stepp et al., 2002).

7.5.4 The Use of RNAi to Understand Cellular Processes

The failure to rescue and validate the requirement for LM-332 in MDCK cell proliferation may have been caused by an off-target effect of the Ad-shLMα3 shRNA. RNAi target sequences, despite the fact that they are becoming increasingly easy to design and deliver into almost any cell line, are known to generate a large number of off-target effects (Jackson et al., 2003). An increased understanding is slowly being gained as to how to design and modify siRNAs to minimize of off-target effects (Jackson et al., 2006; Lin et al., 2005b) but currently,

they are unavoidable. The use of certain controls is therefore crucial to interpret results from studies using RNAi. Based on lessons learned from our Ad-shLMα3 validation experiments and the recommendations from Echeverri *et al*, all RNAi experiments should contain four components: 1) the parental, non-RNAi expressing cells, 2) a negative RNAi control, which is a target sequence that does not align and silence any gene within the cell-line of interest, 3) multiple RNAi target sequences against the target of interest, and 4) a mechanism for rescue (Echeverri et al., 2006). The most important of these being the comparison of the parental cells to multiple RNAi target sequences, as negative shRNA controls can also produce off-target effect-mediated cellular phenotypes, and the functionality of some proteins can be difficult to rescue for a variety of reasons. Indeed, in our studies, infection of cells with the shControls, Ad-shPKCα and Ad-shLacZ caused an increase in cell area, and; overexpression of integrin α6 in MDCK cells causes the α6 integrin to inappropriately dimerize with β1 integrin instead of β4 integrin, resulting in alteration of MDCK cell morphology (data not shown). Unfortunately, perusal through molecular biology journals reveal that many current studies using RNAi techniques do not employ the proper controls, which is cause for alarm, as without controls, there is no proof that the phenotype is not due to RNAi off-targeting.

7.6 Additional Future Directions

7.6.1 Generation of Stable shLMα3 Cell-lines and Assessment of the Requirement for LM-332 in Formation of the Epithelium

Although efficient transient suppression of LMα3 was achieved through expression of siRNA duplexes, this system has several disadvantages. The most significant limitation is that all experiments have to be completed within 48 hours, as at 48 hours, protein expression is beginning to return (Figure 6.10). It is unclear to what extent this small amount of expression

may be important, but could potentially be significant, as sustained inhibition may be required to observe alterations of some cellular processes, such as proliferation. For future studies, it will be important to generate retroviral shRNA knockdowns with the new LMα3 target sequences. Retroviral delivery of shRNA, similar to adenoviral delivery, results in significant shRNA expression and target suppression. The advantage of this system over transient expression of the duplexes is two-fold. First, retroviral expression of the shRNA should maintain the knockdown of LMα3 for longer than 48 hours. Second, as retroviral delivery integrates the plasmid encoding the shRNA directly into the genome, stable knockdown cell lines can be generated. Importantly, if LMα3 is required for proliferation as the literature suggests, we will be unable to generate stable cell lines, but at least would have a system in which longer-term suppression of LMα3 can be achieved.

Once the retrovirus' encoding for the LMα3 shRNAs are generated, and potentially, after stable LMα3 knockdown cell lines are generated, a broad scale phenotypical analysis should be performed in MDCK cells to confirm the requirement for LM-332 in re-formation of the epithelium, specifically in regards to proliferation, migration, cellular adhesion, polarization, and apoptosis.

7.6.2 Phenotypic Compensation by LM-511

In addition to LM-332, MDCK cells also express LM-511 (Mak et al., 2006). LM-511 binds to the same integrin receptors as LM-332, integrins α3β1 and α6β4 (Kikkawa et al., 2000); at low density, is expressed simultaneously to LM-332 (Mak et al., 2006; Gonzalez-Greciano, unpublished); and LM-511 can promote similar cellular phenotypes as LM-332, specifically adhesion, motility, and proliferation (Ferletta and Ekblom, 1999; Kikkawa et al., 2004; Pouliot et

al., 2001). Our laboratory has also recently generated a stable knockdown of LMα5 (Gonzalez-Greciano, unpublished). We have determined that loss of the α chain expression from one laminin does not alter the expression levels of the other laminin for both LMα3 and LMα5 (Figure 4.7 and Gonzalez-Greciano, unpublished). As LM-511 continues to be expressed in the absence of LM-332 however, it could potentially compensate functionally for LM-332 when LM-332 is absent. Assessing how loss of one may alter biological activity of the other, specifically in regards to adhesion, motility, and proliferation, will also be an important consideration for future studies.

7.6.3 In Vivo Renal Repair in the Absence of LM-332

Renal ischemia, which is defined as a decrease in the blood supply to the kidney due to blood vessel obstruction, results in either the shedding or depolarization of tubular epithelial cells (Racusen, 1998). Failure to repair the renal epithelium following ischemic injury to the kidney can lead to renal disease and hepatic damage (Golab et al., 2009; Pagtalunan et al., 1999), and may also promote cardiovascular disease (Sarnak et al., 2003). Studies from our laboratory have shown that LM-332 is not expressed in the normal rat kidney. Following ischemic injury however, high levels of LM-332 are observed throughout the length of the nephrons (Zuk and Matlin, 2002). Given the requirement for LM-332 in wound healing of other tissues, and given that the studies presented in this work also implicate LM-332 in the regulation of cell spreading, morphogenesis, and possibly proliferation, it is interesting to speculate that LM-332 expression is required following ischemic injury to repair the wounded renal epithelium *in vivo.* An important future direction therefore will be to use a conditional LMα3 knockout mouse to determine the requirement for LM-332 in renal injury repair following ischemic injury.

7.6.4 Laminin-332 and Tumorigenesis

The full-length LMα3 chain, which contains the LG4-5 domain at the Carboxy-terminus, is only observed upon the initial wounding of keratinocytes, similar to MDCK cells, and its overexpression in keratinocytes promotes tumorigenesis (Sigle et al., 2004; Tran et al., 2008). Furthermore, high levels of LM-332 are observed in renal cancer and polycystic kidney disease, and many squamous cell carcinomas, and high levels of the LG4-5 domain are detected in many squamous cell carcinomas (Joly et al., 2003; Lohi et al., 1996; Marinkovich, 2007; Tran et al., 2008). As discussed in section *7.5.2*, the differences in how the expression of full-length LM-332 in MDCK cell versus other cell types may mediate cell functions are unclear. Nevertheless, the data from Tran *et al* raise the possibility that continuous expression of the unprocessed form of LM-332, containing the full-length LMα3, may promote tumorigenesis within renal epithelia. In addition to the shRNA system described in this work, another useful tool for understanding LM-332 function was generated: the MDCK-hLMα3 overexpression system. LMα3 overexpressing cells could therefore be used to determine 1) if continuous expression of the unprocessed LMα3 may promote phenotypes, such as loss of contact inhibition, leading to renal disease *in vitro,* and 2) if overexpression of LMα3 in renal epithelial cells promotes tumorigenicity *in vivo*.

REFERENCES

Abercrombie, M. (1979). Contact inhibition and malignancy. Nature *281*, 259-262.

Afrakhte, M., Heldin, N. E., and Westermark, B. (1998). Inhibition of G1 cyclin-dependent kinase activity in cell density-dependent growth arrest in human fibroblasts. Cell Growth Differ *9*, 983-988.

Alam, N., Goel, H. L., Zarif, M. J., Butterfield, J. E., Perkins, H. M., Sansoucy, B. G., Sawyer, T. K., and Languino, L. R. (2007). The integrin-growth factor receptor duet. J Cell Physiol *213*, 649-653.

Alberts, B. (2008). Molecular biology of the cell, 5th edn (New York: Garland Science).

Alt, J. R., Gladden, A. B., and Diehl, J. A. (2002). p21(Cip1) Promotes cyclin D1 nuclear accumulation via direct inhibition of nuclear export. J Biol Chem *277*, 8517-8523.

Aoshiba, K., Tsuji, T., and Nagai, A. (2003). Bleomycin induces cellular senescence in alveolar epithelial cells. Eur Respir J *22*, 436-443.

Assoian, R. K. (1997). Anchorage-dependent cell cycle progression. J Cell Biol *136*, 1-4.
Atadja, P., Wong, H., Veillete, C., and Riabowol, K. (1995). Overexpression of cyclin D1 blocks proliferation of normal diploid fibroblasts. Exp Cell Res *217*, 205-216.

Aumailley, M., Bruckner-Tuderman, L., Carter, W. G., Deutzmann, R., Edgar, D., Ekblom, P., Engel, J., Engvall, E., Hohenester, E., Jones, J. C*., et al.* (2005). A simplified laminin nomenclature. Matrix Biol *24*, 326-332.

Bao, W., Thullberg, M., Zhang, H., Onischenko, A., and Stromblad, S. (2002). Cell attachment to the extracellular matrix induces proteasomal degradation of p21(CIP1) via Cdc42/Rac1 signaling. Mol Cell Biol *22*, 4587-4597.

Beck, K., Dixon, T. W., Engel, J., and Parry, D. A. (1993). Ionic interactions in the coiled-coil domain of laminin determine the specificity of chain assembly. J Mol Biol *231*, 311-323.

Beck, K., Hunter, I., and Engel, J. (1990). Structure and function of laminin: anatomy of a multidomain glycoprotein. FASEB J *4*, 148-160.

Bello, V., Sirour, C., Moreau, N., Denker, E., and Darribere, T. (2008). A function for dystroglycan in pronephros development in Xenopus laevis. Dev Biol *317*, 106-120.

Ben-Porath, I., and Weinberg, R. A. (2005). The signals and pathways activating cellular senescence. Int J Biochem Cell Biol *37*, 961-976.

Bernier, S. M., Utani, A., Sugiyama, S., Doi, T., Polistina, C., and Yamada, Y. (1995). Cloning and expression of laminin alpha 2 chain (M-chain) in the mouse. Matrix Biol *14*, 447-455.

Besson, A., Dowdy, S. F., and Roberts, J. M. (2008). CDK inhibitors: cell cycle regulators and beyond. Dev Cell *14*, 159-169.

Birmingham, A., Anderson, E. M., Reynolds, A., Ilsley-Tyree, D., Leake, D., Fedorov, Y., Baskerville, S., Maksimova, E., Robinson, K., Karpilow, J.*, et al.* (2006). 3' UTR seed matches, but not overall identity, are associated with RNAi off-targets. Nat Methods *3*, 199-204.

Blystone, S. D., Slater, S. E., Williams, M. P., Crow, M. T., and Brown, E. J. (1999). A molecular mechanism of integrin crosstalk: alphavbeta3 suppression of calcium/calmodulin-dependent protein kinase II regulates alpha5beta1 function. J Cell Biol *145*, 889-897.

Brehm, A., Miska, E. A., McCance, D. J., Reid, J. L., Bannister, A. J., and Kouzarides, T. (1998). Retinoblastoma protein recruits histone deacetylase to repress transcription. Nature *391*, 597-601.

Carter, W. G., Kaur, P., Gil, S. G., Gahr, P. J., and Wayner, E. A. (1990). Distinct functions for integrins alpha 3 beta 1 in focal adhesions and alpha 6 beta 4/bullous pemphigoid antigen in a new stable anchoring contact (SAC) of keratinocytes: relation to hemidesmosomes. J Cell Biol *111*, 3141-3154.

Chartier, N. T., Oddou, C. I., Laine, M. G., Ducarouge, B., Marie, C. A., Block, M. R., and Jacquier-Sarlin, M. R. (2007). Cyclin-dependent kinase 2/cyclin E complex is involved in p120 catenin (p120ctn)-dependent cell growth control: a new role for p120ctn in cancer. Cancer Res *67*, 9781-9790.

Cheng, M., Olivier, P., Diehl, J. A., Fero, M., Roussel, M. F., Roberts, J. M., and Sherr, C. J. (1999). The p21(Cip1) and p27(Kip1) CDK 'inhibitors' are essential activators of cyclin D-dependent kinases in murine fibroblasts. EMBO J *18*, 1571-1583.

Cheng, Y. S., Champliaud, M. F., Burgeson, R. E., Marinkovich, M. P., and Yurchenco, P. D. (1997). Self-assembly of laminin isoforms. J Biol Chem *272*, 31525-31532.

Child, E. S., and Mann, D. J. (2006). The intricacies of p21 phosphorylation: protein/protein interactions, subcellular localization and stability. Cell Cycle *5*, 1313-1319.

Clarke, A. S., Lotz, M. M., Chao, C., and Mercurio, A. M. (1995). Activation of the p21 pathway of growth arrest and apoptosis by the beta 4 integrin cytoplasmic domain. J Biol Chem *270*, 22673-22676.

Coleman, M. L., Marshall, C. J., and Olson, M. F. (2003). Ras promotes p21(Waf1/Cip1) protein stability via a cyclin D1-imposed block in proteasome-mediated degradation. EMBO J *22*, 2036-2046.

Cruet-Hennequart, S., Maubant, S., Luis, J., Gauduchon, P., Staedel, C., and Dedhar, S. (2003). alpha(v) integrins regulate cell proliferation through integrin-linked kinase (ILK) in ovarian cancer cells. Oncogene *22*, 1688-1702.

D'Amico, M., Hulit, J., Amanatullah, D. F., Zafonte, B. T., Albanese, C., Bouzahzah, B., Fu, M., Augenlicht, L. H., Donehower, L. A., Takemaru, K.*, et al.* (2000). The integrin-linked kinase regulates the cyclin D1 gene through glycogen synthase kinase 3beta and cAMP-responsive element-binding protein-dependent pathways. J Biol Chem *275*, 32649-32657.

Dans, M., Gagnoux-Palacios, L., Blaikie, P., Klein, S., Mariotti, A., and Giancotti, F. G. (2001). Tyrosine phosphorylation of the beta 4 integrin cytoplasmic domain mediates Shc signaling to extracellular signal-regulated kinase and antagonizes formation of hemidesmosomes. J Biol Chem *276*, 1494-1502.

Decline, F., and Rousselle, P. (2001). Keratinocyte migration requires alpha2beta1 integrin-mediated interaction with the laminin 5 gamma2 chain. J Cell Sci *114*, 811-823.

DeMali, K. A., and Burridge, K. (2003). Coupling membrane protrusion and cell adhesion. J Cell Sci *116*, 2389-2397.

Diehl, J. A. (2002). Cycling to cancer with cyclin D1. Cancer Biol Ther *1*, 226-231.

Diehl, J. A., Cheng, M., Roussel, M. F., and Sherr, C. J. (1998). Glycogen synthase kinase-3beta regulates cyclin D1 proteolysis and subcellular localization. Genes Dev *12*, 3499-3511.

Diehl, J. A., and Sherr, C. J. (1997). A dominant-negative cyclin D1 mutant prevents nuclear import of cyclin-dependent kinase 4 (CDK4) and its phosphorylation by CDK-activating kinase. Mol Cell Biol *17*, 7362-7374.

Durbeej, M. (2010). Laminins. Cell Tissue Res *339*, 259-268.

Echeverri, C. J., Beachy, P. A., Baum, B., Boutros, M., Buchholz, F., Chanda, S. K., Downward, J., Ellenberg, J., Fraser, A. G., Hacohen, N.*, et al.* (2006). Minimizing the risk of reporting false positives in large-scale RNAi screens. Nat Methods *3*, 777-779.

Echtermeyer, F., Streit, M., Wilcox-Adelman, S., Saoncella, S., Denhez, F., Detmar, M., and Goetinck, P. (2001). Delayed wound repair and impaired angiogenesis in mice lacking syndecan-4. J Clin Invest *107*, R9-R14.

Elbashir, S. M., Harborth, J., Lendeckel, W., Yalcin, A., Weber, K., and Tuschl, T. (2001a). Duplexes of 21-nucleotide RNAs mediate RNA interference in cultured mammalian cells. Nature *411*, 494-498.

Elbashir, S. M., Harborth, J., Weber, K., and Tuschl, T. (2002). Analysis of gene function in somatic mammalian cells using small interfering RNAs. Methods *26*, 199-213.

Elbashir, S. M., Lendeckel, W., and Tuschl, T. (2001b). RNA interference is mediated by 21- and 22-nucleotide RNAs. Genes Dev *15*, 188-200.

Elenius, K., Vainio, S., Laato, M., Salmivirta, M., Thesleff, I., and Jalkanen, M. (1991). Induced expression of syndecan in healing wounds. J Cell Biol *114*, 585-595.

Elenius, V., Gotte, M., Reizes, O., Elenius, K., and Bernfield, M. (2004). Inhibition by the soluble syndecan-1 ectodomains delays wound repair in mice overexpressing syndecan-1. J Biol Chem *279*, 41928-41935.

Engel, J. (1989). EGF-like domains in extracellular matrix proteins: localized signals for growth and differentiation? FEBS Lett *251*, 1-7.

Engel, J., Odermatt, E., Engel, A., Madri, J. A., Furthmayr, H., Rohde, H., and Timpl, R. (1981). Shapes, domain organizations and flexibility of laminin and fibronectin, two multifunctional proteins of the extracellular matrix. J Mol Biol *150*, 97-120.

Erickson, A. C., and Couchman, J. R. (2001). Basement membrane and interstitial proteoglycans produced by MDCK cells correspond to those expressed in the kidney cortex. Matrix Biol *19*, 769-778.

Fears, C. Y., and Woods, A. (2006). The role of syndecans in disease and wound healing. Matrix Biol *25*, 443-456.

Fedorov, Y., Anderson, E. M., Birmingham, A., Reynolds, A., Karpilow, J., Robinson, K., Leake, D., Marshall, W. S., and Khvorova, A. (2006). Off-target effects by siRNA can induce toxic phenotype. RNA *12*, 1188-1196.

Fedorov, Y., King, A., Anderson, E., Karpilow, J., Ilsley, D., Marshall, W., and Khvorova, A. (2005). Different delivery methods-different expression profiles. Nat Methods *2*, 241.

Fenteany, G., Janmey, P. A., and Stossel, T. P. (2000). Signaling pathways and cell mechanics involved in wound closure by epithelial cell sheets. Curr Biol *10*, 831-838.

Ferletta, M., and Ekblom, P. (1999). Identification of laminin-10/11 as a strong cell adhesive complex for a normal and a malignant human epithelial cell line. J Cell Sci *112 (Pt 1)*, 1-10.

Ferrigno, O., Virolle, T., Galliano, M. F., Chauvin, N., Ortonne, J. P., Meneguzzi, G., and Aberdam, D. (1997). Murine laminin alpha3A and alpha3B isoform chains are generated by usage of two promoters and alternative splicing. J Biol Chem *272*, 20502-20507.

Fire, A., Xu, S., Montgomery, M. K., Kostas, S. A., Driver, S. E., and Mello, C. C. (1998). Potent and specific genetic interference by double-stranded RNA in Caenorhabditis elegans. Nature *391*, 806-811.

Fish, E. M., and Molitoris, B. A. (1994). Alterations in epithelial polarity and the pathogenesis of disease states. N Engl J Med *330*, 1580-1588.

Friedl, P., Hegerfeldt, Y., and Tusch, M. (2004). Collective cell migration in morphogenesis and cancer. Int J Dev Biol *48*, 441-449.

Frisch, S. M., and Francis, H. (1994). Disruption of epithelial cell-matrix interactions induces apoptosis. J Cell Biol *124*, 619-626.

Fristrom, D. (1988). The cellular basis of epithelial morphogenesis. A review. Tissue Cell *20*, 645-690.

Fu, M., Wang, C., Li, Z., Sakamaki, T., and Pestell, R. G. (2004). Minireview: Cyclin D1: normal and abnormal functions. Endocrinology *145*, 5439-5447.

Furuyama, A., and Mochitate, K. (2000). Assembly of the exogenous extracellular matrix during basement membrane formation by alveolar epithelial cells in vitro. J Cell Sci *113 (Pt 5)*, 859-868.

Galliano, M. F., Aberdam, D., Aguzzi, A., Ortonne, J. P., and Meneguzzi, G. (1995). Cloning and complete primary structure of the mouse laminin alpha 3 chain. Distinct expression pattern of the laminin alpha 3A and alpha 3B chain isoforms. J Biol Chem *270*, 21820-21826.

Gallo, R., Kim, C., Kokenyesi, R., Adzick, N. S., and Bernfield, M. (1996). Syndecans-1 and -4 are induced during wound repair of neonatal but not fetal skin. J Invest Dermatol *107*, 676-683.

Gambaletta, D., Marchetti, A., Benedetti, L., Mercurio, A. M., Sacchi, A., and Falcioni, R. (2000). Cooperative signaling between alpha(6)beta(4) integrin and ErbB-2 receptor is required to promote phosphatidylinositol 3-kinase-dependent invasion. J Biol Chem *275*, 10604-10610.

Gartel, A. L., and Radhakrishnan, S. K. (2005). Lost in transcription: p21 repression, mechanisms, and consequences. Cancer Res *65*, 3980-3985.

Gaulin, J. F., Fiset, A., Fortier, S., and Faure, R. L. (2000). Characterization of Cdk2-cyclin E complexes in plasma membrane and endosomes of liver parenchyma. Insulin-dependent regulation. J Biol Chem *275*, 16658-16665.

Gaush, C. R., Hard, W. L., and Smith, T. F. (1966). Characterization of an established line of canine kidney cells (MDCK). Proc Soc Exp Biol Med *122*, 931-935.

Giancotti, F. G., and Tarone, G. (2003). Positional control of cell fate through joint integrin/receptor protein kinase signaling. Annu Rev Cell Dev Biol *19*, 173-206.

Gladden, A. B., and Diehl, J. A. (2005). Location, location, location: the role of cyclin D1 nuclear localization in cancer. J Cell Biochem *96*, 906-913.

Goel, H. L., Breen, M., Zhang, J., Das, I., Aznavoorian-Cheshire, S., Greenberg, N. M., Elgavish, A., and Languino, L. R. (2005). beta1A integrin expression is required for type 1 insulin-like growth factor receptor mitogenic and transforming activities and localization to focal contacts. Cancer Res *65*, 6692-6700.

Golab, F., Kadkhodaee, M., Zahmatkesh, M., Hedayati, M., Arab, H., Schuster, R., Zahedi, K., Lentsch, A. B., and Soleimani, M. (2009). Ischemic and non-ischemic acute kidney injury cause hepatic damage. Kidney Int *75*, 783-792.

Goldfinger, L. E., Hopkinson, S. B., deHart, G. W., Collawn, S., Couchman, J. R., and Jones, J. C. (1999). The alpha3 laminin subunit, alpha6beta4 and alpha3beta1 integrin coordinately regulate wound healing in cultured epithelial cells and in the skin. J Cell Sci *112 (Pt 16)*, 2615-2629.

Goldfinger, L. E., Stack, M. S., and Jones, J. C. (1998). Processing of laminin-5 and its functional consequences: role of plasmin and tissue-type plasminogen activator. J Cell Biol *141*, 255-265.

Goncalves, M. A., and de Vries, A. A. (2006). Adenovirus: from foe to friend. Rev Med Virol *16*, 167-186.

Gong, J., Ardelt, B., Traganos, F., and Darzynkiewicz, Z. (1994). Unscheduled expression of cyclin B1 and cyclin E in several leukemic and solid tumor cell lines. Cancer Res *54*, 4285-4288.

Gonzales, M., Haan, K., Baker, S. E., Fitchmun, M., Todorov, I., Weitzman, S., and Jones, J. C. (1999). A cell signal pathway involving laminin-5, alpha3beta1 integrin, and mitogen-activated protein kinase can regulate epithelial cell proliferation. Mol Biol Cell *10*, 259-270.

Graham, F. L., Smiley, J., Russell, W. C., and Nairn, R. (1977). Characteristics of a human cell line transformed by DNA from human adenovirus type 5. J Gen Virol *36*, 59-74.

Guadagno, T. M., Ohtsubo, M., Roberts, J. M., and Assoian, R. K. (1993). A link between cyclin A expression and adhesion-dependent cell cycle progression. Science *262*, 1572-1575.

Hall, D. E., Reichardt, L. F., Crowley, E., Holley, B., Moezzi, H., Sonnenberg, A., and Damsky, C. H. (1990). The alpha 1/beta 1 and alpha 6/beta 1 integrin heterodimers mediate cell attachment to distinct sites on laminin. J Cell Biol *110*, 2175-2184.
Han, E. K., Ng, S. C., Arber, N., Begemann, M., and Weinstein, I. B. (1999). Roles of cyclin D1 and related genes in growth inhibition, senescence and apoptosis. Apoptosis *4*, 213-219.

Hashimoto, J., Kariya, Y., and Miyazaki, K. (2006). Regulation of proliferation and chondrogenic differentiation of human mesenchymal stem cells by laminin-5 (laminin-332). Stem Cells *24*, 2346-2354.

Hay, E. D. (1991). Cell biology of extracellular matrix, 2nd edn (New York: Plenum Press).

Herzlinger, D. A., Easton, T. G., and Ojakian, G. K. (1982). The MDCK epithelial cell line expresses a cell surface antigen of the kidney distal tubule. J Cell Biol *93*, 269-277.

Higginson, J. R., and Winder, S. J. (2005). Dystroglycan: a multifunctional adaptor protein. Biochem Soc Trans *33*, 1254-1255.

Hormia, M., Falk-Marzillier, J., Plopper, G., Tamura, R. N., Jones, J. C., and Quaranta, V. (1995). Rapid spreading and mature hemidesmosome formation in HaCaT keratinocytes induced by incubation with soluble laminin-5r. J Invest Dermatol *105*, 557-561.

Howe, C. C., and Dietzschold, B. (1983). Structural analysis of three subunits of laminin from teratocarcinoma-derived parietal endoderm cells. Dev Biol *98*, 385-391.

Humphries, M. J. (1996). Integrin activation: the link between ligand binding and signal transduction. Curr Opin Cell Biol *8*, 632-640.

Hwang, A., Maity, A., McKenna, W. G., and Muschel, R. J. (1995). Cell cycle-dependent regulation of the cyclin B1 promoter. J Biol Chem *270*, 28419-28424.

Hwang, H. C., and Clurman, B. E. (2005). Cyclin E in normal and neoplastic cell cycles. Oncogene *24*, 2776-2786.

Itahana, K., Dimri, G. P., Hara, E., Itahana, Y., Zou, Y., Desprez, P. Y., and Campisi, J. (2002). A role for p53 in maintaining and establishing the quiescence growth arrest in human cells. J Biol Chem *277*, 18206-18214.

Jacinto, A., Martinez-Arias, A., and Martin, P. (2001). Mechanisms of epithelial fusion and repair. Nat Cell Biol *3*, E117-123.

Jackson, A. L., Bartz, S. R., Schelter, J., Kobayashi, S. V., Burchard, J., Mao, M., Li, B., Cavet, G., and Linsley, P. S. (2003). Expression profiling reveals off-target gene regulation by RNAi. Nat Biotechnol *21*, 635-637.

Jackson, A. L., Burchard, J., Leake, D., Reynolds, A., Schelter, J., Guo, J., Johnson, J. M., Lim, L., Karpilow, J., Nichols, K.*, et al.* (2006). Position-specific chemical modification of siRNAs reduces "off-target" transcript silencing. RNA *12*, 1197-1205.

Jeffrey, P. D., Russo, A. A., Polyak, K., Gibbs, E., Hurwitz, J., Massague, J., and Pavletich, N. P. (1995). Mechanism of CDK activation revealed by the structure of a cyclinA-CDK2 complex. Nature *376*, 313-320.

Joly, D., Berissi, S., Bertrand, A., Strehl, L., Patey, N., and Knebelmann, B. (2006). Laminin 5 regulates polycystic kidney cell proliferation and cyst formation. J Biol Chem *281*, 29181-29189.

Joly, D., Morel, V., Hummel, A., Ruello, A., Nusbaum, P., Patey, N., Noel, L. H., Rousselle, P., and Knebelmann, B. (2003). Beta4 integrin and laminin 5 are aberrantly expressed in polycystic kidney disease: role in increased cell adhesion and migration. Am J Pathol *163*, 1791-1800.

Jones, J. C., Lane, K., Hopkinson, S. B., Lecuona, E., Geiger, R. C., Dean, D. A., Correa-Meyer, E., Gonzales, M., Campbell, K., Sznajder, J. I., and Budinger, S. (2005). Laminin-6 assembles into multimolecular fibrillar complexes with perlecan and participates in mechanical-signal transduction via a dystroglycan-dependent, integrin-independent mechanism. J Cell Sci *118*, 2557-2566.

Kagawa, S., Fujiwara, T., Kadowaki, Y., Fukazawa, T., Sok-Joo, R., Roth, J. A., and Tanaka, N. (1999). Overexpression of the p21 sdi1 gene induces senescence-like state in human cancer cells: implication for senescence-directed molecular therapy for cancer. Cell Death Differ *6*, 765-772.

Kallunki, P., Sainio, K., Eddy, R., Byers, M., Kallunki, T., Sariola, H., Beck, K., Hirvonen, H., Shows, T. B., and Tryggvason, K. (1992). A truncated laminin chain homologous to the B2 chain: structure, spatial expression, and chromosomal assignment. J Cell Biol *119*, 679-693.

Kardassis, D., Papakosta, P., Pardali, K., and Moustakas, A. (1999). c-Jun transactivates the promoter of the human p21(WAF1/Cip1) gene by acting as a superactivator of the ubiquitous transcription factor Sp1. J Biol Chem *274*, 29572-29581.

Karin, M. (1995). The regulation of AP-1 activity by mitogen-activated protein kinases. J Biol Chem *270*, 16483-16486.

Kariya, Y., Kato, R., Itoh, S., Fukuda, T., Shibukawa, Y., Sanzen, N., Sekiguchi, K., Wada, Y., Kawasaki, N., and Gu, J. (2008). N-Glycosylation of laminin-332 regulates its biological functions. A novel function of the bisecting GlcNAc. J Biol Chem *283*, 33036-33045.

Kariya, Y., Kawamura, C., Tabei, T., and Gu, J. (2010). Bisecting GlcNAc residues on laminin-332 down-regulate galectin-3-dependent keratinocyte motility. J Biol Chem *285*, 3330-3340.

Kariya, Y., Yasuda, C., Nakashima, Y., Ishida, K., Tsubota, Y., and Miyazaki, K. (2004). Characterization of laminin 5B and NH2-terminal proteolytic fragment of its alpha3B chain: promotion of cellular adhesion, migration, and proliferation. J Biol Chem *279*, 24774-24784.

Kikkawa, Y., Sanzen, N., Fujiwara, H., Sonnenberg, A., and Sekiguchi, K. (2000). Integrin binding specificity of laminin-10/11: laminin-10/11 are recognized by alpha 3 beta 1, alpha 6 beta 1 and alpha 6 beta 4 integrins. J Cell Sci *113 (Pt 5)*, 869-876.

Kikkawa, Y., Yu, H., Genersch, E., Sanzen, N., Sekiguchi, K., Fassler, R., Campbell, K. P., Talts, J. F., and Ekblom, P. (2004). Laminin isoforms differentially regulate adhesion, spreading, proliferation, and ERK activation of beta1 integrin-null cells. Exp Cell Res *300*, 94-108.

Kim, J. P., Zhang, K., Chen, J. D., Wynn, K. C., Kramer, R. H., and Woodley, D. T. (1992). Mechanism of human keratinocyte migration on fibronectin: unique roles of RGD site and integrins. J Cell Physiol *151*, 443-450.

Klein, G., Langegger, M., Timpl, R., and Ekblom, P. (1988). Role of laminin A chain in the development of epithelial cell polarity. Cell *55*, 331-341.

Kligys, K., Claiborne, J. N., DeBiase, P. J., Hopkinson, S. B., Wu, Y., Mizuno, K., and Jones, J. C. (2007). The slingshot family of phosphatases mediates Rac1 regulation of cofilin phosphorylation, laminin-332 organization, and motility behavior of keratinocytes. J Biol Chem *282*, 32520-32528.

Knoll, R., Postel, R., Wang, J., Kratzner, R., Hennecke, G., Vacaru, A. M., Vakeel, P., Schubert, C., Murthy, K., Rana, B. K.*, et al.* (2007). Laminin-alpha4 and integrin-linked kinase mutations cause human cardiomyopathy via simultaneous defects in cardiomyocytes and endothelial cells. Circulation *116*, 515-525.

Kwon, Y. H., Jovanovic, A., Serfas, M. S., Kiyokawa, H., and Tyner, A. L. (2002). P21 functions to maintain quiescence of p27-deficient hepatocytes. J Biol Chem *277*, 41417-41422.

LaBaer, J., Garrett, M. D., Stevenson, L. F., Slingerland, J. M., Sandhu, C., Chou, H. S., Fattaey, A., and Harlow, E. (1997). New functional activities for the p21 family of CDK inhibitors. Genes Dev *11*, 847-862.

Langhofer, M., Hopkinson, S. B., and Jones, J. C. (1993). The matrix secreted by 804G cells contains laminin-related components that participate in hemidesmosome assembly in vitro. J Cell Sci *105 (Pt 3)*, 753-764.

LeBleu, V. S., Macdonald, B., and Kalluri, R. (2007). Structure and function of basement membranes. Exp Biol Med (Maywood) *232*, 1121-1129.

Legate, K. R., Wickstrom, S. A., and Fassler, R. (2009). Genetic and cell biological analysis of integrin outside-in signaling. Genes Dev *23*, 397-418.

Li, N., Zhang, Y., Naylor, M. J., Schatzmann, F., Maurer, F., Wintermantel, T., Schuetz, G., Mueller, U., Streuli, C. H., and Hynes, N. E. (2005a). Beta1 integrins regulate mammary gland proliferation and maintain the integrity of mammary alveoli. Embo J *24*, 1942-1953.

Li, S., Gerrard, E. R., Jr., and Balkovetz, D. F. (2004). Evidence for ERK1/2 phosphorylation controlling contact inhibition of proliferation in Madin-Darby canine kidney epithelial cells. Am J Physiol Cell Physiol *287*, C432-439.

Li, S., Liquari, P., McKee, K. K., Harrison, D., Patel, R., Lee, S., and Yurchenco, P. D. (2005b). Laminin-sulfatide binding initiates basement membrane assembly and enables receptor signaling in Schwann cells and fibroblasts. J Cell Biol *169*, 179-189.

Lin, D. I., Barbash, O., Kumar, K. G., Weber, J. D., Harper, J. W., Klein-Szanto, A. J., Rustgi, A., Fuchs, S. Y., and Diehl, J. A. (2006). Phosphorylation-dependent ubiquitination of cyclin D1 by the SCF(FBX4-alphaB crystallin) complex. Mol Cell *24*, 355-366.

Lin, F., Ren, X. D., Doris, G., and Clark, R. A. (2005a). Three-dimensional migration of human adult dermal fibroblasts from collagen lattices into fibrin/fibronectin gels requires syndecan-4 proteoglycan. J Invest Dermatol *124*, 906-913.

Lin, X., Ruan, X., Anderson, M. G., McDowell, J. A., Kroeger, P. E., Fesik, S. W., and Shen, Y. (2005b). siRNA-mediated off-target gene silencing triggered by a 7 nt complementation. Nucleic Acids Res *33*, 4527-4535.

Liu, S., Yamashita, H., Weidow, B., Weaver, A. M., and Quaranta, V. (2010). Laminin-332-beta1 integrin interactions negatively regulate invadopodia. J Cell Physiol *223*, 134-142.

Lochmuller, H., Jani, A., Huard, J., Prescott, S., Simoneau, M., Massie, B., Karpati, G., and Acsadi, G. (1994). Emergence of early region 1-containing replication-competent adenovirus in stocks of replication-defective adenovirus recombinants (delta E1 + delta E3) during multiple passages in 293 cells. Hum Gene Ther *5*, 1485-1491.

Lohi, J., Tani, T., Leivo, I., Linnala, A., Kangas, L., Burgeson, R. E., Lehto, V. P., and Virtanen, I. (1996). Expression of laminin in renal-cell carcinomas, renal-cell carcinoma cell lines and xenografts in nude mice. Int J Cancer *68*, 364-371.

Lucibello, F. C., Sewing, A., Brusselbach, S., Burger, C., and Muller, R. (1993). Deregulation of cyclins D1 and E and suppression of cdk2 and cdk4 in senescent human fibroblasts. J Cell Sci *105 (Pt 1)*, 123-133.

Lukas, C., Sorensen, C. S., Kramer, E., Santoni-Rugiu, E., Lindeneg, C., Peters, J. M., Bartek, J., and Lukas, J. (1999). Accumulation of cyclin B1 requires E2F and cyclin-A-dependent rearrangement of the anaphase-promoting complex. Nature *401*, 815-818.

Madin, S. H., Andriese, P. C., and Darby, N. B. (1957). The in vitro cultivation of tissues of domestic and laboratory animals. Am J Vet Res *18*, 932-941.

Mainiero, F., Murgia, C., Wary, K. K., Curatola, A. M., Pepe, A., Blumemberg, M., Westwick, J. K., Der, C. J., and Giancotti, F. G. (1997). The coupling of alpha6beta4 integrin to Ras-MAP kinase pathways mediated by Shc controls keratinocyte proliferation. Embo J *16*, 2365-2375.

Mak, G. Z., Kavanaugh, G. M., Buschmann, M. M., Stickley, S. M., Koch, M., Goss, K. H., Waechter, H., Zuk, A., and Matlin, K. S. (2006). Regulated synthesis and functions of laminin 5 in polarized madin-darby canine kidney epithelial cells. Mol Biol Cell *17*, 3664-3677.

Marinkovich, M. P. (2007). Tumour microenvironment: laminin 332 in squamous-cell carcinoma. Nat Rev Cancer *7*, 370-380.

Masuda-Hirata, M., Suzuki, A., Amano, Y., Yamashita, K., Ide, M., Yamanaka, T., Sakai, M., Imamura, M., and Ohno, S. (2009). Intracellular polarity protein PAR-1 regulates extracellular laminin assembly by regulating the dystroglycan complex. Genes Cells *14*, 835-850.

Matlin, K. S., Reggio, H., Helenius, A., and Simons, K. (1981). Infectious entry pathway of influenza virus in a canine kidney cell line. J Cell Biol *91*, 601-613.

Matoltsy, A. G., and Viziam, C. B. (1970). Further observations on epithelialization of small wounds: an autoradiographic study of incorporation and distribution of 3H-thymidine in the epithelium covering skin wounds. J Invest Dermatol *55*, 20-25.

Matsui, C., Wang, C. K., Nelson, C. F., Bauer, E. A., and Hoeffler, W. K. (1995). The assembly of laminin-5 subunits. J Biol Chem *270*, 23496-23503.

Mayer, U., Poschl, E., Gerecke, D. R., Wagman, D. W., Burgeson, R. E., and Timpl, R. (1995). Low nidogen affinity of laminin-5 can be attributed to two serine residues in EGF-like motif gamma 2III4. FEBS Lett *365*, 129-132.

McGowan, K. A., and Marinkovich, M. P. (2000). Laminins and human disease. Microsc Res Tech *51*, 262-279.

McKee, K. K., Capizzi, S., and Yurchenco, P. D. (2009). Scaffold-forming and Adhesive Contributions of Synthetic Laminin-binding Proteins to Basement Membrane Assembly. J Biol Chem *284*, 8984-8994.

Meder, D., Shevchenko, A., Simons, K., and Fullekrug, J. (2005). Gp135/podocalyxin and NHERF-2 participate in the formation of a preapical domain during polarization of MDCK cells. J Cell Biol *168*, 303-313.

Meister, G., and Tuschl, T. (2004). Mechanisms of gene silencing by double-stranded RNA. Nature *431*, 343-349.

Meloche, S., and Pouyssegur, J. (2007). The ERK1/2 mitogen-activated protein kinase pathway as a master regulator of the G1- to S-phase transition. Oncogene *26*, 3227-3239.

Meng, X., Klement, J. F., Leperi, D. A., Birk, D. E., Sasaki, T., Timpl, R., Uitto, J., and Pulkkinen, L. (2003). Targeted inactivation of murine laminin gamma2-chain gene recapitulates human junctional epidermolysis bullosa. J Invest Dermatol *121*, 720-731.

Michelson, P. H., Tigue, M., and Jones, J. C. (2000). Human bronchial epithelial cells secrete laminin 5, express hemidesmosomal proteins, and assemble hemidesmosomes. J Histochem Cytochem *48*, 535-544.

Midwood, K. S., Valenick, L. V., Hsia, H. C., and Schwarzbauer, J. E. (2004). Coregulation of fibronectin signaling and matrix contraction by tenascin-C and syndecan-4. Mol Biol Cell *15*, 5670-5677.

Miner, J. H., and Li, C. (2000). Defective glomerulogenesis in the absence of laminin alpha5 demonstrates a developmental role for the kidney glomerular basement membrane. Dev Biol *217*, 278-289.

Miner, J. H., and Yurchenco, P. D. (2004). Laminin functions in tissue morphogenesis. Annu Rev Cell Dev Biol *20*, 255-284.

Misfeldt, D. S., Hamamoto, S. T., and Pitelka, D. R. (1976). Transepithelial transport in cell culture. Proc Natl Acad Sci U S A *73*, 1212-1216.

Mitsuuchi, Y., Johnson, S. W., Selvakumaran, M., Williams, S. J., Hamilton, T. C., and Testa, J. R. (2000). The phosphatidylinositol 3-kinase/AKT signal transduction pathway plays a critical role in the expression of p21WAF1/CIP1/SDI1 induced by cisplatin and paclitaxel. Cancer Res *60*, 5390-5394.

Miyagoe, Y., Hanaoka, K., Nonaka, I., Hayasaka, M., Nabeshima, Y., Arahata, K., and Takeda, S. (1997). Laminin alpha2 chain-null mutant mice by targeted disruption of the Lama2 gene: a new model of merosin (laminin 2)-deficient congenital muscular dystrophy. FEBS Lett *415*, 33-39.

Mizuguchi, H., and Kay, M. A. (1998). Efficient construction of a recombinant adenovirus vector by an improved in vitro ligation method. Hum Gene Ther *9*, 2577-2583.

Mizushima, H., Hirosaki, T., Miyata, S., Takamura, H., Miyagi, Y., and Miyazaki, K. (2002). Expression of laminin-5 enhances tumorigenicity of human fibrosarcoma cells in nude mice. Jpn J Cancer Res *93*, 652-659.

Montanaro, F., Lindenbaum, M., and Carbonetto, S. (1999). alpha-Dystroglycan is a laminin receptor involved in extracellular matrix assembly on myotubes and muscle cell viability. J Cell Biol *145*, 1325-1340.

Montgomery, M. K., Xu, S., and Fire, A. (1998). RNA as a target of double-stranded RNA-mediated genetic interference in Caenorhabditis elegans. Proc Natl Acad Sci U S A *95*, 15502-15507.

Moore, J. D., Yang, J., Truant, R., and Kornbluth, S. (1999). Nuclear import of Cdk/cyclin complexes: identification of distinct mechanisms for import of Cdk2/cyclin E and Cdc2/cyclin B1. J Cell Biol *144*, 213-224.

Morgan, D. O. (1997). Cyclin-dependent kinases: engines, clocks, and microprocessors. Annu Rev Cell Dev Biol *13*, 261-291.

Moro, L., Dolce, L., Cabodi, S., Bergatto, E., Boeri Erba, E., Smeriglio, M., Turco, E., Retta, S. F., Giuffrida, M. G., Venturino, M.*, et al.* (2002). Integrin-induced epidermal growth factor (EGF) receptor activation requires c-Src and p130Cas and leads to phosphorylation of specific EGF receptor tyrosines. J Biol Chem *277*, 9405-9414.

Murgia, C., Blaikie, P., Kim, N., Dans, M., Petrie, H. T., and Giancotti, F. G. (1998). Cell cycle and adhesion defects in mice carrying a targeted deletion of the integrin beta4 cytoplasmic domain. Embo J *17*, 3940-3951.

Nguyen, B. P., Ryan, M. C., Gil, S. G., and Carter, W. G. (2000). Deposition of laminin 5 in epidermal wounds regulates integrin signaling and adhesion. Curr Opin Cell Biol *12*, 554-562.

Nikolopoulos, S. N., Blaikie, P., Yoshioka, T., Guo, W., Puri, C., Tacchetti, C., and Giancotti, F. G. (2005). Targeted deletion of the integrin beta4 signaling domain suppresses laminin-5-dependent nuclear entry of mitogen-activated protein kinases and NF-kappaB, causing defects in epidermal growth and migration. Mol Cell Biol *25*, 6090-6102.

Noakes, P. G., Gautam, M., Mudd, J., Sanes, J. R., and Merlie, J. P. (1995a). Aberrant differentiation of neuromuscular junctions in mice lacking s-laminin/laminin beta 2. Nature *374*, 258-262.

Noakes, P. G., Miner, J. H., Gautam, M., Cunningham, J. M., Sanes, J. R., and Merlie, J. P. (1995b). The renal glomerulus of mice lacking s-laminin/laminin beta 2: nephrosis despite molecular compensation by laminin beta 1. Nat Genet *10*, 400-406.

Odenthal, U., Haehn, S., Tunggal, P., Merkl, B., Schomburg, D., Frie, C., Paulsson, M., and Smyth, N. (2004). Molecular analysis of laminin N-terminal domains mediating self-interactions. J Biol Chem *279*, 44504-44512.

Ojeh, N., Hiilesvuo, K., Warri, A., Salmivirta, M., Henttinen, T., and Maatta, A. (2008). Ectopic expression of syndecan-1 in basal epidermis affects keratinocyte proliferation and wound re-epithelialization. J Invest Dermatol *128*, 26-34.

Okamoto, O., Bachy, S., Odenthal, U., Bernaud, J., Rigal, D., Lortat-Jacob, H., Smyth, N., and Rousselle, P. (2003). Normal human keratinocytes bind to the alpha3LG4/5 domain of unprocessed laminin-5 through the receptor syndecan-1. J Biol Chem *278*, 44168-44177.

Olsen, J., Lefebvre, O., Fritsch, C., Troelsen, J. T., Orian-Rousseau, V., Kedinger, M., and Simon-Assmann, P. (2000). Involvement of activator protein 1 complexes in the epithelium-specific activation of the laminin gamma2-chain gene promoter by hepatocyte growth factor (scatter factor). Biochem J *347*, 407-417.

Pagtalunan, M. E., Olson, J. L., Tilney, N. L., and Meyer, T. W. (1999). Late consequences of acute ischemic injury to a solitary kidney. J Am Soc Nephrol *10*, 366-373.

Pardee, A. B. (1974). A restriction point for control of normal animal cell proliferation. Proc Natl Acad Sci U S A *71*, 1286-1290.

Patton, B. L., Connoll, A. M., Martin, P. T., Cunningham, J. M., Mehta, S., Pestronk, A., Miner, J. H., and Sanes, J. R. (1999). Distribution of ten laminin chains in dystrophic and regenerating muscles. Neuromuscul Disord *9*, 423-433.

Patton, B. L., Cunningham, J. M., Thyboll, J., Kortesmaa, J., Westerblad, H., Edstrom, L., Tryggvason, K., and Sanes, J. R. (2001). Properly formed but improperly localized synaptic specializations in the absence of laminin alpha4. Nat Neurosci *4*, 597-604.

Patton, B. L., Miner, J. H., Chiu, A. Y., and Sanes, J. R. (1997). Distribution and function of laminins in the neuromuscular system of developing, adult, and mutant mice. J Cell Biol *139*, 1507-1521.

Paulsson, M., Deutzmann, R., Timpl, R., Dalzoppo, D., Odermatt, E., and Engel, J. (1985). Evidence for coiled-coil alpha-helical regions in the long arm of laminin. EMBO J *4*, 309-316.

Pei, X. H., and Xiong, Y. (2005). Biochemical and cellular mechanisms of mammalian CDK inhibitors: a few unresolved issues. Oncogene *24*, 2787-2795.

Pennock, S., and Wang, Z. (2003). Stimulation of cell proliferation by endosomal epidermal growth factor receptor as revealed through two distinct phases of signaling. Mol Cell Biol *23*, 5803-5815.

Pertsemlidis, A., and Fondon, J. W., 3rd (2001). Having a BLAST with bioinformatics (and avoiding BLASTphemy). Genome Biol *2*, REVIEWS2002.

Peters, B. P., Hartle, R. J., Krzesicki, R. F., Kroll, T. G., Perini, F., Balun, J. E., Goldstein, I. J., and Ruddon, R. W. (1985). The biosynthesis, processing, and secretion of laminin by human choriocarcinoma cells. J Biol Chem *260*, 14732-14742.

Peterson, M. D., Bement, W. M., and Mooseker, M. S. (1993). An in vitro model for the analysis of intestinal brush border assembly. II. Changes in expression and localization of brush border proteins during cell contact-induced brush border assembly in Caco-2BBe cells. J Cell Sci *105 (Pt 2)*, 461-472.

Peterson, M. D., and Mooseker, M. S. (1992). Characterization of the enterocyte-like brush border cytoskeleton of the C2BBe clones of the human intestinal cell line, Caco-2. J Cell Sci *102 (Pt 3)*, 581-600.

Pines, J., and Hunter, T. (1989). Isolation of a human cyclin cDNA: evidence for cyclin mRNA and protein regulation in the cell cycle and for interaction with p34cdc2. Cell *58*, 833-846.

Plopper, G., Falk-Marzillier, J., Glaser, S., Fitchmun, M., Giannelli, G., Romano, T., Jones, J. C., and Quaranta, V. (1996). Changes in expression of monoclonal antibody epitopes on laminin-5r induced by cell contact. J Cell Sci *109 (Pt 7)*, 1965-1973.

Poon, R. Y., and Hunter, T. (1998). Expression of a novel form of p21Cip1/Waf1 in UV-irradiated and transformed cells. Oncogene *16*, 1333-1343.

Pouliot, N., Nice, E. C., and Burgess, A. W. (2001). Laminin-10 mediates basal and EGF-stimulated motility of human colon carcinoma cells via alpha(3)beta(1) and alpha(6)beta(4) integrins. Exp Cell Res *266*, 1-10.

Price, L. S., Leng, J., Schwartz, M. A., and Bokoch, G. M. (1998). Activation of Rac and Cdc42 by integrins mediates cell spreading. Mol Biol Cell *9*, 1863-1871.

Pulkkinen, L., Christiano, A. M., Gerecke, D., Wagman, D. W., Burgeson, R. E., Pittelkow, M. R., and Uitto, J. (1994). A homozygous nonsense mutation in the beta 3 chain gene of laminin 5 (LAMB3) in Herlitz junctional epidermolysis bullosa. Genomics *24*, 357-360.

Pyke, C., Salo, S., Ralfkiaer, E., Romer, J., Dano, K., and Tryggvason, K. (1995). Laminin-5 is a marker of invading cancer cells in some human carcinomas and is coexpressed with the receptor for urokinase plasminogen activator in budding cancer cells in colon adenocarcinomas. Cancer Res *55*, 4132-4139.

Racusen, L. C. (1998). Epithelial cell shedding in acute renal injury. Clin Exp Pharmacol Physiol *25*, 273-275.

Raghavan, S., Bauer, C., Mundschau, G., Li, Q., and Fuchs, E. (2000). Conditional ablation of beta1 integrin in skin. Severe defects in epidermal proliferation, basement membrane formation, and hair follicle invagination. J Cell Biol *150*, 1149-1160.

Ragione, F. D., Russo, G. L., Oliva, A., Mercurio, C., Mastropietro, S., Pietra, V. D., and Zappia, V. (1996). Biochemical characterization of p16INK4- and p18-containing complexes in human cell lines. J Biol Chem *271*, 15942-15949.

Remy, L., Trespeuch, C., Bachy, S., Scoazec, J. Y., and Rousselle, P. (2006). Matrilysin 1 influences colon carcinoma cell migration by cleavage of the laminin-5 beta3 chain. Cancer Res *66*, 11228-11237.

Retta, S. F., Cassara, G., D'Amato, M., Alessandro, R., Pellegrino, M., Degani, S., De Leo, G., Silengo, L., and Tarone, G. (2001). Cross talk between beta(1) and alpha(V) integrins: beta(1) affects beta(3) mRNA stability. Mol Biol Cell *12*, 3126-3138.

Rodius, S., Indra, G., Thibault, C., Pfister, V., and Georges-Labouesse, E. (2007). Loss of alpha6 integrins in keratinocytes leads to an increase in TGFbeta and AP1 signaling and in expression of differentiation genes. J Cell Physiol *212*, 439-449.

Rousselle, P., Keene, D. R., Ruggiero, F., Champliaud, M. F., Rest, M., and Burgeson, R. E. (1997). Laminin 5 binds the NC-1 domain of type VII collagen. J Cell Biol *138*, 719-728.

Rousselle, P., Lunstrum, G. P., Keene, D. R., and Burgeson, R. E. (1991). Kalinin: an epithelium-specific basement membrane adhesion molecule that is a component of anchoring filaments. J Cell Biol *114*, 567-576.

Ruoslahti, E. (1996). RGD and other recognition sequences for integrins. Annu Rev Cell Dev Biol *12*, 697-715.

Russo, A. A., Jeffrey, P. D., Patten, A. K., Massague, J., and Pavletich, N. P. (1996). Crystal structure of the p27Kip1 cyclin-dependent-kinase inhibitor bound to the cyclin A-Cdk2 complex. Nature *382*, 325-331.

Ryan, M. C., Lee, K., Miyashita, Y., and Carter, W. G. (1999). Targeted disruption of the LAMA3 gene in mice reveals abnormalities in survival and late stage differentiation of epithelial cells. J Cell Biol *145*, 1309-1323.

Ryan, M. C., Tizard, R., VanDevanter, D. R., and Carter, W. G. (1994). Cloning of the LamA3 gene encoding the alpha 3 chain of the adhesive ligand epiligrin. Expression in wound repair. J Biol Chem *269*, 22779-22787.

Sanderson, R. D., Fitch, J. M., Linsenmayer, T. R., and Mayne, R. (1986). Fibroblasts promote the formation of a continuous basal lamina during myogenesis in vitro. J Cell Biol *102*, 740-747.

Santoro, M. M., and Gaudino, G. (2005). Cellular and molecular facets of keratinocyte reepithelization during wound healing. Exp Cell Res *304*, 274-286.

Sarnak, M. J., Levey, A. S., Schoolwerth, A. C., Coresh, J., Culleton, B., Hamm, L. L., McCullough, P. A., Kasiske, B. L., Kelepouris, E., Klag, M. J.*, et al.* (2003). Kidney disease as a risk factor for development of cardiovascular disease: a statement from the American Heart Association Councils on Kidney in Cardiovascular Disease, High Blood Pressure Research, Clinical Cardiology, and Epidemiology and Prevention. Hypertension *42*, 1050-1065.

Sato, G. (1981). Functionally differentiated cell lines, (New York: A.R. Liss).

Schenk, S., Hintermann, E., Bilban, M., Koshikawa, N., Hojilla, C., Khokha, R., and Quaranta, V. (2003). Binding to EGF receptor of a laminin-5 EGF-like fragment liberated during MMP-dependent mammary gland involution. J Cell Biol *161*, 197-209.

Schock, F., and Perrimon, N. (2002). Molecular mechanisms of epithelial morphogenesis. Annu Rev Cell Dev Biol *18*, 463-493.

Schoenenberger, C. A., Zuk, A., Zinkl, G. M., Kendall, D., and Matlin, K. S. (1994). Integrin expression and localization in normal MDCK cells and transformed MDCK cells lacking apical polarity. J Cell Sci *107 (Pt 2)*, 527-541.

Schwartz, M. A., and Ginsberg, M. H. (2002). Networks and crosstalk: integrin signalling spreads. Nat Cell Biol *4*, E65-68.

Schwarz, D. S., Hutvagner, G., Du, T., Xu, Z., Aronin, N., and Zamore, P. D. (2003). Asymmetry in the assembly of the RNAi enzyme complex. Cell *115*, 199-208.

Scibetta, A. G., Copier, J., Barrett, A., Chaplin, T., and Taylor-Papadimitriou, J. (2005). Gene expression changes induced by a recombinant E1-/E3- adenovirus type 5 vector in human mammary epithelial cells. Intervirology *48*, 350-361.

Sehgal, B. U., DeBiase, P. J., Matzno, S., Chew, T. L., Claiborne, J. N., Hopkinson, S. B., Russell, A., Marinkovich, M. P., and Jones, J. C. (2006). Integrin beta4 regulates migratory behavior of keratinocytes by determining laminin-332 organization. J Biol Chem *281*, 35487-35498.

Severino, J., Allen, R. G., Balin, S., Balin, A., and Cristofalo, V. J. (2000). Is beta-galactosidase staining a marker of senescence in vitro and in vivo? Exp Cell Res *257*, 162-171.

Shang, M., Koshikawa, N., Schenk, S., and Quaranta, V. (2001). The LG3 module of laminin-5 harbors a binding site for integrin alpha3beta1 that promotes cell adhesion, spreading, and migration. J Biol Chem *276*, 33045-33053.

Shaulian, E., and Karin, M. (2001). AP-1 in cell proliferation and survival. Oncogene *20*, 2390-2400.

Shaulian, E., and Karin, M. (2002). AP-1 as a regulator of cell life and death. Nat Cell Biol *4*, E131-136.

Shaw, L. M. (2001). Identification of insulin receptor substrate 1 (IRS-1) and IRS-2 as signaling intermediates in the alpha6beta4 integrin-dependent activation of phosphoinositide 3-OH kinase and promotion of invasion. Mol Cell Biol *21*, 5082-5093.

Sigle, R. O., Gil, S. G., Bhattacharya, M., Ryan, M. C., Yang, T. M., Brown, T. A., Boutaud, A., Miyashita, Y., Olerud, J., and Carter, W. G. (2004). Globular domains 4/5 of the laminin alpha3 chain mediate deposition of precursor laminin 5. J Cell Sci *117*, 4481-4494.

Simons, K., and Fuller, S. D. (1985). Cell surface polarity in epithelia. Annu Rev Cell Biol *1*, 243-288.

Singer, J. D., Gurian-West, M., Clurman, B., and Roberts, J. M. (1999). Cullin-3 targets cyclin E for ubiquitination and controls S phase in mammalian cells. Genes Dev *13*, 2375-2387.

Smyth, N., Vatansever, H. S., Murray, P., Meyer, M., Frie, C., Paulsson, M., and Edgar, D. (1999). Absence of basement membranes after targeting the LAMC1 gene results in embryonic lethality due to failure of endoderm differentiation. J Cell Biol *144*, 151-160.

Sonnenberg, A., Daams, H., Van der Valk, M. A., Hilkens, J., and Hilgers, J. (1986). Development of mouse mammary gland: identification of stages in differentiation of luminal and myoepithelial cells using monoclonal antibodies and polyvalent antiserum against keratin. J Histochem Cytochem *34*, 1037-1046.

St Croix, B., Sheehan, C., Rak, J. W., Florenes, V. A., Slingerland, J. M., and Kerbel, R. S. (1998). E-Cadherin-dependent growth suppression is mediated by the cyclin-dependent kinase inhibitor p27(KIP1). J Cell Biol *142*, 557-571.

Stepp, M. A., Gibson, H. E., Gala, P. H., Iglesia, D. D., Pajoohesh-Ganji, A., Pal-Ghosh, S., Brown, M., Aquino, C., Schwartz, A. M., Goldberger, O.*, et al.* (2002). Defects in keratinocyte activation during wound healing in the syndecan-1-deficient mouse. J Cell Sci *115*, 4517-4531.

Stoker, M., O'Neill, C., Berryman, S., and Waxman, V. (1968). Anchorage and growth regulation in normal and virus-transformed cells. Int J Cancer *3*, 683-693.

Sugiyama, S., Utani, A., Yamada, S., Kozak, C. A., and Yamada, Y. (1995). Cloning and expression of the mouse laminin gamma 2 (B2t) chain, a subunit of epithelial cell laminin. Eur J Biochem *228*, 120-128.

Suzuki, N., Hozumi, K., Urushibata, S., Yoshimura, T., Kikkawa, Y., Gumerson, J. D., Michele, D. E., Hoffman, M. P., Yamada, Y., and Nomizu, M. (2010). Identification of alpha-dystroglycan binding sequences in the laminin alpha2 chain LG4-5 module. Matrix Biol *29*, 143-151.

Takada, Y., and Puzon, W. (1993). Identification of a regulatory region of integrin beta 1 subunit using activating and inhibiting antibodies. J Biol Chem *268*, 17597-17601.

Talts, J. F., Andac, Z., Gohring, W., Brancaccio, A., and Timpl, R. (1999). Binding of the G domains of laminin alpha1 and alpha2 chains and perlecan to heparin, sulfatides, alpha-dystroglycan and several extracellular matrix proteins. EMBO J *18*, 863-870.

Tchou, W. W., Rom, W. N., and Tchou-Wong, K. M. (1996). Novel form of p21(WAF1/CIP1/SDI1) protein in phorbol ester-induced G2/M arrest. J Biol Chem *271*, 29556-29560.

Thiery, J. P. (2002). Epithelial-mesenchymal transitions in tumour progression. Nat Rev Cancer *2*, 442-454.

Thyboll, J., Kortesmaa, J., Cao, R., Soininen, R., Wang, L., Iivanainen, A., Sorokin, L., Risling, M., Cao, Y., and Tryggvason, K. (2002). Deletion of the laminin alpha4 chain leads to impaired microvessel maturation. Mol Cell Biol *22*, 1194-1202.

Timpl, R., Rohde, H., Robey, P. G., Rennard, S. I., Foidart, J. M., and Martin, G. R. (1979). Laminin--a glycoprotein from basement membranes. J Biol Chem *254*, 9933-9937.

Timpl, R., Tisi, D., Talts, J. F., Andac, Z., Sasaki, T., and Hohenester, E. (2000). Structure and function of laminin LG modules. Matrix Biol *19*, 309-317.

Todd, D. E., Densham, R. M., Molton, S. A., Balmanno, K., Newson, C., Weston, C. R., Garner, A. P., Scott, L., and Cook, S. J. (2004). ERK1/2 and p38 cooperate to induce a p21CIP1-dependent G1 cell cycle arrest. Oncogene *23*, 3284-3295.

Tran, M., Rousselle, P., Nokelainen, P., Tallapragada, S., Nguyen, N. T., Fincher, E. F., and Marinkovich, M. P. (2008). Targeting a tumor-specific laminin domain critical for human carcinogenesis. Cancer Res *68*, 2885-2894.

Trusolino, L., Bertotti, A., and Comoglio, P. M. (2001). A signaling adapter function for alpha6beta4 integrin in the control of HGF-dependent invasive growth. Cell *107*, 643-654.

Tsubota, Y., Yasuda, C., Kariya, Y., Ogawa, T., Hirosaki, T., Mizushima, H., and Miyazaki, K. (2005). Regulation of biological activity and matrix assembly of laminin-5 by COOH-terminal, LG4-5 domain of alpha3 chain. J Biol Chem *280*, 14370-14377.

Tunggal, P., Smyth, N., Paulsson, M., and Ott, M. C. (2000). Laminins: structure and genetic regulation. Microsc Res Tech *51*, 214-227.

Utani, A., Nomizu, M., Matsuura, H., Kato, K., Kobayashi, T., Takeda, U., Aota, S., Nielsen, P. K., and Shinkai, H. (2001). A unique sequence of the laminin alpha 3 G domain binds to heparin and promotes cell adhesion through syndecan-2 and -4. J Biol Chem *276*, 28779-28788.

Valentich, J. D. (1981). Morphological similarities between the dog kidney cell line MDCK and the mammalian cortical collecting tubule. Ann N Y Acad Sci *372*, 384-405.

Warren, J. C., Rutkowski, A., and Cassimeris, L. (2006). Infection with replication-deficient adenovirus induces changes in the dynamic instability of host cell microtubules. Mol Biol Cell *17*, 3557-3568.

Waterman, E. A., Sakai, N., Nguyen, N. T., Horst, B. A., Veitch, D. P., Dey, C. N., Ortiz-Urda, S., Khavari, P. A., and Marinkovich, M. P. (2007). A laminin-collagen complex drives human epidermal carcinogenesis through phosphoinositol-3-kinase activation. Cancer Res *67*, 4264-4270.

Watson, J. V., Chambers, S. H., and Smith, P. J. (1987). A pragmatic approach to the analysis of DNA histograms with a definable G1 peak. Cytometry *8*, 1-8.

Weaver, V. M., Lelievre, S., Lakins, J. N., Chrenek, M. A., Jones, J. C., Giancotti, F., Werb, Z., and Bissell, M. J. (2002). beta4 integrin-dependent formation of polarized three-dimensional architecture confers resistance to apoptosis in normal and malignant mammary epithelium. Cancer Cell *2*, 205-216.

Weber, J. D., Hu, W., Jefcoat, S. C., Jr., Raben, D. M., and Baldassare, J. J. (1997a). Ras-stimulated extracellular signal-related kinase 1 and RhoA activities coordinate platelet-derived growth factor-induced G1 progression through the independent regulation of cyclin D1 and p27. J Biol Chem *272*, 32966-32971.

Weber, J. D., Raben, D. M., Phillips, P. J., and Baldassare, J. J. (1997b). Sustained activation of extracellular-signal-regulated kinase 1 (ERK1) is required for the continued expression of cyclin D1 in G1 phase. Biochem J *326 (Pt 1)*, 61-68.

Weir, M. L., Oppizzi, M. L., Henry, M. D., Onishi, A., Campbell, K. P., Bissell, M. J., and Muschler, J. L. (2006). Dystroglycan loss disrupts polarity and beta-casein induction in mammary epithelial cells by perturbing laminin anchoring. J Cell Sci *119*, 4047-4058.

Xian, X., Gopal, S., and Couchman, J. R. (2010). Syndecans as receptors and organizers of the extracellular matrix. Cell Tissue Res *339*, 31-46.

Yang, B., Jung, D., Motto, D., Meyer, J., Koretzky, G., and Campbell, K. P. (1995). SH3 domain-mediated interaction of dystroglycan and Grb2. J Biol Chem *270*, 11711-11714.

Yang, J., and Kornbluth, S. (1999). All aboard the cyclin train: subcellular trafficking of cyclins and their CDK partners. Trends Cell Biol *9*, 207-210.

Yu, W., Datta, A., Leroy, P., O'Brien, L. E., Mak, G., Jou, T. S., Matlin, K. S., Mostov, K. E., and Zegers, M. M. (2005). Beta1-integrin orients epithelial polarity via Rac1 and laminin. Mol Biol Cell *16*, 433-445.

Yurchenco, P. D., and O'Rear, J. J. (1994). Basal lamina assembly. Curr Opin Cell Biol *6*, 674-681.

Yurchenco, P. D., Quan, Y., Colognato, H., Mathus, T., Harrison, D., Yamada, Y., and O'Rear, J. J. (1997). The alpha chain of laminin-1 is independently secreted and drives secretion of its beta- and gamma-chain partners. Proc Natl Acad Sci U S A *94*, 10189-10194.

Yurchenco, P. D., Tsilibary, E. C., Charonis, A. S., and Furthmayr, H. (1985). Laminin polymerization in vitro. Evidence for a two-step assembly with domain specificity. J Biol Chem *260*, 7636-7644.

Zboralski, D., Bockmann, M., Zapatka, M., Hoppe, S., Schoneck, A., Hahn, S. A., Schmiegel, W., and Schwarte-Waldhoff, I. (2008). Divergent mechanisms underlie Smad4-mediated positive regulation of the three genes encoding the basement membrane component laminin-332 (laminin-5). BMC Cancer *8*, 215.

Zegers, M. M., Forget, M. A., Chernoff, J., Mostov, K. E., ter Beest, M. B., and Hansen, S. H. (2003). Pak1 and PIX regulate contact inhibition during epithelial wound healing. Embo J *22*, 4155-4165.

Zent, R., Bush, K. T., Pohl, M. L., Quaranta, V., Koshikawa, N., Wang, Z., Kreidberg, J. A., Sakurai, H., Stuart, R. O., and Nigam, S. K. (2001). Involvement of laminin binding integrins and laminin-5 in branching morphogenesis of the ureteric bud during kidney development. Dev Biol *238*, 289-302.

Zhang, H. S., Gavin, M., Dahiya, A., Postigo, A. A., Ma, D., Luo, R. X., Harbour, J. W., and Dean, D. C. (2000). Exit from G1 and S phase of the cell cycle is regulated by repressor complexes containing HDAC-Rb-hSWI/SNF and Rb-hSWI/SNF. Cell *101*, 79-89.

Zhang, X., Ma, L., Enkemann, S. A., and Pledger, W. J. (2003). Role of Gadd45alpha in the density-dependent G1 arrest induced by p27(Kip1). Oncogene *22*, 4166-4174.

Zhao, J., Pestell, R., and Guan, J. L. (2001). Transcriptional activation of cyclin D1 promoter by FAK contributes to cell cycle progression. Mol Biol Cell *12*, 4066-4077.

Zhu, X., Ohtsubo, M., Bohmer, R. M., Roberts, J. M., and Assoian, R. K. (1996). Adhesion-dependent cell cycle progression linked to the expression of cyclin D1, activation of cyclin E-cdk2, and phosphorylation of the retinoblastoma protein. J Cell Biol *133*, 391-403.

Zinkl, G. M., Zuk, A., van der Bijl, P., van Meer, G., and Matlin, K. S. (1996). An antiglycolipid antibody inhibits Madin-Darby canine kidney cell adhesion to laminin and interferes with basolateral polarization and tight junction formation. J Cell Biol *133*, 695-708.

Zuk, A., and Matlin, K. S. (2002). Induction of a laminin isoform and alpha(3)beta(1)-integrin in renal ischemic injury and repair in vivo. Am J Physiol Renal Physiol *283*, F971-984.